TNF Superfamily and Neurotrophin Signalling Differentially Regulate Paravertebral and Prevertebral Development in the Sympathetic Nervous System

Osman Yipkin Calhan

A thesis submitted to Cardiff University in accordance with the requirements for the degree of Doctor of Philosophy in the discipline of Neuroscience

School of Biosciences, Cardiff University

December 2020

Dedicated to all scientists separated from their dreams

during a long, COVID year…

ACKNOWLEDGEMENTS

First and foremost, I would like to thank Professor Alun Davies for giving me the opportunity to continue my scientific journey in the incredibly positive environment of his lab. He was a source of inspiration and creativity and I am deeply grateful to him for sharing his knowledge so generously throughout my Ph.D. studies. I am also thankful to him for his endless support for my academic and non-academic endeavours. He made a hard Ph.D. journey so much easier with his guidance and direction.

I am also deeply grateful to Dr. Sean Wyatt for his great mentorship. I thank him for all the patience he showed towards my countless questions. He greatly helped me to keep my focus on the essential parts of the projects presented in this thesis. I am also very thankful to him for being so generous with his time whenever I needed help, regardless of weekends and holidays. I also thank him for reading this thesis so thoroughly and giving me such highly constructive feedback to improve the quality of the ideas presented here.

I thank Dr. Laura Howard for sharing all her expertise with me. I thank Dr. Clara Erice Jurecky for her great help in teaching me skills and for her support at the beginning of my Ph.D. journey. I also thank Dr. Paulina Carriba, Dr. Blanca Paramo, and Dr. Anthony Horton for firstly helping me with all my questions during daily experiments, and then creating such a nice and friendly environment during my Ph.D. studies.

I thank Professor Yves Barde and his lab at Cardiff University. He showed his genuine support every time I needed him and his lab during my Ph.D. studies.

I thank Cheryl and Malcolm Jones. They kindly and warmly opened the doors of their home to me and let me finish writing my thesis in their home, while at the same time letting me trash their glassware one by one.

I thank and remember my lovely family, Riza, Nihal, and Tijin Calhan. Although they were miles away from me, they never stopped showing their love and support for a single day. Their unending support gave me the confidence to stay dedicated to my Ph.D. studies.

I thank Thelma and Louise. They have kept me company for the long days and long nights while I was writing my thesis. I am truly sure at some point they were as stressed as much as me.

My final and biggest gratitude is to Dr. Hayley Dingsdale. This thesis would not be written without her infinite support. She created such a great environment in which thoughts and ideas could easily flourish throughout my Ph.D. studies. Our long and fruitful discussions helped to grow and shape many ideas involved in this thesis. I am deeply grateful to her for her never-ending scientific and emotional support. I am also grateful to her for reading this thesis many times, and for giving me so much positive and valuable feedback.

ABSTRACT

The sympathetic nervous system (SNS) has two distinct divisions: paravertebral and prevertebral. Previous work on the well-characterised and relatively accessible superior cervical ganglia (SCG, a paravertebral model), discovered a significant role for tumour necrosis factor (TNF) superfamily members in SNS development. The most intriguing were TNFR1-promoted TNF-α-mediated reverse signalling, and CD40-activated CD40L-mediated reverse signalling, identified as major physiological regulators of neurite outgrowth. This thesis asked whether these TNF signalling mechanisms function universally throughout the SNS, or differ across the two divisions.

The innervation density of prevertebral targets (spleen, kidney, and stomach) from *Tnf*-, *Tnfrsf1a*-, and *Cd40*-deficient mice was investigated. In addition, the mechanisms underlying TNF signalling were compared between SCG, and coeliac and superior mesenteric ganglia (prevertebral ganglia; PVG), used here as a prevertebral model.

TNF-α-reverse signalling only enhanced innervation density of paravertebral, but not prevertebral, targets. Similarly, CD40L-reverse signalling suppressed innervation of prevertebral targets, opposite to that seen in paravertebral targets. These *in vivo* differences paralleled *in vitro* findings. Whereas TNF-α-reverse signalling enhanced neurite outgrowth in SCG neurons, PVG neurons only responded to TNF-α-forward signalling. Similarly, whereas CD40L-reverse signalling enhanced neurite outgrowth of SCG neurons, this pathway suppressed PVG neurite outgrowth. These substantial differences between the two SNS divisions led to further investigations into more fundamental signalling, the neurotrophins. Nerve growth factor (NGF) and neurotrophic factor 3 (NT-3) increased neurite outgrowth of SCG and PVG neurons in a concentration-dependent manner. However, SCG neurons were significantly more responsive to NGF and NT-3 than PVG neurons. Surprisingly, these neurotrophins had no differential effects on cell survival between SCG and PVG neurons.

Data here suggest that PVG and SCG neurons differ substantially in their response to both TNF and neurotrophin signalling during SNS development. Thus, future research should consider also including the prevertebral division in the study of the developing SNS.

Table of Contents

List of Figures

Chapter 1

Chapter 2

Chapter 3

Chapter 4

Chapter 5

List of Tables

Chapter 2

Abbreviations

ADAM	A disintegrin and metalloprotease
ADAM17	ADAM metallopeptidase domain 17
AIF	Apoptosis-inducing factor
Apaf-1	Apoptotic protease-activating factor-1
APRIL	A proliferation-inducing ligand
Bad	Bcl-2 associated agonist of cell death
BAFF	B-cell activating factor
Bax	Bcl-2 associated X-protein
BBB	Blood-brain-barrier
Bcl	B-cell lymphoma
BCMA	B-cell maturation antigen
BDNF	Brain-derived neurotrophic factor
BH	Bcl-2 homology
Bik	Bcl-2-interacting killer
Bim	Bcl-2-like protein 11
BMPs	Bone morphogenetic proteins
Bok	Bcl-2 related ovarian killer protein
BSA	Bovine serum albumin
C	Cervical
CAD	Caspase-activated DNase
CD	Cluster of differentiation
CD40L	CD40 ligand
CG	Coeliac ganglia
cIAP	Cellular inhibitors of apoptosis proteins
CNS	Central nervous system
CNTF	Ciliary neurotrophic factor
CRD	Cysteine-rich domain
DAPI	4',6-Diamidino-2-Phenylindole, Dihydrochloride
DBE	Dibenzyl ether
DED	Death effector domain
DISC	Death-inducing signalling complex

DMSO	Dimethylsulfoxide
DPBS	Dulbecco's Phosphate Buffered Saline
DR	Death receptor
DRG	Dorsal root ganglia
E	Embryonic day
EDA	Ectodysplasin A
Edn3	Endothelin-3
EdnrA	Edn3 receptor
EMT	Epithelial to mesenchymal transition
ERK	Extracellular signal regulated kinase
FADD	Fas-associated death domain
FGFs	Fibroblast growth factors
GAPDH	Glyceraldehyde phosphate dehydrogenase
GDNF	Glial cell-line derived neurotrophic factor
GFRα3	GDNF family receptor alpha-3
GITR	Glucocorticoid-induced TNFR-related protein
GITRL	GITR ligand
HBSS	Hanks' Balanced Salt Solution
HGF	Hepatocyte growth factor
HPRT1	Hypoxanthine phosphoribosyltransferase 1
HVEM	Herpesvirus entry mediator
IAPs	Inhibitory apoptosis proteins
iDISCO	Immunolabeling-enabled three-dimensional imaging of solvent cleared organs
IKKβ	Inhibitor of NF-κB
IML	Intermediolateral cell column
JNK	Jun NH_2 terminal kinase
kDa	Kilodalton
L	Lumbar
LIF	Leukaemia inhibitory factor
LIGHT	Lymphotoxin-related inducible ligand that competes for glycoprotein D binding to herpes virus entry mediator on T cells
LT-α	Lymphotoxin alpha

LTβR	Lymphotoxin-β receptor
MAGE-G1	Melanoma-associated antigen
mCD40	Transmembrane CD40
mTNF-α	Transmembrane TNF-α
mTNFSF	Transmembrane TNFSF
mTOR	Mammalian target of rapamycin
NADE	Neurotrophin-associated cell death executor
NCCs	Neural crest stem cells
NF-κB	Nuclear factor-κB
NGF	Nerve growth factor
NK	Natural killer
NRAGE	Melanoma-associated antigen homologue
NSCs	Neural stem cells
NT	Neurotrophin
P	Postnatal day
$p75^{NTR}$	75kDa neurotrophin receptor
PBS	Phosphate buffered saline
PCR	Polymerase chain reaction
PFA	Paraformaldehyde
PI3K	Phosphatidylinositol-3-kinase
PKC	Protein kinase C
PLC	Phospholipase C
PNS	Peripheral nervous system
PTwH	0.2% Tween-20 with 10 μg/ml heparin in PBS
Puma	p53 upregulator of apoptosis
PVG	Prevertebral ganglia
RANK	Receptor-activator of NF-κB
RANKL	RANK ligand
RIP	Receptor-interacting protein
RIPK1	Receptor-interacting serine/threonine protein kinase 1
RT	Room temperature
RT-qPCR	Reverse transcription quantitative PCR
sCD40	Soluble CD40

sCD40L	Soluble CD40L
SCG	Superior cervical ganglia
SDHA	Succinate dehydrogenase
SG	Submandibular gland
Smac/DIABLO	Second mitochondria-derived activator of caspase/ direct inhibitor of apoptosis-binding protein with low pI
SMG	Superior mesenteric ganglia
SNS	Sympathetic nervous system
SODD	Silencer of death domains
SPNs	Sympathetic preganglionic neurons
sTNF-α	Soluble TNF-α
sTNFR	Soluble TNFR
sTNFSF	Soluble TNFSF
TACE	TNF-converting enzyme
TH	Tyrosine hydroxylase
THD	TNF homology domain
THF	Tetrahydrofuran
TNF	Tumour necrosis factor
TNFR	TNF receptor
TNFSF	TNF superfamily
TNFRSF	TNF receptor superfamily
TRADD	TNF-associated death domain
TRAF	TNF-receptor-associated factor
TRAIL	TNF-related apoptosis-inducing ligand
TRANCE	TNF-related activation-induced cytokine
Trk	Tropomyosin receptor kinase
TWEAK	TNF-like weak inducer of apoptosis
TWE-PRIL	Naturally occurring fusion protein with the extracellular portion of APRIL, and transmembrane and intracellular domain of TWEAK
VEGI	Vascular endothelial growth inhibitor

Chapter 1

General Introduction

1.1 Background Information

The adult mammalian nervous system has two anatomically distinct components: the central nervous system (CNS) and the peripheral nervous system (PNS). The CNS is composed of the brain and the spinal cord, whereas the PNS consists of clusters of neurons (ganglia) and peripheral nerves (Kandel et al. 2013). The nervous system is made up of millions of highly organised and precisely connected neurons which communicate in the form of electrical signals, called action potentials. Neurons convey these signals across distances ranging from 0.1 mm to 2 m in humans, and, in doing so, create a highly complex network from which behaviour, movement and cognition emerge (Kandel et al. 2013).

Neurons, the basic signalling unit of the nervous system, share the same morphological architecture: a cell body, several dendrites and an axon. The cell body (soma) controls many of the functions of the cell, and contains organelles and a nucleus. In most neurons the cell body is connected to short processes (dendrites) and long extensions (axons). While dendrites are responsible for receiving the signals from other neurons, axons carry the signal to other neurons. The site at which neurons transmit the action potential to other neurons is called a synapse (Kandel et al. 2013).

There are estimated to be many hundreds of types of neurons in the nervous system. Technological and scientific advances in molecular and cellular biology have provided great insight into the structure and organisation of the nervous system. Especially, rapid advances in genome sequencing technologies offer scientists access to the entire genome of two workhorses of developmental biology: the nematode worm *Caenorhabditis elegans* and *Drosophila melanogaster* (fruit fly) (Brenner 2000). Many of the molecular mechanisms underlying the development of the vertebrate nervous system were uncovered from studies conducted on these two organisms. Similarly other model organisms relatively more amenable to genetic modifications such as *Xenopus laevis* (frog), *Danio rerio* (zebrafish), *Gallus gallus* (chicken) and *Mus musculus* (mouse) helped tremendously in the discovery of the key molecules shaping the

organisation of the nervous system. Although there are huge organisational differences in the nervous systems of these organisms, they still share common principles at the molecular level which have been conserved throughout evolution (Wolpert et al. 2002).

In this introduction, I intend to give an overview of mechanisms controlling the development of the sympathetic nervous system. This will start with the early formation of the neural plate in the neurulation stage of development. It will continue with the emergence and first migration of neural stem cells to their respective positions to start the formation of the sympathetic paravertebral and prevertebral neurons, together with the rest of the sympathetic nervous system. I will continue to outline how the 'neurotrophic theory' casts light on sympathetic neuronal survival during development. Later, I will lay out the basic mechanisms that play a role in the elongation of neurites from sympathetic ganglia to their target organs. Finally, I will describe the involvement of the tumour necrosis superfamily members in controlling sympathetic neuronal outgrowth and target organ innervation. As *Mus musculus* is the only animal model utilised in this thesis, the explanation of the basic tenets of nervous system development will be explained in the context of vertebrate development only.

1.2 Development of the Vertebrate Nervous System

The formation of the highly complex nervous system begins in the early embryonic stages of development and continues until postnatal ages (Tam and Behringer 1997). Early mammalian embryos transform themselves from simple clusters of cells into a more complex layering of distinct cell types. These layers of cells are known as germ layers. The mouse embryo consists of three germ layers which develop throughout embryonic stages (Tam and Behringer 1997). These layers are the ectoderm (Itoh and Sokol 2015) (outer layer), mesoderm (middle layer) (Feldman 2015) and endoderm (inner layer) (Wlizla and Zorn 2015). Each of the developing germ layers gives rise to different types of cells which form tissues, and consequently constitute organs and systems. For

example, cells from the endoderm give rise to the gut, liver and lungs (Wlizla and Zorn 2015). Cells from the mesoderm give rise to muscle, cartilage, bone, blood, and organs including the kidney and heart (Feldman 2015). Lastly, cells from the ectoderm give rise to both the skin and the nervous system (Itoh and Sokol 2015).

The cup-shaped early embryo forms an indentation called the primitive streak at the posterior part of the inner cell mass, the epiblast (Tam and Behringer 1997). The primitive streak is a trench-like structure at the midline area through which the pluripotent epiblast cells migrate to specialised locations in the developing embryo to form future germ layers (Lawson 2003) (Fig. 1.1). The formation of the primitive streak also marks the beginning of the gastrulation period (Ang and Behringer 2002).

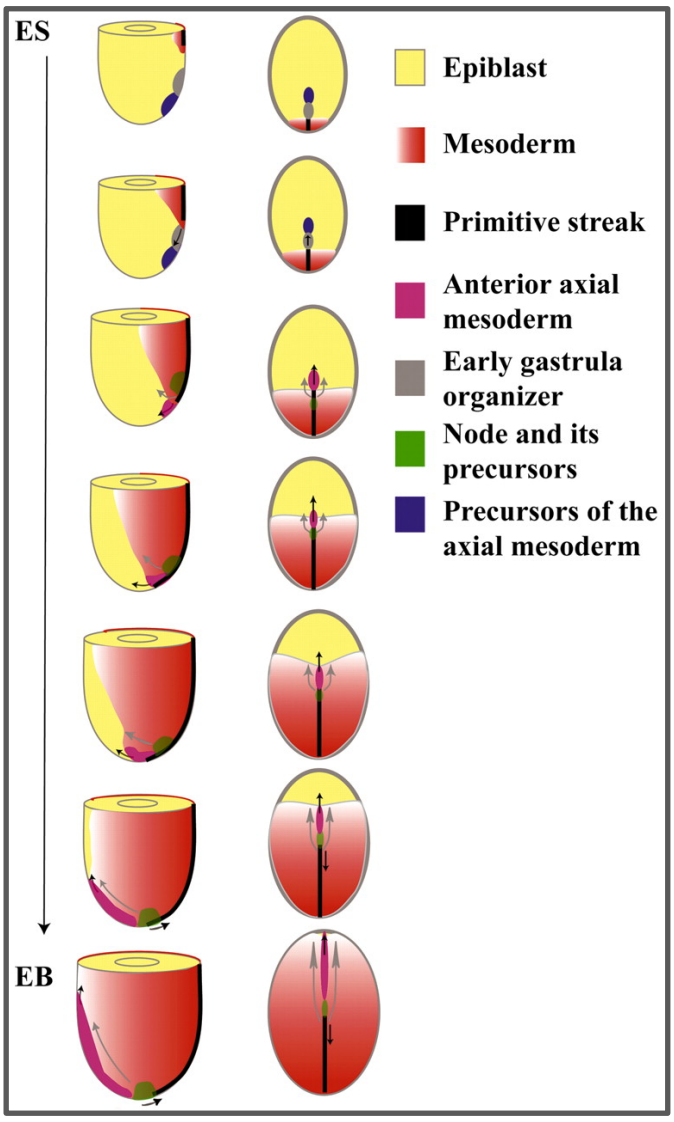

Figure 1.1. Extension of the Primitive Streak Across the Cup-Shaped Embryo. The formation of the primitive streak at the beginning of the gastrulation period from epiblast cells. Precursor cells derive from the organiser centres, and move to form the mesoderm germ layer. *Left:* lateral view of the embryo (anterior shown to the left). *Right*: flattened dorsal view of the embryo (anterior shown at the top). EB: early-bud; ES: early streak. Figure from (Kinder et al. 2001).

As Lewis Wolpert famously said in 1986: “It is not birth, marriage or death, but gastrulation which is truly the most important time in your life” (Vicente 2015). During gastrulation, epiblast cells begin to converge on the primitive streak, which extends through the embryonic midline and forms the anterior-posterior body axis of the embryo. At the primitive streak, epiblast cells undergo epithelial to mesenchymal transition (EMT), and later form the definitive mesoderm and endoderm (Downs 2009; Roelen 2018). The epiblast cells that stay on the surface of the primitive streak give rise to the ectoderm (Sadler 2005).

The notochord is formed from cells that migrate through the primitive node (the cranial end of the primitive streak) and travel cranially; this marks the beginning of the neurulation stage in the developing embryo (Sadler 2005). While the process of gastrulation continues at the posterior end, the notochord formation at the anterior end of the embryo induces the formation of the neural plate from the ectoderm cells above the notochord. Soon after the neural plate forms, it begins to rise up as a pair on both sides of the midline of the neuronal plate to fold and give rise to the neural tube (Fig. 1.2) (Sadler 2005). The neural tube later develops into the brain and the spinal cord (Sadler 2005).

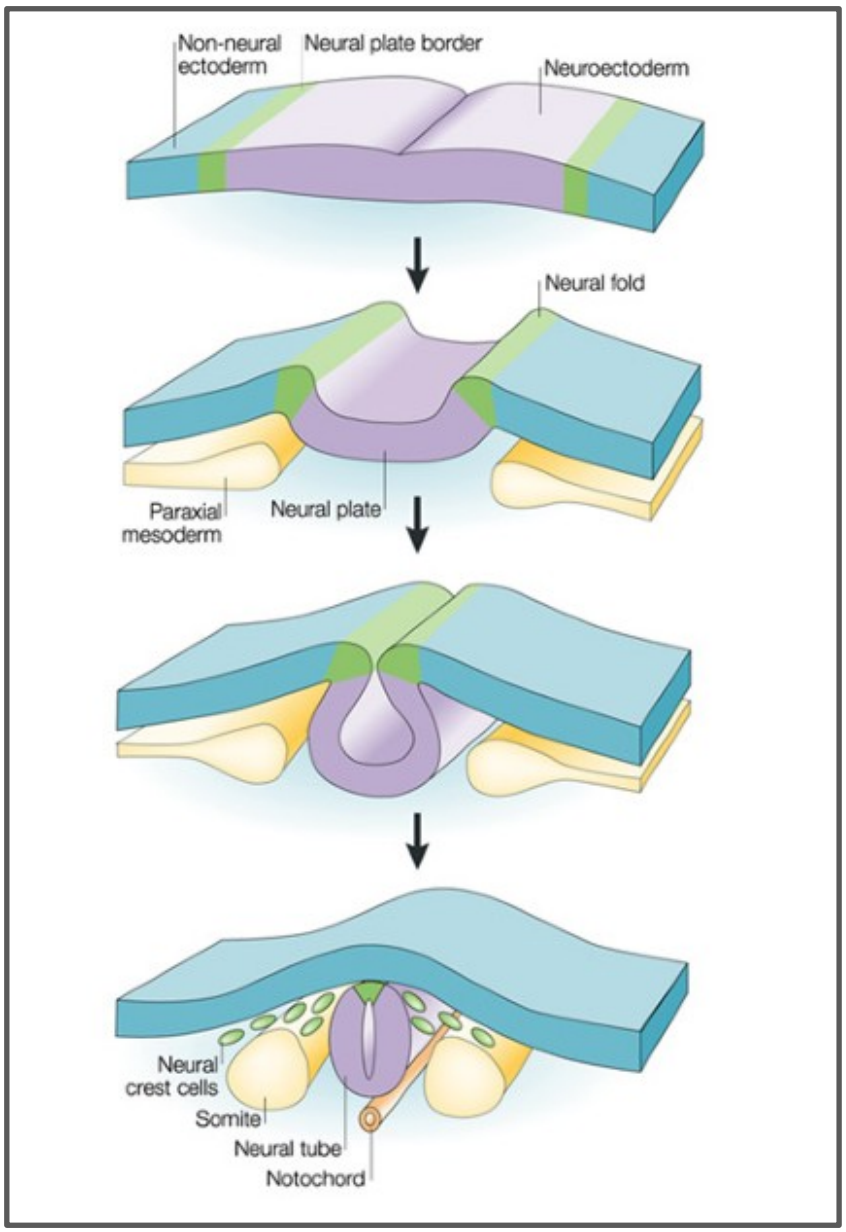

Figure 1.2. The Neural Plate Folds to Give Rise to the Neural Tube. The neural plate folds and rises up on both side of the midline to give rise to the neural tube. Neuroectoderm: Purple; Neural plate border and neural crest cells delaminating from neural plate border: Green; Non-neural Ectoderm: Blue; Paraxial mesoderm: Yellow. Figure from (Gammill and Bronner-Fraser 2003).

1.3 The Peripheral Nervous System Originates Mostly from Neural Crest Precursor Cells

The adult brain has billions of nerve cells, however these originate from a relatively small number of cells from the neural plate. Ectodermal neural stem cells are the most primordial and uncommitted cells in the developing nervous system. These early progenitor cells are multipotent neural stem cells (NSCs) with the ability to produce both neurons and glial cells in the nervous system (Kriegstein and Alvarez-Buylla 2009). NSCs can undergo two different types of cell divisions (Kriegstein and Alvarez-Buylla 2009). In the self-renewing *symmetric cell divisions*, NSCs divide to produce two identical daughter stem cells to expand the population of proliferative progenitor cells. In *asymmetric cell division*, however, NSCs produce only one progenitor stem cell and one daughter cell, the latter of which is programmed to differentiate into a non-stem cell fate such as neurons, astrocytes and oligodendrocytes in the nervous system (Kriegstein and Alvarez-Buylla 2009).

The peripheral nervous system mostly derives from a group of neuroepithelial cells, called neural crest stem cells (NCCs) at the boundary of the neural plate (Selleck and Bronner-Fraser 1995). NCCs are a multipotent, migratory cell population with the capacity to differentiate into impressively diverse cell populations including: cartilage cells; melanocytes of the epidermis; and neurons and glia of the peripheral nervous system (Gilbert 2000). After specification of the neural crest, NCCs undergo EMT which initiates delamination of NCCs. NCCs then undertake extensive migration from the neural tube as a multipotent progenitor population, colonising various distant sites in the embryo (Huang and Saint-Jeannet 2004). This migration is highly ordered, and different subcategories of NCCs (classified by axial level) each follow specific migration routes. The four subcategories of NCCs are: 1) cranial, 2) vagal and sacral, 3) cardiac and 4) trunk NCCs (Crane and Trainor 2006). (The model systems used in this thesis originate from trunk NCCs) (Fig. 1.3).

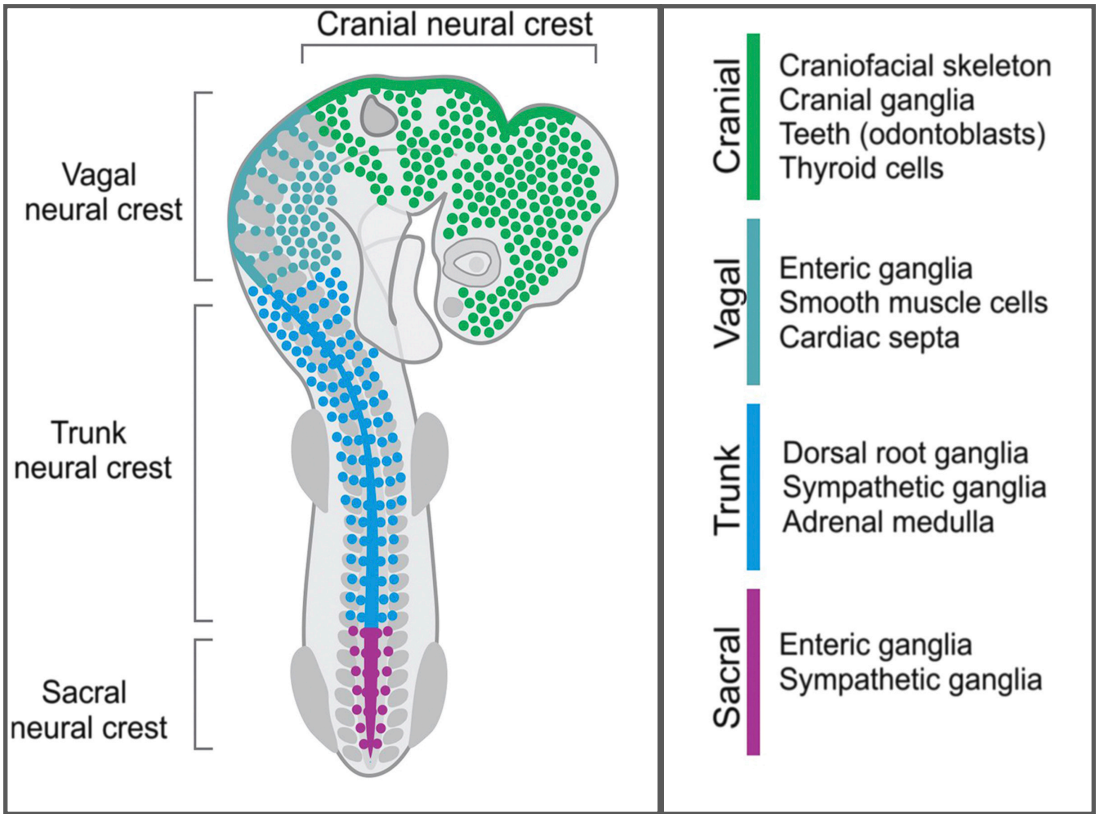

Figure 1.3. Neural Crest Cells are Categorised Based on Their Axial Level. Neural crest cells arise at the boundary between the neural plate and the non-neural ectoderm. The major subdivisions of the neuroaxis are seen: cranial (green), vagal (turquoise), trunk (blue) and sacral (purple). These neural crest cell subpopulations give rise to specific cell populations during development. Figure from (Rothstein et al. 2018).

Trunk NCCs take two main routes to travel to their final destinations in the developing embryo: 1) a dorsolateral pathway which takes NCCs into the ectoderm. NCCs that take this route will transform into pigment cells of the skin; 2) a ventral pathway which takes NCCs ventrally through the anterior of the somites. NCCs taking this route will transform into sensory neurons of the dorsal root ganglia (DRG). Some of the trunk NCCs that follow the ventral route traverse through the medial part of the somite in the direction of the dorsal aorta and differentiate into adrenal medulla and sympathetic ganglia (Fig. 1.4)(Gilbert 2000).

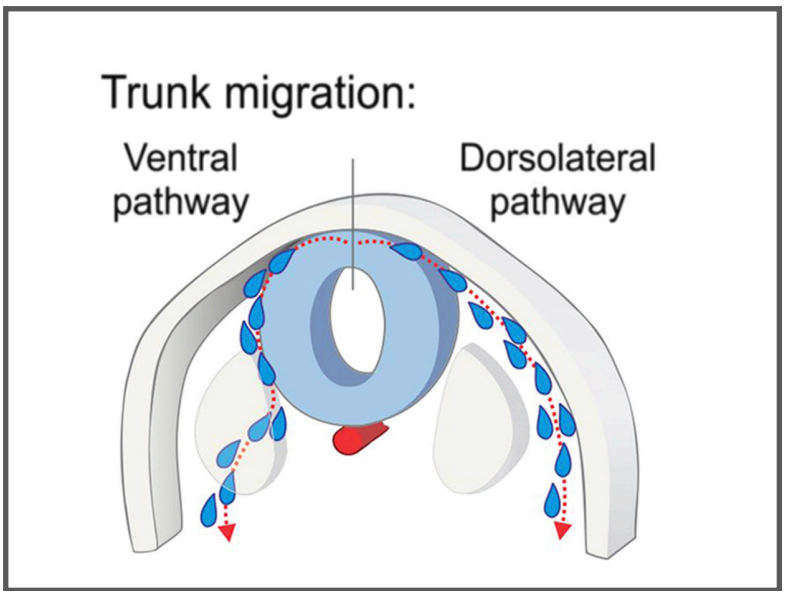

Figure 1.4. Trunk Neural Crest Cells Migrate Along Two Distinct Routes. Migration routes of neural crest cells from the trunk axial level, beginning at the border of the neural tube. Figure from (Rothstein et al. 2018).

Trunk NCCs contribute to sympathetic nervous system (SNS) development. The differentiation of trunk NCCs can take place in two potential ways. First, progenitor NCCs are specified before their migration begins from the neural tube and their fate as a distinct cell type at the final target heavily relies on intrinsic signals. Second, differentiation of multipotent NCCs can be dependent on extracellular signals emerging from the tissues with which they communicated along their migration (Ruhrberg and Schwarz 2010). Bone morphogenetic proteins (BMPs), fibroblast growth factors (FGFs), glucocorticoids, Wnts, and Smads are some of the extrinsic factors that play a crucial role in the differentiation of NCCs during SNS development. In addition, *Mash1, Phox2a/2b, Hand2,* and *Gata3* genes regulate the fate of different sympathetic subpopulations arising from trunk NCC differentiation (Kameda 2014).

In addition to NCCs, several populations of cranial sensory neurons originate from placodes, ectodermal thickenings in defined locations in the cranial region. The trigeminal placode gives rise to a subset of neurons in the trigeminal ganglion, the otic placode gives rise to neurons of the vestibular and spiral ganglia, and the epibranchial placodes give rise to neurons of the geniculate, petrosal and nodose ganglia. All the satellite cells of these ganglia are derived from NCCs.

1.4 Establishment of the Sympathetic Nervous System

The sympathetic nervous system comprises one of the two components of the autonomic nervous system and is essential for maintaining mammalian homeostasis in fight-or-flight conditions. The other half of the autonomic nervous system comprises the parasympathetic nervous system. The sympathetic nervous system can be considered as consisting of two anatomically separate parts, the paravertebral and prevertebral parts (Szurszewski and Linden 2012). Sympathetic nervous system development begins with NCCs that delaminate between somites seven to twenty-eight on

the neural tube. These NCCs give rise to most sensory neurons, sympathetic neurons, glia, chromaffin cells and melanocytes (Kameda 2014).

Information generated by the CNS is transmitted to the target tissue (the effector tissue) via a chain of two neuron types, pre- and postganglionic neurons. Preganglionic neurons are located in the lateral horn of the grey matter of spinal segments cervical (C)8 to lumbar (L)2 (Deuchars and Lall 2015). At sympathetic ganglia, preganglionic neurons synapse with postganglionic neurons (sympathetic paravertebral and prevertebral neurons), which then innervate target tissues via fast excitatory action potentials (Fig. 1.5) (Deuchars and Lall 2015). The focus of this thesis was the comparison of paravertebral and prevertebral neurons. The ganglia used in my studies were primarily the superior cervical ganglia (SCG; the first and largest ganglion of the paravertebral sympathetic chain), and the coeliac ganglia (CG) and superior mesenteric ganglia (SMG), both large prevertebral ganglia.

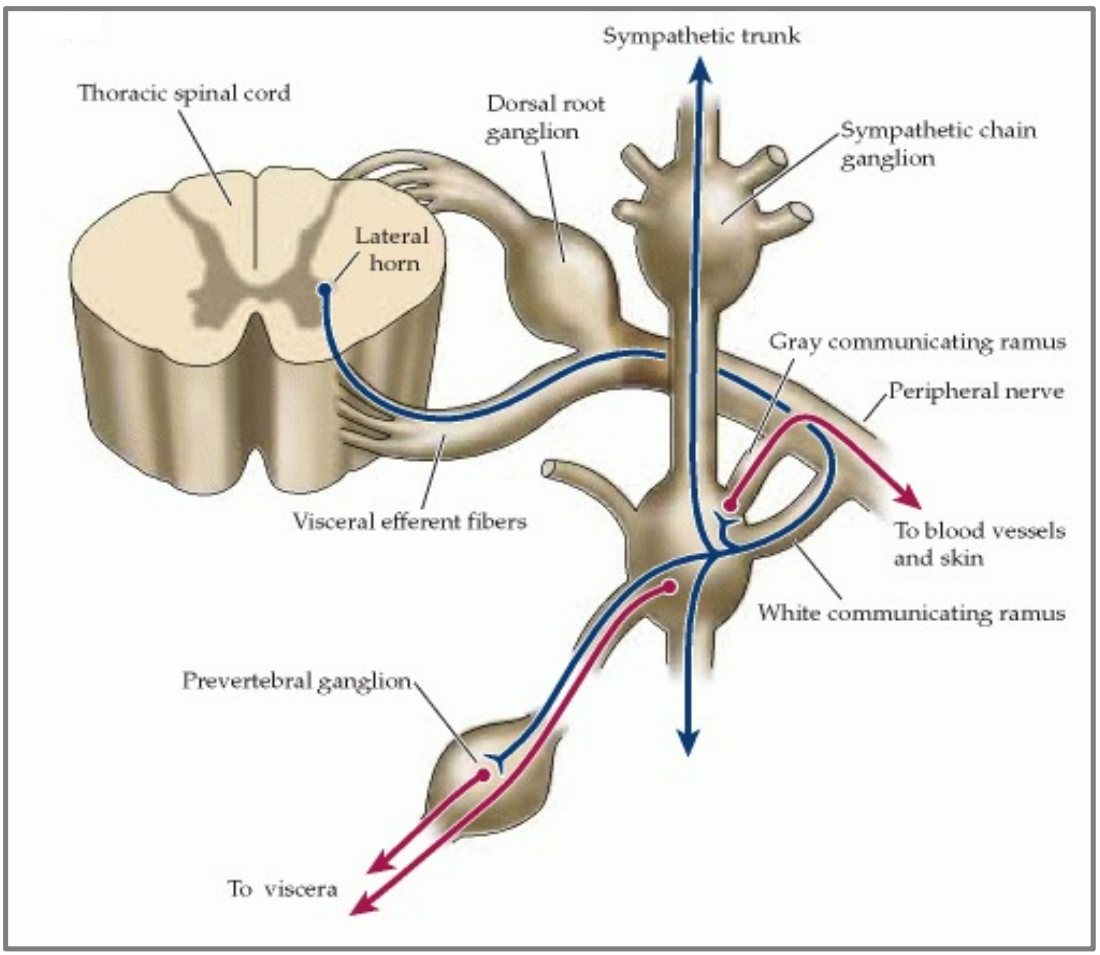

Figure 1.5. Location of Preganglionic Neurons, and Route of Transmission of Sympathetic Information. Transmission route of sympathetic information. Preganglionic neurons (blue) lie in the spinal cord and brain stem (not shown). The axons of preganglionic neurons reach to postganglionic neurons (red) either via the ventral pathway (to the sympathetic chain) or project into splanchnic nerves and form synapses in the prevertebral ganglia. Postganglionic sympathetic neurons travel towards the viscera. Figure from (Purves et al. 2001).

1.4.1 Preganglionic Neurons in the Sympathetic Nervous System

Sympathetic preganglionic neurons (SPNs) control all neurons in the sympathetic nervous system. Cell bodies of SPNs lie in the spinal cord and project their short and myelinated axons to sympathetic ganglia (Deuchars and Lall 2015). The majority of SPNs are located in the intermediolateral cell column (IML) of the spinal cord, near the lateral border of the spinal grey matter at the level of the central canal (Deuchars and Lall 2015). SPNs extend mainly between C8 and L2 levels forming bilateral and symmetrical columns within the IML. However, these columns are not uniform in shape. Rather, SPNs are clusters of 20-150 neurons known as *nests* (Deuchars and Lall 2015).

SPN axons target paravertebral ganglia and prevertebral ganglia (Gilbey and Michael Spyer 1993). SPNs project their axons to sympathetic ganglia in ipsilateral fashion to form synapses onto postganglionic neurons. The axons of SPNs project from the spinal cord through the ventral route and then enter white rami communicantes, which are mostly myelinated nerve branches, before reaching the sympathetic ganglia. Once the preganglionic axons travel across rami communicantes, they either form synapses on paravertebral ganglia or they move on out of the paravertebral chain into prevertebral ganglia (collateral) in the abdominal cavity, anterior to the vertebral column (Fig. 1.5) (Gilbey and Michael Spyer 1993; Deuchars and Lall 2015).

Highly diverse synaptic organisation is seen between the pre- and postganglionic sympathetic neurons — in humans, for example, even though the ratio of SPNs to postganglionic neurons is 1:15, a single fibre from SPNs can innervate 200 different postganglionic neurons (Deuchars and Lall 2015). During synapse formation, SPN fibres release acetylcholine as a neurotransmitter, which is a ligand for the nicotinic receptors (ligand-gated cation channel) of all postganglionic neurons (McCorry et al. 2007). Compared to preganglionic axons, mostly unmyelinated postganglionic fibres are longer as they travel relatively far to reach target organs (Jänig and McLachlan 1992). Therefore, one SPN can broadly act on different areas of the sympathetic system and affect widely distributed peripheral organs.

SPNs require neurotrophic factors for their survival, development and maintenance. Sympathetic neurons, and chromaffin cells in the adrenal medulla and cortex, deliver the required neurotrophic support retrogradely to the SPNs in the IML column of the thoracic spinal cord (Causing et al. 1997). Biochemical analyses have showed that increased concentrations of brain-derived neurotrophic factor (BDNF) and its cognate receptor tropomyosin receptor kinase (Trk) B in transgenic mice leads to preganglionic hyperinnervation on SCGs (Causing et al. 1997). Similarly, neurotrophin-4 (NT-4) deficient mice show marked reduction in the preganglionic sympathetic neuron population in the IML of the thoracic spinal cord, evidence to the importance of this neurotrophic factor for the maintenance of SPNs. While the NT-4 deficiency diminishes the development of the SPNs, the neuron numbers in the paravertebral and prevertebral ganglia remain unchanged. However, the number of synapses between SPNs and postganglionic neurons are reduced (Roosen et al. 2001). In the same way, neurotrophin-3 (NT-3) is a survival factor for sympathetic primordia cells, though whether it has any role on synapse formation between preganglionic axons and sympathetic neurons has not yet been confirmed. Studies showing that SPNs express the NT-3 cognate receptor TrkC, and that some postganglionic neurons and non-neuronal cells neighbouring the SPNs express NT-3, increase the likelihood that NT-3 plays a role in preganglionic synapse formation (Verdi et al. 1996). Unlike the significant roles of the aforementioned neurotrophic factors, *in vivo* studies have shown that nerve growth factor (NGF), the first discovered neurotrophic factor, is not required for preganglionic axon growth from the spinal cord into sympathetic ganglia (Sharma et al. 2010). In addition to neurotrophic factors, neurocytokines, such as FGFs, interleukins, transforming growth factors β, ciliary neurotrophic factor (CNTF), and insulin-like growth factors and their receptors are important in the survival and axonal growth of SPNs (Schober and Unsicker 2001).

1.4.2 Postganglionic Neurons in the Sympathetic Nervous System

Postganglionic sympathetic neurons (sympathetic neurons) are the last step in the delivery of regulatory responses from the CNS to a multitude of tissues spread over the entire body. Sympathetic neurons receive information from preganglionic neurons and convey this to target organs by direct innervation (Gilbey and Michael Spyer 1993).

Postganglionic neurons are derived from NCCs during development. A subset of NCCs take a medial ventral path from the dorsal end of the neural tube during their migration. These cells end their migration clustered near the dorsal aorta to form the sympathetic primordia, primitive sympathetic neurons, at mouse embryonic day 10.5 (E10.5) (Kameda 2014). These sympathetic primordia undergo specification and begin to gain their first sympathetic characteristics (Kameda 2014). The progenitor cells coalesce segmentally; extending bilaterally as two uniform paravertebral chains on both sides of the dorsal aorta. They lie lateral to the vertebral column to form a *one ganglion per segment* structure at all cervical levels (Furness 2015). SCGs are an exception to the one ganglion per segment rule of the sympathetic chain, as the sympathetic primordia colonise several segments (between cervical levels 1 and 3) for the organisation of SCGs at E13.5 (Kameda 2014). While some of the primordial cells rostrally migrate from the dorsal aorta to establish SCGs, some of them ventrally migrate to give rise to prevertebral ganglia (PVGs) which are located close to the ventral branches of the carotid artery (Furness 2015).

Postganglionic axonal elongations of sympathetic nerves leave SCGs, and establish communication branches with the vagus and glossopharyngeal nerves to innervate mainly head muscles, neck muscles, and the salivary gland (Wehrwein et al. 2016; Mitsuoka et al. 2017). Neuronal extensions from SCGs also provide postganglionic fibres to the lacrimal gland (Wehrwein et al. 2016). Similarly, PVGs receive connections from preganglionic neurons, then set out their postganglionic elongations to innervate visceral organs in the abdomen and pelvis, such as the stomach, kidney, liver, spleen, and pancreas (Miolan and Niel 1996; Wehrwein et al. 2016).

1.4.3 Sympathetic Ganglia Anatomy

SCGs have a white and fusiform appearance, shaped like a spindle (Hedger and Webber 1976; Ladd et al. 2014). The SCG begins at the cranial base and reaches approximately to the level of the fourth cervical vertebra, running parallel to the internal carotid artery (Hedger and Webber 1976; Barral and Croibier 2009). SCGs are located dorsal to the bifurcation of the common carotid artery, and their caudo-dorsal sides are adjacent to the distal ganglia of the vagus nerve (Ladd et al. 2014). The rostro-dorsal sides of the SCGs point toward to the jugular foramen. The size of SCGs from the adult rat is around 3.3 mm in length, 0.9 mm in width and 0.6 mm in thickness (Ladd et al. 2014). At the neuronal level, SCG neurons are generally circular in shape and easy to recognise due to their relatively larger size (Ladd et al. 2014).

The prevertebral ganglia in mammals are located near the abdominal aorta, and its main branches constitute the abdominal plexus, a large group of ganglia and nerve trunks. The paired CG and the SMG are located caudo-lateral to the roof of the coeliac artery. While the CG has two lobes connected to each other by short commissures, the SMG is a single ganglion connected to the CG by short nerve trunks. Extensively vascularised prevertebral ganglia are encapsulated by connective tissues and they receive their preganglionic innervations from thoracic splanchnic nerves which are descending branches from the thoracic sympathetic ganglia (Furness 2015).

To briefly summarise the developmental stages described thus far: neural precursors of crest cells migrate from the neural tube and specify to form sympathetic pre- and postganglionic neurons. While preganglionic neurons receive synaptic information though their dendrites from the CNS, they at the same time reach out for postganglionic pre- and paravertebral sympathetic neurons to establish synaptic connections. After this, postganglionic neurons are responsible for transmitting the information to the corresponding final destinations throughout the body. In the rest of the introduction section, I will describe the last two stages of sympathetic nervous system development. In the next section, I will focus on why some sympathetic neurons are able to survive

until their axons reach target organs, while a large proportion of the sympathetic neurons fail during this process. Then, I will describe how sympathetic neurons determine and find the correct pathways during axon elongation, and the factors affecting this process during sympathetic development.

1.5 Sympathetic Neuron Survival & The Neurotrophic Theory

During the development of the peripheral nervous system, cell death is inevitable and essential. Immature neuron death via programmed cell signalling, apoptosis, is a fundamental characteristic of the developing nervous system. Apoptosis ensures the removal of many immature neurons to generate an effective and efficient neuronal circuitry for a well-functioning nervous system (Davies 2003).

The neurotrophic theory, a well-established and elegant concept in the field of neuronal development, highlights the importance of programmed cell death for the developing sympathetic nervous system. It is based on the central principle that developing peripheral neurons undergo programmed cell death if they cannot access sufficient amounts of the appropriate neurotrophic factor. These factors are secreted in limited quantities from target fields, and neurons compete for limited supplies of these factors for their survival (Oppenheim 1989; Davies 2003). This theory explains how, after the proliferation and differentiation of embryonic stem cells generates about twice as many neurons as needed, the surplus undergo cell death immediately after synaptic contacts are established between sympathetic neurons and their innervation targets (Oppenheim 1989; Davies 2003).

The origin of the neurotrophic theory goes back to the 1950s, to the pioneering studies of Rita Levi-Montalcini, Viktor Hamburger and Stanley Cohen on NGF, the founding member of the neurotrophin family (Levi-Montalcini and Angeletti 1968; Thoenen and Barde 1980; Levi-Montalcini 1987). Their early investigations demonstrated that administration of NGF antiserum to sympathetic and certain sensory neuron subpopulations resulted in their

failure to survive *in vitro*, and to undergo normal peripheral neuron development *in vivo* (Levi-Montalcini and Angeletti 1968; Levi-Montalcini 1987).

The influence of target organs on developing peripheral neurons was identified in studies where a complete or partial ablation of targets resulted in a decrease in the survival of innervating neurons (Oppenheim 1985). By contrast, approaches to increase size or availability of targets succeeded in reducing naturally occurring cell death significantly in innervating neurons (Oppenheim 1985). In concert with experiments demonstrating the localisation of NGF to target tissue, and its significant role in neuronal survival (Thoenen and Barde 1980), these experiments clearly demonstrated that, at least in part, naturally occurring cell death is controlled by NGF.

The fundamental principles of the neurotrophic theory were mainly built up by studies with NGF. However, with the discovery of other neurotrophic factors – BDNF (Barde et al. 1982), NT-3 (Hohn et al. 1990) and NT-4 (Hallböök et al. 1991) – the theory further developed. The discovery of these other members challenged the original framework of the neurotrophic theory. Initial theories postulated that populations of neurons compete for only a single neurotrophic factor; later studies have instead identified that the survival of each subtype of peripheral neuron can be promoted synergistically by more than one single neurotrophic factor (Davies 1996). Several studies revealed that while this cooperation between neurotrophins can act during the same time period for some sensory neurons (e.g. in proprioceptive neurons from the trigeminal mesencephalic nucleus (Davies 1986; Davies et al. 1986)), sequential dependence on different neurotrophins can also be seen throughout development (e.g. in mouse trigeminal neurons) (Buchman and Davies 1993).

Several studies have proposed ideas contradictory to the main tenets of the theory. First, the neurotrophic hypothesis originally described neurons competing for limited quantities of survival factors during the restricted window of naturally occurring cell death. However, *in vitro* studies showed that mouse trigeminal neurons become dependent on BDNF and NT-3 for their

survival before this stage, and finally become responsive to NGF at the time of naturally occurring cell death. This BDNF and NT-3 release indicates that sufficient amount of neurotrophic factor synthesis takes place to promote survival of early trigeminal neurons earlier than naturally occurring cell death (Lumsden and Davies 1983; Buchman and Davies 1993). Second, the original theory suggested that neurotrophic factors are only produced in their target fields, and are retrogradely transported to the corresponding developing neurons. However, a number of studies on several populations of developing neurons have reported that afferents, axonal projections that arrive at target organs, also influence the survival of the neurons by using the anterograde route to transport neurotrophins. For example, removal of the dorsal root of the chick (reducing afferent influence) increases neuronal cell death at the period of naturally occurring cell death. On the other hand, enlarged afferent supply increases neuronal survival as seen in the nucleus of the optic tract (Linden 1994). Third, autocrine trophic support has been shown as an alternative route to retrograde transport of the neurotrophic factors. For example, sensory DRG neurons from chick embryos cultured in neurotrophin-free medium can undergo BDNF-required maturational changes while their axons grow out to their target organs. This suggests that early DRG neurons respond to BDNF by an autocrine signalling mechanism in the course of axonal growth (Wright et al. 1992).

The pioneering discovery of the prototypical neurotrophic factor NGF, and subsequent advances in the understanding of neurotrophic factors, has resulted in the recent iteration of the neurotrophic theory. The neurotrophic theory provides the most plausible explanation as to why only a proportion of developing neurons can survive during nervous system development.

1.5.1 Programmed Cell Death

Energy-dependent apoptosis, characterised by distinct morphological and biochemical changes, is tightly controlled by a wide range of transmembrane and intracellular molecules, and is in the end, executed by a specific protease

family, caspases (Pfisterer and Khodosevich 2017). Apoptotic events are classified into two main categories, as either extrinsic or intrinsic apoptosis, depending on whether the initial signal is mediated by a receptor protein (Fig. 1.6) (Elmore 2007).

The intrinsic, mitochondrial, pathway is activated by various exogenous and endogenous stimuli, growth factors, cytokines, DNA damage, hypoxia, infection, and other cell stress factors (Elmore 2007). These stressors cause alterations in the mitochondrial membrane that result in an increase in the permeability of the mitochondrial outer membrane. The structural changes in the membrane lead to a loss of the mitochondrial transmembrane potential and release of proteins from the intermembrane space of mitochondria into the cytosol (Fig. 1.6) (Elmore 2007).

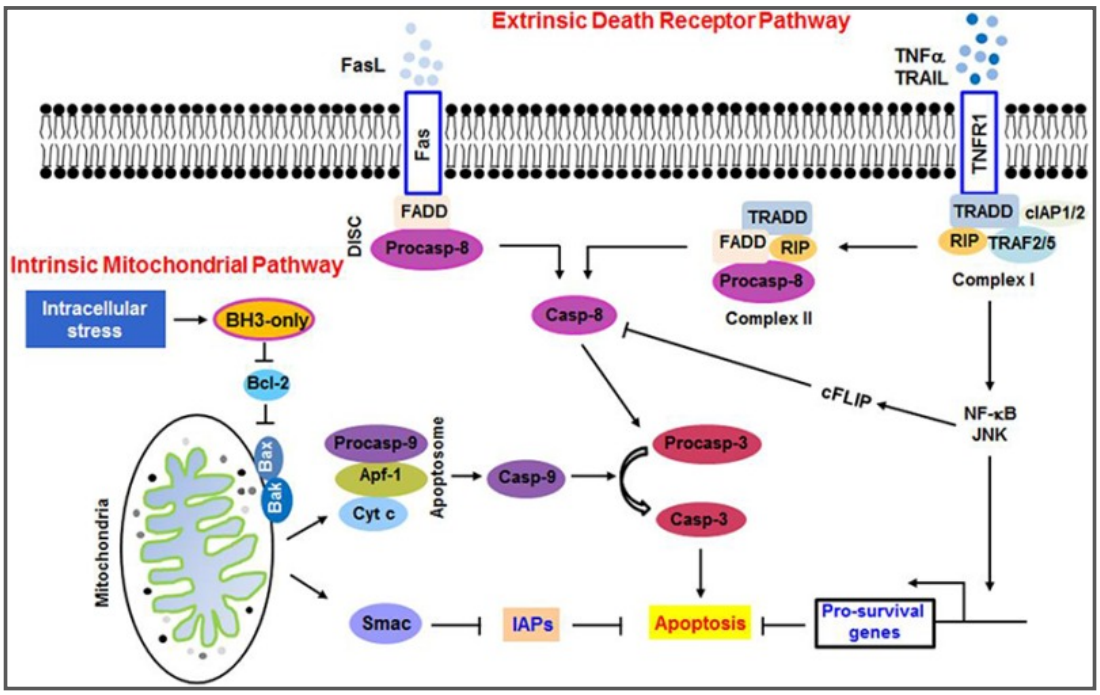

Figure 1.6. Intrinsic and Extrinsic Cell Death Pathways. Both intracellular and extracellular stimuli can trigger cell death pathways. In the extrinsic pathway, activation of death receptors by extracellular ligands such as Fas and TNF-α triggers recruitment of FADD and TRADD proteins. This, in turn, leads to downstream activation of caspase-8 and-3, leading to cell apoptosis. The intrinsic cell death pathway is activated by intracellular stressors, e.g. oxidative stress. Activation of mitochondrial-associated effector proteins leads to release of cytochrome c from the mitochondria, activation of caspase-9 and -3 sequentially, and subsequent cell death. Figure from (Zhou and Li 2015).

B-cell lymphoma 2 (Bcl-2) family members and other closely homologous proteins are some of the most essential components of the intrinsic apoptotic pathway. Bcl-2 family member protein Bcl-2 plays a prominent role in inhibiting the release of pro-apoptotic proteins into the cytosol, such as cytochrome c, second mitochondria-derived activator of caspase/direct inhibitor of apoptosis-binding protein with low pI (Smac/DIABLO) and Omi/HtrA2 (Cory and Adams 2002). In mammals, at least 20 proteins have been discovered which share the same Bcl-2 homology (BH) domain. Among them, pro-apoptosis proteins Bcl-2 associated X-protein (Bax) and Bcl-2-related ovarian killer protein (Bok) (Bax family members), and Bcl-2-like protein 11 (Bim), Bcl-2-interacting killer (Bik), Bcl-2 associated agonist of cell death (Bad), Noxa and p53 upregulated modulator of apoptosis (Puma) (BH3-only family members), contribute to the permeabilisation of the mitochondrial membrane after cytotoxic signals. On the other hand, Bcl-x_L, Bcl-w, A1, and Mcl1 proteins are some of the pro-survival members of the Bcl-2 family, which promote cell survival (Cory and Adams 2002).

In a healthy cell, Bcl-2 and its pro-survival homologues maintain the integrity of the mitochondrial outer membrane by sequestrating Bax and Bok proteins. However, when apoptotic stimuli occur, BH-3-only protein members in a 'sensitiser' role (e.g., Bad, Noxa, and Bik) bind to Bcl-2; other BH-3-only proteins in an 'activator' role (e.g., Bim, Bid, or Puma) bind to Bax proteins (released from Bcl-2 interaction) (Nechushtan et al. 2001; Kim et al. 2006) to induce oligomerisation of these proteins, which results in the loss of mitochondrial membrane integrity (Green and Reed 1998; Gross et al. 1999). Formation of the homo-oligomers is an essential part of the intrinsic pathway as they provide the conduit for the exit of apoptogenic proteins from the mitochondria through channel formation (Nechushtan et al. 2001; Cory and Adams 2002).

One of the biochemical hallmarks of intrinsic apoptosis is the release of cytochrome-c and other caspase-activating factors from the mitochondrial transmembrane into the cytosol (Saraste 2000). Released cytochrome-c

immediately associates with apoptotic protease-activating factor-1 (Apaf-1), which in turn results in activation of procaspase-9 to form an apaptosome multiprotein complex, and consequently activation of caspase-3 as the last executioner before cell death (Srinivasula et al. 1998; Elmore 2007). In addition to cytochrome-c, pro-apoptotic proteins such as Smac/DIABLO and Omi/HtrA2 are released from mitochondria and act in apoptosis by antagonising the inhibitory apoptosis proteins (IAPs) (Elmore 2007). Furthermore, the flavoprotein apoptosis-inducing factor (AIF) (Joza et al. 2001), endonuclease G (Li et al. 2001), and caspase-activated DNase (CAD) (Enari et al. 1998) are also released from mitochondria to translocate into the nucleus; these are considered to be part of the chromatic condensation and DNA fragmentation process of apoptosis (Elmore 2007).

The extrinsic pathway is mediated by transmembrane death receptors that transduce external signals carried by ligands into apoptotic cell fate decisions. Death receptors belong to a subset of the tumour necrosis factor (TNF) receptor superfamily (TNFRSF), which share cysteine-rich repeats in their extracellular domain and contain a cytoplasmic sequence called the death domain (Ashkenazi 1998). FasL/FasR, TNF-α/TNFR1, TNF-like weak inducer of apoptosis (TWEAK)/death receptor (DR) 3, TNF-related apoptosis-inducing ligand (TRAIL)/DR4 and TRAIL/DR5 are some of the characterised ligand-death receptor pairs (Fig. 1.6) (Ashkenazi 1998).

Ligand binding triggers receptor trimerisation that leads to allosteric conformational activation of the receptors (Ashkenazi 1998). Reorganisation of the receptors allows the formation of the death-inducing signalling complex (DISC), which serves as a docking site for intracellular mediator molecules (Krammer 2000).

FasL/FasR and TNF-α/TNFR1 are two of the most well-characterised ligand/receptor pairs in terms of the machinery of the extrinsic apoptosis pathway (Ashkenazi 1998). In the FasL/FasR complex, the Fas DISC promotes the binding of three Fas-associated death domain (FADD) proteins into the complex via their own death domain. FADD also has a so-called death-effector

domain (DED) which facilitates association of the DED-containing procaspase-8, also known as FLICE, into the DISC (Ashkenazi 1998; Wajant 2002). Here, dimerised procaspase-8 is proteolytically activated and released from DISC into the cytoplasm as active caspase-8, activating various downstream proteins such as procaspase-3, which drives the completion of the cell death programme (Wajant 2002). Although the general mechanisms of the Fas pathway closely resemble that of TNF-α/TNFR1-activated extrinsic apoptosis, there are a few differences in the recruitment of downstream mediator proteins. Similar to Fas signalling, the TNF-α/TNFR1 interaction induces clustering of the receptor, which forms a trimer in response to TNF-α binding; this results in clustering of the receptors' death domain. Subsequently, TNF-associated death domain (TRADD) is recruited into the receptor complex. Thereafter, FADD and receptor-interacting protein (RIP) couple to the TRADD for the activation of caspase-8 and downstream effector caspases which, in turn, activate caspase-3 to execute the cell's death sentence (Ashkenazi 1998).

1.5.2 Neurotrophic Factors

The neurotrophic factors, or neurotrophins, are a family of NGF-related growth factors. Although originally classified as survival factors for developing sensory and sympathetic neuron populations, they have been implicated in many other processes in the nervous system, such as axonal growth, guidance, and neuronal differentiation (Davies 2008).

The discovery of the remarkable role of NGF in the survival of peripheral neurons drove the search for other possible neurotrophic factors with similar effects in neuronal development. The first indication that other family members might exist was the survival and axonal elongation of dissociated sensory ganglia from the chick embryo promoted by a factor released from cultured glioma cells (Barde et al. 1978). Such observations led to the discovery and purification of the second neurotrophin, BDNF, from pig brain (Barde et al. 1982). Molecular cloning of BDNF revealed the full primary molecular structure of the protein with its amino acid sequence. Sequence comparisons of NGF and

BDNF revealed high structural homology between the two factors and further experiments demonstrated that these proteins also shared similarities in function (Leibrock et al. 1989). Identification of the third member of the neurotrophin family, NT-3, took advantage of the sequence similarities between NGF and BDNF, as NT-3 also showed striking sequence homology to the previously discovered neurotrophins, including catalytically active cysteine residues (Hohn et al. 1990; Kaisho et al. 1990; Maisonpierre et al. 1990; Rosenthal et al. 1990). Like NGF and BDNF, NT-3 also promoted the development of peripheral neurons (Maisonpierre et al. 1990; Wyatt et al. 1997; Francis et al. 1999). Finally, the last member of the neurotrophin family, NT-4, was isolated from both human and rat cells. Despite its evolutionarily less conserved genomic structure compared to the other family members, NT-4 displayed similar bioactivity and, later, receptor specificity (Ip et al. 1992). The similar functions and structures of these four proteins strongly suggested that they were members of the same neurotrophin family (Hohn et al. 1990).

Mature neurotrophins are initially synthesised as long precursors, called proneurotrophins, with molecular weights of 30-35 kDa. Proneurotrophins are cleaved by a wide spectrum of enzymes, including proprotein convertases, matrix metalloprotease 7, and plasmin, to form mature neurotrophins. For a long time, proneurotrophins were thought of as functionally inactive precursors (Lee 2001). However, later studies suggested this was not the case. In contrast to the cell survival role of mature neurotrophins, proneurotrophins mostly promote cell apoptosis. The dual roles of neurotrophins in a given cell population, mediated by two different forms of the protein, provide a diverse and complex regulatory system for controlling cell responses (Lee 2001).

Structurally, mature neurotrophins consist of two non-covalently associated peptide chains, each 12-13 kDa. The homodimer structure of the neurotrophins forms a twisted four-stranded β-sheet which elongates and stabilises the catalytically active site containing three intertwined sulphide bonds. This highly stable tertiary structure is known as a cysteine knot (Butte et al. 1998). Even though there are some notable structural differences between

the neurotrophins, such as surface loops that are highly important for receptor binding, they all share the same specific dimer formation. The dimerisation provides an extensive hydrophobic surface and sites for nonpolar contacts, which stabilises the core of the structure and enables the neurotrophins to bind their receptors to initiate downstream signalling (Butte et al. 1998; Butte 2001).

1.5.3 Neurotrophic Receptors

The four mammalian neurotrophins signal through two major receptor classes: Trk and so-called low-affinity neurotrophin receptor (75kDa Neurotrophin receptor, $p75^{NTR}$). Although the neurotrophins are homologous in amino acid sequence and share similar biochemical roles, they are selective in their interactions with Trk receptors. Three different tyrosine kinase receptors – TrkA, TrkB, and TrkC – preferentially bind to NGF, BDNF and NT-4, and NT-3, respectively (Huang and Reichardt 2003). NT-3, as the only exception, can also interact with one alternatively spliced isoform of TrkA, although this is with a lower binding efficacy than NGF (Clary and Reichardt 1994; Huang and Reichardt 2003). Neurotrophic receptors are expressed by sympathetic neurons, as well as other neuron types in the PNS, and are detectable from early ages; their expression is tightly controlled throughout the development of sympathetic neurons. Although initially the known functions of neurotrophin receptors were restricted to their critical role in classical target-derived survival, a subsequent plethora of studies have uncovered their much broader role throughout the development of the PNS.

1.5.3.1 Trk Receptors

Trk receptors are single pass transmembrane receptors. The extracellular domain consists of a cysteine-rich domain followed by three heavily glycosylated leucine-rich repeats, then another cysteine-rich domain and Ig-like domains proximal to the transmembrane region (Fig. 1.7) (Huang and Reichardt 2003). The Trk receptors bind to their cognate ligands using the second Ig domain. The intracellular tyrosine kinase domain, with several

tyrosine residues, mediates signalling by creating docking sites for effector proteins and enzymes. Ligand binding to full-length Trk results in receptor dimerisation, and subsequent receptor activation through transphosphorylation of the kinase domains (Huang and Reichardt 2003).

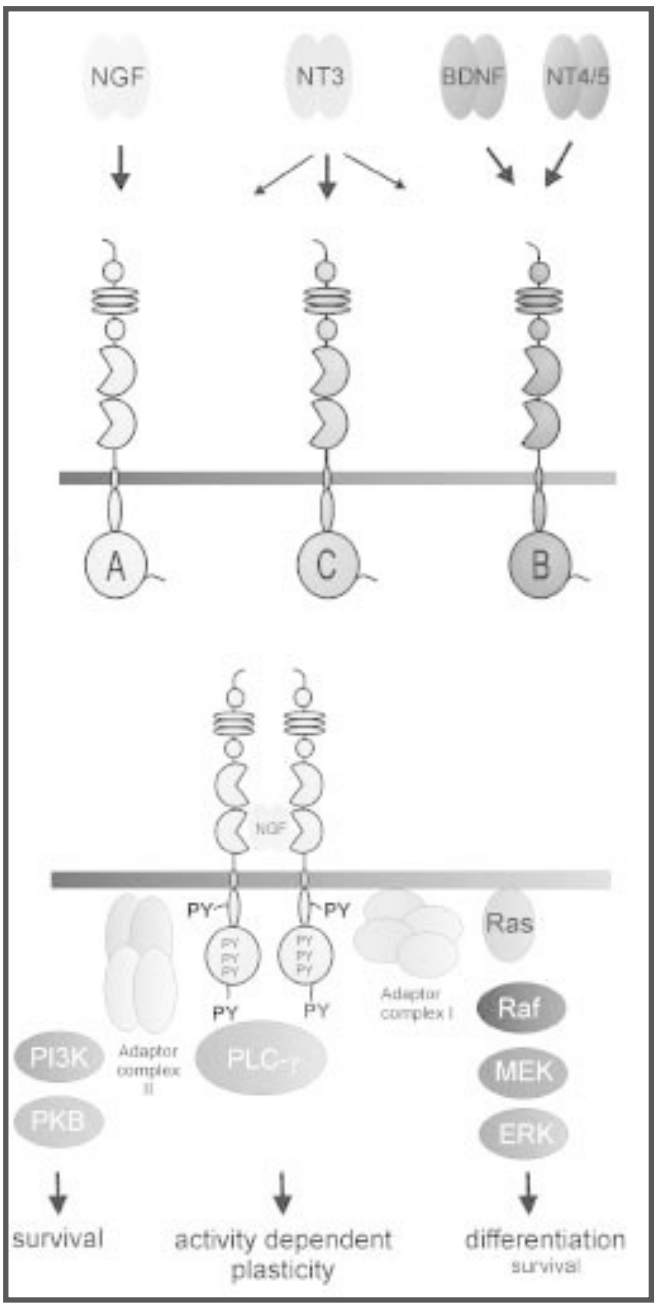

Figure 1.7. Neurotrophins and Their Trk Receptors. Neurotrophins bind their cognate transmembrane Trk receptors with high affinity. **(A)** Receptors have several homologous domains in the extracellular region, these include cysteine clusters (circles) sandwiching leucine-rich regions (ovals), and Ig-like C2 domains (circular sectors). **(B)** Binding of neurotrophins leads to auto-phosphorylation of Trk receptors on intracellular sites, and leads to activation of several downstream signalling cascades, e.g. PI3K, PLC-γ, and ERK1/2. Figure from (Dechant and Neumann 2013).

Alternative splicing of Trk mRNA creates Trk isoforms with varying extracellular domains, which may positively affect the binding affinity of the secondary neurotrophins while showing no effect on the specificity of primary neurotrophins (Clary and Reichardt 1994; Huang and Reichardt 2003). In addition, splicing variants can bring about deletion of large sites in the cytoplasmic domain, including the catalytic tyrosine kinase domain, creating truncated Trk receptors. The truncated Trks are dominant negative receptors that inhibit activity of the full-length receptors by sequestering neurotrophins. They can also stimulate intracellular signalling cascades as an active signalling molecule (Fenner 2012).

Mature neurotrophin binding initiates signalling by triggering Trk phosphorylation at specific tyrosine residues. Each Trk receptor undergoes neurotrophin-activated dimerisation that leads to trans-autophosphorylation of each receptor at tyrosine sites, such as Y490 and Y785 (Deinhardt and Chao 2014). These phosphorylated residues serve as docking sites for the recruitment of adaptor proteins to convey neurotrophin-initiated downstream signalling. In this process, Ras, extracellular signal regulated kinase (ERK), phospholipase C (PLC)-γ and phosphatidylinositol-3-kinase (PI3K)-Akt are the major cell signalling pathways activated by Trk receptors (Deinhardt and Chao 2014).

1.5.3.2 $p75^{NTR}$ Receptor

The other receptor that neurotrophins interact with is the 75 kDa neurotrophin receptor $p75^{NTR}$. This receptor was initially labelled as a 'low affinity receptor' for NGF on sensory and sympathetic neurons. However, further studies showed that $p75^{NTR}$ actually has high binding affinity to proneurotrophins, similar to the ligand-cognate receptor interactions seen with the mature neurotrophins (Vilar 2017). $p75^{NTR}$ is also a non-selective receptor for mature neurotrophins, with a low binding affinity seen across the family. Activation of $p75^{NTR}$ by proneurotrophin binding controls apoptotic responses, in contrast to the cell survival effects of mature neurotrophin/$p75^{NTR}$ signalling.

For example, binding of $p75^{NTR}$ to mature NGF promotes cell survival and axon growth in sympathetic neurons; conversely, proNGF binding brings about cell death (Deinhardt and Chao 2010), and axon degeneration (Meeker and Williams 2015). Similarly, proBDNF mediates cell apoptosis in sympathetic neurons through $p75^{NTR}$, even though sympathetic neurons lack the BDNF cognate receptor, TrkB (Teng et al. 2005). The complex interactions between pro- and mature neurotrophins, and $p75^{NTR}$ and Trk receptors provide a powerful control mechanism by which to regulate the survival of cell populations.

$p75^{NTR}$ is a transmembrane glycoprotein and a member of the TNF receptor superfamily. It contains a death domain in its intracellular region, as also seen in TNFR1 and FasR (Meeker and Williams 2015). In the cytosol, $p75^{NTR}$ interacts with proteins, including TNF-receptor-associated factors (TRAF) 2 and 6, RIP2, melanoma-associated antigen homologue (NRAGE), neurotrophin-associated cell death executor (NADE) and melanoma-associated antigen (MAGE-G1) (Deinhardt and Chao 2010). These interactions lead to activation of the nuclear factor (NF)-κB pathway for cell survival or the Jun NH_2 terminal kinase (JNK) pathway for apoptosis (Deinhardt and Chao 2010). In the extracellular domain, $p75^{NTR}$ has four cysteine-rich domains through which $p75^{NTR}$ interacts with neurotrophins (Meeker and Williams 2015). $p75^{NTR}$ is also able to utilise signalling mechanisms similar to the Notch pathway. In this process, metalloproteases cleave the $p75^{NTR}$ extracellular domain close to the membrane, followed by another cleavage at the intracellular site by γ-secretase, to initiate signalling events in the nucleus (Vilar 2017).

1.5.4 Superior Cervical Ganglion Survival

Neurotrophins and their receptors play a significant role in the survival of sympathetic neurons. To date, the vast majority of the evidence for the role of neurotrophins and their receptors in promoting and regulating the survival of sympathetic neurons during development has come from the numerous *in vitro* and *in vivo* studies of SCG neurons. SCG neurons can be dissected

beginning at E11.5; at this stage however, these neurons are accepted as precursor cells, called neuroblasts, immature forms of sympathetic neurons (Rohrer 1990). E13 is the stage at which mRNA expression of $p75^{NTR}$ and TrkA receptors can first be detected in SCG neurons, although at low levels. Robust TrkA expression is observed at E15 and increases markedly throughout gestational development. Similarly, SCG sensitivity to NGF increases with age. The number of neurons in the SCG increases from E13 and reaches the highest level at E18 (Wyatt and Davies 1995). SCG neurons from TrkA-deficient mice show markedly increased numbers of dying cells from E15 to E18 compared to wild-type counterparts (Fagan et al. 1996). Strikingly, deletion of the TrkA receptor produces severe neuropathies in the postnatal period and is mostly lethal within one month. This lethality is due to extensive neuronal loss in sympathetic, as well as sensory, ganglia and the loss of some neurons from the central nervous system, including from the hippocampus and cortex (Smeyne et al. 1994). In accordance with this role of the TrkA receptor, deletion of the *Ngf* gene produces profound SCG neuron loss during naturally occurring cell death and the virtual absence of SCG neurons at the beginning of the postnatal period (Crowley et al. 1994). These results suggest that disruption of NGF/TrkA signalling cannot be compensated for by other neurotrophins (Fagan et al. 1996) or by other molecular activities, and maintenance of the development of SCG neurons is lost.

In addition to NGF/TrkA signalling, some other neurotrophic factors, growth factors, and ligand/receptor interactions acquire the ability to support SCG survival throughout development. First, NT-3-deficient mouse embryos have demonstrated the requirement for NT-3 in SCG survival. SCG neurons start responding to NT-3 at E18 and become dependent on NT-3 during the postnatal period (Wyatt et al. 1997). However, the exact signalling mechanism (including NGF, NT-3, the TrkA receptor, and $p75^{NTR}$ as components) that coordinates SCG cell survival remains elusive (Kuruvilla et al. 2004). Second, hepatocyte growth factor (HGF) and its receptor Met have been shown to promote the survival and differentiation of cultured sympathetic neuroblasts, but not sympathetic

neurons, by autocrine or local paracrine signalling (Maina et al. 1998; Maina and Klein 1999). Third, glial cell-line derived neurotrophic factor (GDNF) family member artemin and its receptors, the Ret/GFRα3 complex, have direct effects on neuronal survival (Honma et al. 2002). Lastly, postnatally, the influence of cholinergic differentiation factor/leukaemia inhibitory factor (LIF) and CNTF on the survival of SCG neurons has been shown in the presence of NGF at P5 (Kotzbauer et al. 1994).

1.6 Neuronal Outgrowth in the Peripheral Nervous System

Aside from their classic role in neuronal cell survival, neurotrophins and their receptors are also critically important to neuronal process outgrowth. The formation of neuronal connections begins during embryonic development, in which axons extend over long distances and integrate many environmental cues within a constantly changing environment to reach their final destinations. A failure to generate appropriate connections, or conserve established connections, can cause misdirection of neuronal signals, or worse, instigate partial or complete loss of neuronal systems. The essential cellular construct responsible for axonal elongation and pathfinding is a highly specialised and dynamic structure at the tip of the axon, the growth cone, first identified by the pioneering neurobiologist Ramón y Cajal after his examination of histochemical sections (Kandel et al. 2014).

1.6.1 Axon Growth and Guidance

The growth cone has three main compartments based on its cytoskeletal make-up (Lowery and Van Vactor 2009). While the core domain is rich in microtubules and organelles, the peripheral domain is dominated by actin filaments. Arrays of uniformly polarised and bundled F-actin filaments at the leading edge of the growth cone have long finger-like dynamic extensions called filopodia that sense environmental cues *en route*. Between the filopodia, motile and less polarised lamellipodia-like filament structures are also formed by F-actin filaments, the third main compartment of the growth cone (Lowery and

Van Vactor 2009). The constant exploratory behaviour of the cone relies on the dynamic polymerisation, turnover, and protein organisation of F-actin filaments.

Neuronal guidance cues are responsible for directing the precise extension, connectivity, and target innervation of the neurites from the 80 billion neurons in the human body. The role of these extrinsic cues is to provide spatial information to extending neurites during the development of neuronal wiring. These cues are also capable of adhering axons together to produce axon bundles, i.e., fasciculation (Kolodkin and Tessier-Lavigne 2011).

The four major protein families of guidance cues include netrins, slits, semaphorins, and ephrins (Stoeckli 2018). Directional changes in the growth cone occur when filipodia encounter these environmental signals. These signals can be in the form of substrate-bound cues such as extracellular matrix proteins (including laminin, fibronectin, and thrombospondins), cell surface adhesion molecules of the immunoglobulin or cadherin superfamily, anti-adhesive surface-bound molecules (e.g. slits, ephrins), diffusible chemotrophic cues (e.g. netrins, semaphorins), morphogens, growth factors (e.g. Wnt, Shh, BMPs, BDNF), neurotransmitters, and transcription factors (Fig. 1.8) (Kolodkin and Tessier-Lavigne 2011).

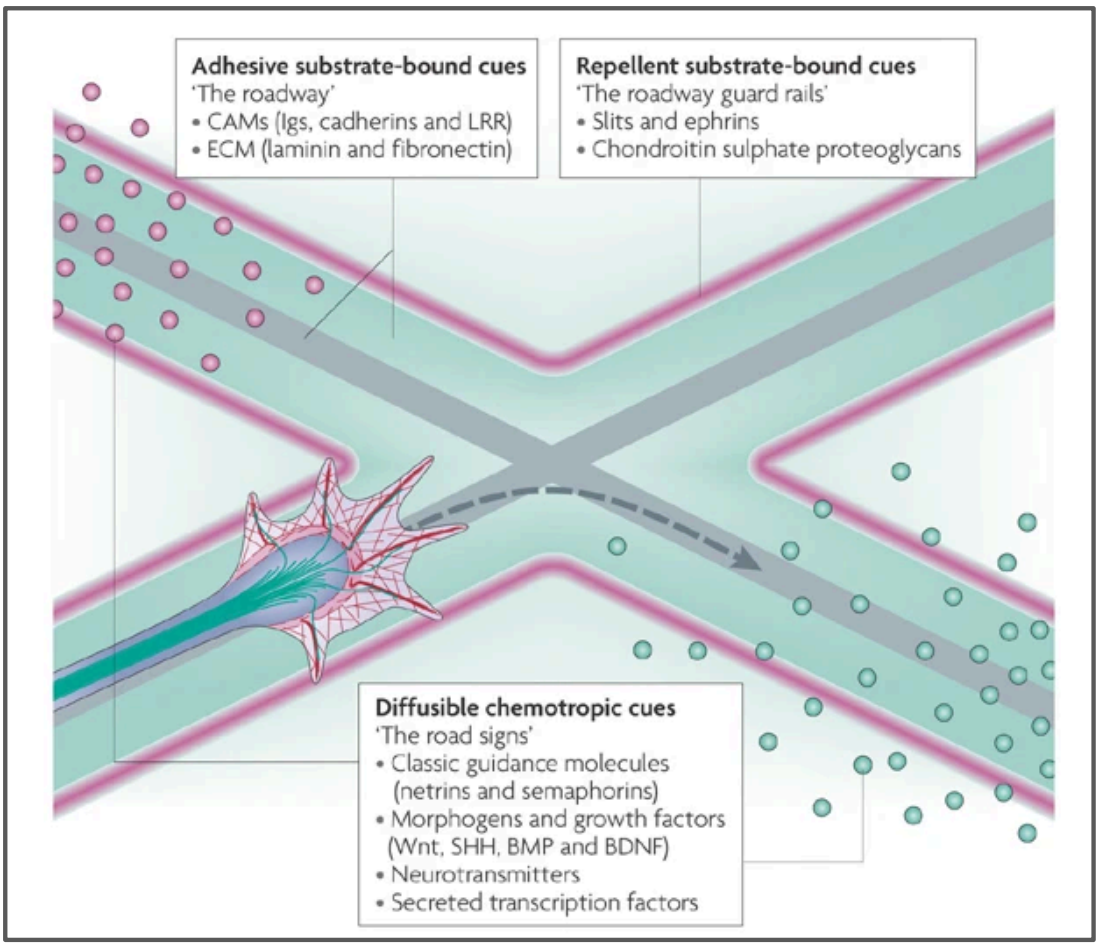

Figure 1.8. The Growth Cone Navigates with the Help of Chemoattractants and Chemorepellents. Chemotropic cues can direct growth cone movement in several ways. These cues exist as diffusible factors and substrate-bound factors. Figure from (Lowery and Van Vactor 2009).

Cytoskeletal elements provide the motor function to steer the growth cone forward, backwards and sideways. Actin-myosin sliding and continuous depolymerisation and polymerisation of actin molecules at the peripheral domain of the growth cone provide the necessary engine power for the movement of the membrane along the substrate (Dickson 2002). Pathfinding does not only consist of the motor function but also requires a translational system, a sensory function, to convert and integrate environmental cues into local signals to control the dynamics of the cytoskeletal machinery. The binding of cue ligands to their receptors on filipodia initiate signal transduction cascades which determine the organisation of the cytoskeleton and consequently the organisational changes deciding the direction of the growth cone (Dickson 2002).

Although many secondary messengers exist in this process, the most studied include calcium ions, kinases, and phosphatases (Rho-family GTPases). These molecules underlie the conversion of ligand-receptor binding into mechanical instructions that orient the growth cone (Huber et al. 2003; Bashaw and Klein 2010).

Neurotrophins can also function as molecular cues in the navigation of growing neurites in the developing nervous system, playing a significant role in the formation of appropriate neuronal circuits in target fields. The next section will provide an overview of the actions of neurotrophins and other significant guidance cues in the development of neuronal connections.

1.6.2 The Role of Neurotrophic Factors in Sympathetic Neuron Outgrowth

It is now known that neurotrophic factors act on axonal guidance and elongation during development. Studies have found that the neurotrophic factors can function both as attractant and repellent, depending on axon types. In addition, while the same axon type may respond specifically to different neurotrophin cues, the specificity of axons towards certain neurotrophic factors can change during development (Huber et al. 2003).

Early studies hypothesised that target field-secreted NGF forms a gradient to attract growing axons to their correct destination (Huber et al. 2003; Kolodkin and Tessier-Lavigne 2011). This proposal was apparently supported *in vitro* by results showing that following the application of high concentrations of NGF to chick dorsal root neurons that had already innervated their targets, growth cones made a 80° turn and started growing towards the source of NGF in the culture environment (Gundersen and Barrett 1980). Neurotrophin addition to cultures can be spatially controlled by the use of capillaries when adding ligands. NGF, BDNF and NT-3 administration through such a capillary into NGF-, BDNF- and NT-3-dependent embryonic DRG cultures, respectively, results in a significant increase in F-actin content in the leading edge of growth cones, facilitating axonal growth towards the relevant cues. In contrast, treating NGF- or NT-3-dependent DRG neurons with BDNF or NT-4 causes a decrease in the total filopodia number in the growth cone, and subsequent retraction of neurite growth and reversion to lamellipodia (Paves and Saarma 1997). Another study with DRG neurons also demonstrated that NGF directly activates actin-dependent movement of axons towards NGF-coated polystyrene bead structures *in vitro*. Axonal growth cones of sensory neurons form filopodial sprouts at sites closest to the beads, which induce filopodial extension and microtubule rearrangements along the axonal shaft to advance towards NGF-coated beads (Gallo and Letourneau 1998). Moreover, in embryonic rat DRG neurons, growth cone turning assays found chemo attractive and repulsive properties of the neurotrophic factors in sensory neurons. While NGF enhanced axon growth of NGF- and BDNF-dependent DRG neurons, NT-3 acted as a chemoattractant to all except NT-4-dependent neuron cultures. On the other hand, BDNF and NT-4 inhibited axon growth in NGF and NT-3-dependent sensory neurons (Paves and Saarma 1997). However, the demonstration that NGF synthesis in the target field only begins after the earliest axons reach their targets demonstrates that NGF cannot be a long-range guidance molecule in normal development (Davies 1996). Taken together, these results raise the possibility that NGF may act as a short-range guidance molecule within the

target field after the axons of NGF-dependent neurons have reached and starting innervating their targets.

Neurotrophic factors can induce changes in the organisation and composition of cytoskeletal proteins to regulate axonal elongation in the developing PNS. The treatment of various neurotrophin-dependent cell cultures with the appropriate neurotrophic factors results in either a net loss of actin filaments and microtubules – causing growth cone collapse or retraction – or an increase in cytoskeletal elements in the growth cone – driving the growth cone towards the source of neurotrophins (Gillespie 2003).

Neurotrophins directly affect the growth of sensory and sympathetic axons in the PNS. Throughout studies into the function of neurotrophins, a core difficulty has always been to separate the axonal growth role of neurotrophins from their survival effect for embryonic neurons. To tease these two functions apart, a null mutant mouse model was generated in which the *Bax* gene, a pro-apoptotic Bcl-2 member, was deleted. This was used to study the function of NGF solely in axonal outgrowth during organ innervation, independent of its function in cell survival (White et al. 1998; Middleton and Davies 2001). Later, these *Bax*-deficient mice were crossed with *Ngf*-deficient mice to generate a *Ngf*$^{-/-}$*;Bax*$^{-/-}$ mouse model. In this model, naturally occurring death of SCG neurons during development was successfully prevented. The role of NGF in the innervation patterns of sympathetic target organs could be clearly mapped out with the mouse models, *Ngf*$^{-/-}$*;Bax*$^{-/-}$ and *TrkA*$^{-/-}$*;Bax*$^{-/-}$ (Glebova and Ginty 2005). Consistent with the conclusion that NGF does not play a role in long-range axon guidance, axons reached their targets in *Ngf*$^{-/-}$*;Bax*$^{-/-}$ and *TrkA*$^{-/-}$*;Bax*$^{-/-}$ mice, but failed, to varying extents, to branch and ramify within their targets. For example, while the innervation of salivary glands was completely ablated, there was a large reduction in the heart, a moderate reduction in the kidneys and no effect at all in the trachea (Glebova and Ginty 2005). These results highlighted the critical importance of NGF in the innervation of almost all sympathetic neuron targets, independently of its role as a cell survival factor.

There is also strong evidence that other extracellular signalling proteins can influence the growth of sympathetic axons during development, besides neurotrophic factors. Artemin plays a significant role as an axon growth-promoting molecule in sympathetic precursors (Davies 2009). Transgenic mice lacking artemin and its receptors Ret and GDNF family receptor alpha-3 (GFRα3) exhibit abnormal axon projection patterns from neuronal precursors during sympathetic axon development (Nishino et al. 1999; Enomoto et al. 2001; Honma et al. 2002). Endothelin family member endothelin-3 (Edn3) also acts as a chemoattractant molecule for sympathetic neuronal axons as they travel towards their final target organs (Davies 2009). In mice lacking *Edn3* and its receptor *EdnrA*, a complete lack of SCG axonal growth along the external carotid arteries was seen, and SCG neuronal axons were poorly developed compared to their wild-type counterparts (Makita et al. 2008).

The discovery of a novel role for the TNF superfamily and their receptors in promoting axonal elongation and target innervation ushered in a new era in research into the regulation of neuron development. The Davies group was one of the pioneers of this research field, providing strong evidence for the regulatory role of these extracellular signalling proteins in the development of the nervous system, and characterising the involvement of many TNF-receptor/ligand pairs in this process. As the main focus of this thesis is the role of this family in sympathetic neuron development, the next sections will discuss the TNF family in more detail.

1.7 TNF and TNFR Superfamilies

The TNF family was first described as a family of tumour regression factors, and was first identified in humans after bacterial infections (Aggarwal et al. 2012). Research into TNF began with the purification and characterisation of TNF, the first member of the family discovered. It was later established that the TNF family is not only essential to the regulation of the immune system, but that it also controls many different cellular signalling pathways including cell differentiation, gene activation, and apoptosis signals (Aggarwal 2003).

TNF initially showed great promise as an anti-cancer agent, although phase I clinical investigations found little potential for TNF in the suppression of cancer; this was mainly because intravenously-administered TNF resulted in groups of symptoms in different organ systems (Feinberg et al. 1988). However, later investigations that targeted matrix metalloproteases to reduce the toxicity of TNF (through the use of broad-spectrum matrix metalloprotease inhibitors) once again highlighted the potential therapeutic role of the TNFSF and TNFRSF members in the treatment of various diseases, such as lethal hepatitis and cancer types. Additionally, the TNFSF and TNFRSF function in the orchestration of the immune system through their pro-apoptotic family members, e.g. TNF, cluster of differentiation (CD) 95 ligand (CD95L), and TRAIL. TNF superfamily-induced apoptotic signals can regulate and eliminate hyperproliferated, cytotoxic, or virus-infected cells (Aggarwal et al. 1985; Chuntharapai et al. 2001; Ichikawa et al. 2001; Kelley et al. 2001; Wielockx et al. 2001).

1.7.1 TNFSF Ligands

To date, 19 different ligands have been identified as members of the TNFSF. Of these, 17 members are type II transmembrane glycoproteins, with intracellular N-termini and extracellular C-termini. Vascular endothelial growth inhibitor (VEGI) and lymphotoxin alpha (LT-α) are the only exceptions, and these lack a transmembrane domain (Fig. 1.9). These proteins are characterised by a conserved 'TNF homology domain' (THD) at the C-terminus, sharing 20-30% amino acid identity, which is responsible for receptor binding. All TNF ligands form non-covalently bound homo-trimers to interact with their receptors. Although TNF superfamily ligands are generated as membrane-bound proteins, they can also be proteolytically cleaved by distinct proteases to generate soluble extracellular factors. For example: metalloprotease TNF-converting enzyme (TACE, also known as 'a disintegrin and metalloprotease (ADAM) metallopeptidase domain 17 (ADAM17)) releases TNF (Adrain et al. 2012) and receptor activator of NF-κB (RANK) ligand (RANKL); matrilysin

cleaves FasL (Powell et al. 1999); and the furin family severs B-cell activating factor (BAFF), ectodysplasin A (EDA), TWEAK, and 'a proliferation-inducing ligand' (APRIL) (Schneider et al. 1999). Both membrane and soluble forms of these ligands act promiscuously, coupling with more than one receptor, to form a complex signalling network.

1.7.2 TNFSF Receptors

In humans, 29 receptors have been identified as members of the TNFRSF so far (Fig. 1.9). Of these receptors, 55 kDa TNF receptor 1 (TNFR1) and 75 kDa TNF receptor 2 (TNFR2) are the most well-characterised and studied members of the superfamily. The majority of the TNFRSF are type I transmembrane proteins, with extracellular N-termini and intracellular C-termini. As seen in TNF ligands, proteolytic cleavage can also generate soluble forms in some of the receptors, such as TNFR1, TNFR2, CD40, CD30, CD27, and Fas (Gruss and Dower 1995). Shedding of the TNF receptors into the extracellular space is highly important in the regulation of the inflammatory response by membrane-bound receptors. As soluble forms of these receptors are in competition for the cognate ligands, it is thought that inflammatory responses are diminished by soluble forms of the receptors (McDermott et al. 1999). TNF receptors are characterised by a 'cysteine-rich domain' (CRD) in the extracellular region. These domains are repeats of cysteine subdomains bridged with disulphide molecules, and the number of CRDs varies across receptor types. TNF receptors are mainly classified into two distinct groups based on the presence or absence of a conserved 68-80 amino acid sequence on their cytoplasmic side, named the death domain. The death domain is required for apoptotic signal transduction by TNF receptors and these receptors are often referred to as *death receptors* (Itoh and Nagata 1993); these include TNFR1, Fas, DR-3, and DR-6. Apoptosis is initiated by the interaction of death receptors with adaptor proteins, which occurs via the death domain present in both partners. This interaction forms a protein scaffolding complex, which initiates the recruitment of caspases.

Contrary to the death receptors, non-death receptors lack a death domain, and they instead recruit TRAF proteins for their downstream signalling pathways.

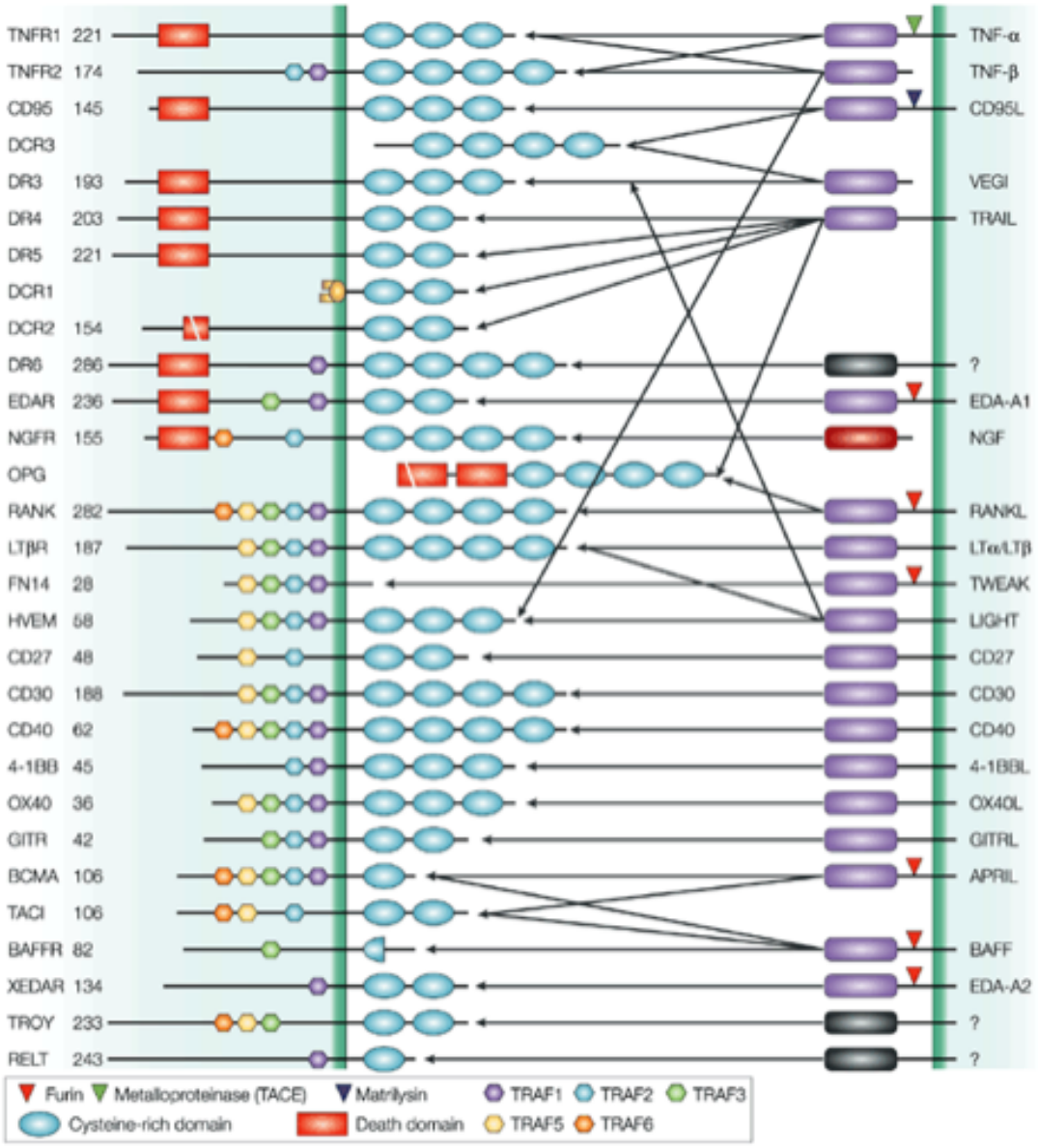

Figure 1.9. Ligand/Receptor Pairs of the TNF Superfamily.

The TNF receptor superfamily and their ligands. Several receptors have intracellular death domains and are known as death receptors. Except VEGI and LTα, ligands are produced as transmembrane ligands and cleaved into soluble factors by metalloproteases. Figure from (Aggarwal 2003).

1.7.3 TNF-α

TNF-α was the second member of the TNFSF discovered (after LT-α). It is involved in numerous cell signalling pathways mediating pro-inflammatory responses, cell survival, differentiation, and death signals (Aggarwal 2003). It is due to this diverse and complex signalling that there is a keen interest in understanding the mediator function of this protein, in the pursuit of treatments for many diseases, including cancer and autoimmune conditions (Aggarwal 2003).

TNF-α is a 27 kDa, 233 amino acid, type II transmembrane protein, expressed by a vast array of cell types, including macrophages, natural killer cells, T cells, B cells, endothelial cells, fibroblasts, dendritic cells, and microglia in the central nervous system (Parameswaran and Patial 2010). The activation of TNF-α gene transcription is linked to various stimuli such as: pathogens; mitogens; radiation; chemical stresses; calcium ionophores; and receptors such as pattern recognition receptors (Toll-like receptors) and many other antigen receptors, including Fc receptors (Falvo et al. 2010). Transmembrane TNF-α (mTNF-α) is a precursor for the soluble form of TNF-α (sTNF-α). After processing by TACE between an alanine[76] and valine[77] residue, 17 kDa, 157 amino acid sTNF-α forms a trimer and is released into blood plasma to circulate throughout the body and exert its biological function at distant sites. The remaining 10 kDa peptide at the cytoplasmic site migrates towards the nucleus in transport vesicles to influence the transcription of another cytokine, interleukin-1 beta (Domonkos et al. 2001).

1.7.4 TNF-α Receptors: TNFR1 and TNFR2

TNF-α owes its highly diverse signalling functions to the expression of TNF receptor proteins, either TNFR1 (*Tnfrsf1a*) and TNFR2 (*Tnfrsf1b*), on almost all nucleated cell types (Ye et al. 2018). Although TNFR1 and TNFR2 are completely different receptors in terms of their expression, structure, and induction of signalling pathways, they can share overlapping functions within cells, and receptor crosstalk exists (Grell et al. 1994; Bradley 2008). In their

extracellular domain, TNFR1 and TNFR2 share 28% homology, with 4 repeated cysteine-rich domains; conversely, their intracellular segments bear no homologous sequences and activate distinct pathways (Naismith and Sprang 1998; MacEwan 2002). A conserved extracellular domain in the receptors – the pre-ligand-binding assembly domain – is necessary for the assembly of the trimeric receptor complex independent from ligand binding (Chan et al. 2000). TNFR1 and TNFR2 can also be processed into soluble forms, sTNFR1 and sTNFR2, by TACE. Both soluble forms of these TNF receptors can interact with mTNF-α and sTNF-α (Leibrock et al. 1989; Solomon et al. 1999). Whereas the ubiquitously expressed TNFR1 (Grell et al. 1998) shows high affinity, rapid binding, and slow dissociation rates for sTNF-α, the TNFR2 expression profile is more restricted to certain cell types (Faustman and Davis 2010; Probert 2015) (immune, neuronal, and endothelial cells), and can only be fully activated by mTNF-α (Yang et al. 2018).

TNF-α binding induces the internalisation of its receptors. Internalisation is an important regulation mechanism by which the long-term activity of TNFR1 and TNFR2 can be strictly controlled (Higuchi and Aggarwal 1994). While internalisation of TNFR1 has been established to rely on specific cytoplasmic phosphorylation sites (Cottin et al. 1999), TNFR2 internalisation is dependent on a di-leucine motif (Fischer et al. 2011).

TNFR1 is a death receptor, as it contains an intracellular death domain (Tartaglia et al. 1993). Thus, TNF-α interaction with TNFR1 can trigger cell apoptosis and necrosis pathways via the recruitment of caspase proteins, under the coordination of TRADD and FADD, also known as complex II formation (Hsu et al. 1995; Fischer et al. 2011). However, this interaction can alternatively lead to the recruitment of a separate series of proteins to activate pro-inflammatory and cell survival pathways. Recruitment of proteins such as TRAF2 and 5, silencer of death domains (SODD) protein, cellular inhibitors of apoptosis protein (cIAP), and receptor-interacting serine/threonine protein kinase 1 (RIPK1) around the TRADD (in the absence of FADD), called a complex I formation, can activate pathways including the JNK, p38, ERK and NF-κB

pathways (MacEwan 2002; Grivennikov et al. 2006; Yang et al. 2018; Dostert et al. 2019).

On the other hand, TNFR2 does not have a death domain, making it a non-death receptor. Despite this, TNFR2 still recruits TRAF proteins, through which downstream signalling results in cellular apoptosis. There are essentially two main pathways for TNFR2-initated apoptosis, with each including some variants: 1) TNFR2 independently activates an apoptotic signalling pathway; 2) TNFR2 can cross-talk with TNFR1 and induce complex II formation. The latter depends on TNFR1 downstream proteins or cIAP pool exhaustion, due to overstimulation of TNFR2 under stress conditions. Although TNFR2 is able to activate apoptotic pathways, TNF-α relies largely on TNFR1 for the promotion of cell death, and on TNFR2 for contributions to cell survival, cell proliferation, and cell regeneration; this is primarily due to the different expression profiles of these two receptors (Domonkos et al. 2001; Krippner-Heidenreich et al. 2002; Faustman and Davis 2010; Yang et al. 2018; Wajant and Siegmund 2019).

1.7.5 CD40 Ligand and CD40 Receptor

The interaction of the CD40 ligand (CD40L) with its receptor CD40, and its downstream signalling, regulates antibody production, expression of surface molecules, cell survival, and cellular apoptosis as part of the adaptive immune response. The significant role of CD40L and its receptor in immune cell activation makes it of key interest in the context of immune-related diseases, and there is a search for corresponding therapeutic approaches centred around this signal transduction system (Banchereau et al. 1994; Fries et al. 1995; Henn et al. 1998; Schönbeck and Libby 2001; Aird 2007).

CD40L is a member of the TNFSF with a molecular mass of 32-33 kDa and a tertiary conformation similar to TNF. CD40L is both expressed on the cell surface as an integral membrane protein (where it forms a homotrimeric structure (van Kooten et al. 2000)), and is also cleaved to an 18 kDa soluble form, which carries similar functional roles to the membrane-bound form (Graf et al. 1995; Mazzei et al. 1995). CD40L is expressed transiently in immune cells, e.g. T

cells, B cells, platelets and other immune cells in response to inflammatory conditions (Karpusas et al. 1995; Carbone et al. 1997).

The receptor, CD40, is a member of the TNFRSF composed of a 305 amino acid sequence, with a molecular mass of 48 kDa. The identical biochemical structure formed by the extracellular cysteine residues in both the human and mouse protein suggests that CD40 folds into the same active tertiary structure in both species (van Kooten et al. 2000). CD40 was initially found to be constitutively expressed on B cells; however, it is also expressed much more broadly, such as in dendritic cells, monocytes, platelets, and macrophages, as well as on fibroblasts, epithelial cells, and endothelial cells (Banchereau et al. 1995; van Kooten and Banchereau 1997).

The cytoplasmic site of CD40 has no specific domain to initiate signal cascades. Therefore, CD40 must first recruit other intracellular adapter proteins to activate downstream signalling. TRAF proteins undertake an essential part in this process (Hu et al. 1994; Cheng et al. 1995; Pullen et al. 1999). The coupling of CD40L with CD40 results in direct or secondary recruitment of trimeric TRAF1, TRAF2, TRAF3, TRAF5 and TRAF6 proteins on the cytoplasmic domain. Following trimeric TRAF binding, several downstream kinase signalling molecules are phosphorylated to activate canonical and non-canonical NF-κB, ERK1/2, p38, PI3K, PLC-γ and JNK pathways to regulate transcription factors (Elgueta et al. 2009). CD40 signalling leads to a breadth of cellular and immune responses, mediated by cell-type specific activities of TRAF proteins to activate or inhibit expression of transcription factors (Bishop et al. 2007; Elgueta et al. 2009; Graham et al. 2009).

1.7.6 Reverse Signalling of the TNF Ligand Superfamily

Some of the TNF ligand superfamily members have unique properties that allow their membrane-bound forms to receive, as well as convey, signals for their respective cellular activities. Their cognate TNFR family members can serve as ligands to carry signals whilst the TNF ligands act as receptors to transmit the signals into the cell. This two-way communication mechanism

generated by TNF-TNFR coupling is called *reverse signalling*, *bi-directional signalling*, or *outside-to-inside signalling* (Fig. 1.10). TNF-α, CD40L, CD30L, lymphotoxin-related inducible ligand that competes for glycoprotein D binding to herpes virus entry mediator on T cells (LIGHT), FasL, TRAIL, TNF-related activation-induced cytokine (TRANCE), 4-1BBL, CD70L, and OX40L are all members of the TNF ligand superfamily with reverse signalling functions in the immune system (Eissner et al. 2004; Sun and Fink 2007; Horiuchi et al. 2010; Juhász et al. 2013).

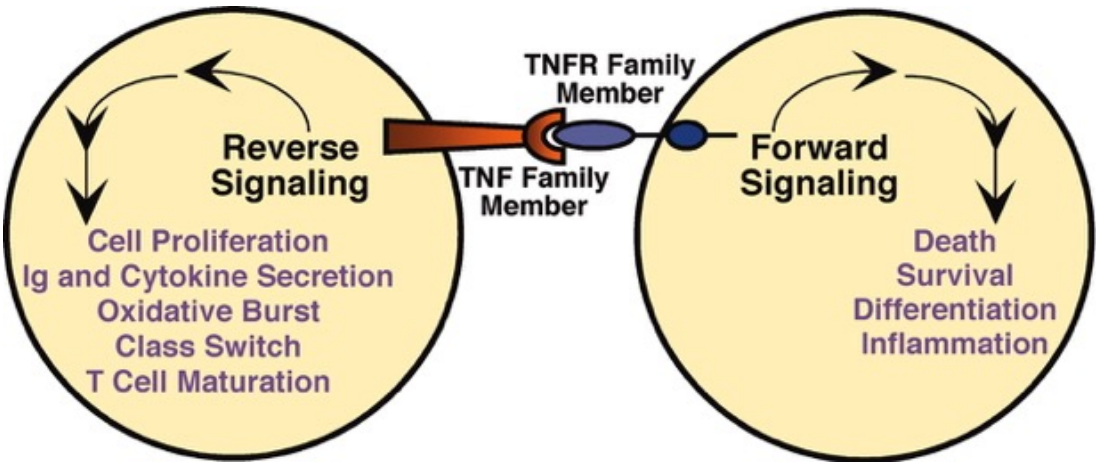

Figure 1.10. Bidirectional Signalling in the TNF Superfamily. Several members of the TNF superfamily can function both as ligands and receptors, allowing forward and reverse signalling pathways with often opposing cellular outcomes. Figure from (Sun and Fink 2007).

Although a diverse array of experimental data from various studies proves the existence of reverse signalling, the exact signal transduction mechanisms employed by TNFSF members remains uncertain. Since TNFSF members share little homology in their cytoplasmic domain, it is likely that they use no shared or common pathway for reverse signalling. Nonetheless, some studies reported that a few family members with bi-directional capacity, including TNF-α and CD40L, possess a casein kinase 1 phosphorylation site in their intracellular domain; the exact role of this domain is still unclear but the similarity between ligands suggests the potential for a common pathway (Eissner et al. 2004; Sun and Fink 2007; Horiuchi et al. 2010; Juhász et al. 2013).

Although the exact molecular mechanisms controlling mTNF-α reverse signalling are still unclear, there have been some relevant findings. Site-directed mutagenesis experiments using the isolated mTNF-α showed that the ligand is phosphorylated at Ser-05 at the cytoplasmic N-terminal end. Upon binding of the TNFR, this site is dephosphorylated, which leads to an increase in intracellular calcium concentrations. In addition, Cys-47 palmitoylation at the boundary between the transmembrane and the cytoplasmic domains of mTNF-α is suggested to be a posttranslational modification that may also participate in reverse signalling (Utsumi et al. 2001).

More experimental data are also required to obtain a clear picture about the biological relevance of reverse signalling in TNF-bearing cells. Observations thus far suggest that reverse signalling promotes the expression of various factors and cytokines involved in the regulation of cell proliferation, Ig and cytokine secretion, oxidative bursts, class switching, and T-cell maturation in the immune system (Domonkos et al. 2001; Eissner et al. 2004; Sun and Fink 2007; Horiuchi et al. 2010; Juhász et al. 2013).

1.7.7 Role of TNFSF and TNFRSF in the Development of the Peripheral Nervous System

Over the last 20 years, there have been extensive studies into the roles of various members of the TNFSF and TNFRSF in the development of the PNS

(Gutierrez et al. 2008; O'Keeffe et al. 2008; Gavalda et al. 2009; Gutierrez et al. 2013; Kisiswa et al. 2013; McWilliams et al. 2015; Kisiswa et al. 2017; Howard et al. 2018; Calhan et al. 2019; Erice et al. 2019). These studies have thus far revealed that almost none of the members of the TNFSF and TNFRSF affect the survival of sympathetic and sensory neurons during PNS development. TNF-α and its receptor TNFR1 have been the only exception to this concept, as disruption of the TNF-α/TNFR1 interaction in E16 sympathetic SCG and sensory trigeminal neurons causes an increase in the survival of these neurons (Barker et al. 2001).

In contrast, many TNFSF and TNFRSF members play a significant role in regulating the growth of sympathetic and sensory axons during PNS development. High expression of both TNFSF and TNFRSF members in the neuron populations of the PNS initially highlighted them as potential extracellular regulators of axonal growth of peripheral neurons at various developmental stages: ranging from early embryonic stages of sympathetic neuron formation to target field innervation (Gutierrez et al. 2008; O'Keeffe et al. 2008; Gavalda et al. 2009; Gutierrez et al. 2013; Kisiswa et al. 2013; McWilliams et al. 2015). One of the first TNFSF/TNFRSF pairs shown to be crucially involved in the regulation of axon growth and target field innervation *in vivo* was glucocorticoid-induced TNFR-related protein (GITR) and its ligand (GITRL). GITR and GITRL are co-expressed in SCG neurons at high levels during the period of target innervation and naturally occurring cell death (O'Keeffe et al. 2008). Elaborate *in vivo* and *in vitro* analyses revealed that inhibition of the GITR-GITRL interaction reduces NGF-promoted neurite growth from cultured SCG neurons in the immediate postnatal period; target organ innervation is also decreased in mice lacking GITR (*Tnfrsf18*$^{-/-}$) (O'Keeffe et al. 2008). The GITRL-GITR interaction is required for the phosphorylation of intracellular ERK1/ERK2 by NGF that is essential in sympathetic neuron development (O'Keeffe et al. 2008).

Next, the co-expression and localisation of LIGHT with its two receptors lymphotoxin-β receptor (LTβR) and herpesvirus entry mediator (HVEM) in mouse nodose ganglia (as a type of sensory neuron), reiterated the importance

of TNF ligand/receptor pairs in PNS development (Gavalda et al. 2009). Overexpression of LIGHT reduced BDNF-promoted neurite growth in developing sensory neurons. Although the expression of both LTβ and HVEM receptors has been detected in the mouse nodose ganglia, only HVEM receptor inhibition results in significantly greater and more branched neurite growth in sensory neurons (Gavalda et al. 2009). Overexpression of LIGHT showed that LIGHT/HVEM signalling inactivates the NF-κB pathway, acting as an effective negative regulator of neurite growth in developing sensory neurons. The discovery of the negative regulatory role of LIGHT/HVEM signalling was the first evidence of its role in the developing nervous system (Gavalda et al. 2009).

Signalling between RANKL (*Tnfsf11*) and its membrane-bound receptor RANK has, similar to LIGHT, a negative regulatory role in neurotrophin-induced neurite growth in sympathetic and sensory neurons of the developing mouse PNS (Gutierrez et al. 2013). RANKL/RANK signalling mainly acts in the immune system, e.g. dendritic cell survival, maturation and T-cell response. It has been demonstrated however that RANKL-treated sympathetic SCG neurons and sub-populations of sensory neurons (both NGF-dependent trigeminal and BDNF-dependent nodose) have diminished neurite length and complexity. Inhibitor of NF-κB (IKKβ)-dependent canonical activation of NF-κB mediates RANK signalling to exert its inhibitory effect on neurite growth and branching during perinatal periods of PNS development (Gutierrez et al. 2013).

TNF-α inhibits the elongation and branching of cultured P0 SCG neurons by NF-κB signalling. TNF-α-treated SCG neurons show marked reductions in both their neurite length and complexity via IKKβ-dependent phosphorylation of p65 in the classical NF-κB pathway (Gutierrez et al. 2008).

Members of the TNF superfamily are known for their role in the regulation of neurite outgrowth at later embryonic and early postnatal stages of development. However, Howard *et al.* for the first time showed that CD40L/CD40 autocrine signalling enhances the neurite outgrowth of early embryonic sensory neurons (Howard et al. 2019). CD40L-treated cultured E12 DRG neurons exhibited significantly increased neurite lengths and complexity,

independent of neurotrophins. Similarly, *in vivo* analysis showed that spinal nerves emerging from DRG were significantly shorter in E12 *Cd40*$^{-/-}$ embryos compared with littermate *Cd40*$^{+/+}$ embryos (Howard et al. 2019).

As the examples highlighted in this section clearly demonstrate, members of the TNFSF and TNFRSF contribute to neurite outgrowth of neuronal subpopulations within the PNS, and consequently the development of the PNS. These relatively early pioneering studies (and one more recent study) primarily characterised the role of TNF superfamily members in forward signalling-related mechanisms only. However, later studies found that in addition to forward signalling, members of the TNFSF and TNFRSF can also utilise reverse signalling to regulate neuronal outgrowth in the PNS.

1.7.8 The Role of TNF Reverse Signalling in the Developing Peripheral Nervous System

Reverse signalling through some of the TNF superfamily members has been a long-established phenomenon in immune system-related pathways (Sun and Fink 2007); however, the report of Kisisiwa *et al.* was the first demonstration of a significant involvement of TNF superfamily reverse signalling in the mouse nervous system (Kisiswa et al. 2013). In this report, both *in vitro* and *in vivo* analyses revealed that, in the presence of NGF, TNFR1-promoted TNF-α-mediated reverse signalling promotes the outgrowth of paravertebral SCG neurons during the developmental window when these neurons are reaching out to, and ramifying, their target organs (Kisiswa et al. 2013). TNFR1-Fc (previously shown to be a potent and specific reverse signalling ligand for TNF-α (Eissner et al. 2000)) -treated cultured SCG neurons had significantly longer and more complex neurite processes compared with non-treated control neurons (Kisiswa et al. 2013). *In vivo* experiments investigating TNF-α-reverse signalling in the paravertebral sympathetic nervous system found significant decreases in the sympathetic innervation density of paravertebral target organs, such as the iris, nasal tissue and submandibular gland, when either TNF-α- or TNFR1 were knocked out (Kisiswa et al. 2013). Further analyses elucidated that

T-type Ca^{2+} channels (Kisiswa et al. 2017) and ERK1/2 pathways (Kisiswa et al. 2013) function downstream of TNF-α-reverse signalling during its role in the outgrowth of SCG neurons.

Further evidence of the contribution of TNF ligand superfamily-mediated reverse signalling to the development of the sympathetic nervous system came from McWilliams *et al.* who demonstrated that CD40 acts as a ligand to promote sympathetic neurite elongation and branching via an autocrine loop (McWilliams et al. 2015). This study found that cultured SCG neurons show significant decreases in their neurite outgrowth when the CD40L-CD40 interaction was disrupted, either biochemically (such as by using function-blocking antibodies) or as a result of genetic manipulations (e.g. with knockout *Cd40*$^{-/-}$ mice) (McWilliams et al. 2015). Phenotype rescue experiments also showed that SCG neurons dissociated from *Cd40*$^{-/-}$ mice presented rescued neurite lengths when they were treated with CD40-Fc (McWilliams et al. 2015). In the same study, the physiological effect of CD40-reverse signalling was also demonstrated by the significant reduction in sympathetic innervation density of target tissues in the absence of *Cd40* (McWilliams et al. 2015).

A very recent study investigated TWE-PRIL, a naturally occurring fusion protein, consisting of the extracellular portion of APRIL (a TNFSF member), and the transmembrane and intracellular domains of TWEAK (another TNFSF member). TWE-PRIL suppressed neurite outgrowth of SCG neurons, and reduced tissue innervation of paravertebral target organs, through reverse signalling (Howard et al. 2018). Cultured SCG neurons from *April*$^{-/-}$ (*Tnfsf13*$^{-/-}$) embryos have significantly longer and more complex neurite structures compared with neurons from wild-type littermates. Similarly, sympathetic neurons innervating the E16 embryonic head exhibited significantly longer fibres in *April*$^{-/-}$ mice compared with their *April*$^{+/+}$ littermates (Howard et al. 2018).

1.8 Aim

Studies so far have identified the TNF and TNFR superfamilies as playing significant roles in the regulation of NGF-driven neuronal outgrowth and survival. Forward signalling is one mechanism by which this occurs; however reverse signalling, a more recently discovered concept, has been shown to be as effective. The post-ganglionic sympathetic nervous system consists of two anatomically distinct populations, the paravertebral and prevertebral. To date, investigations into the TNF and TNFR superfamilies have only made use of paravertebral ganglia as model systems. This raised the question: to what extent do findings obtained using paravertebral neurons apply to the sympathetic nervous system as a whole?

This thesis aims to compare and contrast the role of TNF superfamily signalling in neuronal outgrowth and survival between paravertebral and prevertebral neurons. SCG neurons will be used as a source of paravertebral neurons, and coeliac and superior mesenteric ganglia used as sources of prevertebral neurons. Two different ligand/receptor signalling pairs, TNF-α/TNFR1 and CD40L/CD40, will be analysed. Finally, the underlying origin of any differences between the two anatomically distinct kinds of sympathetic neurons will be investigated, by comparing the effect of neurotrophins on the survival and outgrowth of paravertebral and prevertebral neurons.

These investigations will identify if there are universal signals in the sympathetic nervous system, or whether a wider range of signalling and response mechanisms exist. Ultimately, these findings should help inform future studies into the physiology of the sympathetic nervous system.

Chapter 2

Materials and Methods

2.1 Animal Husbandry

All animal experiments in this research project were carried out in accordance with the Home Office Animals (Scientific Procedures) Act 1986. Animal safety and wellbeing was monitored regularly throughout each day, and any disruptions or discomfort to the animals were minimised as quickly as possible. The standard animal husbandry requirements, including racks, shelving, bedding, feeding, and sanitation of general equipment were provided by Cardiff University in agreement with the Act. Mouse pregnancy was tested by checking for vaginal plugs 12-14 h following breeding. The first day of gestation (E1) was taken as the day after the plug was seen in the instance of pregnancy. In this thesis, three knockout mouse strains were used, TNF-α (Körner et al. 1997), TNFR1 (Peschon et al. 1998) and CD40 (Kawabe et al. 1994). All mouse models were of C57BL/6 background. Homozygous knockout offspring were obtained from crosses between heterozygous parents. Mendelian frequency was observed in offspring from all three strains. Conventional polymerase chain reaction (PCR) was used to confirm genotypes (see Appendix). Experiments involving neurons from wild-type animals were obtained from CD-1 wild-type mice.

The Tnf-α knockout mouse strain used in this thesis was originally created by inactivation of the *Tnf* gene encoding Tnf-α (located at the H-2 locus on chromosome 17) by homologous recombination in embryonic stem cells, a kind gift from Professor K. Fox (Cardiff University). Homozygous $Tnf^{-/-}$ mice are viable and fertile. This mouse model lacks B cell follicles and shows abnormalities in the lymphoid organ structure. Histopathological characterisation of the mouse model found no structural abnormalities in the lungs, liver, kidney, spleen, thymus, or brain (Körner et al. 1997). Similarly, over a span of 20 years, our lab has not reported any significant abnormalities related to the development of this mouse model.

TNFR1 mice were generated by targeting the *Tnfrsf1*a gene by homologous recombination, and were a kind gift from Dr. D. Copland (University of Bristol). A targeting vector was used to replace exons 2 to 5 with

a neo-cassette. Characterisation of the mouse strain found selective deficits in host and inflammatory responses in homozygous knockout mice; whereas, development, and the thymocyte and lymphocyte population numbers, were unaltered (Peschon et al. 1998). During the studies in this chapter, neither heterozygous or homozygous knockout *Tnfrsf1a* mice showed any gross organ- or reproduction-related abnormalities. Both genotypes had normal lifespans.

CD40 knockout mice on a C57BL6/J background were ordered from The Jackson Laboratory (Bar Harbor, ME, USA) (Kawabe et al. 1994). The *Cd40* mutation was created by homologous recombination of a neomycin-resistance gene cassette with the third exon. No abnormalities were detected in terms of gross development, specific organ development or reproduction in this mouse model.

2.2 Primary Neuron Cultures

Sympathetic neurons dissected from paravertebral and prevertebral ganglia were used in outgrowth, survival, and microfluidic assays, for immunocytochemical analyses, and in gene expression analyses. For all these experiments, the same dissection protocol was followed. Experiment-specific differences, such as animal ages and concentrations of individual exogenous proteins, Tnf-α (410-MT-010; R&D Systems, Minneapolis, MN, USA), TNFR1-Fc (372-R1-050; R&D Systems), TNFR2-Fc (726-R2-050; R&D Systems), CD40L (Alx-522-120-C010; Enzo Life Sciences, New York, NY, USA), CD40-Fc (1215-CD-050; R&D Systems), and control Fc fusion protein (Alx-203-004-C050; Enzo Life Sciences), are defined in each results chapter. After each dissection, sympathetic neurons were supplemented with 1 or 10 ng/ml NGF (R&D Systems), and 25 μM caspase inhibitor III (218745; Merck, Darmstadt, Germany), to prevent neurons from undergoing apoptosis. As the only exception, SCG and PVG neurons were not supplemented with caspase inhibitor after dissection when used for cell survival analysis.

2.2.1 Preparation of Culture Dishes

2.2.1.1 Poly-ornithine Solution

150 mM boric acid (in distilled water; Sigma-Aldrich, Darmstadt, Germany) was adjusted to pH 8.4 using 5 M NaOH. 500 mg poly-DL-ornithine hydrobromide (p8638; Sigma-Aldrich) was then dissolved in the borate solution, and the solution filter sterilised. The poly-ornithine solution was stored at 4 ^{o}C for a maximum of 2 weeks.

2.2.1.2 Coating of Culture Dishes

35 mm culture dishes (627160 (with no inner rings) and 627170 (with 4 inner rings); Greiner Bio-one, Stonehouse, UK) were coated with 1 ml poly-ornithine solution overnight at room temperature (RT). The next day, the poly-ornithine was aspirated and the dishes washed with sterile water twice. Dishes were then left to air dry in a laminar flow hood. Prior to each experiment, culture dishes were coated with 20 µg/µl laminin (L2020; Sigma-Aldrich) in Hanks' Balanced Salt Solution (HBSS, 14170070; Thermo Fisher Scientific, Waltham, MA, USA), and incubated at 37 °C, 5% CO_2 in a humidified chamber, for at least 1 h.

2.2.2 Dissection and Culture of Sympathetic Neurons

All dissection procedures were conducted in a laminar flow cabinet applying standard sterilisation procedures on working areas and tools. Sympathetic neurons (SCG and PVG neurons) were dissected from knockout animals or CD1 litters at various embryonic ages between E16 and p5, using electrolytically-sharpened 0.5 mm diameter tungsten needles (Davies 1995). Dissected tissues were transferred to 35 mm cell culture dishes containing 1-2 ml Ca^{2+}/Mg^{2+}-free Dulbecco's Phosphate Buffered Saline (DPBS) (59331C; Sigma-Aldrich). Tissues were then transferred into 10 ml polypropylene tubes containing 0.95 ml fresh Ca^{2+}/Mg^{2+}-free HBSS with 0.05 ml trypsin (Sigma-Aldrich). Tissues were incubated with this trypsin for 15-25 min (age-dependent:

E16, 15 min; to P5, 25 min) at 37 °C for trypsinisation. To subsequently inactivate the trypsin, 5 ml Ham's F12 media (51448C; Sigma-Aldrich) containing 10% heat-inactivated horse serum (Sigma-Aldrich) was added to the tissue, before centrifugation at 2, 000 x g for 2 min at RT. 5 ml of the media supernatant was then exchanged for 5 ml fresh Ham's F12 media, and the tissue was again centrifuged at 2, 000 x g for 2 min at RT. The supernatant was then discarded carefully and the cell pellet re-suspended in 0.1 ml defined Ham's F14 nutrient media (L0138-500; VWR, Radnor, PA, USA) supplemented with 2 mM L-Glutamine (Gibco Biosciences, Dublin, Ireland), 2.5% Albumax (11020021; Thermo Fisher Scientific), 100 U/ml penicillin, and 100 µg/ml streptomycin (Sigma-Aldrich). Tissues were mechanically dissociated into a single cell suspension by gentle trituration with siliconised Pasteur pipettes. After the trituration, 400 µl F14 was added into the single cell suspension to bring the final volume to 500 µl. 1, 2, 3 or 4 µl cell suspension was added into separate wells of a 4-well plate containing 100 µl F14 media to check cell density. Cells were plated at a very low density (<60-80 cells per 4-ringed dish) for neurite outgrowth assays, and at a relatively higher density (<600-800 per 4-ringed dish) for cell survival assays. Based on adjusted cell density, sympathetic cells were plated onto laminin/poly-ornithine-coated, 35 mm cell culture dishes. Cells were cultured at 37 °C, for 18-24 h, in a 5% CO_2 humidified chamber.

2.2.3 Neurite Outgrowth

For neurite outgrowth assays, neurons were allowed to grow for a maximum of 18 h following plating. Neurons were labelled with the green fluorescent, cell-permeant dye, calcein-AM (C1430; Thermo Fisher Scientific) using the following protocol: 1 µl of 1 mg/ml calcein-AM was added to 1 ml warm F14 solution and incubated for 10 min at 37 °C (calcein-AM solution). This was then added to cells and 20 minutes incubation (at 37 °C, in a 5% CO_2 humidified chamber) allowed for processing of non-fluorescent calcein-AM into fluorescent calcein.

Following this incubation, between 60-100 neurons (15-25 per inner ring) were imaged per condition by fluorescence microscopy (Zeiss-Axiovert 200; Zeiss, Oberkochen, Germany). Acquired images were analysed to quantify the growth and complexity of neuronal processes using a modified and automated version of the conventional Sholl analysis (Gutierrez and Davies 2007) in MATLAB (MathWorks, Natick, MA, USA). This analysis is based on virtual concentric rings, with the rings positioned to place the soma at the centre. The number of neurites intersecting each ring was quantified. Sholl profiles were used to present the number of intersections at each distance from the soma, and illustrate neuronal morphology. Use of the automated Sholl analysis reduced the time required to perform the analysis, and improved accuracy (Gutierrez and Davies 2007). Each experiment was performed at least three times. All imaging and quantification was performed blind to genotype.

2.2.4 Cell Survival Assays

For cell survival experiments, NGF (R&D Systems) or NT-3 (CYT-688; Prospect, Brisbane, CA, USA) treated cells (numbering 150-200) were plated into each inner ring of 35 mm dishes (with 4 inner rings) per condition. Four hours after plating, the number of attached cells was counted by phase-contrast microscopy, and this designated as the total cell number. Cell numbers were then counted 24 and 48 h later to quantify percentage cell survival at each time point. Parameters used to identify surviving cells were a bright, non-fragmented nucleus, and the presence of non-fragmented neurite extensions. These parameters were used as dying cells have dense chromatin structures in their nucleus, and fragmented neurite extensions. All experiments were repeated at least three times, and imaging and quantification was performed blind to genotype.

2.3 Immunocytochemistry

SCG and PVG neurons were dissected as described in **Section 2.2.2**. Dissociated sympathetic neurons were cultured at high density in 1 ml F14

media supplemented with 10 ng/ml NGF, on poly-ornithine/laminin-coated 35 mm dishes (with no inner rings). After an overnight incubation at 37 °C, in a 5% CO_2 humidified chamber, the culture media was carefully aspirated and neurons twice washed with 1 ml warm sterile DPBS. Next, cells were fixed with 1 ml 4% paraformaldehyde (PFA, 28908; Thermo Fisher Scientific) diluted in DPBS, for 20 min, and washed three times with DPBS. To block non-specific binding, sympathetic neurons were incubated for 1 h in 5% bovine serum albumin (BSA; Sigma-Aldrich) and 0.2% Triton X-100 (Sigma-Aldrich) at RT. After blocking, cells were washed with DPBS. Cells were then incubated overnight at 4 °C in primary antibody (Table 2.1) diluted in 1% BSA and 0.2% Triton X-100 in DPBS, with gentle rocking. The next day, cells were washed three times with DPBS and incubated for 1 h in secondary antibody (Table 2.2) diluted in 1% BSA in DPBS at RT in the dark. Cells were then washed twice with 1 ml DPBS in the dark to remove non-bound secondary antibody. To counterstain nuclei, cells were incubated with 1:4000 4',6-Diamidino-2-Phenylindole, Dihydrochloride (DAPI, 10236276001; Sigma-Aldrich) in DPBS for 20 min. Cells were washed twice with 1 ml DPBS, before 2 ml DPBS was added into dishes after the final wash. Images of fluorescently stained sympathetic neurons were captured by confocal microscopy (Zeiss Axio Z2 Imager).

Table 2.1. Primary Antibodies and Their Dilutions Used in Immunocytochemical Analyses.

Primary Antibody	Host	Cat. No.; Company	Dilution
TNF-α	Rabbit	ab34674; Abcam	1:500
TNFR1	Rabbit	ab19139; Abcam	1:500
TNFR2	Goat	AF-426-PB; R&D	1:40
CD40L	Rabbit	ab2391; Abcam	1:200
CD40	Mouse	MA5-15535; Invitrogen	1:500
β-III tubulin	Chicken	ab41489; Abcam	1:1500

Table 2.2. Secondary Antibodies and Their Dilutions Used in Immunocytochemical Analyses.

Fluorophore	Type	Cat. No.; Company	Dilution
Alexa Fluor 488	Donkey anti-rabbit IgG	A21206; Thermo Fisher	1:500
Alexa Fluor 488	Donkey anti- goat IgG	A11055; Thermo Fisher	1:500
Alexa Fluor 488	Donkey anti-rabbit IgG	A32790; Thermo Fisher	1:500
Alexa Fluor 488	Goat anti-mouse IgG	A11001; Thermo Fisher	1:500
Alexa Fluor 594	Goat anti-chicken IgY	A11042; Thermo Fisher	1:500

2.4 Microfluidic Compartments

Four-compartment microfluidic devices (SND 150; Xona Microfluidics, Triangle Research Park, NC, USA) were sterilised in a 70% EtOH bath for 15 min, and washed with sterilised water twice on first use and after each experiment. Washed devices were left to air dry in a laminar flow cabinet. Cleaned devices were kept in sterilised conditions, and each device was used a maximum of three times.

Prior to experiments, devices were placed onto poly-ornithine-coated 35 mm cell culture dishes (without inner rings), and slight pressure applied to adhere them to the surface of the dish. Each compartment of the devices was coated with 20 µg/µl laminin in HBSS for 20-25 min in a 5% CO_2 humidified chamber. After dissection of SCG and PVGs, sympathetic neurons were seeded at very high densities into one side of the device only, designated as the soma compartment (Fig. 2.1). After 45 min incubation in a 5% CO_2 humidified chamber, allowing neurons to attach to the surface of the culture dish, both soma and axon compartments were supplemented with 1:1000 caspase inhibitor and 1 ng/ml NGF in F14 media. TNF-α or TNFR1-Fc treatments were also added as stated (see results section in **Chapter 3**). Cultures were then incubated at 37 °C in a 5% CO_2 humidified chamber. After 18 h, calcein-AM solution was added into only the axon compartments, and the devices were returned to the incubator for 30 min. Cell bodies and neurite extensions of sympathetic neurons were imaged using fluorescence microscopy. During the imaging process, the entire imaging area was divided into virtual sections, to prevent repeated capture of the same neurons and their processes, and each section was imaged separately from top to bottom.

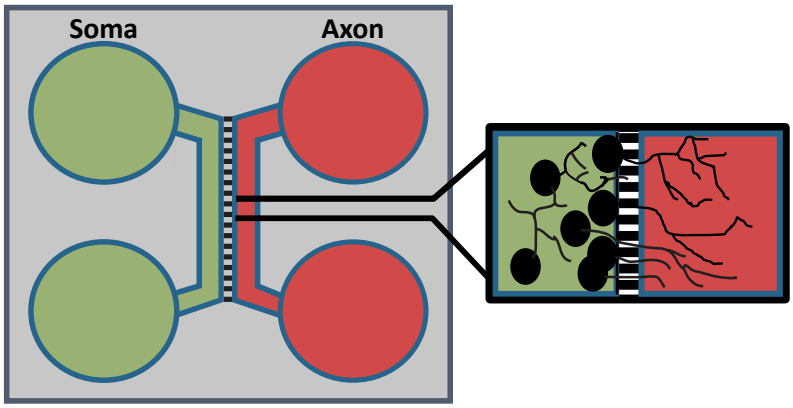

Figure 2.1. Schematic of the Microfluidic Device Used for Region-Specific Analysis of TNF Signalling in Sympathetic Neurons. Schematic of the four-compartment microfluidic device used to analyse TNF signalling in soma and axonal regions of sympathetic neurons. Neurons were seeded into the soma compartment. Inset illustrates axons projecting from the soma compartment through microchannels into the axon compartment.

Neurite length was quantified by a modified version of a previously described method (Ronn et al. 2000). A grid of 200 μm² squares was placed over the axon compartment only of each image in ImageJ. The number of intersections between neurites and this grid was counted manually and normalised to the number of fluorescently-labelled cell bodies in the soma compartment. During calculations sympathetic neurite extensions in the soma compartment were excluded as most of the neuron cell bodies were situated close to the microgrooves; thus their neurite length was negligible. In addition, neurite extensions were not individually traced back to their original soma, as the mathematical formula used relies instead on the total number of cell bodies. Average neurite length per projecting cell body was calculated using the formula developed by Ronn *et al.* (2000): L = DI/2, where L is the estimated length, D is the interline interval, and I is the average number of intersections per projecting cell body (Ronn et al. 2000). Measurements were taken across all fields along the microfluidic barrier, with care taken to avoid overlapping images.

2.5 Immunolabeling-enabled three-dimensional imaging of solvent-cleared organs (iDISCO) Method

Analysis of sympathetic nerve innervation of intact, sympathetic target organs was performed using the iDISCO method. The volume imaging of solvent-cleared whole-mount immunolabelled target tissues (the kidney, stomach and spleen) was performed either from P6 (**Chapter 3**) or P10 (**Chapter 4**) knockout mice.

2.5.1 Sample Collection

Animals were culled by decapitation and sympathetic target organs were collected into phosphate buffered saline (PBS). All harvested organ samples were fixed in 4% PFA in PBS for 2 h at RT.

2.5.2 Tissue Pre-treatment in Methanol

All fixed tissues were washed three times in PBS for 30 min, then sequentially in 20%, 40%, 60%, and 80% MeOH in PBS for 30 min each. Lastly, tissues were washed in 100% MeOH for at least 1 h. To bleach samples, tissues were treated with 5% H_2O_2 in MeOH at 4 °C overnight. Following bleaching, tissues were washed in 80% MeOH in PBS for 30 min. Next, tissues were washed sequentially with 80%, 60%, 40%, and 20% MeOH with 0.2% Triton X-100 in PBS for 30 min each. Finally, tissues were washed twice in 0.2% Triton X-100 in PBS for 1 h. At the end of the day, samples were transferred into 0.2% Triton X-100, 20% dimethylsulfoxide (DMSO) and 0.3 M glycine (G7126; Sigma-Aldrich) in PBS, and incubated at 37 °C over two nights.

2.5.3 Tissue Immuno-labelling

Pre-treated tissues were blocked in 0.2% Triton X-100, 10% DMSO and 6% freshly prepared and sterilised donkey serum in PBS for 4 days at 37 °C. Blocked samples were washed twice in 0.2% Tween-20 with 10 μg/ml heparin (H3393; Sigma-Aldrich) in PBS (PTwH) for 1 h at RT. Then, tissues were incubated with 1:200 rabbit anti-tyrosine hydroxylase (TH) primary antibody (AB152; Merck) in PTwH with 5% DMSO and 3% donkey serum at 37 °C for 4 days. Tissues were then washed in freshly prepared PTwH at RT for 10 min, 15 min, 1 h, 2 h and overnight by replacing the PTwH solution at each washing step. Next, tissues were incubated with 1:300 Alexa Fluor 594-conjugated donkey anti-rabbit IgG secondary antibody (21207; Thermo Fisher Scientific) diluted in PTwH with 3% donkey serum at 37 °C for 4 days. Lastly, tissues were washed in PTwH for one day following the same protocol as described in the primary antibody staining step, to prepare tissues for clearing steps.

2.5.4 Tissue Clearing

The following day, samples were washed in PTwH in 2 h washing cycles until the end of the day. Samples were then incubated in 50% v/v tetrahydrofuran (THF, 401757; Sigma-Aldrich) in distilled water overnight.

Samples were then incubated for 1 h in 80% THF in distilled water, and then for 1 h, twice, in 100% THF. Next the organs were incubated in dichloromethane until the samples sank to the bottom of the vial (less than 1 h). Lastly, samples were incubated in dibenzyl ether (DBE; Sigma-Aldrich) until they were clear (approximately 2 h), and then vials were completely filled with DBE for further storage at RT in the dark, until imaging.

2.5.5 Imaging of Sympathetic Target Organs

The target organs were placed in a 3D-printed chamber (sized appropriate to each organ) and submerged in DBE before imaging. The images of the whole kidney, stomach and spleen were captured using confocal microscopy (Zeiss Axio Z2 Imager).

2.5.6 Analysis of the Sympathetic Target Organs

For each organ examined, the same anatomical regions were quantified to ensure consistency in the analysis of samples. Kidney samples were analysed in their entirety. As spleen samples were curled at the caudal and cranial ends (which would affect the precise measurement of sympathetic nerve length) these ends were excluded from quantification. At this stage of development the stomach of pups still contain milk, which introduces curvature and an uneven surface area. Therefore, the greater curvature was excluded from quantification, and the most intensely innervated regions of the stomach were analysed: the lesser curvature, cardia, fundus, and the upper half the body.

After imaging by confocal microscopy, individual z-stacks were merged into maximum intensity projections using Zen software (Zen 2012, Zeiss) and imported into FIJI (Schindelin et al. 2012). TH immunoreactivity was analysed using a user-defined macro to perform semi-automated quantification as follows. The Feature Extraction tool (FeatureJ Hessian (Sato et al. 1998)) was used, with parameters set at a 1.5 smooth scale, and the lowest eigenvalue of Hessian tensor employed. A threshold value for background subtraction was manually chosen after preliminary visual inspection of the image sets for each

organ (across all genotypes). The same background subtraction settings were applied to all organ images collected from wild-type and knockout mice. To analyse the innervation density, a region of interest was drawn around the organs, and the percentage of pixels in the specified areas above the threshold was quantified. This percentage was presented as the innervation density. During this process, empty spaces, which occasionally occurred in the areas of interest due to the rehydration step of iDISCO, were excluded from the measurement of total area to ensure that the stained pixels were expressed as a percentage of viable tissue area only. All imaging and quantification was performed blind to genotype. Data are expressed as a percentage of the average from wild-type littermates.

2.6 Gene Expression Analysis

The levels of *Tnf*, *Tnfrsf1a* and *Tnfrsf1b*, *Cd40*, and *Ngf* mRNA were measured in both sympathetic target organs, and paravertebral and prevertebral ganglia by reverse transcription-quantitative PCR (RT-qPCR), and normalised to mRNA levels of the housekeeping enzymes: glyceraldehyde phosphate dehydrogenase (*Gapdh*), succinate dehydrogenase (*Sdha*), and hypoxanthine phosphoribosyltransferase 1 (*Hprt1*). In this method, mRNA was first extracted from samples, then reverse transcribed into cDNA. cDNA was quantified using qPCR with fluorescently labelled probes.

2.6.1 RNA Extraction

Freshly dissected sympathetic target organs or dissociated sympathetic neurons were immediately treated with RNAlater solution (Applied Biosystems, Thermo Fisher Scientific) to stabilise and protect the integrity of RNA. These tissues and cells were incubated at 4 ^{o}C overnight, before storage at -80 ^{o}C until processing for RT-qPCR. In each gene expression analysis, tissues samples and sympathetic neurons were collected from at least three different embryos or pups (before RNA extraction), and for each genotype this process was repeated at least three times. Total RNA was extracted and

purified using the RNeasy Lipid Mini extraction kit (74804; Qiagen, Crawley, UK) following the manufacturer's protocol.

2.6.2 Reverse Transcription

10 µl of extracted RNA was reverse transcribed using an AffinityScript reverse transcription kit (Agilent, Berkshire, UK). The reaction mix contained 2 µl AffinityScript reverse transcriptase, 5 mM dNTPs and 10 µM random hexamers. RNA samples were reverse transcribed at 45 °C for 1 h.

2.6.3 qPCR

PCR products were detected using dual-labelled FAM/BHQ1 hybridisation probes (MWG/Eurofins, Ebersberg, Germany) specific to each cDNA. Primer and probe sequences were designed using Beacon Designer software (Premier Biosoft, Palo Alto, CA, USA) and are shown in Table 2.3. The reaction mix for qPCR consisted of 2 µl cDNA in a total reaction volume of 20 µl. cDNA, forward and reverse primers (150 nM), and dual labelled probes (300 nM) were diluted with 12.5 µl Brilliant III ultrafast qPCR master mix (Agilent). qPCR reactions were performed using a Stratagene MX3000P thermal cycler (Agilent), using the following protocol: 30 s at 95 °C; followed by 45 cycles of 95 °C for 10 s and 60 °C for 35 s. Standard curves were generated for each cDNA for each run, using reverse-transcribed mouse adult spleen total RNA (Zyagen, San Diego, CA, USA) at five-fold dilution steps, for quantification of *Tnf*, *Tnfrsf1a* and *Tnfrsf1b, Cd40* and *Ngf,* and reference genes. Relative mRNA levels were quantified in four separate sets of dissected tissues and dissociated neurons for each experiment.

Table 2.3. Primer and probe sequences used in qRT-PCR analysis.

Gene	Primer /Probe	Sequence (5' to 3')
Tnf	Forward	CTC CCT CTC ATC AGT TCT AT
	Reverse	CTA CAG GCT TGT CAC TCG
	Probe	FAM-CCC AGA CCC TCA CAC TCA GAT-BHQ1
Tnfrsf1a	Forward	TTC CCA GAA TTA CCT CAG
	Reverse	AAC TGG TTC TCC TTA CAG
	Probe	FAM-CAC CGT GTC CTT GTC AGC-BHQ1
Tnfrsf1b	Forward	CTC CAA GCA TCC TTA CAT
	Reverse	GTC CTA ACA TCA GCA GAC
	Probe	FAM-ATG TCA CTC CAA CAA TCA GAC CAA T-BHQ1
Cd40	Forward	CTT TGG AGT TAT GGA GAT G
	Reverse	ATG ACT GAT TGG AGA AGA
	Probe	FAM-CCA CTG AGA CCA CTG ATA CCG-BHQ1
Ngf	Forward	AAA CGG AGA CTC CAC TCA CC
	Reverse	GTC CTG TTG AAA GGG ATT GTA CC
	Probe	FAM-TGT TCA GCA CCC AGC CTC CAC CCA- BHQ1
Gapdh	Forward	GAG AAA CCT GCC AAG TAT G
	Reverse	GGA GTT GCT GTT GAA GTC
	Probe	FAM-AGA CAA CCT GGT CCT CAG TGT-BHQ1
Sdha	Forward	GGA ACA CTC CAA AAA CAG
	Reverse	CCA CAG CAT CAA ATT CAT
	Probe	FAM-CCT GCG GCT TTC ACT TCT CT-BHQ1
Hprt1	Forward	TTA AGC AGT ACA GCC CCA AAA TG
	Reverse	AAG TCT GGC CTG TAT CCA ACA C
	Probe	FAM-TCG AGA GGT CCT TTT CAC CAG CAA G-BHQ1

2.7 Statistics

Data were assessed for normality using the Kolmogorov-Smirnov test. Kruskal-Wallis test followed by Dunn's multiple comparison *post-hoc* test was used for group analysis of non-normally distributed data, whilst one-way ANOVAs performed for multiple comparisons with Dunnett's *post-hoc* analysis, was used for normally distributed data. A Student's *t*-test (normally distributed data) or a Mann-Whitney test (non-normally distributed data) were conducted for pair-wise comparisons of data. $p<0.05$ was considered significant. GraphPad Prism software (Prism 5 for Windows, V.5.03; GraphPad) was used to perform statistical analysis and produce graphs.

Chapter 3

A Comparison of TNF Forward and Reverse Signalling in the Development of the Paravertebral and Prevertebral Divisions of the Sympathetic Nervous System

3.1 Introduction

Tumour necrosis factor (TNF) superfamily (TNFSF) proteins are synthesised as type II transmembrane proteins with a common TNF domain. All 19 TNFSF members begin as membrane-associated forms, but can be released from the cell membrane through proteolytic cleavage by metalloproteases. Therefore, two distinct forms of TNFSF members are involved in the regulation of cellular activities: soluble TNFSF (sTNFSF) and transmembrane TNFSF (mTNFSF). Similarly, TNF receptor (TNFR) superfamily (TNFRSF) members can also be present in both forms, either as transmembrane receptor proteins on the cell surface, or as soluble receptor proteins in the extracellular space (Aggarwal 2003). A member of the TNFSF, 26 kDa transmembrane tumour necrosis factor-alpha (mTNF-α), can be proteolytically cleaved by Tnf-α converting enzyme (TACE), a member of the ADAM family of metalloproteases, to be released as 17 kDa soluble TNF-α (sTNF-α) (Black 2002; Sedger and McDermott 2014). TNF-α has two receptor proteins, called TNF receptor 1 (TNFR1, also known as *TNFRSF1A*) and TNF receptor 2 (TNFR2, also known as *TNFRSF1B*). TNFR1 is expressed on almost all nucleated cell types while TNFR2 expression is mostly restricted to immune and tumour cells. Both TNFR1 and TNFR2 can also be cleaved by TACE to generate two soluble forms of TNFRs (Sedger and McDermott 2014). TNF-α acts as a ligand both as a type II transmembrane protein and as a classical soluble cytokine; therefore, the signalling between cells is established through either direct cell-to-cell contact or by different forms of chemical signalling, such as autocrine, paracrine, and endocrine (Parameswaran and Patial 2010; Yang et al. 2018).

In 1994, Smith *et al*. for the first time discussed the ligand-receptor interaction between TNFSF and TNFRSF from a different angle, and suggested the possibility of '*bipolar signalling*', stating "direct cell-cell contact is blurring the distinction between receptor and ligand" (Smith et al. 1994). In the same year Ferran *et al*. used *in vivo* and *in vitro* experiments to show for the first time that TNF-α can function as a cell surface-associated receptor with signal transduction potential (Ferran et al. 1994). Subsequently, an increasing number

of publications reported that TNF ligands can act as receptors and generate intracellular signalling cascades, while cognate receptors can behave as ligands. Although the membrane bound 26 kDa protein complex of mTNF-α does not have any identifiable enzymatic activity in its cytoplasmic domain, it is predicted that mTNF-α promotes signalling cascades in reverse signalling through adaptor proteins, which have not yet been discovered. Reverse signalling, as in forward signalling, mediates many diverse immunological responses on mTNF-α bearing cells. For example, TNFR1-activated TNF-α-mediated reverse signalling causes activation of T and B cells, differentiation of osteoclasts, and apoptosis of active macrophages; TNFR2-activated reverse signalling in tumour cells promotes tumour cell survival and resistance to apoptotic cell death through the NF-κB pathway. Beyond these examples, TNF-α reverse signalling has many other important roles in the immune system with a direct relevance to therapeutic strategies through its cytokine modulation role (Eissner et al. 2004; Sun and Fink 2007; Pallai et al. 2016; Ba et al. 2017; Qu et al. 2017; Lee et al. 2019).

Studies investigating the spatial and temporal distribution of TNF-α in the developing nervous system date back to the beginning of the 1990s (Gendron et al. 1991). In the last twenty years however, research on the role of TNF-α and its receptors on different aspects of neuronal development has progressed rapidly. Specific to sympathetic nervous system (SNS) development for example, Barker *et al*. reported that TNF-α is involved in the death of NGF-deprived sympathetic superior cervical ganglia (SCG) neurons in embryonic mice (Barker et al. 2001). Gutierrez *et al*. explored the molecular mechanism of TNF-α forward signalling that inhibits neurite growth of cultured neonatal mouse SCG neurons (Gutierrez et al. 2008). In 2013 Kisiswa *et al*. made an important contribution to the field by implicating the reverse signalling mechanism for the first time in the development of the SNS. In this study, TNFR1-activated TNF-α-mediated reverse signalling promoted sympathetic axon growth and branch complexity as sympathetic axons ramified in their target organs. *In vitro* experiments carried out with postnatal SCG neurons, and

in vivo studies conducted with the SCG neuron-target organs (submandibular gland, iris, and nasal tissue) from either postnatal *Tnf* or *Tnfrsf1a* knockout mice, showed that disruption of TNFR1-activated TNF-α-mediated reverse signalling resulted in significantly reduced SCG axon growth and branching, and consequently diminished innervation density in target organs (Kisiswa et al. 2013). In their following studies, they also reported that TNF-α reverse signalling activates T-type Ca^{2+} channels and promotes downstream ERK1/2 signalling pathways (Kisiswa et al. 2013; Kisiswa et al. 2017).

These studies confirmed a critical role for TNF-α and its receptors in SNS development. In particular, the discovery of TNF-α reverse signalling in SNS development, and demonstration of the physiological effects of reverse signalling *in vivo,* underlined the complexity of target organ innervation by sympathetic neurons. Despite their pioneering role in uncovering the significance of TNF-α and its receptors in the development of the SNS, these studies had one distinct drawback. All our knowledge about the role of TNF-α and its receptors in the development of the SNS derive only from studies using paravertebral SCG neurons as a model system, as these are the most well-characterised SNS neurons. However, prevertebral sympathetic ganglia (PVG), which are the other subdivision of the SNS, are as crucial as paravertebral ganglia in providing sympathetic input to many organs, e.g. the spleen, stomach, liver and kidneys. More importantly, studies show that paravertebral and prevertebral sympathetic neurons differ from each other in many aspects, such as functional, structural, electrophysiological and biochemical (Szurszewski 1981; Elfvin et al. 1993; Wang and McKinnon 1995; Boyd et al. 1996). Therefore, it is important to explore the nature of the differences between paravertebral and prevertebral systems to more fully understand the principles that underlie the development and functioning of the SNS.

In this chapter, I aim to further explore the contributions of TNF-α-dependent signalling mechanisms to the development of the sympathetic nervous system. I will investigate the extent to which findings reported from the paravertebral division are also applicable to the prevertebral division of the

sympathetic nervous system. To achieve this, I will first analyse the innervation of the spleen and the stomach in TNF-α-deficient and TNFR1-deficient mouse models, as these organs receive their sympathetic innervation primarily from PVG neurons. Following *in vivo* analysis, I will assess whether there are differences in the neuronal responses of prevertebral ganglia to TNF-α forward and reverse signalling mechanisms *in vitro*, in comparison to those seen in paravertebral ganglia. In this context, I introduce coeliac ganglia and superior mesenteric ganglia (CG-SMG) cultures as a prevertebral neuron model system to examine TNF-α signalling mechanisms that regulate innervation of prevertebral sympathetic target organs.

3.2 Results

3.2.1 The Role of TNF-α and TNFR1 in the Innervation of PVG Target Organs During Sympathetic Nervous System Development

The spleen and the stomach are two organs which receive their major sympathetic innervation from the CG, together with some minor innervation from the SMG, and minimal contributions from the paravertebral thoracic sympathetic chain (Chevendra and Weaver 1991; Trudrung et al. 1994; Quinson et al. 2001; Phillips and Powley 2007; Rosas-Ballina et al. 2008). Kisiswa *et al.* demonstrated that TNFR1 is expressed by paravertebral SCG target organs (iris, submandibular gland and nasal tissues) and acts as a ligand for mTNF-α expressed along the axons of SCG neurons, defined as TNFR1-activated TNF-α-mediated reverse signalling. They found that TNF-α-reverse signalling was one of the mechanisms that played a role in regulating the innervation of SCG target organs, and a lack of TNFR1 and TNF-α proteins resulted in hypoinnervation in all three SCG targets (Kisiswa et al. 2013). Here, the sympathetic innervation of the spleen and the stomach were analysed in postnatal TNF-α-deficient and TNFR1-deficient mice to determine whether TNF-α/TNFR1 forward or reverse signalling plays a role in modulating target innervation by prevertebral sympathetic neurons.

Tyrosine hydroxylase (TH) staining in iDISCO tissue preparations was used to compare sympathetic (noradrenergic) fibre density between TNF-α-deficient (Körner et al. 1997) and TNFR1-deficient mice (Pfeffer et al. 1993), and their heterozygous and wild-type littermates. TH is the rate-limiting enzyme in the biosynthesis of dopamine and noradrenaline; it is a well-established protocol to use an antibody against TH to visualise sympathetic innervation fibres (Phillips and Powley 2007). During analysis, sympathetic innervation density was assessed by quantifying the immunostaining of TH-expressing sympathetic fibres. Analysis was carried out in P6 mice, as by this age sympathetic fibres have completed their journey to target organs and have

extensively innervated the tissues (Kisiswa et al. 2013). Experiments were performed blind to genotypes from the beginning of the iDISCO protocol to the end of data analysis.

Fig. 3.1A shows representative images of spleen tissue from wild-type, heterozygous and homozygous *Tnf* knockout mice. TH-expressing sympathetic fibres can be seen on the gastric surface, between the superior and inferior border of the spleen. In contrast to the hypoinnervation recorded in SCG target organs in response to deletion of *Tnf*, the representative images illustrate that *Tnf* deletion had no effect on innervation density of the spleen. Quantification of innervation density confirmed that there were no significant differences between spleen tissues from $Tnf^{+/+}$ (100 ± 24%), $Tnf^{+/-}$ (125 ± 27%) and $Tnf^{/-}$ (102 ± 35%) littermates (Fig. 3.1B).

Whilst knockdown of *Tnf* had no effect on spleen innervation density, knockdown of its receptor protein, *Tnfrsf1a* did affect innervation density. Representative images of spleen tissue from wild-type, heterozygous and homozygous *Tnfrsf1a* knockout mice are shown in Fig. 3.1C. These images of TH-stained spleen tissues from mice lacking either one or both copies of *Tnfrsf1a* indicate that there was an increase in sympathetic neuron innervation when TNFR1 protein expression was reduced or removed. Quantification of sympathetic fibres confirmed that both $Tnfrsf1a^{+/-}$ and $Tnfrsf1a^{-/-}$ animals displayed a significant increase in sympathetic neuron innervation density compared with wild-type littermates (Fig. 3.1D, $p<0.05$, $n=9$ animals per genotype, Kruskal-Wallis test). Heterozygous animals showed a 49 ± 6% increase in innervation density compared to wild-type animals (100 ± 9%), and homozygous animals showed a 69 ± 16% increase; there was no significant difference between heterozygous and homozygous animals.

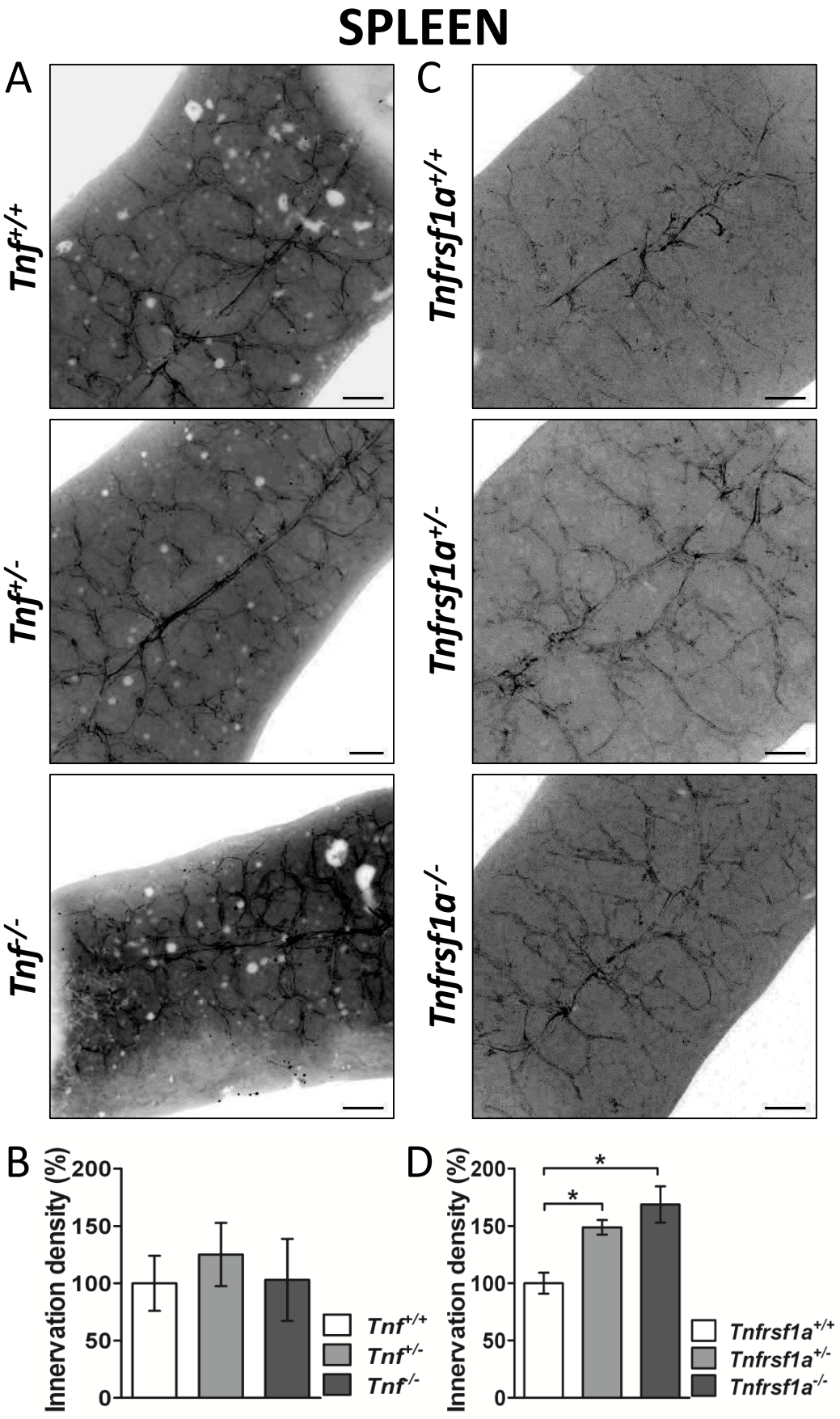

Fig. 3.1. Legend on following page.

Figure 3.1. Sympathetic Innervation of the PVG-Innervated Spleen in Wild-Type, and *Tnf* and *Tnfrsf1a* Knockout Mice. (A&C) Representative images of iDISCO-stained whole mount spleens from P6 wild-type, heterozygous and homozygous *Tnf* **(A)** and *Tnfrsf1a* **(C)** knockout mice. Sympathetic nerves are labelled with an anti-tyrosine hydroxylase antibody. Scale bars represent 200 μm. Each image is representative of 8 $Tnf^{+/+}$, 8 $Tnf^{+/-}$, 9 $Tnf^{-/-}$ and 9 $Tnfrsf1a^{+/+}$, 9 $Tnfrsf1a^{+/-}$, 6 $Tnfrsf1a^{-/-}$ animals. **(B&D)** Quantification of innervation density of sympathetic fibres in spleens from P6 wild-type, heterozygous and homozygous *Tnf* **(B)** and *Tnfrsf1a* **(D)** knockout mice. Values were normalised to those obtained from wild-type animals, and data are presented as the mean ± standard error. n is as stated in (A&C). *: $p<0.05$ (Kruskal-Wallis, with Dunn's *post-hoc* test). PVG: prevertebral ganglia (coeliac and superior mesenteric ganglia.

The sympathetic innervation of the stomach of wild-type, heterozygous and homozygous *Tnf* and *Tnfrsf1a* knockout mice was also analysed. Representative images of stomach tissues from each genotype illustrate the typical anatomical distribution of nerve fibres (Fig. 3.2). TH-stained sympathetic fibres start innervating the tissue around the superior opening of the stomach, called the cardia area, and from there they continue their ramification towards other anatomical divisions of the stomach. iDISCO images of stomach tissues revealed that there were no detectable differences in sympathetic fibre density between either $Tnf^{+/+}$, $Tnf^{+/-}$, and $Tnf^{/-}$ littermates, or between $Tnfrsf1a^{+/+}$, $Tnfrsf1a^{+/-}$, and $Tnfrsf1a^{-/-}$ littermates (Fig. 3.2A & 3.2C). Quantification of sympathetic fibres in the wild-type and *Tnf* knockout mice demonstrated that innervation densities were not significantly different between the three genotypes (Fig. 3.2B). Similarly, there were no significant differences in the TH immunofluorescence density between stomach tissues from $Tnfrsf1a^{+/+}$, $Tnfrsf1a^{+/-}$, and $Tnfrsf1a^{-/-}$ littermates (Fig. 3.2D).

These iDISCO experiments demonstrated that manipulation of TNF signalling pathways affected the sympathetic innervation of organs innervated by prevertebral (CG-SMG) neurons in a different manner compared to organs innervated by paravertebral neurons (SCG).

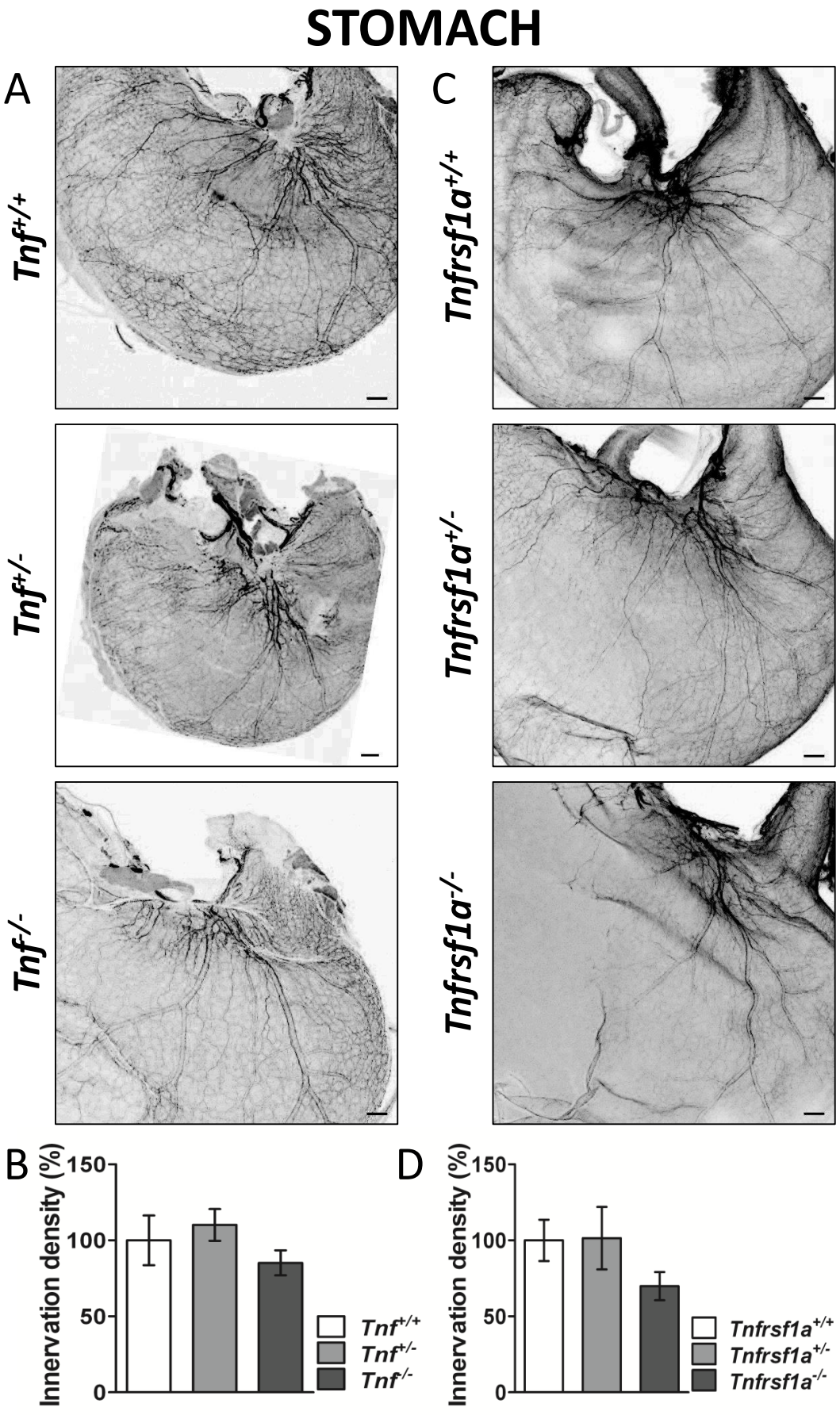

Fig. 3.2. Legend on following page.

Figure 3.2. Sympathetic Innervation of the PVG-Innervated Stomach in Wild-Type, and *Tnf* and *Tnfrsf1a* Knockout Mice. (A&C) Representative images of iDISCO-stained whole mount stomachs from P6 wild-type, heterozygous and homozygous *Tnf* **(A)** and *Tnfrsf1a* **(C)** knockout mice. Sympathetic nerves are labelled with an anti-tyrosine hydroxylase antibody. Scale bars represent 200 μm. Each image is representative of 8 $Tnf^{+/+}$, 8 $Tnf^{+/-}$, 8 $Tnf^{-/-}$ and 9 $Tnfrsf1a^{+/+}$, 7 $Tnfrsf1a^{+/-}$, 8 $Tnfrsf1a^{-/-}$ animals. **(B&D)** Quantification of innervation density of sympathetic fibres in stomachs from P6 wild-type, heterozygous and homozygous *Tnf* **(B)** and *Tnfrsf1a* **(D)** knockout mice. Values were normalised to those obtained from wild-type animals, and data are presented as the mean ± standard error. n is as stated in (A&C). PVG: prevertebral ganglia (coeliac and superior mesenteric ganglia).

3.2.2 The Different Contribution of TNFR1-Activated TNF-α Reverse Signalling to the Development of Paravertebral and Prevertebral Neurons

The iDISCO experiments clearly indicated that deletion of *Tnf* and *Tnfrsf1a* was not associated with hypoinnervation in PVG-innervated target organs, as was previously reported for SCG-innervated target organs. Kisiswa *et al.* demonstrated that TNFR1 is released from target organs and acts as a ligand for TNF-α to enhance SCG innervation into the target organs through TNF-α reverse signalling (Kisiswa et al. 2013). The marked differences between the innervation of SCG-innervated target organs and CG-SMG-innervated target organs led to an investigation to determine whether these differences were due to different responses of paravertebral and prevertebral neurons to TNF-α reverse signalling. To test this, SCG (as a positive control) and CG-SMG were dissected from litters of CD1 pups on postnatal day 0 (P0). P0 is a developmental time-point at which both paravertebral and prevertebral neurons are innervating their sympathetic target organs (Glebova and Ginty 2005). Sympathetic ganglia from all the pups in a litter (average litter size was 10-15 pups) were pooled, with paravertebral ganglia separated from prevertebral ganglia. These postnatal SCG and CG-SMG neurons were then dissociated and seeded into low-density cultures in the presence of NGF to sustain neuron survival and to promote axon growth. Sympathetic neuron cultures were supplemented with soluble, divalent TNFR1 fusion protein (TNFR1-Fc chimera, in which the extracellular domains of two TNFR1 molecules are linked to the Fc part of the human IgG1 antibody (Eissner et al. 2000)) to determine whether TNFR1-activated TNF-α-mediated reverse signalling enhances axon growth. The TNFR1-Fc chimera has been proven to be a strong reverse-signalling ligand for TNF-α activation in both immune cells and neurons (Eissner et al. 2004; Kisiswa et al. 2013).

After 18 h incubation, dissociated P0 SCG neurons treated with TNFR1-Fc had larger and more branched neurons than those incubated with NGF alone (Fig. 3.3A). Quantification of the size and complexity of SCG neuron arbours showed that those treated with TNFR1-Fc had significantly increased neurite

elongation and higher numbers of branch points than the NGF-only control groups (Fig. 3.3B & 3.3C respectively). Sholl profiles, which count neurite intersections with virtual concentric rings at a given distance from the soma to measure neurite complexity, also confirmed that SCG neurons supplemented with TNFR1-Fc were more complex than neurons cultured with NGF alone (Fig. 3.3D).

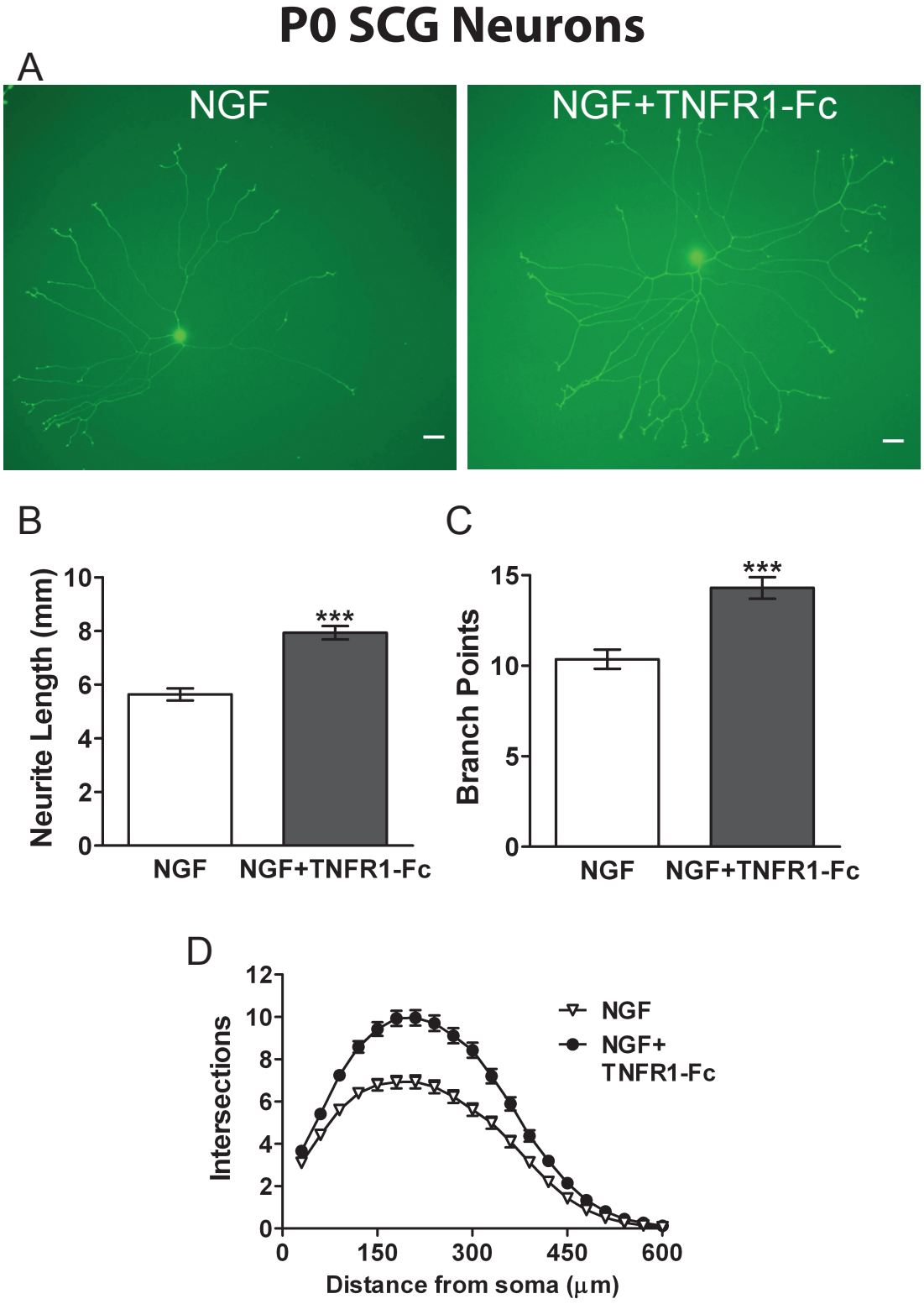

Fig. 3.3. Legend on following page.

Figure 3.3. TNFR1-Promoted TNF-α Reverse Signalling in Po SCG Neurons. (A) Representative images of calcein-AM stained SCG neurons from Po wild-type mice treated with 10 ng/ml NGF ± 30 ng/ml TNFR1-Fc. Scale bars represent 50 µm. Each image is representative of 180 images from at least three experiments. **(B&C)** Quantification of neurite lengths **(B)** and branch points **(C)** of Po wild-type SCG neurons treated as described in (A). Data are presented as the mean ± standard error. Results were collected from the analysis of at least 180 neurons per condition, with at least three separate experiments performed for each condition (60 to 80 neurons analysed per experiment). ***: $p<0.001$ (Mann-Whitney test). **(D)** Sholl analysis of Po wild-type SCG neurons treated as described in (A). Data are presented as the mean ± standard error. At least three separate experiments were performed for each condition (60 to 80 neurons analysed per experiment). NGF: nerve growth factor; SCG: superior cervical ganglia.

The same experimental set-up and conditions were then used to examine the contribution of TNFR1-promoted TNF-α reverse signalling to the growth of PVG neuron processes. CG-SMG, dissected from the same pups from which the SCG neurons were taken, were dissociated and seeded into low-density cultures and the effect of the TNFR1-Fc chimera was tested. Fig. 3.4A illustrates that there were no differences in the extent of process outgrowth between neurons in TNFR1-Fc-treated and NGF-only conditions. Quantification of the neurite length (Fig. 3.4B), the number of branch points (Fig. 3.4C), and Sholl analysis confirmed that there were no significant differences in any of the measured parameters of neuronal complexity between neuron cultures supplemented with TNFR1-Fc chimera and those containing only NGF (Fig. 3.4D).

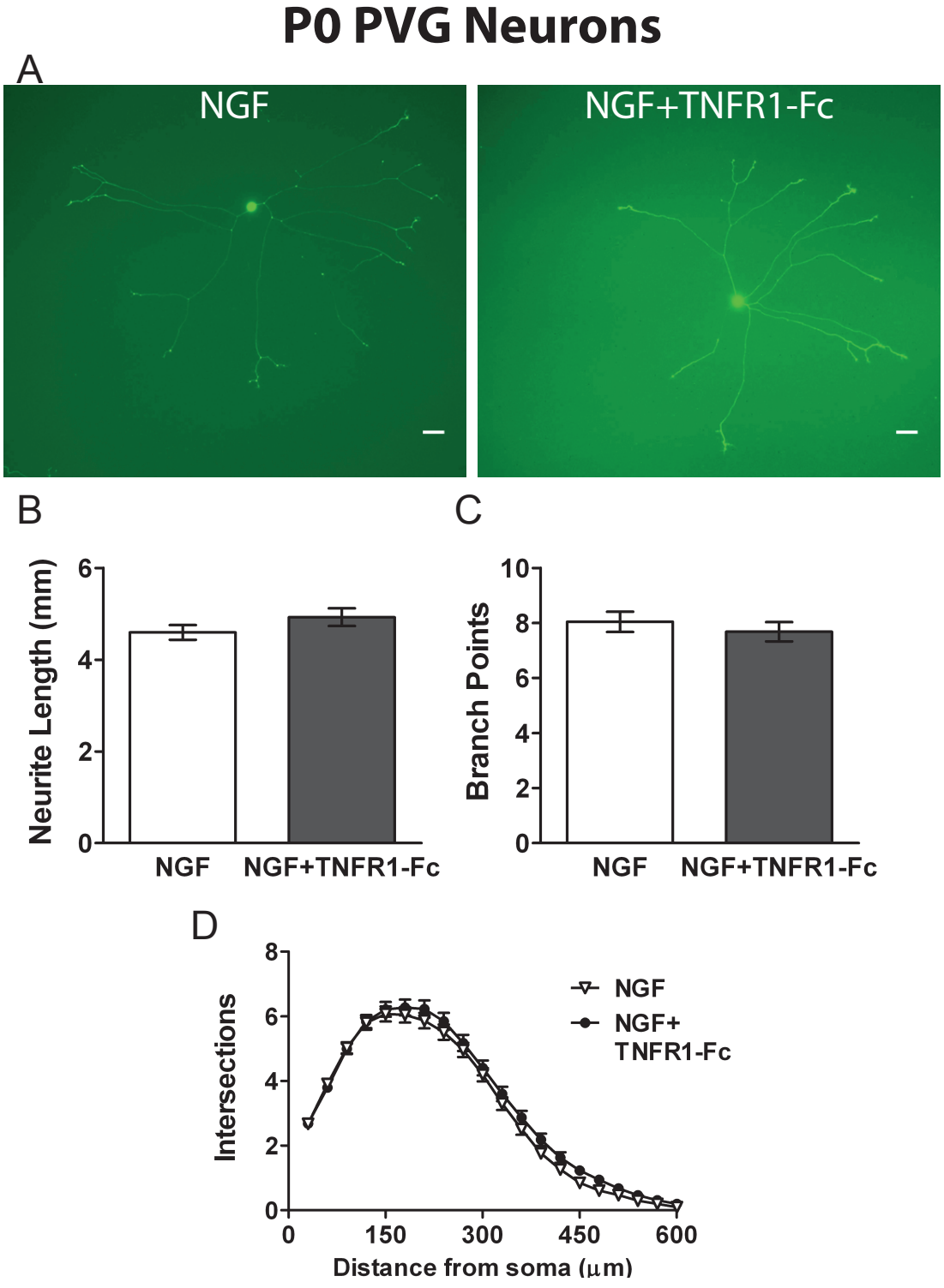

Fig 3.4. Legend on following page.

Figure 3.4. TNFR1-Fc Fails to Activate TNF-α Reverse Signalling in Po PVG Neurons. **(A)** Representative images of calcein-AM stained PVG neurons from Po wild-type mice treated with 10 ng/ml NGF ± 30 ng/ml TNFR1-Fc. Scale bars represent 50 μm. Each image is representative of 180 images from at least three experiments. **(B&C)** Quantification of neurite lengths **(B)** and branch points **(C)** of Po wild-type PVG neurons treated as described in (A). Data are presented as the mean ± standard error. Results were collected from the analysis of at least 180 neurons per condition, with at least three separate experiments performed for each condition (60 to 80 neurons analysed per experiment). **(D)** Sholl analysis of Po wild-type PVG neurons treated as described in (A). Data are presented as the mean ± standard error. At least three separate experiments were performed for each condition (60 to 80 neurons analysed per experiment). NGF: nerve growth factor; PVG: prevertebral ganglia (coeliac and superior mesenteric ganglia).

The modulatory roles of extracellular signals, including TNFSF and TNFRSF members, may be restricted to certain time points during SNS development, depending on the timing of unfolding developmental events. Such events include neuroblast specification and differentiation (between E8-E17), axon growth (between E10-P12), and target organ innervation (between E17-P10) (Glebova and Ginty 2005). Therefore, I investigated the response of SCG and PVG neurons to TNFR1-activated TNF-α reverse signalling at a later time point, P5, to determine whether they have the same responses to P0 neurons at this later stage of target tissue innervation. The ability of TNFR1-Fc to enhance the size and complexity of SCG neuron processes could still be seen at this later stage of development, although its effects were reduced compared to P0 (Fig. 3.5A). Analysis of neurite length and branch point number clearly showed that TNFR1-Fc significantly enhanced SCG neuron process elongation and bifurcation at P5 compared to cultures containing NGF alone (Fig. 3.5B & 3.5C). Sholl analysis also confirmed that P5 SCG neurons had more complex neurite structures when supplemented with TNFR1-Fc compared to neurons cultured with just NGF (Fig. 3.5D). As seen with P0 PVG neurons, P5 PVG neurons also did not respond to TNFR1-Fc with increased process growth and branching at this later developmental stage (Fig. 3.6A). Quantitative analysis showed that TNFR1-Fc did not enhance the mean length or number of branch points of P5 PVG neuron processes compared to NGF-only control cultures (Fig. 3.6B & 3.6C), and Sholl profiles of PVG neurons supplemented with either NGF alone or NGF plus TNFR1-Fc were virtually overlapping (Fig. 3.6D).

In vitro results above have corroborated previous data showing that TNF-α reverse signalling, activated here by TNFR1-Fc, enhances the growth and complexity of paravertebral SCG neuron processes at the developmental ages when their axons would be innervating their target organs *in vivo*. The growth and complexity of prevertebral sympathetic neuron processes however, are not affected by TNFR1-Fc-activated TNF-α reverse signalling when analysed at the same developmental time-points.

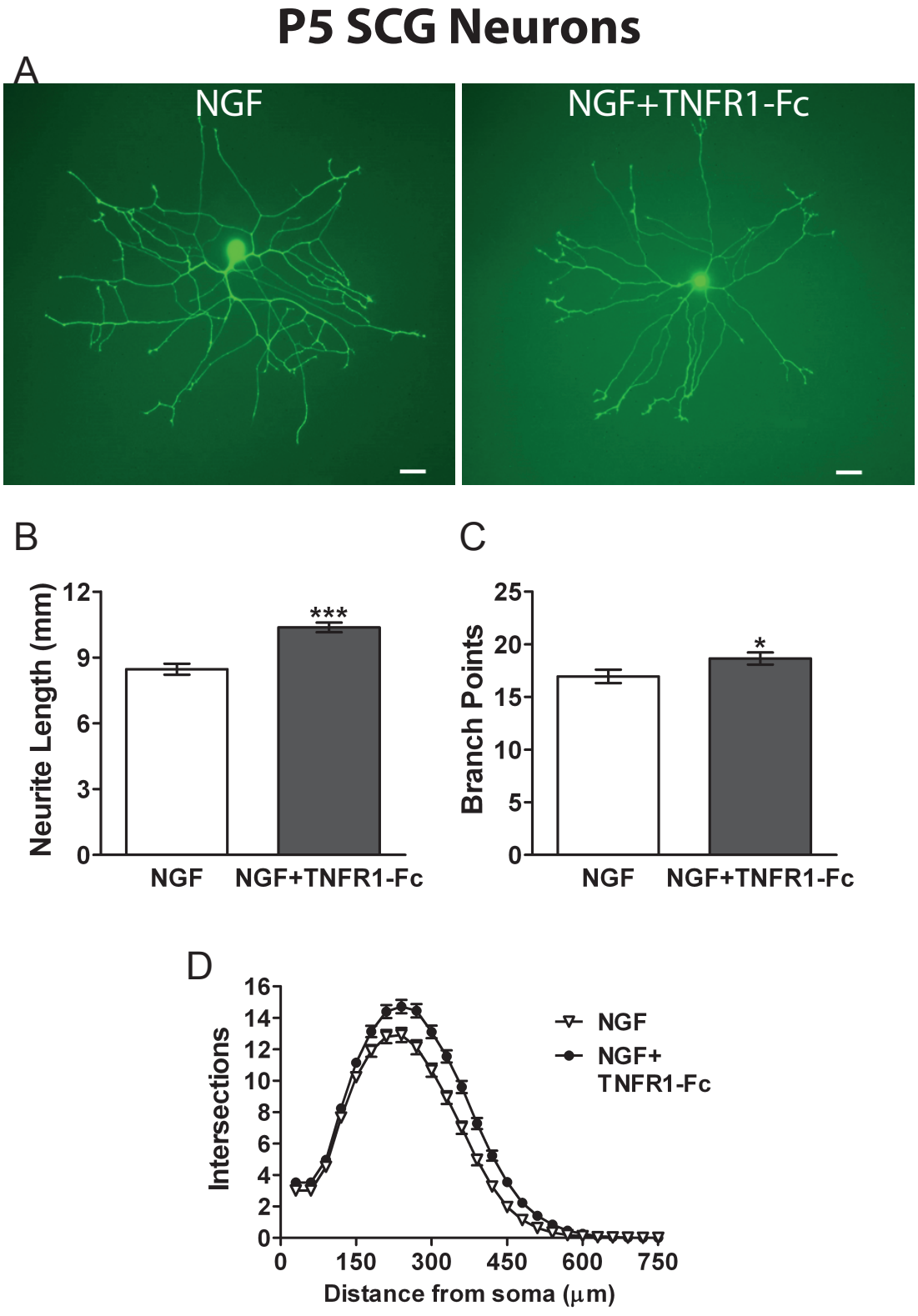

Fig 3.5. Legend on following page.

Figure 3.5. TNFR1-Promoted TNF-α Reverse Signalling in P5 SCG Neurons. (A) Representative images of calcein-AM stained SCG neurons from P5 wild-type mice treated with 10 ng/ml NGF ± 30 ng/ml TNFR1-Fc. Scale bars represent 50 µm. Each image is representative of 180 images from at least three experiments. **(B&C)** Quantification of neurite lengths **(B)** and branch points **(C)** of P5 wild-type SCG neurons treated as described in (A). Data are presented as the mean ± standard error. Results were collected from the analysis of at least 180 neurons per condition, with at least three separate experiments performed for each condition (60 to 80 neurons analysed per experiment). *: $p<0.05$, ***: $p<0.001$ (Mann-Whitney test). **(D)** Sholl analysis of P5 wild-type SCG neurons treated as described in (A). Data are presented as the mean ± standard error. At least three separate experiments were performed for each condition (60 to 80 neurons analysed per experiment). NGF: nerve growth factor; SCG: superior cervical ganglia.

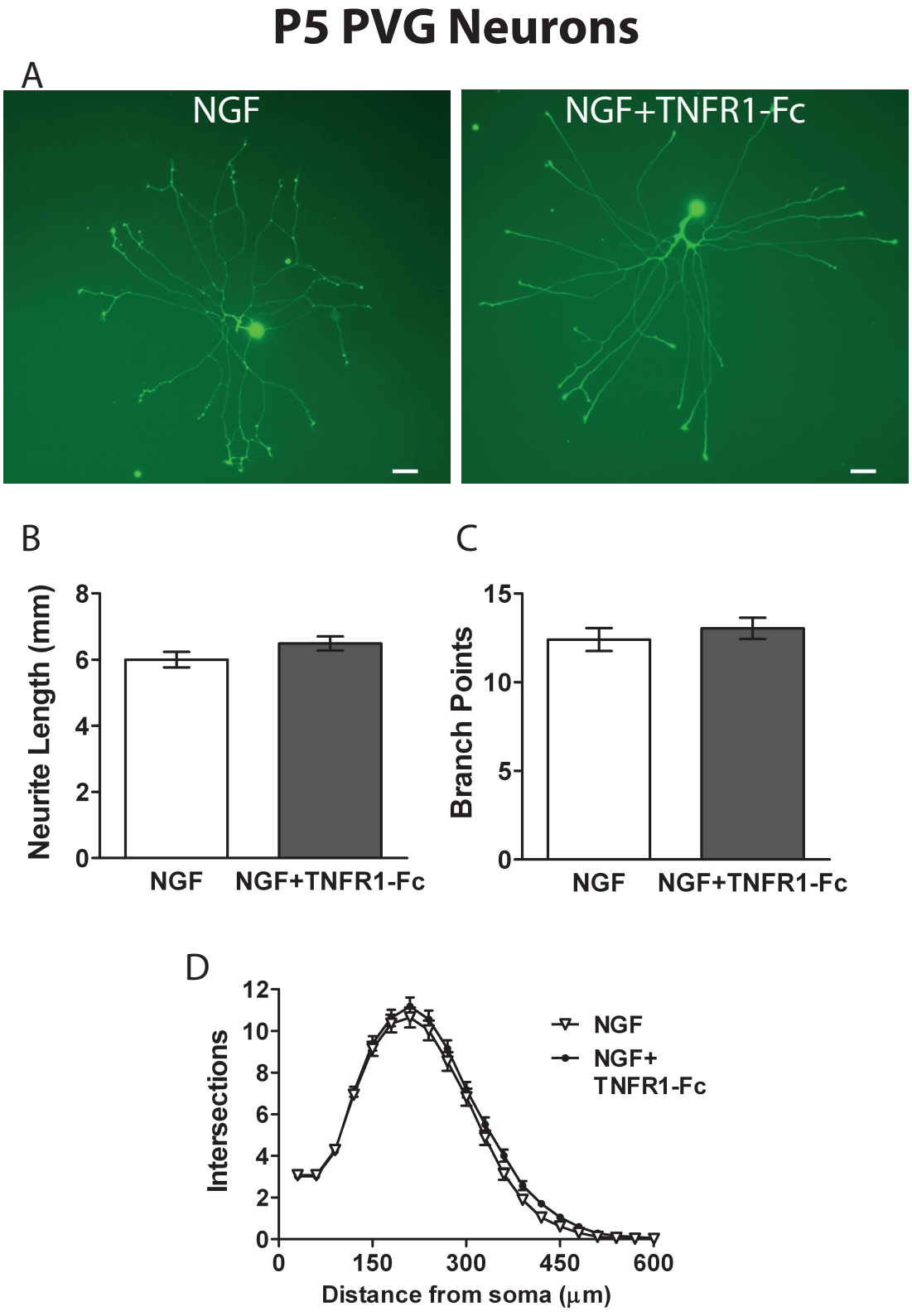

Fig 3.6. Legend on following page.

Figure 3.6. TNFR1-Fc Fails to Activate TNF-α Reverse Signalling in P5 PVG Neurons. **(A)** Representative images of calcein-AM stained PVG neurons from P5 wild-type mice treated with 10 ng/ml NGF ± 30 ng/ml TNFR1-Fc. Scale bars represent 50 μm. Each image is representative of 180 images from at least three experiments. **(B&C)** Quantification of neurite lengths **(B)** and branch points **(C)** of P5 wild-type PVG neurons treated as described in (A). Data are presented as the mean ± standard error. Results were collected from the analysis of at least 180 neurons per condition, with at least three separate experiments performed for each condition (60 to 80 neurons analysed per experiment). **(D)** Sholl analysis of P5 wild-type PVG neurons treated as described in (A). Data are presented as the mean ± standard error. At least three separate experiments were performed for each condition (60 to 80 neurons analysed per experiment). NGF: nerve growth factor; PVG: prevertebral ganglia (coeliac and superior mesenteric ganglia).

3.2.3 TNFR2-Activated TNF-α Reverse Signalling Fails to Enhance Axon Growth in Paravertebral and Prevertebral Neurons

For the past 20 years, studies focusing on tumour progression have characterised the positive and negative regulatory effects of TNFR2-activated TNF-α-mediated reverse signalling in different tumour micro-environments (Qu et al. 2017). These studies have not only identified signalling pathways that play pivotal roles in TNFR2-activated reverse signalling in several different cell lines; they have also succeeded in targeting these TNFR2-activated reverse signalling pathways in the development of treatment strategies for chronic destructive diseases, such as rheumatoid arthritis (Brennan et al. 2002; Rossol et al. 2007; Qu et al. 2017). To determine whether TNFR2-activated TNF-α-mediated reverse signalling also plays a role in SNS development, cultured P0 paravertebral and PVG sympathetic neurons were supplemented with either NGF alone or NGF plus TNFR2-Fc chimera, adopting the same experimental procedures as described for the analysis of the effects of TNFR1-Fc.

No changes in the length and degree of branching of P0 sympathetic neuron processes were seen in response to TNFR2-Fc treatment. Fig. 3.7 shows the analysis of SCG neurons cultured with NGF, either with or without the addition of TNFR2-Fc. Quantification of mean neurite length, number of branch points and Sholl analysis demonstrated that TNFR2-Fc had no significant effect on the growth of P0 SCG neuron processes (Fig. 3.7A-C). It is important to note that the culture experiments investigating the regulatory role of TNFR2 in SCG neurons (Fig. 3.7) were carried out only once (instead of three times; the only occurrence of this in this thesis). This resulted in a relatively smaller total neuron sample size (80 neurons analysed instead of a minimum of 180 neurons), and the error bars are subsequently larger than their equivalents in other sections. Similarly, inspection of neurite process growth and complexity of P0 PVG neurons demonstrated that supplementing these neurons with TNFR2-Fc in the presence of NGF did not have any significant effect on the growth or nature of PVG neuron processes when compared with NGF-only controls (Fig. 3.8A-C).

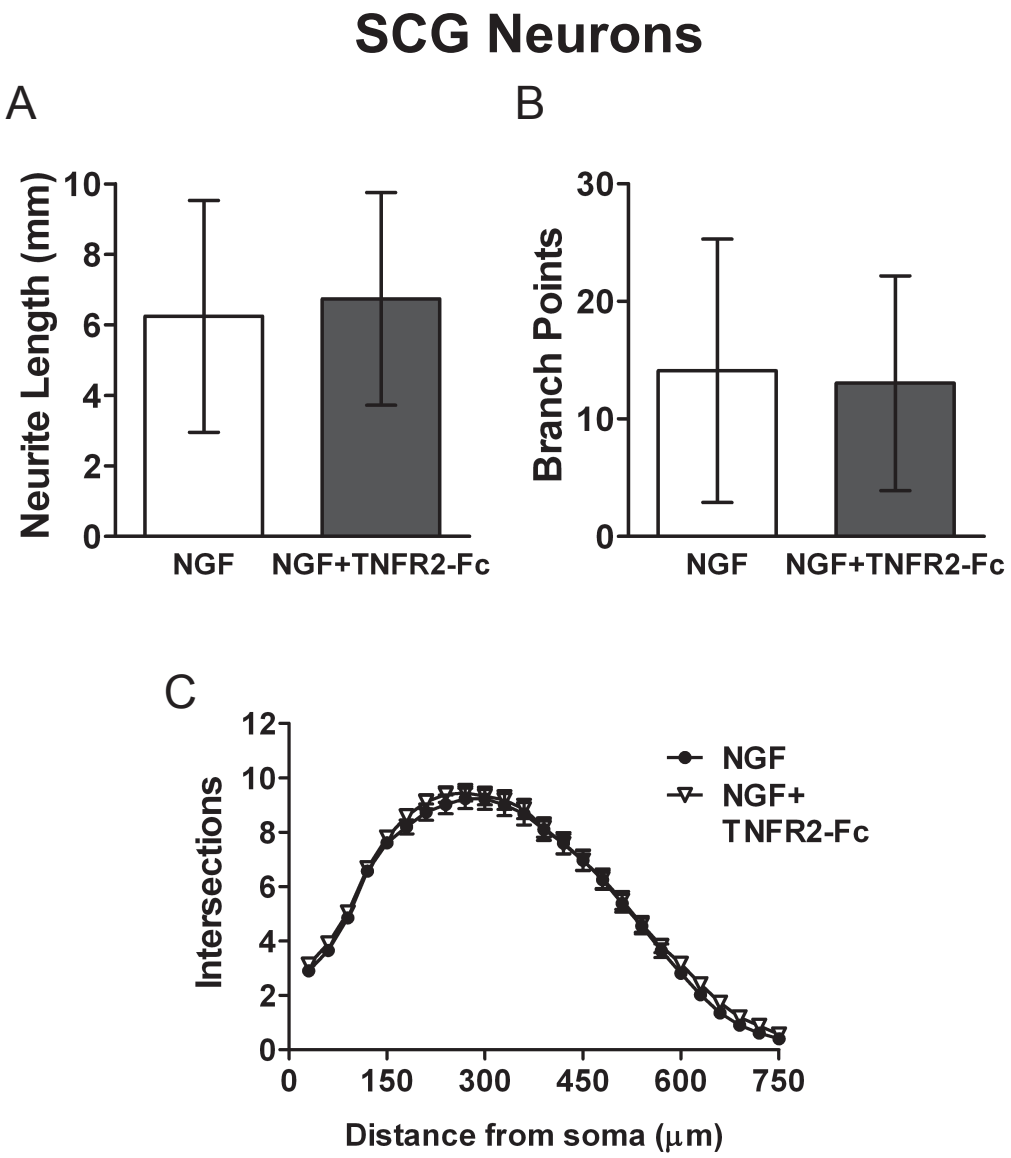

Figure 3.7. TNFR2-Fc Fails to Activate TNF-α Reverse Signalling in Po SCG Neurons. (A&B) Quantification of neurite lengths **(A)** and branch points **(B)** of Po wild-type SCG neurons treated with 10 ng/ml NGF ± 50 ng/ml TNFR2-Fc. Data are presented as the mean ± standard error. Results were collected from the analysis of at least 60 neurons per condition. **(C)** Sholl analysis of Po wild-type SCG neurons treated as described in (A&B). Data are presented as the mean ± standard error. At least 60 neurons were analysed per condition. NGF: nerve growth factor; SCG: superior cervical ganglia.

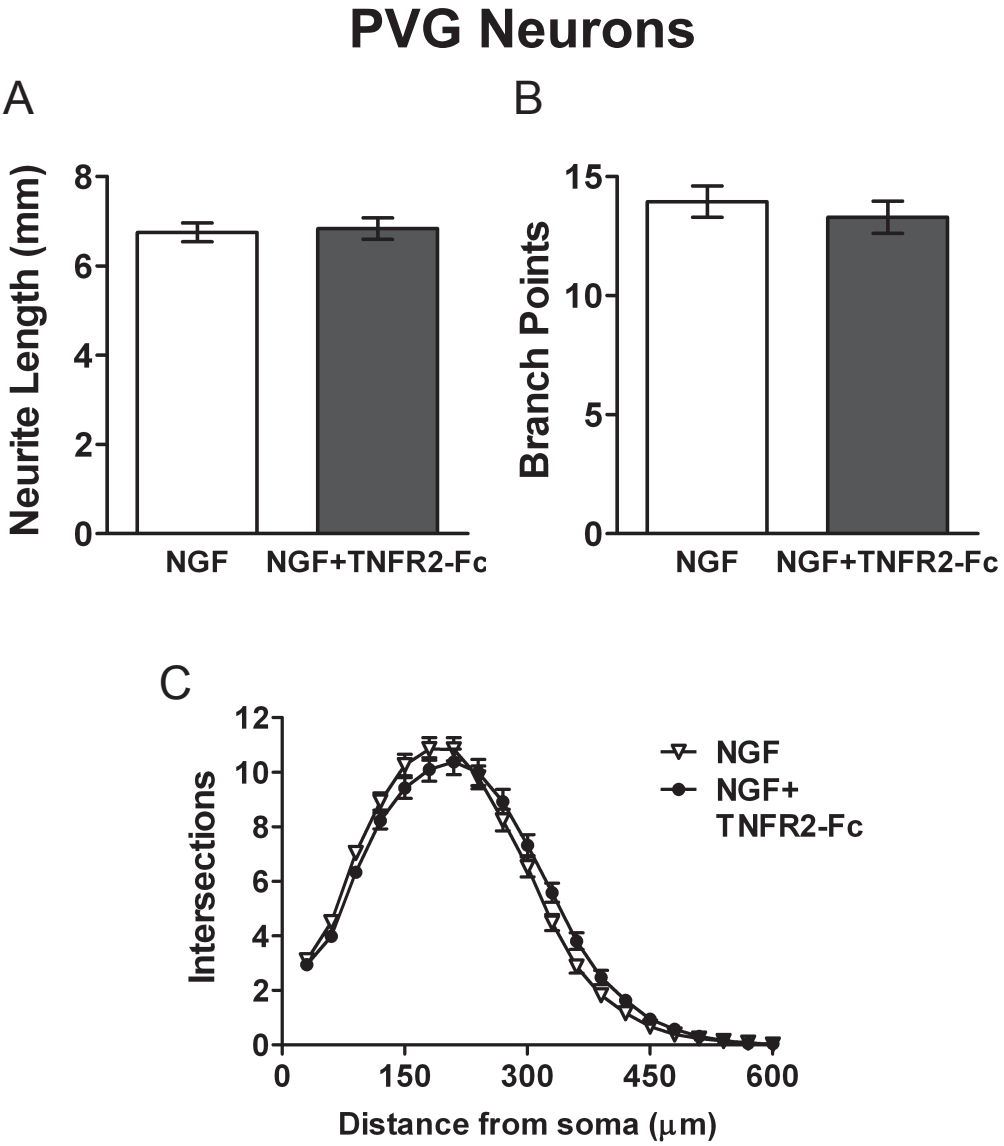

Figure 3.8. TNFR2-Fc Fails to Activate TNF-α Reverse Signalling in Po PVG Neurons. (A&B) Quantification of neurite lengths **(A)** and branch points **(B)** of Po wild-type PVG neurons treated with 10 ng/ml NGF ± 50 ng/ml TNFR2-Fc. Data are presented as the mean ± standard error. At least three separate experiments were performed for each condition (60 to 80 neurons analysed per experiment). **(C)** Sholl analysis of Po wild-type PVG neurons treated as described in (A&B). Data are presented as the mean ± standard error. At least three separate experiments were performed for each condition (60 to 80 neurons analysed per experiment). NGF: nerve growth factor; PVG: prevertebral ganglia (coeliac and superior mesenteric ganglia).

3.2.4 TNF-α-activated TNFR1-mediated Forward Signalling Suppresses NGF-Promoted Axon Growth in Both Paravertebral and Prevertebral Neurons

Prior to the discovery of TNF-α reverse signalling, Gutierrez *et al.* reported that in the presence of NGF, dissociated SCG neuron cultures incubated with sTNF-α show significant reductions in both total process length and branch complexity (Gutierrez et al. 2008). They demonstrated that this suppressive effect of sTNF-α *in vitro* is dependent on TNF-α-activated TNFR1-mediated forward signalling and downstream NF-κB transcriptional activity. Given the different responses of paravertebral SCG and prevertebral CG-SMG neurons to TNF-α-mediated reverse signalling in this chapter, the question arose as to whether TNF-α-activated forward signalling would function to suppress neuronal process growth from prevertebral neurons in the same manner as it does from paravertebral neurons. To investigate TNF-α-activated TNFR1-mediated forward signalling in sympathetic neurons, Po SCG and PVG neurons were treated with sTNF-α in the presence of NGF. To conduct experiments, the same experimental parameters were used as described in detail in **Section 3.2.2**.

Fig. 3.9A shows that NGF+sTNF-α-treated Po SCG neurons had smaller neurites and fewer neurite arbours compared with neurons treated with NGF only. The significant suppressive effect of sTNF-α on total neurite length and the number of branch points are illustrated in Fig. 3.9B & 3.9C, respectively. Fig. 3.9D shows Sholl analysis comparing the overall neurite morphology of NGF-only and NGF+sTNF-α-treated SCG neurons. The overall reduction that was detected in the complexity of the neurite arbours in sTNF-α-treated SCG neurons corroborates previous findings that sTNF-α significantly suppresses NGF-promoted neurite elongation in SCG neurons (Gutierrez et al. 2008).

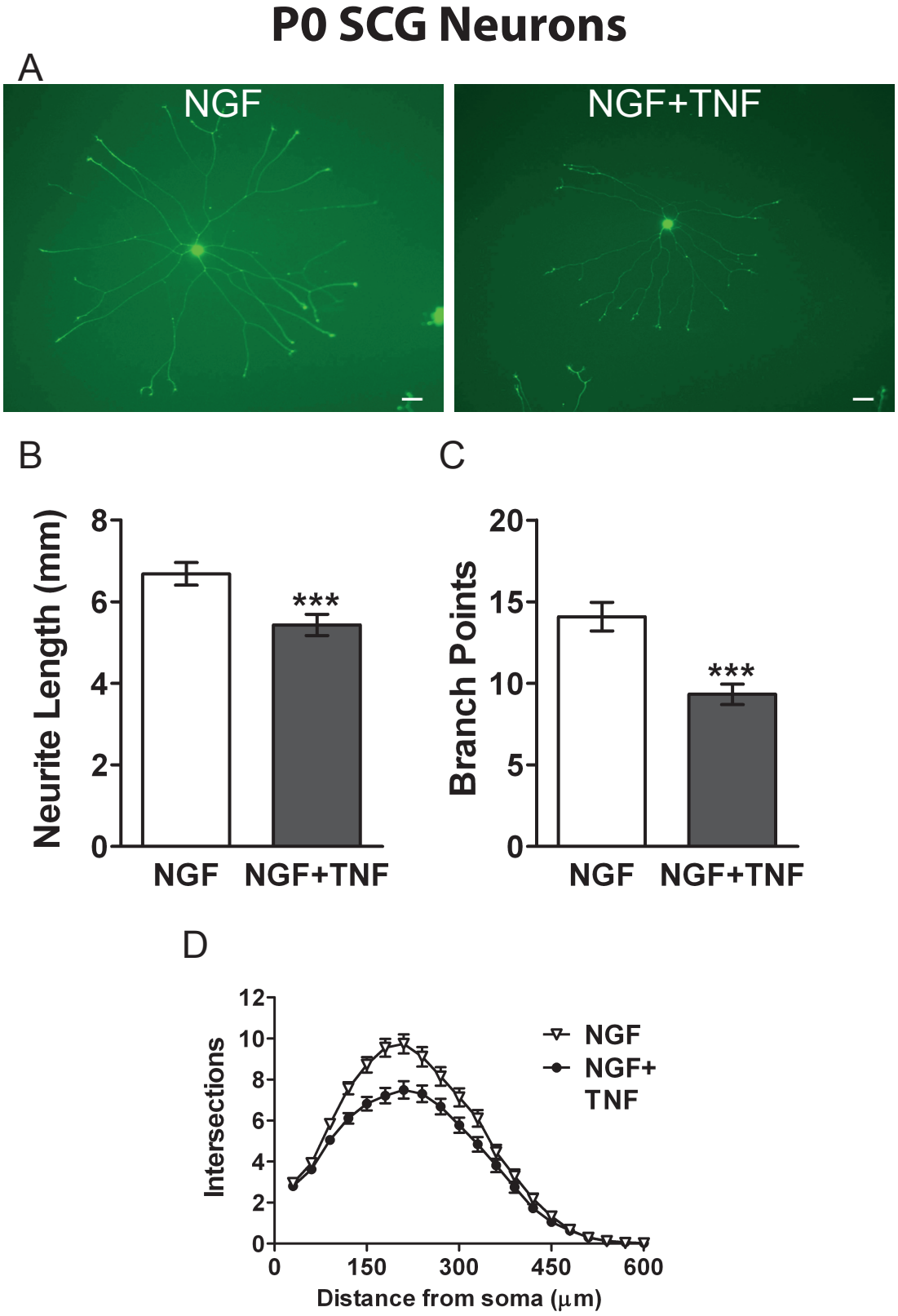

Fig 3.9. Legend on following page.

Figure 3.9. TNF-α-Activated TNFR1-Mediated Forward Signalling in Po SCG Neurons. **(A)** Representative images of calcein-AM stained SCG neurons from Po wild-type mice treated with 10 ng/ml NGF ± 50 ng/ml soluble TNF-α. Scale bars represent 50 μm. Each image is representative of 180 images from at least three experiments. **(B&C)** Quantification of neurite lengths **(B)** and branch points **(C)** of Po wild-type SCG neurons treated as described in (A). Data are presented as the mean ± standard error. Results were collected from the analysis of at least 180 neurons per condition, with at least three separate experiments performed for each condition (60 to 80 neurons analysed per experiment). ***: $p<0.001$ (Mann-Whitney test). **(D)** Sholl analysis of Po wild-type SCG neurons treated as described in (A). Data are presented as the mean ± standard error. At least three separate experiments were performed for each condition (60 to 80 neurons analysed per experiment). NGF: nerve growth factor; SCG: superior cervical ganglia.

Fig. 3.10A illustrates PVG neurons grown in low-density dissociated cultures, either in the presence of NGF alone (control condition) or NGF+sTNF-α. The neurite growth-inhibitory effect of sTNF-α seen in Po SCG neurons was also seen in Po PVG neurons. Treating Po PVG neurons with sTNF-α caused a marked reduction in both total neurite length and branch points (Fig. 3.10B & 3.10C, respectively). These clear inhibitory effects of sTNF-α on the growth of PVG neurons are reflected by the Sholl profile of PVG neurons with or without sTNF-α (Fig. 3.10D).

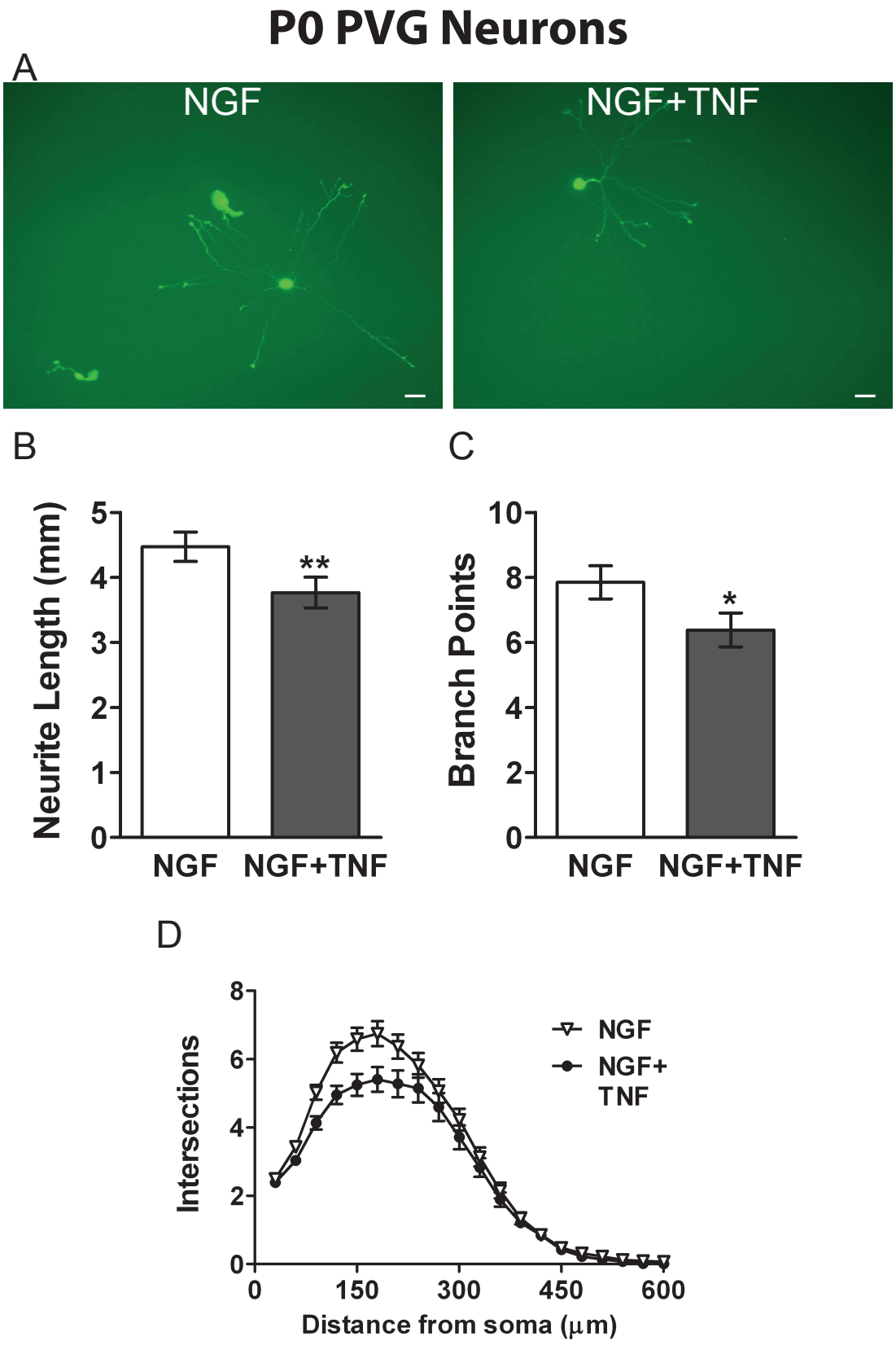

Fig 3.10. Legend on following page.

Figure 3.10. TNF-α-Activated TNFR1-Mediated Forward Signalling in Po PVG Neurons. **(A)** Representative images of calcein-AM stained PVG neurons from Po wild-type mice treated with 10 ng/ml NGF ± 50 ng/ml soluble TNF-α. Scale bars represent 50 μm. Each image is representative of 180 images from at least three experiments. **(B&C)** Quantification of neurite lengths **(B)** and branch points **(C)** of Po wild-type PVG neurons treated as described in (A). Data are presented as the mean ± standard error. Results were collected from the analysis of at least 180 neurons per condition, with at least three separate experiments performed for each condition (60 to 80 neurons analysed per experiment). *: $p<0.05$, **: $p<0.01$ (Mann-Whitney test). **(D)** Sholl analysis of Po wild-type PVG neurons treated as described in (A). Data are presented as the mean ± standard error. At least three separate experiments were performed for each condition (60 to 80 neurons analysed per experiment). NGF: nerve growth factor; PVG: prevertebral ganglia (coeliac and superior mesenteric ganglia).

The response of P5 SCG and PVG neurons to sTNF-α was examined to ascertain whether the neuronal responses of paravertebral and prevertebral sympathetic neurons to sTNF-α differ at later developmental stages when those neurons are nearer to completing target tissue innervation. Similar to P0 SCG neurons, sTNF-α diminished neurite growth in P5 SCG neurons compared to neurons supplemented only with NGF (Fig. 3.11A). After quantification, significant decreases were detected in the total neurite length (Fig. 3.11B) and number of branch points of neurons cultured with sTNF-α (Fig. 3.11C). The Sholl profile of sTNF-α-treated SCG neurons (Fig 3.11D) also showed a less complex neurite morphology. Importantly, the neurite growth-inhibitory effect of sTNF-α on PVG neurons, seen at P0, disappeared by the P5 developmental time point (Fig. 3.12A). There were no significant differences in total neurite length and branch points between NGF-only and NGF+sTNF-α-treated PVG neurons (Fig. 3.12B & 3.12C, respectively). There were also negligible differences in the Sholl profiles of PVG neurons grown with or without sTNF-α (Fig. 3.12D).

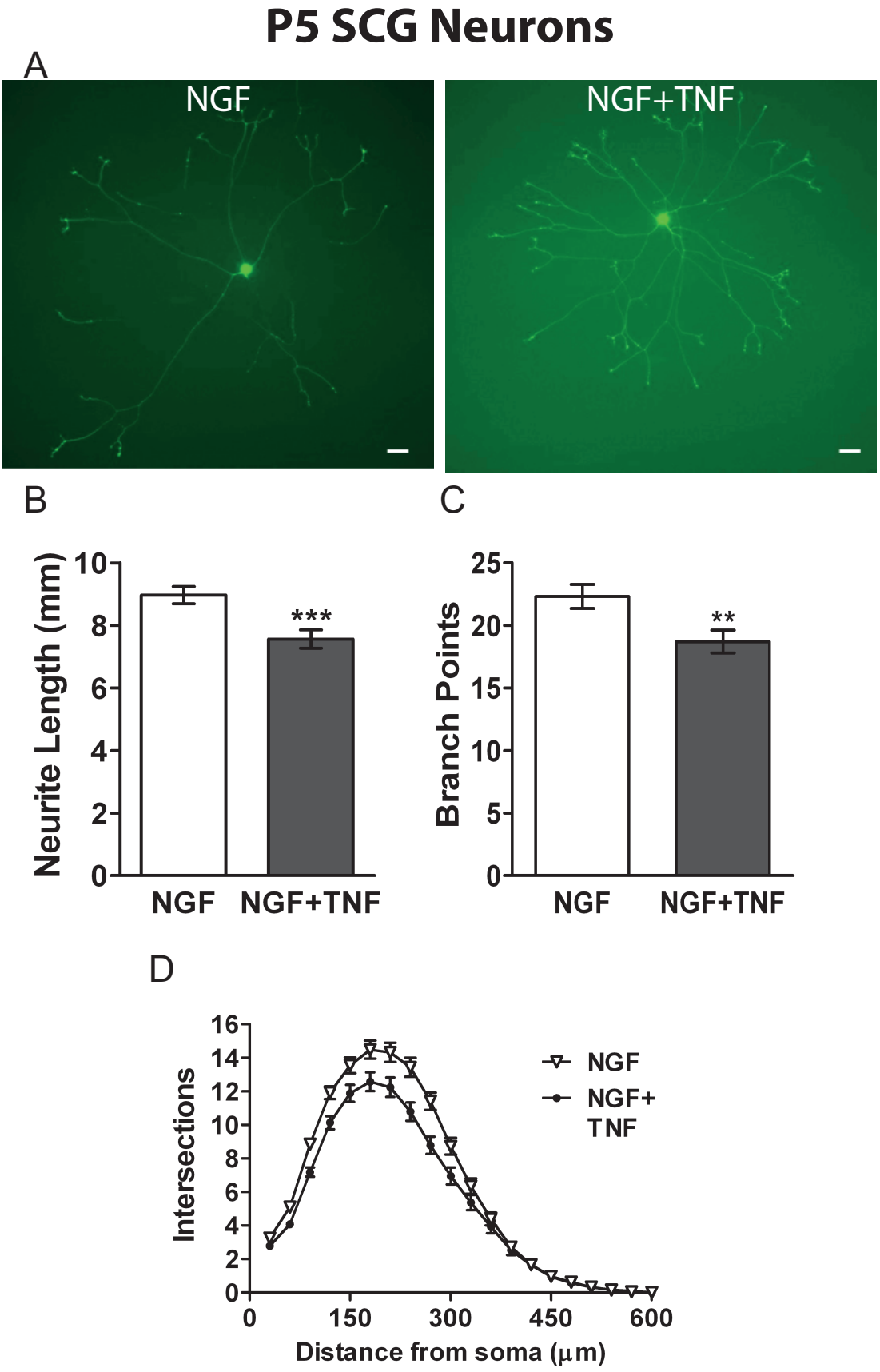

Fig 3.11 Legend on following page.

Figure 3.11. TNF-α-Activated TNFR1-Mediated Forward Signalling in P5 SCG Neurons. (A) Representative images of calcein-AM stained SCG neurons from P5 wild-type mice treated with 10 ng/ml NGF ± 50 ng/ml soluble TNF-α. Scale bars represent 50 μm. Each image is representative of 180 images from at least three experiments. **(B&C)** Quantification of neurite lengths **(B)** and branch points **(C)** of P5 wild-type SCG neurons treated as described in (A). Data are presented as the mean ± standard error. Results were collected from the analysis of at least 180 neurons per condition, with at least three separate experiments performed for each condition (60 to 80 neurons analysed per experiment). **: $p<0.01$, ***: $p<0.001$ (Mann-Whitney test). **(D)** Sholl analysis of P5 wild-type SCG neurons treated as described in (A). Data are presented as the mean ± standard error. At least three separate experiments were performed for each condition (60 to 80 neurons analysed per experiment). NGF: nerve growth factor; SCG: superior cervical ganglia.

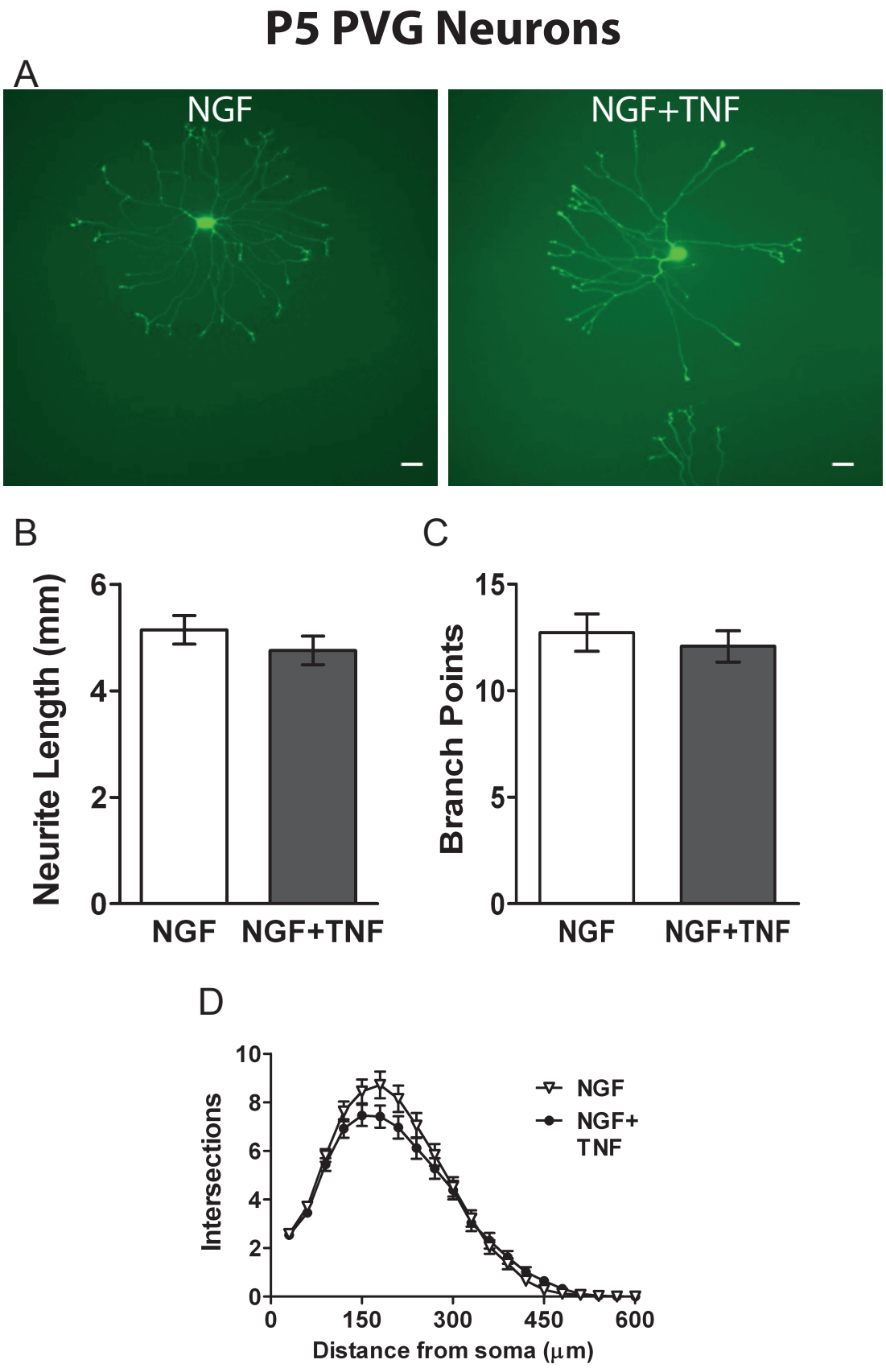

Fig 3.12. Legend on following page.

Figure 3.12. TNF-α-Activated TNFR1-Mediated Forward Signalling in P5 PVG Neurons. **(A)** Representative images of calcein-AM stained PVG neurons from P5 wild-type mice treated with 10 ng/ml NGF ± 50 ng/ml soluble TNF-α. Scale bars represent 50 μm. Each image is representative of 180 images from at least three experiments. **(B&C)** Quantification of neurite lengths **(B)** and branch points **(C)** of P5 wild-type PVG neurons treated as described in (A). Data are presented as the mean ± standard error. Results were collected from the analysis of at least 180 neurons per condition, with at least three separate experiments performed for each condition (60 to 80 neurons analysed per experiment). **(D)** Sholl analysis of P5 wild-type PVG neurons treated as described in (A). Data are presented as the mean ± standard error. At least three separate experiments were performed for each condition (60 to 80 neurons analysed per experiment). NGF: nerve growth factor; PVG: prevertebral ganglia (coeliac and superior mesenteric ganglia).

3.2.5 TNF-α Suppresses Neurite Growth from Different Morphological Regions of Paravertebral and Prevertebral Sympathetic Neurons

Receptors that mediate signal transduction in response to binding of extracellular proteins can be located on different morphological regions of neurons, such as axons, dendrites, or the soma (Ludwig and Pittman 2003; Ludwig and Leng 2006). Kisiswa *et al*. demonstrated that during TNF-α-mediated reverse signalling, TNFR1 binds to its receptor proteins (TNF-α) located on the processes of SCG neurons. However, when they examined TNFR1-mediated forward signalling they found that sTNF-α binds its receptor proteins (TNFR1) located on the soma of SCG neurons (Gutierrez et al. 2008; Kisiswa et al. 2013). Given the *in vivo* and *in vitro* evidence showing that paravertebral and prevertebral sympathetic neurons differ in responses to TNF-related signalling pathways during the innervation of sympathetic target organs, the morphological regions in which TNF-α forward and reverse signalling occurs in PVG neurons was investigated to determine whether this may partly explain the differences in the response of SCG and PVG neurons to TNFR1-Fc and sTNF-α.

To investigate the responses of sympathetic neurons to TNF-α forward and reverse signalling from both soma and processes separately, cell bodies and neurites of cultured Po SCG and PVG neurons were isolated by the use of microfluidic devices. These devices enable users to contain the soma and neurites of a neuron in different compartments, which can be then filled with media supplemented with different factors, thus users are able to assess regional responses of neurons to different media supplements (see Fig. 2.1). The microfluidic culture platform used in these experiments consisted of two main channels separated by 150 μm, high fluidic-resistant, microgrooves. To maintain separation of factors across the two compartments, a larger volume of growth media was used in the wells of one side of the device. The different volumes on each side created hydrostatic pressure which prevented diffusion of soluble compounds across the microgroove (the fluidic integrity of these compartments was previously demonstrated in detail (Taylor et al. 2005)).

Po SCG or PVG neurons were loaded into the soma compartments of these microfluidic devices. Both soma and axon compartments were supplemented with 10 ng/ml NGF to sustain neuron survival, and to enhance axon growth through the arrays of axon-guiding micro-channels into the axon compartment. sTNF-α (to test forward signalling) or TNFR1 (to test reverse signalling) were added either to the soma compartment or to the axon compartment, or excluded from both compartments. Cell cultures were incubated for 18 h, then the fluorescent vital dye, calcein-AM was added only into the axon compartment. The calcein-AM dye retrogradely labelled cells, enabling tracing back to the cell bodies of neurons projecting their axons through the micro-channels. A stereological method was used to quantify neurite elongation into the axonal compartment relative to the number of cell bodies detected in the soma compartment (see **Section 2.4** in **Chapter 2**). All imaging and quantification processes were performed blind to treatment conditions.

Fig. 3.13A shows NGF-only and NGF+sTNF-α-treated Po SCG neurons with their soma and neurites isolated into different compartments, immediately after they were loaded with calcein-AM dye through their neurites. Images vividly show the reduced neurite density in the axonal compartment of SCG neurons that were exposed to sTNF-α through their cell soma, compared with NGF-only treated SCG neurons. Quantification of the neurite length of SCG neurons revealed a highly significant decrease in the neurite growth of SCG neurons when they were exposed to sTNF-α only at their cell soma. However, addition of sTNF-α to the axon compartment did not affect the growth of SCG axons compared with NGF-only treated SCG neurons (Fig. 3.13B).

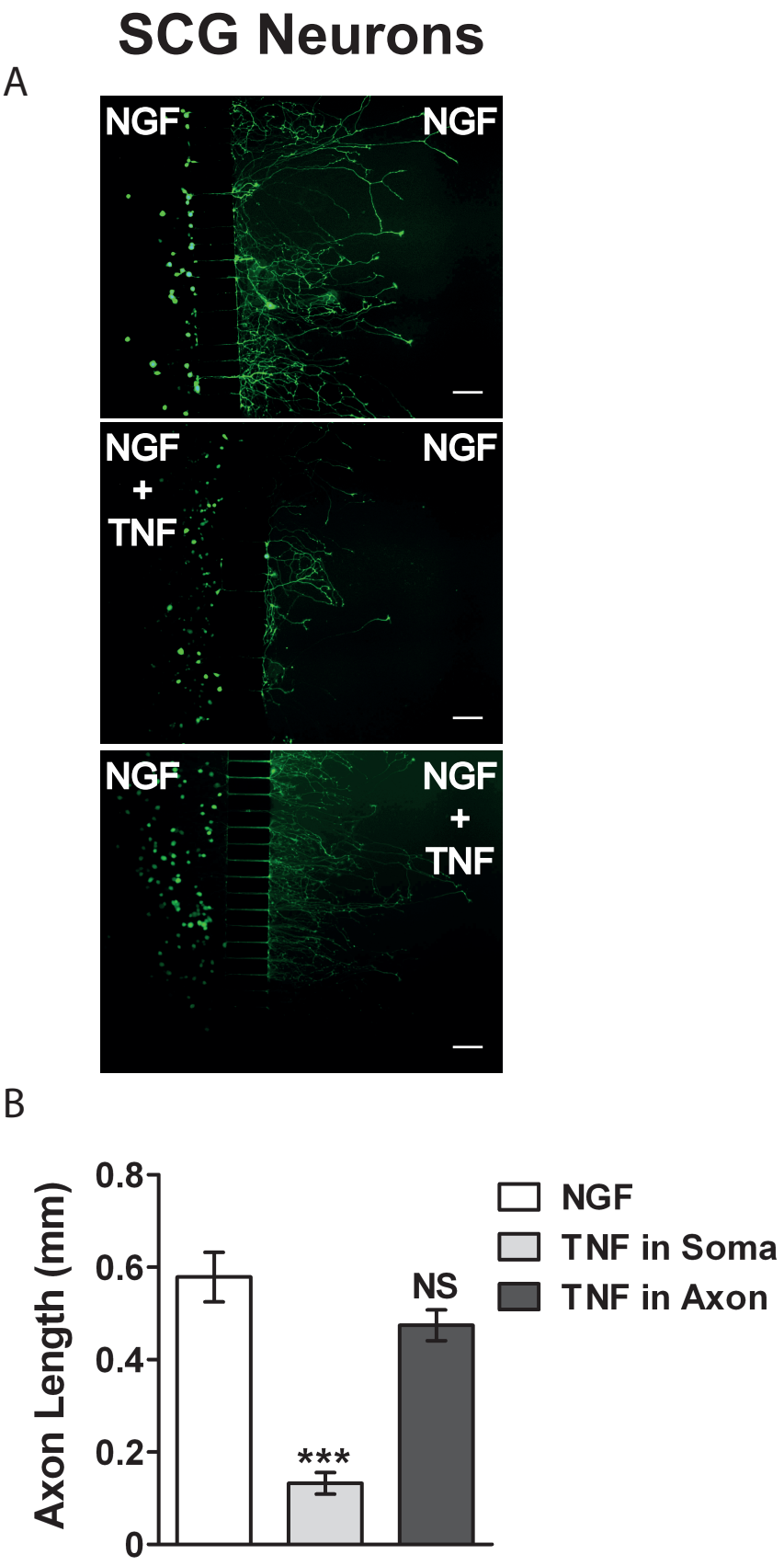

Fig 3.13. Legend on following page.

Figure 3.13. TNF-α-Promoted TNFR1-Mediated Forward Signalling from Soma and Axonal Compartments of Po SCG Neurons. (A) Representative images of calcein-AM stained SCG neurons from Po wild-type mice treated with 10 ng/ml NGF, with 50 ng/ml soluble TNF-α in either the soma (left) or axonal (right) compartment or neither. Scale bars represent 100 μm. Each image is representative of three experiments. **(B)** Quantification of axon lengths of Po wild-type SCG neurons treated as described in (A). Data are presented as the mean ± standard error. n=3 for each condition. ***: $p<0.001$ (Kruskal-Wallis, with Dunn's *post-hoc* analysis). NGF: nerve growth factor; NS: not significant; SCG: superior cervical ganglia.

Fig. 3.14A displays the soma and neurites of Po PVG neurons after they were cultured with or without sTNF-α-treatment in isolated compartments of a microfluidic device. Images indicate that the neurite density of PVG neurons in the axon compartment declined when sTNF-α was added to the axon compartment, compared with NGF-only treated PVG neurons. Quantification of the total neurite lengths in both the axon-supplemented neurons and the NGF-only neurons revealed that axonal treatment with sTNF-α resulted in a decrease in total neurite lengths. Representative images suggest that sTNF-α-did not significantly decrease neurite density when sTNF-α was added to the soma compartment of PVG compartment cultures (Fig. 3.14A) and this observation was borne out by quantification of the neurite length of PVG neurons following supplementation of the cell soma compartment with sTNF-α (Fig. 3.14B). The standard error of the PVG control group in this experiment was larger than other groups, as NGF-only treated PVG neurons showed inconsistent outgrowth in one of the three experimental repeats. This should be taken into consideration during the interpretation of the data.

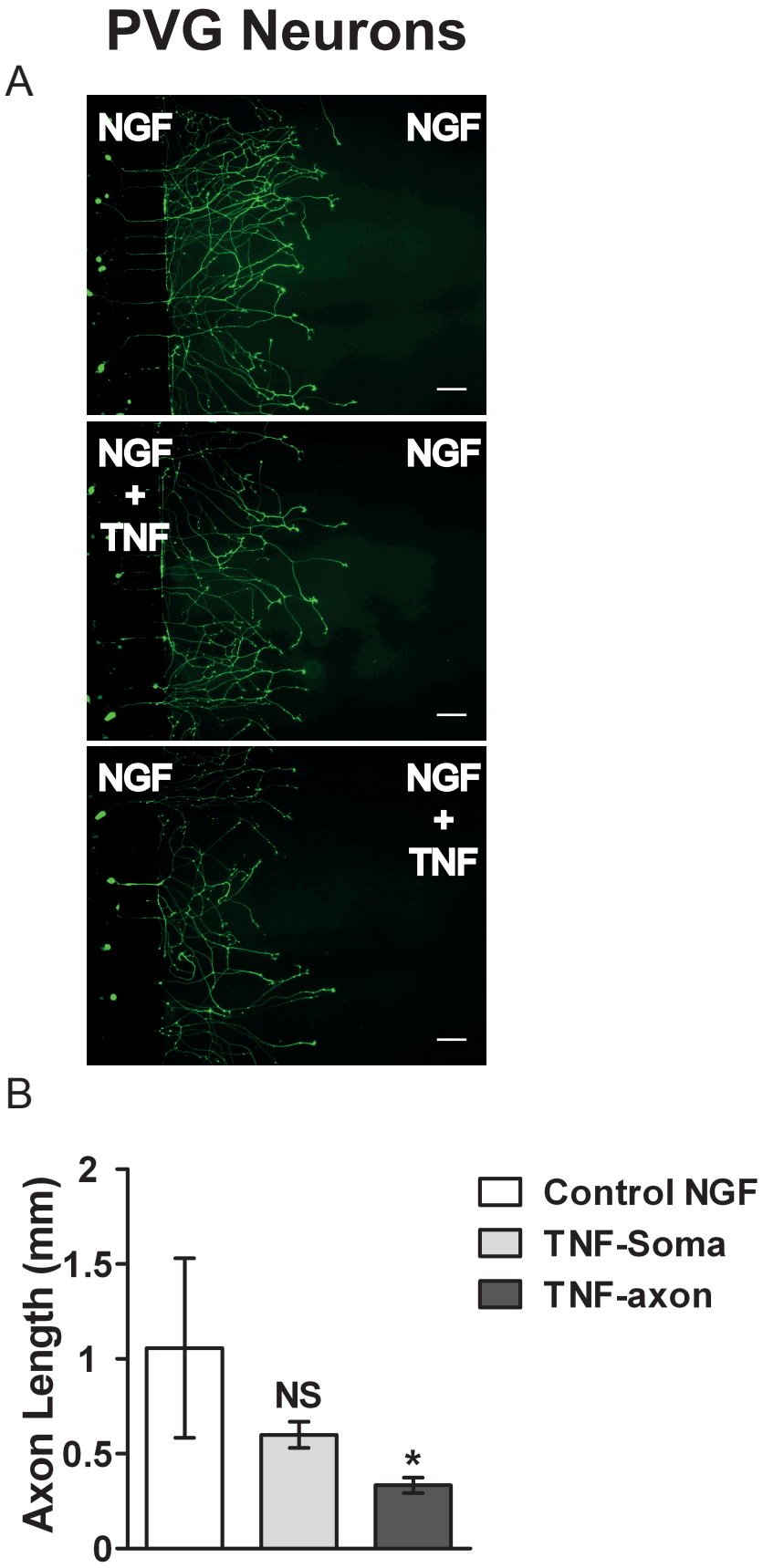

Fig 3.14. Legend on following page.

Figure 3.14. TNF-α-Promoted TNFR1-Mediated Forward Signalling from Soma and Axonal Compartments of Po PVG Neurons. (A) Representative images of calcein-AM stained PVG neurons from Po wild-type mice treated with 10 ng/ml NGF, with 50 ng/ml soluble TNF-α in either the soma (left) or axonal (right) compartment or neither. Scale bars represent 100 μm. Each image is representative of three experiments. **(B)** Quantification of axon lengths of Po wild-type PVG neurons treated as described in (A). Data are presented as the mean ± standard error. n=3 for each condition. *: $p<0.05$ (Kruskal-Wallis, with Dunn's *post-hoc* analysis). NS: not significant; NGF: nerve growth factor; PVG: prevertebral ganglia (coeliac and superior mesenteric ganglia).

To identify if the difference seen in the forward signalling mechanisms also occurred during TNFR1-activated TNF-α-mediated reverse signalling, the effect of TNFR1-Fc on the growth of Po sympathetic neuron processes was analysed after it was added specifically to the cell soma or neurite compartments. As TNFR1-Fc did not affect the growth of PVG neuron processes in the standard culture system (when PVG neurons were exposed to TNFR1-Fc as whole neurons without compartmentalisation) in previous experiments (see **Section 3.2.2** in this chapter), this experiment would also hint at whether different neuron regions could work in opposing directions in regulating process growth in response to the same signal. Quantification of the neurite length of SCG neurons showed that TNFR1-Fc significantly enhanced neurite growth from SCG neurons only when added to the axon compartment (Fig. 3.15A), which also corroborated the report by Kisiswa *et al.* In contrast, quantification of the neurite length of PVG neurons revealed that TNFR1-Fc did not affect neurite growth of PVG neurons when added to either the cell soma or axon compartment (Fig. 3.15B). This is consistent with the previous *in vitro* results showing the insignificant effect of TNFR1-Fc on PVG neurite growth (see Fig. 3.4).

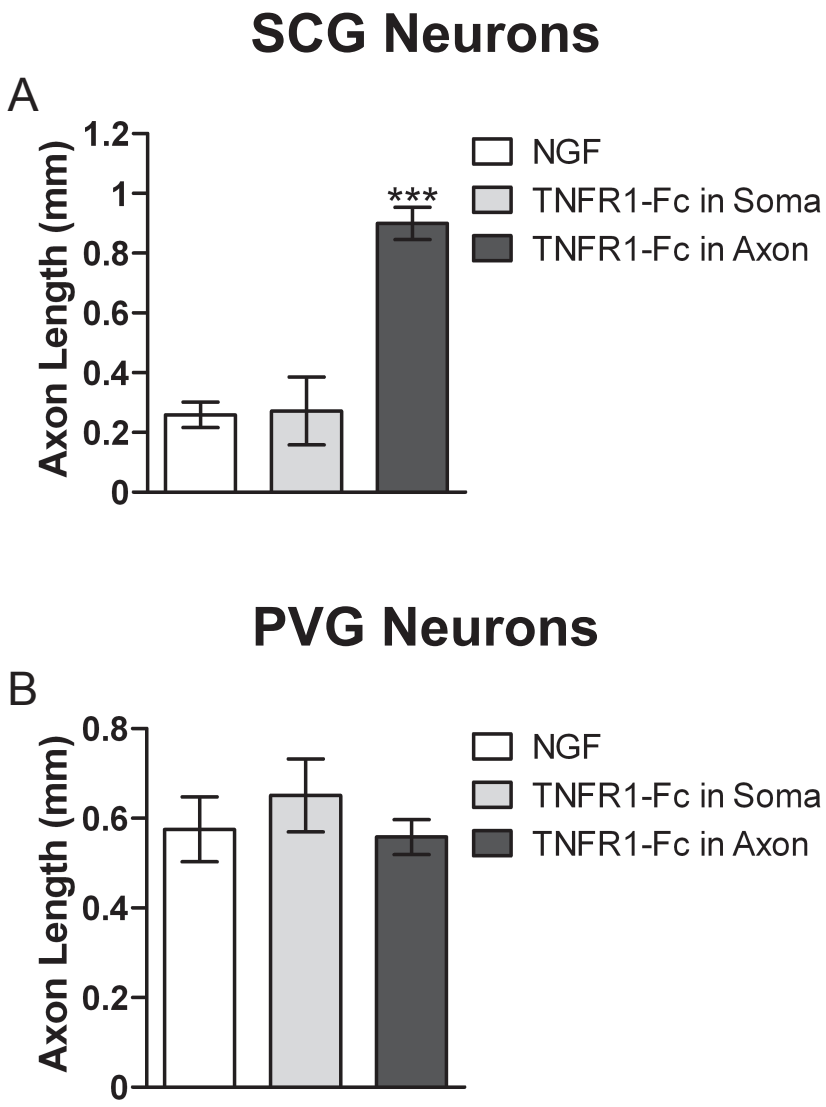

Figure 3.15. TNFR1-Fc-Promoted TNF-α Reverse Signalling from Soma and Axonal Compartments of Po SCG and PVG Neurons. (A) Quantification of axon lengths of Po wild-type SCG neurons treated with 10 ng/ml NGF, with 50 ng/ml TNFR1-Fc in either the soma or axonal compartment, or neither. **(B)** Quantification of axon lengths of Po wild-type PVG neurons treated with NGF, with 50 g/ml TNFR1-Fc in either the soma or axonal compartment, or neither. Data are presented as the mean ± standard error. n=3 for each condition. ***: $p<0.001$ (Kruskal-Wallis, with Dunn's *post-hoc* analysis). NGF: nerve growth factor; PVG: prevertebral ganglia (coeliac and superior mesenteric ganglia); SCG: superior cervical ganglia.

Together, the above findings demonstrate that while sTNF-α significantly inhibits axon growth in both paravertebral and prevertebral sympathetic cultured neurons, sTNF-α exerts its inhibitory effects on these sympathetic neurons from different neuronal regions. Whereas the neurite growth inhibitory-effect of sTNF-α was clear when it was applied to the cell soma of SCG neurons, PVG neurons responded to the same neurite growth-inhibitory effect of sTNF-α only from neurite terminals. Furthermore, findings here support the previous results indicating that TNFR1-Fc enhances neurite growth in paravertebral neurons, but not prevertebral neurons.

3.2.6 Localisation of TNF-α and TNF Receptors Differ in Paravertebral and Prevertebral Sympathetic Neurons

The findings thus far demonstrate evident differences in the responses of paravertebral and prevertebral sympathetic neurons to TNF-related forward and reverse signalling during SNS development. Previously, Kisiswa *et al.* demonstrated that whereas TNF-α immunoreactivity was observed on both the cell soma and axon terminals of SCG neurons, TNFR1 immunoreactivity was restricted to the cell soma (Kisiswa et al. 2013). This raised the possibility that the distribution of TNF-α and its receptors, TNFR1 and TNFR2, may show differences between paravertebral and prevertebral neurons, which may underlie the distinct responses of these two groups of sympathetic neurons to TNF-related signalling. To investigate this, Po SCG and PVG sympathetic neuron cultures were established and incubated for 18 h in the presence of NGF, followed by staining with appropriate primary and secondary antibodies to allow immunofluorescence analysis (see details in **Section 2.3** in **Chapter 2**). A β-III tubulin antibody was used to identify sympathetic neurons and cell nuclei were labelled with the fluorescent nuclear marker, DAPI. The validity and specificity of TNF-α and TNFR1 antibodies were tested in cultures of SCG and CG-SMG neurons established from TNFR1- and TNF-α deficient mice (Fig. 3.16A & 3.16B, respectively). However, due to the lack of a transgenic mouse model for TNFR2, the validation of the specificity of the antibody against TNFR2 was reliant on the manufacturer's validation.

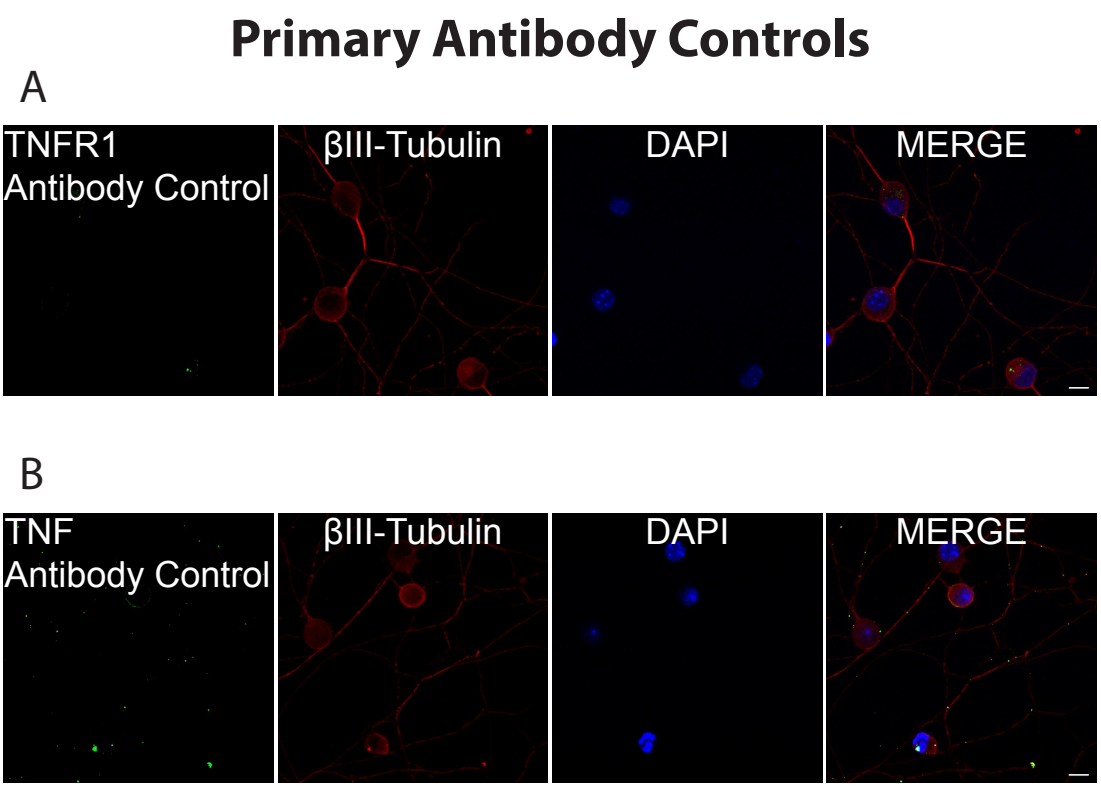

Figure 3.16. Validation of TNFR1 and TNF-α Primary Antibodies Used in Immunocytochemical Analysis of Sympathetic Neurons. (A) Representative images of SCG neurons from Po *Tnfrsf1a*$^{-/-}$ mice. Sympathetic neurons were labelled with anti-TNFR1 (green), β-III tubulin (red), and DAPI was used to stain nuclei. **(B)** Representative images of SCG neurons from Po *Tnf*$^{-/-}$ mice. Sympathetic neurons were labelled with anti-TNF-α (green), β-III tubulin (red), and DAPI was used to stain nuclei. Scale bars represent 10 μm. Each image is representative of at least 30 images. n=1 for each condition. SCG: superior cervical ganglia.

To control for non-specific binding of the secondary antibodies, SCG neurons (Fig. 3.17) and PVG neurons (Fig. 3.18) were first stained omitting primary antibodies. β-III tubulin primary antibody (Fig. 3.17A & 3.18A), TNF-α/TNFR1 primary antibodies (Fig. 3.17B & 3.18B), or TNFR2-primary antibodies (Fig. 3.17C & 3.18C) were omitted in both SCG and PVG preparations. No non-specific binding was detected when primary antibodies were omitted in SCG neurons or PVG neurons. Immunofluorescence images were obtained by confocal microscopy and imaging was carried out blind to neuron type and protein of interest.

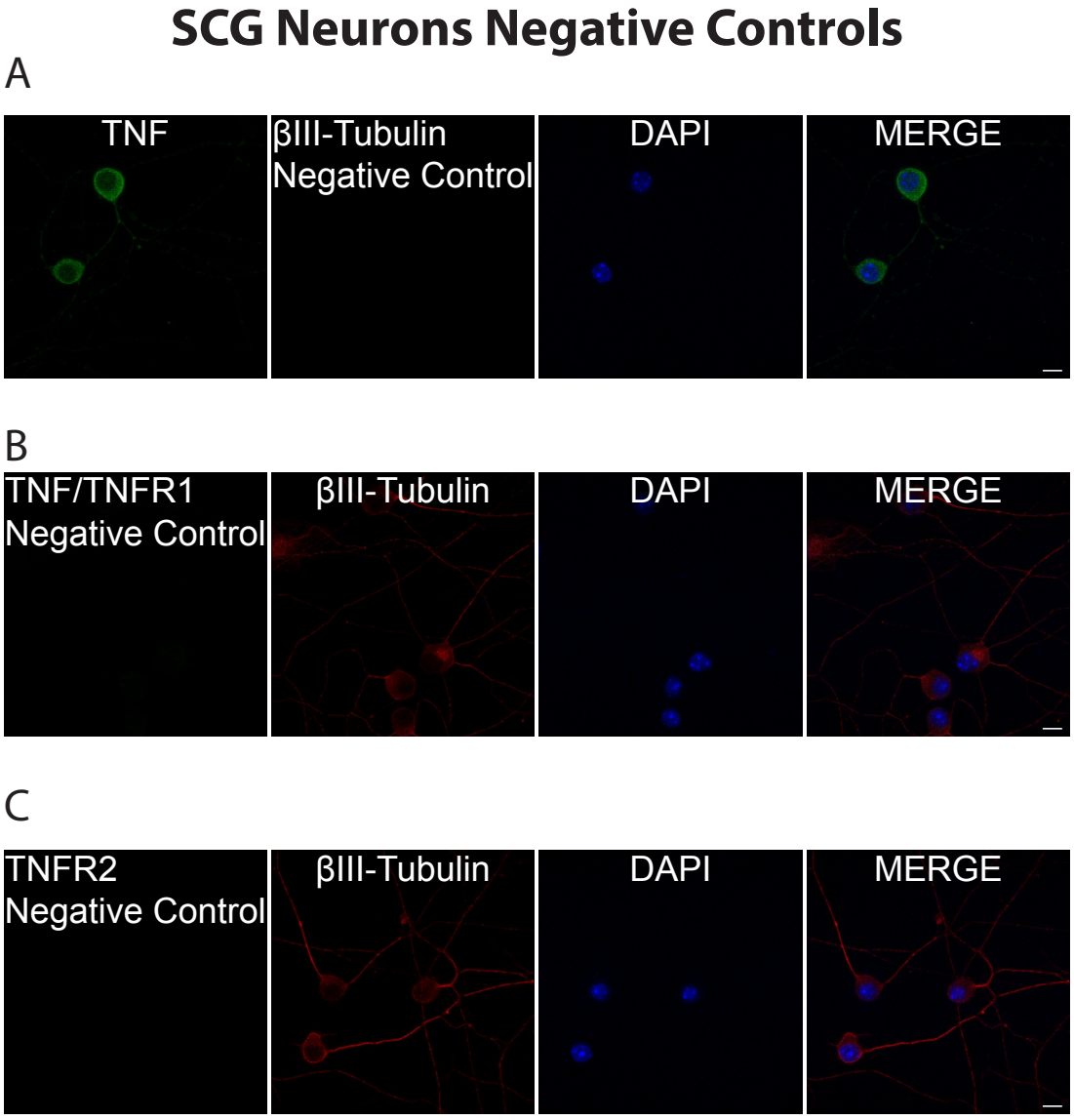

Figure 3.17. Validation of Secondary Antibodies Used in Immunocytochemical Analysis of Po SCG Sympathetic Neurons. (A-C) Representative images of SCG neurons from Po wild-type mice. **(A)** SCG neurons were stained with anti-TNF-α (green) with relevant secondary antibody, and the secondary antibody against the β-III tubulin primary antibody (red; primary antibody omitted). **(B)** SCG neurons were stained with the secondary antibody used against anti-TNF-α and TNFR1 (green; primary antibodies omitted) and primary anti-β-III tubulin (red) with relevant secondary antibody. **(C)** SCG neurons were stained with the secondary antibody used against anti-TNFR2 (green; primary antibody omitted) and primary anti-β-III tubulin (red) with relevant secondary antibody. DAPI was used to stain nuclei. Scale bars represent 10 μm. Each image is representative of at least 30 images. n=3 for each condition. SCG: superior cervical ganglia.

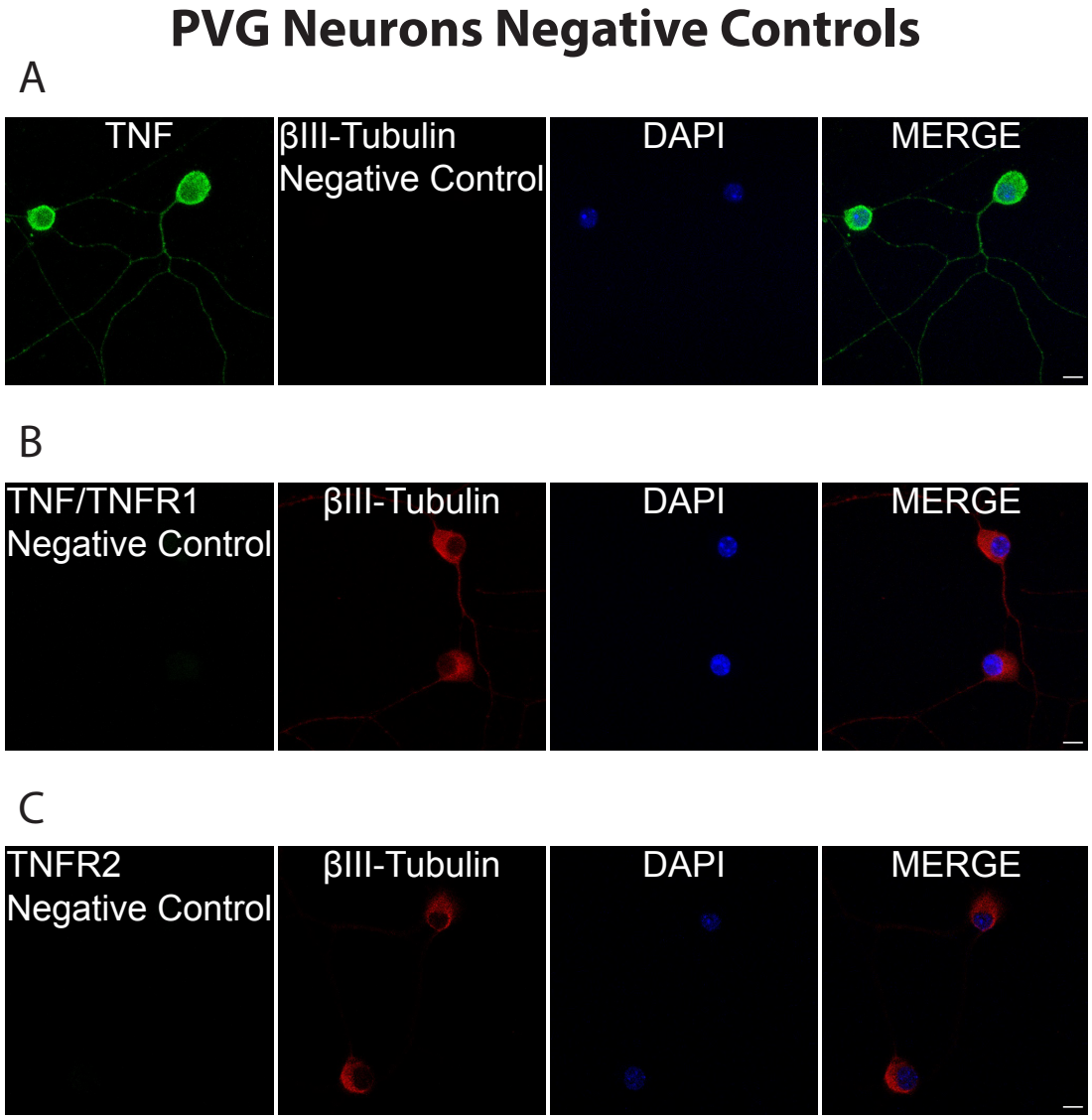

Figure 3.18. Validation of Secondary Antibodies Used in Immunocytochemical Analysis of Po PVG Sympathetic Neurons. (A-C) Representative images of PVG neurons from Po wild-type mice. **(A)** PVG neurons were stained with anti-TNFR1 (green) with relevant secondary antibody, and the secondary antibody against the β-III tubulin primary antibody (red; primary antibody omitted). **(B)** PVG neurons were stained with the secondary antibody used against anti-TNF-α and TNFR1 (green; primary antibodies omitted) and primary anti-β-III tubulin (red) with relevant secondary antibody. **(C)** PVG neurons were stained with the secondary antibody used against TNFR2 (green; primary antibody omitted) and primary anti-β-III tubulin (red) with relevant secondary antibody. DAPI was used to stain nuclei. Scale bars represent 10 μm. Each image is representative of at least 30 images. n=3 for each condition. PVG: prevertebral ganglia (coeliac and superior mesenteric ganglia).

Fig. 3.19 shows the localisation of the TNFR1 protein in dissociated sympathetic neuron cultures established from Po SCG and CG-SMG (PVG). In these immunofluorescence images, TNFR1 protein is shown in green, and β-III tubulin, highlighting sympathetic neuron soma and processes, is shown in red. Merged images show the spatial distribution of TNFR1 protein in sympathetic neurons. The relative localisation of TNFR1 protein expression with β-III tubulin indicates that it is restricted to the cell soma of SCG neurons (Fig. 3.19A). However, labelling of PVG neurons with anti-TNFR1 antibody clearly shows TNFR1 localisation in both the cell soma and neurites (Fig. 3.19B).

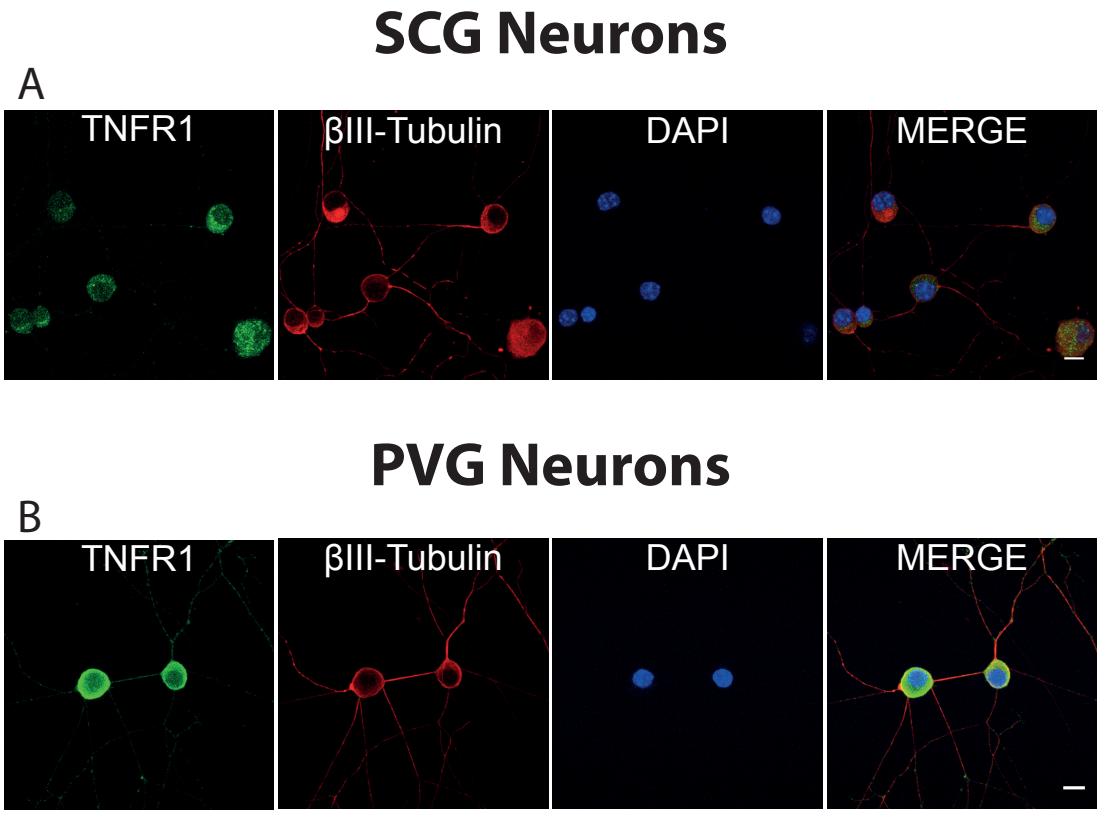

Figure 3.19. TNFR1 Expression by Po SCG and PVG Neurons. (A) Representative images of SCG neurons from Po wild-type mice. Sympathetic neurons were labelled with anti-TNFR1 (green), β-III tubulin (red), and DAPI was used to stain nuclei. **(B)** Representative images of PVG neurons from Po wild-type mice. Sympathetic neurons were labelled with anti-TNFR1 (green), β-III tubulin (red), and DAPI was used to stain nuclei. Scale bars represent 10 μm. Each image is representative of at least 30 images. n=3 for each condition. PVG: prevertebral ganglia (coeliac and superior mesenteric ganglia); SCG: superior cervical ganglia.

Fig. 3.20 shows the distribution of the TNF-α protein in dissociated sympathetic neuron cultures established from Po SCG and PVG. Representative images demonstrate that TNF-α protein (green) co-localises with sympathetic neurons as delineated by β-III tubulin (red). In contrast to TNFR1, TNF-α primary antibody strongly labelled virtually all SCG (Fig. 3.20A) and PVG (Fig. 3.20B) neurons, both on the cell soma and along neurites.

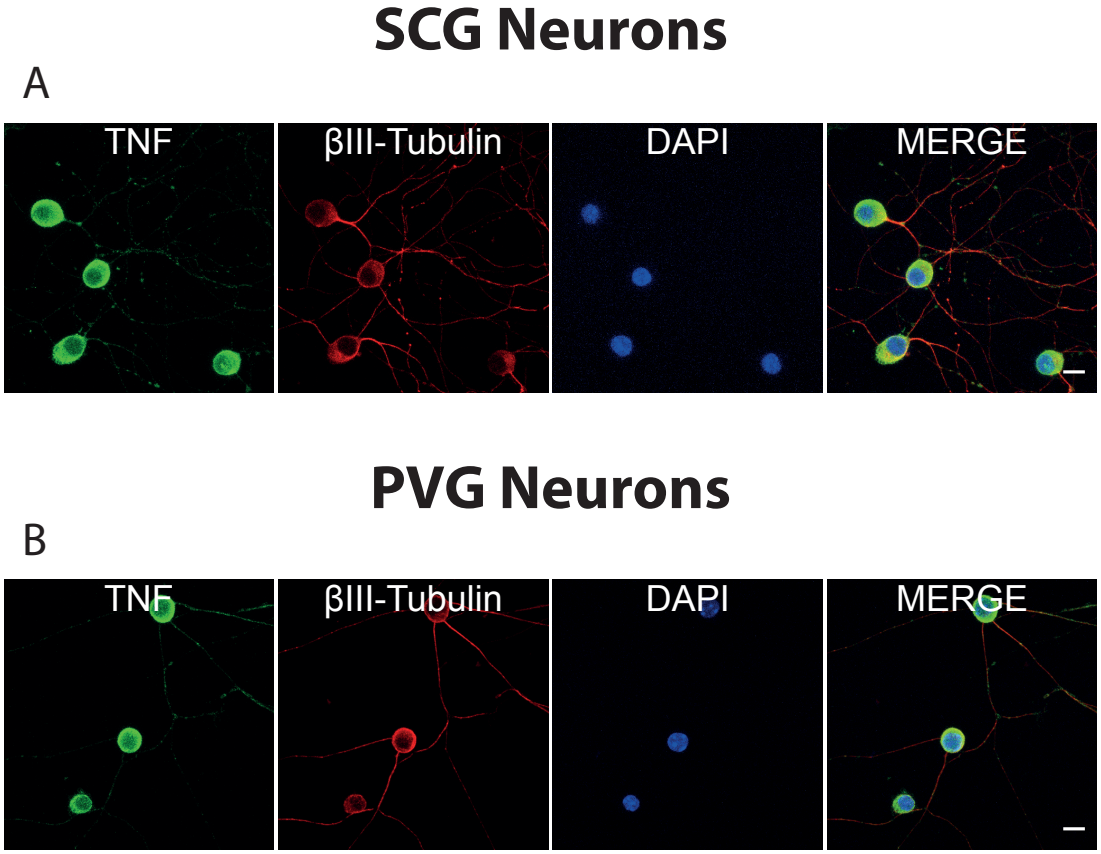

Figure 3.20. TNF-α Expression by Po SCG and PVG Neurons. (A) Representative images of SCG neurons from Po wild-type mice. Sympathetic neurons were labelled with anti-TNF-α (green), β-III tubulin (red), and DAPI was used to stain nuclei. **(B)** Representative images of PVG neurons from Po wild-type mice. Sympathetic neurons were labelled with anti-TNF-α (green), β-III tubulin (red), and DAPI was used to stain nuclei. Scale bars represent 10 μm. Each image is representative of at least 30 images. n=3 for each condition. PVG: prevertebral ganglia (coeliac and superior mesenteric ganglia); SCG: superior cervical ganglia.

Finally, the distribution of the second TNF-α receptor protein, TNFR2, was examined in both cultured Po SCG and PVG neurons. Fig. 3.21 shows the distribution of TNFR2 protein (green) in sympathetic SCG and PVG neurons. TNFR2 protein was distributed on both the cell soma and neurite elongations in both SCG (Fig. 3.21A) and PVG (Fig. 3.21B) neurons.

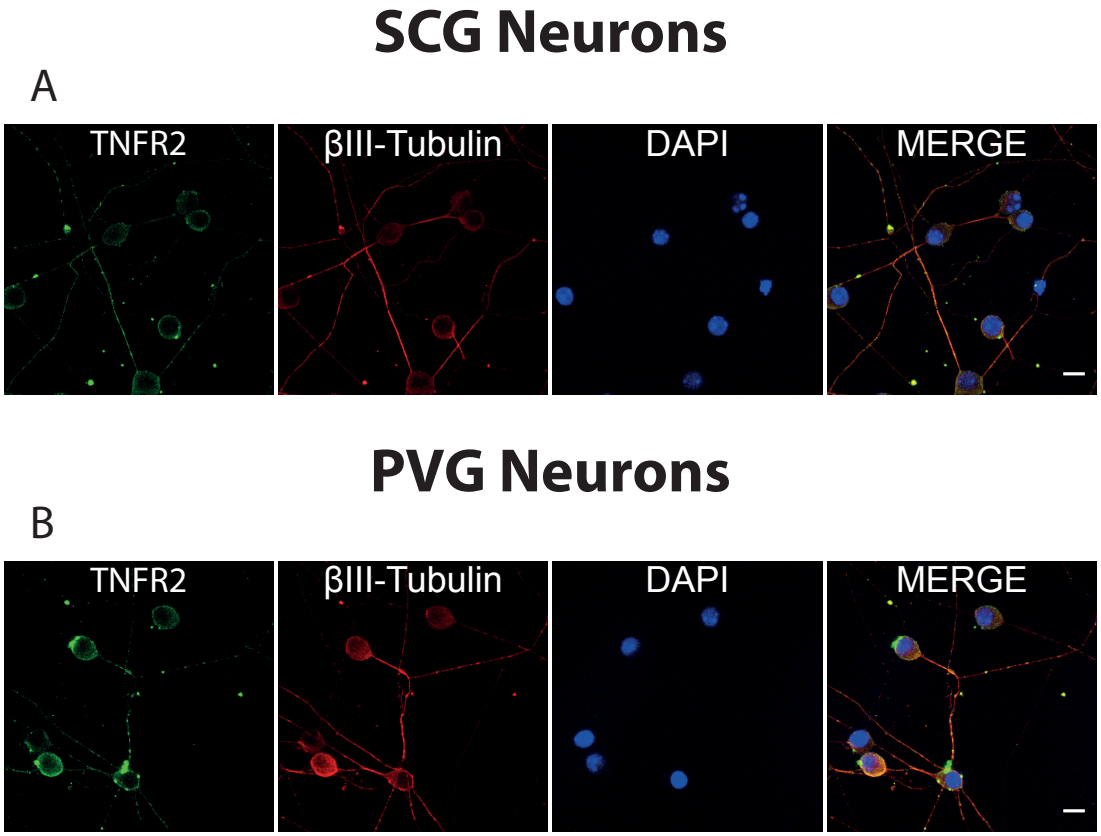

Figure 3.21. TNFR2 Expression by Po SCG and PVG Neurons. (A) Representative images of SCG neurons from Po wild-type mice. Sympathetic neurons were labelled with anti-TNFR2 (green), β-III tubulin (red), and DAPI was used to stain nuclei. **(B)** Representative images of PVG neurons from Po wild-type mice. Sympathetic neurons were labelled with anti-TNFR2 (green), β-III tubulin (red), and DAPI was used stain nuclei. Scale bars represent 10 μm. Each image is representative of at least 30 images. n=3 for each condition. PVG: prevertebral ganglia (coeliac and superior mesenteric ganglia); SCG: superior cervical ganglia.

Immunocytochemical analysis of TNF-α and its receptors in sympathetic paravertebral and prevertebral neurons indicates that whereas localisation of the TNFR1 protein differs between paravertebral and prevertebral neurons, TNF-α and TNFR2 have similar distribution patterns in these sympathetic neurons. As also previously described (Kisiswa et al. 2013), triple immunofluorescence staining revealed that TNFR1 is expressed exclusively in the cell soma of paravertebral neurons. However, TNFR1 does not show differential staining between soma and processes in prevertebral neurons. TNF-α and TNFR2 were found to be expressed in both the neurites and soma of all sympathetic neurons types tested.

3.2.7 Expression of TNF-α, TNFR1 and TNFR2 Transcripts in Paravertebral and Prevertebral Neurons and Their Target Organs

After detection of the TNF ligand and receptor proteins in sympathetic neurons, the expression of the transcripts encoding TNF-related proteins were explored to determine whether there may be differences in the levels of expression of these mRNAs between paravertebral and prevertebral sympathetic neurons and their respective target fields. To do this, mRNAs encoding TNF-α, TNFR1 and TNFR2 were quantified in sympathetic paravertebral and prevertebral neurons, and their target organs, by real-time quantitative PCR (RT-PCR). During this procedure the housekeeping enzymes glyceraldehyde phosphate dehydrogenase *(Gapdh),* hypoxanthine phosphoribosyltransferase 1 (*Hprt1*), and succinate dehydrogenase (*Sdha*) were used as reference genes for the accurate assessment of the expression of target genes.

Fig. 3.22 shows the relative differences in the expression of *Tnf*, *Tnfrsf1a* and *Tnfrsf1b* mRNAs in P0 SCG and PVG neurons when they were normalised to endogenous reference genes. *Tnf* (Fig. 3.22A), *Tnfrsf1a* (TNFR1, Fig. 3.22B) and *Tnfrsf1b* (TNFR2, Fig. 3.22C) transcript levels were not significantly different between the sympathetic neuron populations.

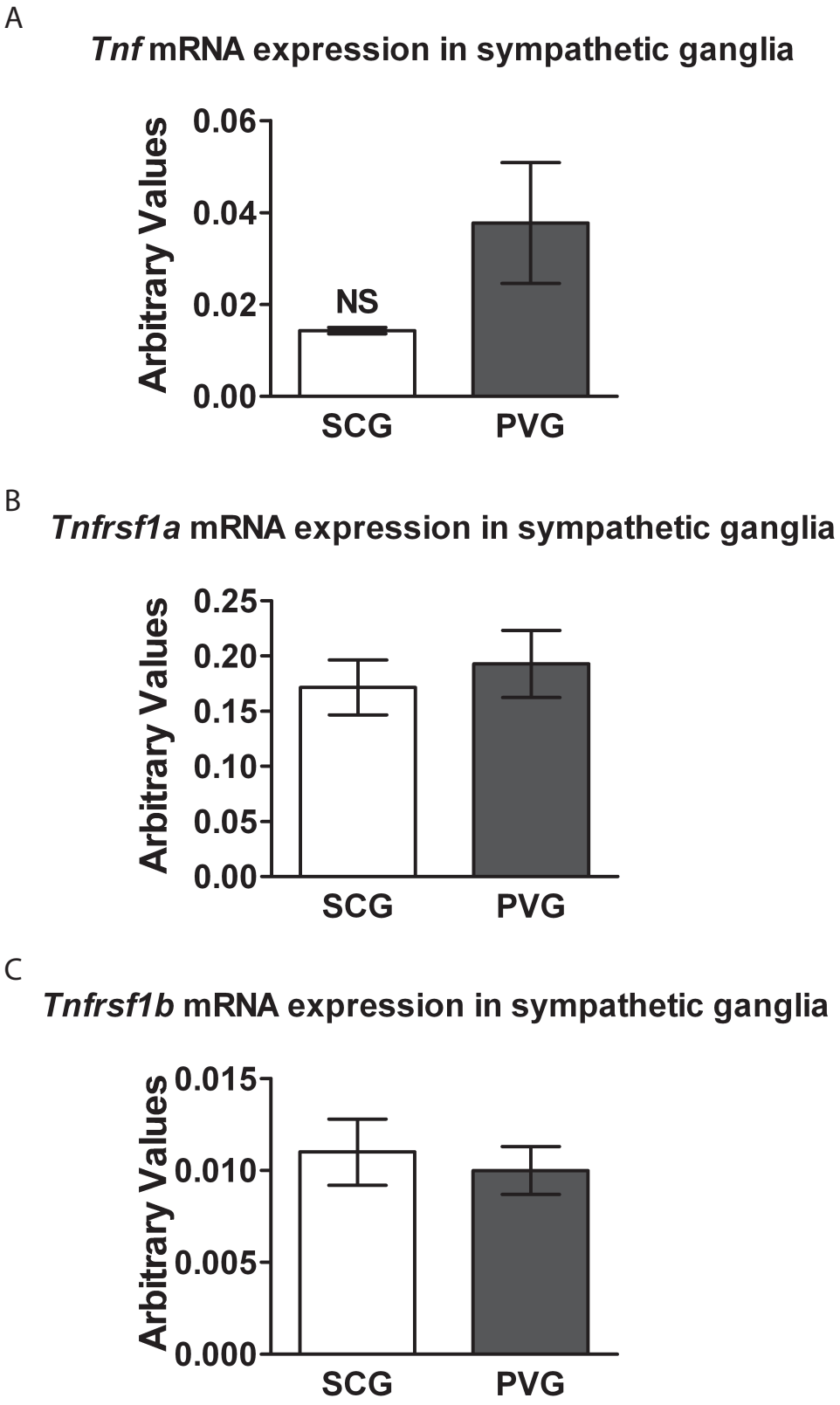

Fig. 3.22. Legend on following page.

Figure 3.22. mRNA Expression Levels of TNF Signalling Components in Po SCG and PVG Neurons. *Tnf* **(A)**, *Tnfrsf1a* **(B)**, and *Tnfrs1b* **(C)** mRNA expression levels in SCG and PVG neurons from Po wild-type mice. mRNA levels were normalised to those of the housekeeping genes *Gapdh*, *Hprt1* and *Sdha*. Each sample (with neurons pooled from at least 5 animals from the same litter) was analysed in triplicate wells for each gene (with the mean value of the triplicates used as one repeat), and n=3 independent experiments. Data are presented as the mean ± standard error. NS: not significant (Student's *t*-test); PVG: prevertebral ganglia (coeliac and superior mesenteric ganglia); SCG: superior cervical ganglia.

Fig. 3.23 shows the relative expression of *Tnf, Tnfrsfia* and *Tnfrsfib* mRNAs in Po submandibular gland (SG) and spleen, target organs of paravertebral and prevertebral sympathetic neurons, respectively. While *Tnf* mRNA levels were significantly higher in the spleen than the SG, there was no difference between *Tnfrsfia* mRNA levels expressed in the SG and spleen tissues.

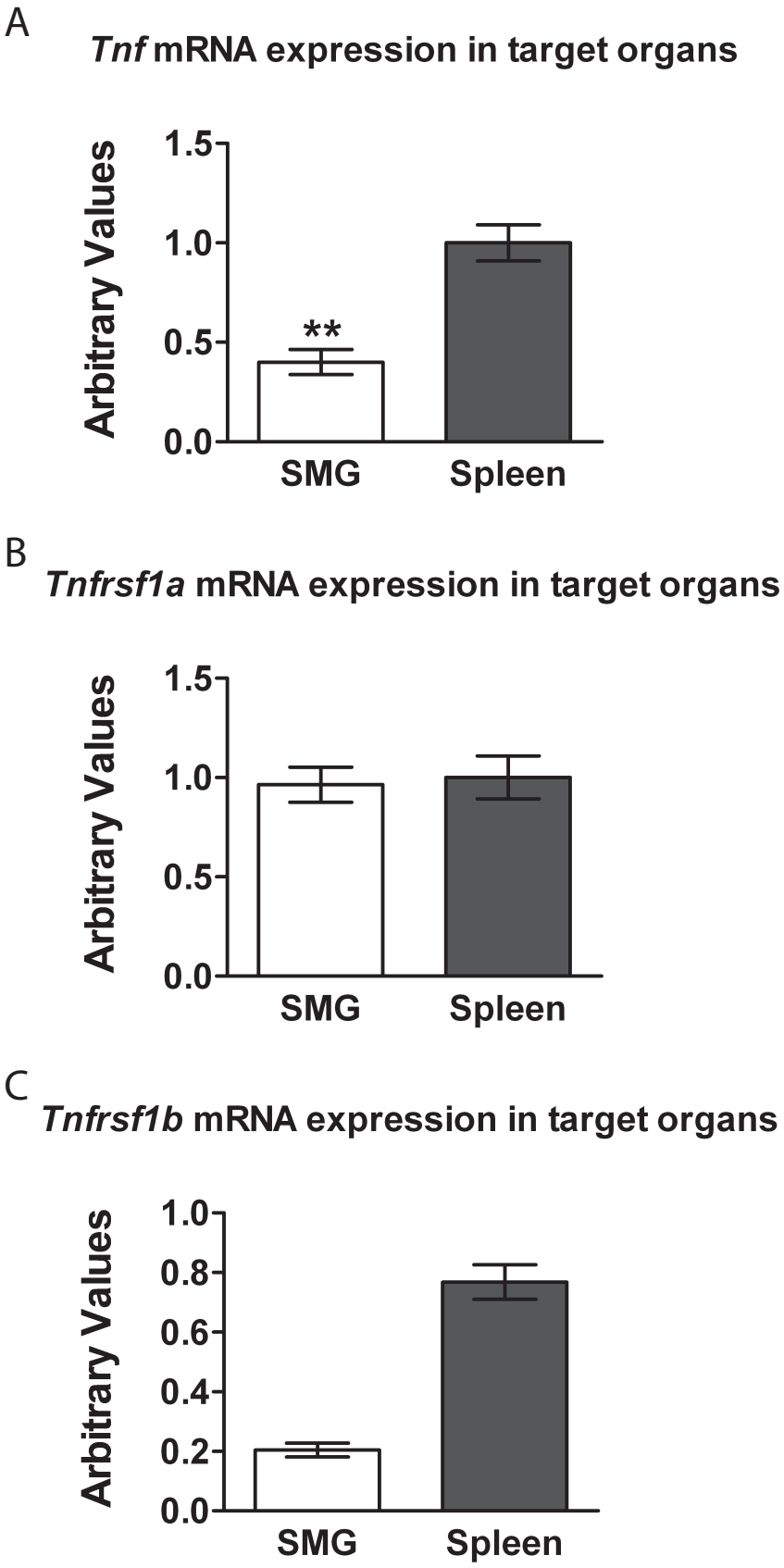

Fig. 3.23. Legend on following page.

Figure 3.23. mRNA Expression Levels of TNF Signalling Components in Paravertebral and Prevertebral Target Organs. *Tnf* **(A)**, *Tnfrsf1a* **(B)**, and *Tnfrsf1b* **(C)** mRNA expression levels in SG (paravertebral target organ) and spleen (prevertebral target organ) from P0 wild-type mice. mRNA levels were normalised to those of the housekeeping genes *Gapdh*, *Hprt1* and *Sdha*. Each sample was analysed in triplicate wells for each gene (with the mean value of the triplicates used as one repeat), and n=3 independent experiments. Data are presented as the mean ± standard error. **: $p<0.01$ (Student's *t*-test). PVG: prevertebral ganglia (coeliac and superior mesenteric ganglia); SCG: superior cervical ganglia; SG: submandibular gland.

3.3 Discussion

The aim of the studies in this chapter was to expand our understanding of the development of the SNS by investigating the extent to which TNF-signalling, known to significantly contribute to the development of the paravertebral SNS, is also relevant to the development of the prevertebral SNS. *In vivo* and *in vitro* experiments were used to explore the contribution of TNF-dependent signalling to the establishment of prevertebral sympathetic innervation of target organs, and to compare the effects of TNF-dependent signalling between paravertebral and prevertebral divisions of the sympathetic nervous system. *In vivo* results showed that knockout of either TNF-α, or its receptor TNFR1, did not affect sympathetic innervation density in target organs receiving their innervation primarily from prevertebral ganglia. One exception to this was in the spleen of TNFR1 knockout animals, where innervation density was significantly increased compared to wild-type animals. This contrasted with findings from the target tissues of SCG neurons, which have consistently shown a decrease in innervation density when either TNF-α or TNFR1 were knocked out. *In vitro* studies clearly revealed that TNF-α and TNFR1 signalling causes different neuronal responses in paravertebral SCG neurons and prevertebral CG-SMG neurons. Experiments with cultured sympathetic neurons demonstrated that TNFR1-activated TNF-α-mediated reverse signalling was a significant mechanism contributing to neurite elongation and branching of paravertebral neurons; however, the same signalling mechanism did not affect neurite growth in prevertebral neurons. On the other hand, although TNF-α-activated TNFR1-mediated forward signalling had similar inhibitory effects on neurite outgrowth in both paravertebral and prevertebral neurons, these sympathetic neurons showed differences in the neuronal region at which they were responsive to TNF-α. Findings in this chapter suggest that TNF-dependent signalling mechanisms play different roles in the development of the paravertebral and prevertebral divisions of the SNS.

In vivo analysis of target tissue innervation highlighted a clear contrast between the paravertebral and prevertebral sympathetic divisions in their

reliance on TNF-signalling mechanisms during target innervation. Previous studies have reported marked reductions (between 20% to 50%) in the innervation of sympathetic organs (submandibular salivary gland, iris, nasal tissues, pineal gland and trachea) in mice lacking either TNF-α or TNFR1 (Kisiswa et al. 2013; Erice et al. 2019). These studies clearly demonstrated that TNF-signalling mechanisms function to enhance sympathetic target field innervation during SNS development. However, all of the sympathetic target tissues previously investigated in these studies were organs receiving their innervation only from SCG neurons. In the present study, the spleen and the stomach (target organs for innervating CG and SMG neurons) were used as the first prevertebral target organs investigated in this context. Whereas knockdown of TNF-α consistently reduced innervation density in SCG-target tissues, no such effect was seen when studying either the spleen or the stomach. Furthermore, whilst TNFR1 knockdown again reduced innervation in SCG-target tissue, no such effect was seen when innervation of the stomach was examined. Surprisingly, in the spleen, TNFR1 knockdown had the opposite effect, causing instead an increase in the innervation density of this organ.

Several possible mechanisms may explain the different responses of SCG and PVG neurons to the knockout of TNF signalling pathway components. Kisiswa *et al.* (2013) concluded, using *in vitro* approaches, that the key element controlling the innervation of SCG-targeted organs is TNFR1-activated TNF-α-mediated reverse signalling. In this reverse signalling pathway, TNFR1 produced by SCG target tissues (e.g. iris and submandibular gland) binds to membrane-integrated TNF-α present on the axons of SCG neurons through cell-to-cell contact and/or paracrine signalling, triggering outgrowth and ramification of the neurons. Knockdown of either the ligand (TNFR1) or the receptor (mTNF-α) leads to a loss of reverse signalling and subsequent hypoinnervation. One explanation for the unaltered innervation of PVG-innervated organs in response to TNF-α knockdown could be that this reverse signalling pathway does not function in PVG neurons. Indeed, *in vitro* experiments using cultured PVG neurons identified that TNFR1-Fc, a known ligand for mTNF-α, failed to

enhance NGF-promoted neurite growth when added to PVG neurons. In contrast, SCG neurons showed a significant increase both in total neurite length and complexity when they were treated with TNFR1-Fc in parallel experiments. The SCG results are consistent with the findings of Kisiswa *et al*. (2013), confirming that the experimental set-up used for this study should detect any TNFR1-Fc mediated changes in the growth of PVG processes.

Microfluidic chambers isolate different morphological regions of neurons, namely the neurites and the cell soma. This enables the identification of the particular neuronal regions that respond to growth-promoting ligands, and minimises the possibility that differential ligand activation at two different neuronal sites may counteract the effects of each other. In SCG neurons, these compartment cultures found that SCG neurons were responsive to TNFR1-Fc only when it was added to neurites, but not to the cell soma, in accordance with data in Kisiswa *et al.* (2013). In contrast, PVG neurons were not responsive to TNFR1-Fc when it was applied to either the cell soma or neurites, confirming the observations seen in non-compartment cultures.

Data from compartment and non-compartment cultures suggest that the innervation differences seen *in vivo* between SCG and PVG target tissues resulted from a lack of TNFR1-activated TNF-α-mediated reverse signalling in PVG neurons. One simple explanation for this could be differential expression of mTNF-α, the receptor that mediates reverse signalling, between SCG and PVG neurons. However, quantification of the *Tnf* mRNA levels in both SCG and PVG neurons did not suggest a significant difference in expression levels of mTNF-α between the different neuron types. Furthermore, immunocytochemistry results confirmed that TNF-α is expressed along the axons and on the cell soma of both SCG and PVG neurons. These results suggest that the intrinsic unresponsiveness of PVG neurons to TNFR1-Fc is not directly related to expression of its receptor protein, mTNF-α. Another explanation for the observed *in vivo* results could be that TNFR1 was not expressed at sufficient levels, or indeed at all, in the target tissues of PVG neurons, thus PVG neurons may not utilise TNF-α reverse signalling during ramification of their target

tissues. However, RT-PCR results revealed that *Tnfrsf1a* mRNA levels were similar between PVG-targeted spleen and SCG-targeted SG. Therefore, *in vivo*, the different responses of SCG and PVG neurons to TNFR1-Fc is not likely to be directly linked to TNFR1 expression levels in target tissues.

Since SCG and PVG neurons respond differently *in vitro* to TNFR1-Fc, despite similar levels and localisation of the relevant receptor, mTNF-α, it is possible that the different cellular responses of SCG and PVG neuron populations to TNFR1-Fc are determined by differences in particular steps of the intracellular signalling cascades arising from activated mTNF-α. In SCG neurons, TNF-α reverse signalling opens voltage-gated T-type Ca^{2+} channels along SCG axons, which enhances protein kinase C (PKC) activity and downstream ERK1/2 activation to promote SCG axon growth (Kisiswa et al. 2013; Kisiswa et al. 2017). Future work should explore at which level of the intracellular signalling cascade PVG neurons diverge from SCG neurons to mute TNFR1-mediated neurite outgrowth.

Whilst there is evidence to suggest that knockdown of TNF-α and TNFR1 does not cause hypoinnervation of PVG-target organs because reverse signalling does not contribute to the normal development of this division of the sympathetic nervous system, it does not explain why deletion of TNFR1 causes an increase in the density of sympathetic innervation in the spleen. sTNF-α-activated TNFR1-mediated forward signalling has previously been shown to suppress neurite outgrowth and branching in cultured SCG neurons (Gutierrez et al. 2008). Analysis of neonatal SCG and PVG neuron responses to sTNF-α in standard neuron cultures in the current study revealed that, as a ligand for forward signalling, sTNF-α had similar inhibitory effects on neurite growth and branching on both SCG and PVG neurons. However, compartment assays identified that cultured SCG and PVG neurons differed in the region that responded to sTNF-α forward signalling. The current SCG *in vitro* results further support previous reports that TNF-α forward signalling exerts its inhibitory effect on the growth of SCG axons through the cell soma (Kisiswa et al. 2013). Surprisingly, PVG neurons were unresponsive to sTNF-α when it was added to

the soma compartment. However, PVG neurons showed a significant decrease in neurite process growth when sTNF-α was added into axon compartments in the presence of NGF. A possible explanation for this difference between SCG and PVG neurons could be differences in the localisation of the TNF-α forward signalling receptor TNFR1 between these neuron types. Immunocytochemistry showed that TNFR1 expression was restricted to the soma of SCG neurons, whereas PVG neurons expressed TNFR1 on both the soma and axons. This difference in the localisation of TNFR1 could contribute to the differences in SCG and PVG target tissue innervation in *Tnf*- and *Tnfrsf1a*-deficient mice *in vivo*. If SCG neurons do not express TNFR1 on axons, they cannot respond to sTNF-α released from their target tissues, whereas PVG neurons may be able to potentially respond to target tissue-derived sTNF-α with reduced axon growth. Interestingly, RT-qPCR showed that the expression of *Tnf* mRNA transcripts in PVG-targeted spleen was higher than in SCG-targeted submandibular gland. Whilst the significantly higher expression levels of *Tnf* mRNA in spleen compared to submandibular gland may enhance the contribution of forward signalling to spleen innervation by PVG neurons, the main reason for the higher TNF-α expression in the spleen may instead be related to the heavy involvement of the spleen in the immune system (Tecklenborg et al. 2018).

A number of questions remain unanswered regarding the roles of TNF-α/TNFR1 signalling in sympathetic neuron development and the molecular mechanisms underlying the differences in the response of paravertebral and prevertebral sympathetic neurons to TNF-α/TNFR1 forward and reverse signalling. For example, future experiments should assess what influences the spatial expression pattern of TNFR1 on SCG and PVG neurons. sTNF-α suppresses NGF-promoted axon growth in cultured SCG neurons by an IKKß-activated NF-κB signalling mechanism (Gutierrez et al. 2008), as such investigation into the role of NF-κB signalling in TNF-α forward signalling in PVG neurons is warranted in further studies.

Another interesting question is whether the ability of TNF-α/TNFR1 signalling to modulate spleen innervation *in vivo* is mediated through cell-to-

cell contact, involving the binding of mTNF-α expressed on the surface of spleen cells to transmembrane TNFR1 expressed by PVG axons, or whether autocrine or paracrine signalling mechanisms are at play. Previously, it has been suggested that TNF-α forward signalling in cultured SCG neurons could occur via autocrine signalling at the cell soma as SCG neurons express TNF-α and TNFR1 proteins in the soma (Gutierrez et al. 2008). In the present study, the neurite growth inhibitory activity of sTNF-α on cultured PVG neurons suggests that these neurons are responsive to TNF-α forward signalling via either paracrine and/or autocrine mechanisms acting at axon terminals, as soluble TNF-α was the ligand in these experiments. PVG neurons express both TNF-α and TNFR1 in their axons, and the spleen expresses TNF-α. However, further work is required to differentiate whether one or both of these signalling mechanisms function *in vivo*. Data in Kisiswa *et al*. supported the view that TNF-α reverse signalling uses either cell-to-cell contact mediated and/or paracrine signalling at axon terminals to promote the growth of SCG axons, as axons were shown to express TNF-α protein, and not TNFR1, whereas SCG target fields expressed TNFR1 at the protein level (Kisiswa et al. 2013). In contrast to TNF-α, other related investigations have asserted that autocrine signalling is likely in the case of additional members of the TNFSF and TNFRSF that modulate target field innervation by developing peripheral neurons. For example: LIGHT-HVEM autocrine signalling suppresses BDNF-promoted sensory neuron neurite growth *in vitro* (Gavalda et al. 2009); GITRL-GITR autocrine signalling enhances NGF-promoted SCG neurite outgrowth *in vitro* (O'Keeffe et al. 2008) and the sympathetic innervation of the nasal mucosa and iris *in vivo*; CD40-CD40L autocrine reverse signalling enhances NGF-promoted SCG neurite outgrowth *in vitro* and the sympathetic innervation of the thymus and periorbital tissue *in vivo* (McWilliams et al. 2015); B-cell maturation antigen (BCMA)-TWE-PRIL autocrine reverse signalling suppresses neurite outgrowth in SCG neurons *in vitro* and greatly reduces TH-positive SCG neuron innervation of the postnatal mouse cranium *in vivo* (Howard et al. 2018). There are three commonalities to the above studies that revealed that TNFSF/TNFRSF autocrine signalling loops operate to modulate process outgrowth from SCG neurons *in vivo*. First, SCG

neurons were shown to express both the ligand and receptor proteins of the signalling system being studied. Second, the extent of process outgrowth was compared between cultured wild-type neurons and cultured knockout neurons that lacked the expression of either the ligand (reverse signalling) or receptor (for forward signalling) of the signalling loop being investigated. Importantly, neurons were cultured at an extremely low density to prevent individual cells from being in close enough proximity to each other to allow paracrine signalling. Third, analysis of target field innervation *in vivo* was carried out in wild-type animals and knockout animals lacking either ligand or receptor expression. In the present study, RT-qPCR analysis showed that TNF-α and TNFR1 were expressed at the mRNA level in PVG neurons and immunocytochemistry confirmed their expression at the protein level. In addition, analysis of spleen innervation *in vivo* in *Tnfrsf1a*-deficient mice revealed hyperinnervation in the absence of TNFR1 expression. Together these pieces of evidence raise the possibility that autocrine signalling may be one of the mechanisms underlying TNF-α forward signalling that suppresses neurite outgrowth of PVG neurons and alters target field innervation. However, comparison of process outgrowth from wild-type and knockout PVG neurons lacking either TNF-α or TNFR1 in very low density cultures was not performed, so it is not possible to preclude either the existence of paracrine signalling, or the possibility of equal contributions from autocrine and paracrine signalling in PVG neurons during target organ innervation. Blocking the interaction of TNF-α with its ligands or receptors using function-blocking antibodies in low-density PVG cultures could help uncover the presence of autocrine signalling in these neurons in future studies.

Further research could also explore whether TNFR2-mediated TNF-α forward or reverse signalling plays a role in the development of the SNS. Immunological studies have reported an effective role for TNFR2 as a ligand in TNFR2-activated TNF-α-mediated reverse signalling (Brennan et al. 2002; Rossol et al. 2007; Qu et al. 2017). RT-qPCR results from the present study indicate that *Tnfrs1b* mRNA is expressed in SCG and PVG neurons, as well as

within the target organs of these neurons. In addition, immunocytochemistry demonstrated that TNFR2 protein was expressed within the cell soma and neurites of SCG and PVG neurons. Therefore, it is possible that TNFR2 could in some way regulate TNF-α forward or reverse signalling during sympathetic target field innervation. Although in the present study TNFR2-Fc alone failed to activate TNF-α reverse signalling in both cultured SCG and PVG neurons (Fig. 3.7 & 3.8, respectively), TNFR2 may still regulate TNFR1-activated TNF-α reverse signalling by modulating the function of TNFR1. *In vitro* experiments comparing the effect of TNFR1-Fc treatment on process outgrowth from SCG and PVG neurons with TNFR1-Fc+TNFR2-Fc treatment could help identify if TNFR2 plays a role in modulating TNF-α reverse signalling. In addition, experiments in this chapter demonstrated that sTNF-α-activated forward signalling induces a significant decrease in neurite growth and complexity from both cultured SCG and PVG neurons. However, the functional role of TNFR2 was not investigated in these experiments, since TNFR2, unlike TNFR1, can only be fully activated by membrane integrated TNF-α, rather than its soluble form (Grell et al. 1995). Therefore, further experiments investigating TNFR2 function in the development of the SNS may consider this. *In vitro*, growing neurons on a layer of cells expressing membrane-integrated TNF-α would help identify the function of TNFR2, whilst *in vivo* analysis of a TNFR2-deficient mouse model would also allow more holistic analysis of the function of TNFR2.

Barker *et al.* discovered that sTNF-α, acting through TNFR1, promotes apoptotic death of developing SCG neurons (Barker et al. 2001). In contrast, TNF-α reverse signalling (Kisiswa et al. 2013) does not affect the survival of developing SCG neurons, neither do TWE-PRIL-reverse (Howard et al. 2018), CD40L-reverse (McWilliams et al. 2015), RANKL-forward (Gutierrez et al. 2013), LIGHT-forward (Gavalda et al. 2009) nor GITRL-forward (O'Keeffe et al. 2008) signalling. PVG neurons share similarities with SCG neurons in the expression and localisation of TNF-α and TNFR1. Since sTNF-α forward signalling mediates apoptosis in cultured SCG neurons, and forward signalling is the only TNF-α signalling mechanism that appears to operate in cultured PVG neurons, it is

plausible that sTNF-α can also trigger apoptosis in PVG neurons in the absence of NGF. Survival assays using antibodies blocking the function of TNF-α and/or TNFR1 or the addition of sTNF-α to neonatal SCG and PVG neurons cultured in the absence of NGF would help uncover shared and converging apoptosis pathways between PVG and SCG neurons. An alternative approach would be to culture PVG neurons from TNF-α deficient neonates and their wild-type littermates in the absence of NGF and determine whether TNF-α deficient neurons show altered survival compared to wild-type neurons.

In conclusion, experiments presented in this chapter represent the first attempt to uncover the contributions of TNF-α forward and reverse signalling to the development of prevertebral neurons of the SNS. Due to their larger size, ease of accessibility, and experimental tractability, SCG neurons have been extensively studied in the investigation of axonal growth regulation and innervation of target fields. As such, the majority of our current understanding about SNS development comes from hypotheses tested on these neuron populations. In this study, data are presented from cultured neurons of the mouse coeliac and superior mesenteric ganglia, alongside data analysing the innervation of organs that receive sympathetic innervation from these prevertebral neurons. The evidence from this study suggests that TNF-α and TNFR1 utilise different signalling mechanisms within SCG and PVG neurons to contribute to the sympathetic innervation of their target tissues. TNFR1-activated TNF-α reverse signalling appears to be the primary mechanism modulating the innervation of SCG target organs, even though SCG neurons have the capacity for both TNF-α forward and reverse signalling. In contrast, PVG neurons seem to only be able to respond to TNF-α forward signalling with altered process outgrowth. This key difference between SCG and PVG neurons could be partly attributable to the regional variation of TNFR1 expression seen between these sympathetic neuron populations. Future projects should focus on the signalling pathways that determine the alterations in TNFR1 localisation between SCG and PVG neurons and explore whether TNFR2 may in some way

modulate TNF-α/TNFR1 mediated regulation of SCG and PVG neuron target field innervation.

Chapter 4

The Contrasting Roles of CD40-CD40L Reverse Signalling in the Development of the Prevertebral and Paravertebral Divisions of the Sympathetic Nervous System

4.1 INTRODUCTION

The costimulatory receptor (CD40) is a member of the TNFRSF, and like other family members, is a type I transmembrane protein with conserved cysteine-rich residues in the extracellular domain. Mouse CD40 is a 48 kDa glycoprotein with a 193 amino acid extracellular domain, 22 amino acid hydrophobic transmembrane domain, and a 90 amino acid intracellular domain (van Kooten et al. 2000). In addition to a transmembrane (mCD40) form, TACE cleaves mCD40 to produce the soluble form of CD40 (sCD40), which together with mCD40 works to regulate cellular functions (Contin et al. 2003). sCD40 can also be generated as an isoform of CD40 by alternative splicing (Tone et al. 2001). The CD40 specific ligand, CD40L, is a member of the TNFSF of cytokines, with a structure and functions characteristic of this family. CD40L is expressed as a cell surface type II transmembrane protein, with a single membrane-spanning domain, an extracellular C-terminus and an intracellular N-terminus. CD40L varies in size between 32 and 39 kDa depending on post-translational modifications (van Kooten et al. 2000). The biochemical configuration of CD40L (β-sheet–α-helix loop–β-sheet) allows the protein to form a trimeric structure to bind to the constitutionally trimeric CD40 receptor complex (Karpusas et al. 1995). CD40L is also expressed in an 18 kDa soluble form (sCD40L) in the intracellular compartments of activated T cells, and this form has the capacity to bind CD40 in a similar trimeric fashion to transmembrane CD40L (Graf et al. 1995). Although sCD40L is a biologically active cytokine (Graf et al. 1995; Mazzei et al. 1995), it is not yet clear whether the soluble form of this glycoprotein can functionally fulfil all the roles of membrane-bound CD40L (Graf et al. 1995; Karpusas et al. 1995).

CD40-CD40L signalling has been shown to be a key player in numerous molecular activities directly linked to humoral and cellular adaptive immune responses, together with anti-tumour immunity (van Kooten et al. 2000; Antoniades et al. 2009; Elgueta et al. 2009; Laman et al. 2017). CD40 is expressed as a surface antigen on B lymphocytes, and binding of CD40L (secreted by platelets and T cells) to its receptor on B cells activates, proliferates and

differentiates B cells. CD40 has other important roles in immune responses, such as modulating antibody production, involvement in the development of autoimmune diseases and regulation of anti-tumour immunity in some carcinomas (van Kooten et al. 2000; Antoniades et al. 2009; Elgueta et al. 2009; Laman et al. 2017). The majority of studies investigating CD40-CD40L signalling have primarily focussed on its potential roles in immunome-related areas, since early discoveries clearly showed that CD40 and CD40L are expressed on a wide range of immune cells. However, relatively recent studies have found that, in addition to immune cells, CD40 and CD40L are also localised on other cell types including the thymic epithelium, endothelium from the skin, fibroblasts, and smooth muscle cells. These studies generated interest into the wider functions of CD40 and CD40L outside of immune cells, by demonstrating the effect of these proteins in wider cellular contexts (van Kooten et al. 2000; Antoniades et al. 2009; Elgueta et al. 2009; Laman et al. 2017).

Expression of CD40 and CD40L has been shown on various neuron types and in different regions of mouse CNS and PNS. For example, the expression of CD40 and CD40L has been detected on cortical neurons, neurons in the dentate gyrus, medium spiny neurons in the striatum, pyramidal neurons in the hippocampus, sensory neurons in dorsal root ganglia (DRG), and sympathetic neurons in the superior cervical ganglia (SCG) (Tan 2002; Hou et al. 2008; Carriba and Davies 2017; Howard et al. 2019; Carriba et al. 2020). CD40-CD40L signalling plays important roles in the maintenance, protection, and the development of the nervous system. Previously, a protective role for CD40-CD40L signalling in age-related neurodegeneration was demonstrated in neuron populations from the neocortex and hippocampus, in which a deficiency of CD40 causes neuron loss and various neuronal and gross brain abnormalities in the mouse (Tan 2002; Hou et al. 2008). CD40-CD40L has been shown to play a modulatory role in neurological diseases, such as human immunodeficiency virus 1-associated neurocognitive disorder, by regulating the integrity of the blood-brain-barrier (BBB), a structure which protects the brain from pathogens and toxins (Ramirez et al. 2010). Similarly, CD40-CD40L signalling induces

brain inflammation, BBB dysfunction and long term cognitive impairment in a mouse model of sepsis (Michels et al. 2015). More recently, CD40-CD40L signalling has been shown to regulate the growth of neuronal processes in the developing nervous system. For example, CD40-CD40L signalling regulates the growth and complexity of mouse hippocampal and striatal neuron dendrites by a PKC-dependent mechanism (with CD40-deficient neurons showing clear abnormalities in the development of their dendrites) (Carriba and Davies 2017; Carriba et al. 2020), and CD40-CD40L signalling enhances early axon growth from developing DRG sensory neurons (Howard et al. 2019).

Perhaps the most notable findings regarding the effects of CD40 signalling on the development of neuron populations were made by McWilliams *et al*., who uncovered a novel relationship between target-derived NGF signalling and an autocrine CD40-CD40L reverse signalling loop that together regulated the growth and branching of paravertebral sympathetic neuron axons during target field innervation (McWilliams et al. 2015). Target-derived NGF governs some crucial developmental processes of sympathetic neurons, including axonal extension and branching, elaboration of dendrites and survival of sympathetic neurons during a period of apoptotic programmed cell death that occurs shortly after sympathetic axons have reached their target fields (Levi-Montalcini 1987; Bennett et al. 2002; Davies 2003). According to the neurotrophic hypothesis, sympathetic neurons are produced in greater numbers than required for optimal functioning of the sympathetic nervous system, and they compete for limiting amounts of NGF expressed in their target organs to survive the period of programmed cell death. In addition to acting as target-derived molecules, neurotrophic factors can also function in a cell-autonomous, autocrine signalling modality in the developing and adult nervous system. In autocrine signalling, an individual neuron expresses both ligand and its specific receptor and the secreted soluble ligand binds to its receptor on the secreting neuron to initiate intracellular signal transduction in that neuron. Such autocrine signalling loops can operate in both forward and reverse signalling modalities. Examples of autocrine signalling within the nervous

system include; an autocrine brain-derived neurotrophic factor (BDNF)-TrkB pathway that plays a role in hippocampus-dependent synaptic plasticity during learning (Colgan et al. 2018), a Wnt10b-mammalian target of rapamycin (mTOR) autocrine pathway that mediates axonal regeneration in the injured CNS (Tassew et al. 2017), an insulin-like growth factor 2 autocrine loop promoting synapse stabilisation in the mammalian hippocampus (Terauchi et al. 2016), and an autocrine Wnt5a-Ror signalling loop that mediates target innervation of sympathetic fibres (Ryu et al. 2013). McWilliams *et al.* discovered that an autocrine CD40-CD40L reverse signalling loop in paravertebral SCG neurons enhanced NGF-promoted target field innervation; however, since NGF negatively regulates autocrine CD40-CD40L signalling, this autocrine signalling loop only enhanced target field innervation in target fields expressing low levels of NGF.

Results from the previous chapter clearly indicated that different modes of TNF-α-TNFR1 signalling (forward and reverse) modulate the innervation of their target fields by paravertebral and prevertebral sympathetic neurons. This raises the possibility that CD40-CD40L signalling may operate differently in regulating target field innervation by prevertebral sympathetic neurons compared to paravertebral sympathetic neurons. This chapter aims to further advance our understanding of the contributions of CD40-CD40L signalling to the development of the sympathetic nervous system by investigating its contribution to target innervation by prevertebral sympathetic neurons and comparing it to CD40-CD40L regulation of paravertebral sympathetic neuron target innervation.

4.2 RESULTS

4.2.1 Perinatal PVG and SCG Neurons Co-Express CD40 and CD40L

Previously, McWilliams *et al.* reported co-expression of CD40 and CD40L on the cell soma and processes of cultured P3 paravertebral SCG neurons (McWilliams et al. 2015). The first step in comparing and contrasting the role of CD40L-CD40 signalling between SCG and PVG neurons was to determine whether expression patterns of CD40 and CD40L show differences in these neuronal subpopulations. To investigate this, sympathetic prevertebral and paravertebral neuron cultures were established from P0 PVG and SCG, respectively. At P0, both PVG and SCG neurons are innervating their target organs and pilot experiments identified P0 as an age at which CD40-CD40L signalling affected PVG neuron axon growth. Neuron cultures were incubated for 24 h in the presence of NGF, followed by staining with CD40- and CD40L-primary, and relevant secondary, antibodies to identify the localisation of these proteins. An anti-βIII tubulin antibody was used to label the sympathetic neurons and cell nuclei were stained with DAPI. The validity and specificity of the anti-CD40 antibody was demonstrated previously by the Davies lab in sensory neuron cultures established from *Cd40*$^{-/-}$ mice (Howard et al. 2019). Immunofluorescence images were captured by confocal microscopy and imaging and quantification of neurons were conducted blind to neuron type and protein of interest. Non-specific binding of secondary antibodies was excluded by including no-primary antibody controls for PVG (Fig. 4.1) and SCG (Fig. 4.2) neurons. When anti-CD40 (Fig. 4.1A & 4.2A), anti-CD40L (Fig. 4.1B & 4.2B), or anti-βIII tubulin primary antibodies (Fig. 4.1C & 4.2C) were omitted, no non-specific binding was detected on either PVG or SCG neurons.

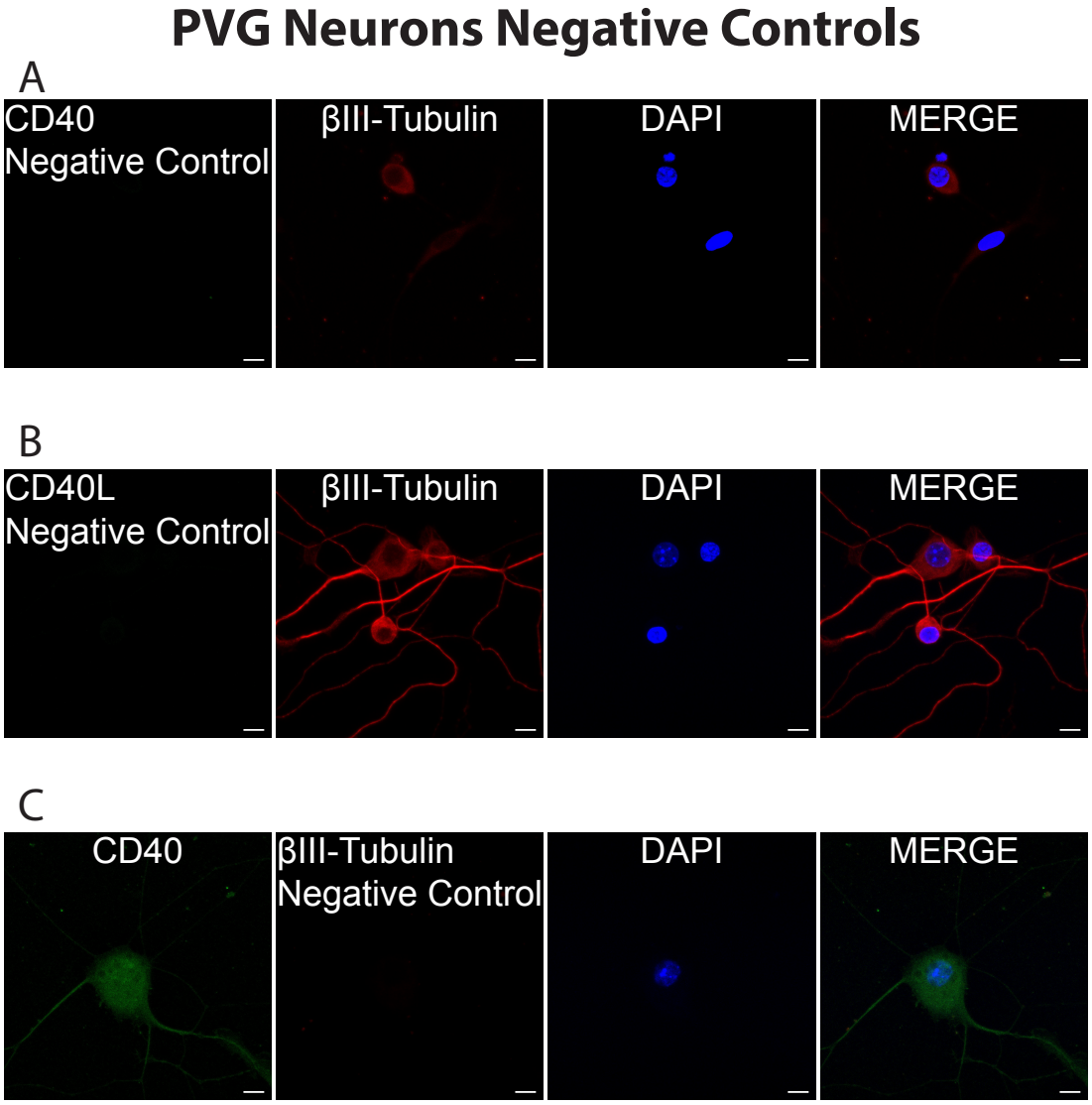

Figure 4.1. Validation of Secondary Antibodies Used in Immunocytochemical Analysis of Po PVG Sympathetic Neurons. (A-C) Representative images of PVG neurons from Po wild-type mice. **(A)** PVG neurons were stained with the secondary antibody against anti-CD40 primary antibody (green, primary antibody omitted) and primary β-III tubulin (red) with relevant secondary antibody. **(B)** PVG neurons were stained with the secondary antibody against anti-CD40L primary antibody (green, primary antibody omitted) and primary β-III tubulin (red) with relevant secondary antibody. **(C)** PVG neurons were labelled with anti-CD40 (green) primary antibody with relevant secondary antibody and the secondary antibody against the β-III tubulin primary antibody (red, primary antibody omitted). DAPI was used to stain nuclei. Scale bars represent 10 μm. Each image is representative of at least 30 images. n=3 for each condition. PVG: prevertebral ganglia (coeliac and superior mesenteric ganglia).

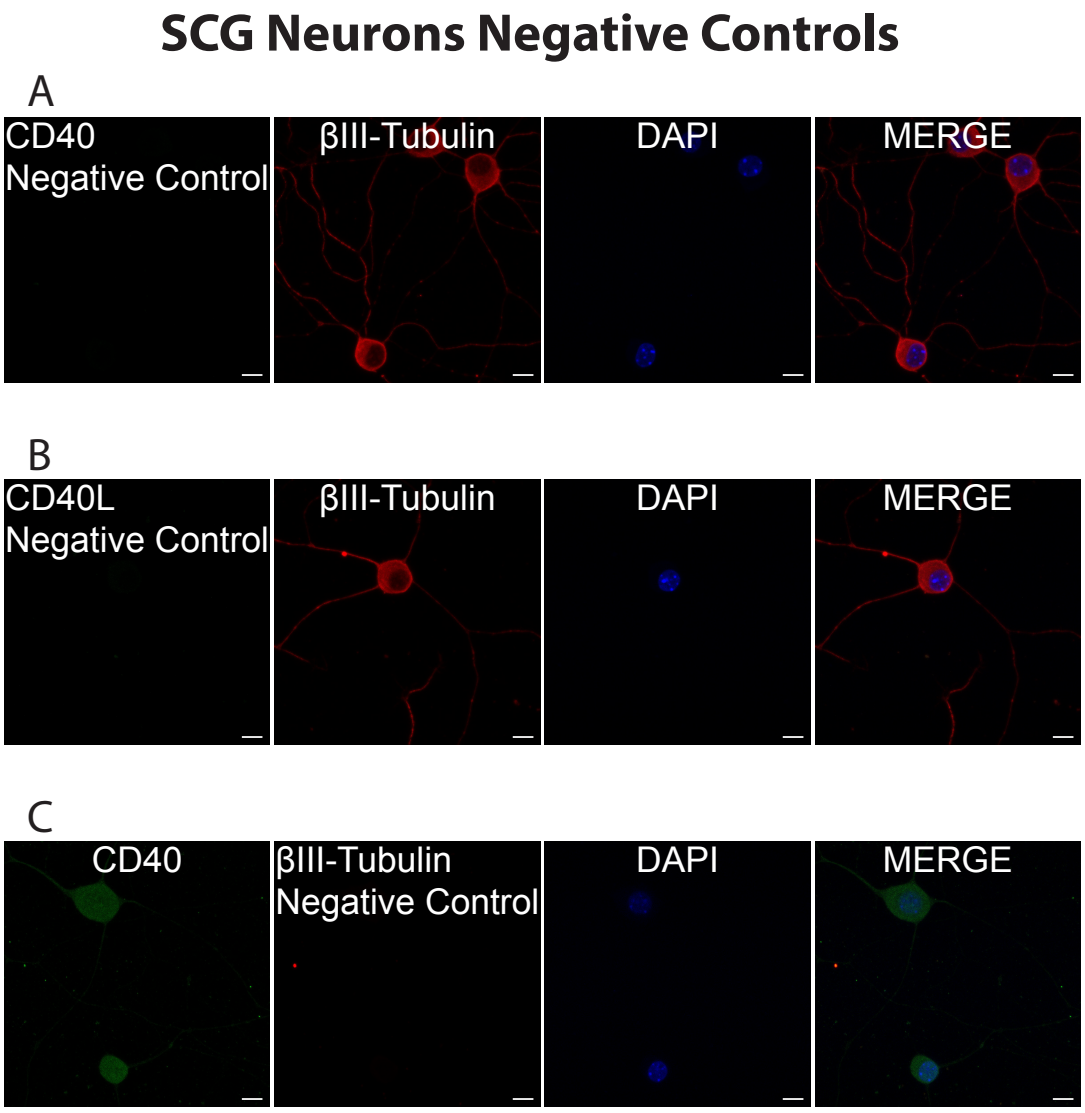

Figure 4.2. Validation of Secondary Antibodies Used in Immunocytochemical Analysis of Po SCG Sympathetic Neurons. (A-C) Representative images of SCG neurons from Po wild-type mice. **(A)** SCG neurons were stained with the secondary antibody against anti-CD40 primary antibody (green, primary antibody omitted) and primary β-III tubulin (red) with relevant secondary antibody. **(B)** SCG neurons were stained with the secondary antibody against anti-CD40L primary antibody (green, primary antibody omitted) and primary β-III tubulin (red) with relevant secondary antibody. **(C)** SCG neurons were labelled with anti-CD40 (green) primary antibody with relevant secondary antibody and the secondary antibody against the β-III tubulin primary antibody (red, primary antibody omitted). DAPI was used to stain nuclei. Scale bars represent 10 μm. Each image is representative of at least 30 images. n=3 for each condition. SCG: superior cervical ganglia.

Fig. 4.3 illustrates that CD40 and CD40L proteins were both expressed and localised in the cell soma and neurite processes of cultured Po PVG neurons. Triple labelling experiments demonstrated that the vast majority of the PVG neurons identified by anti-βIII tubulin antibody were also labelled by anti-CD40 (90 ± 1.5%) and anti-CD40L antibody (92 ± 1.1%), in separate experiments. The distribution of CD40 (Fig. 4.3A) and CD40L (Fig. 4.3B) to the cell soma and neurite arbours of PVG neurons are clearly seen in merged images, where co-localisation with βIII tubulin is demonstrated by yellow pixels.

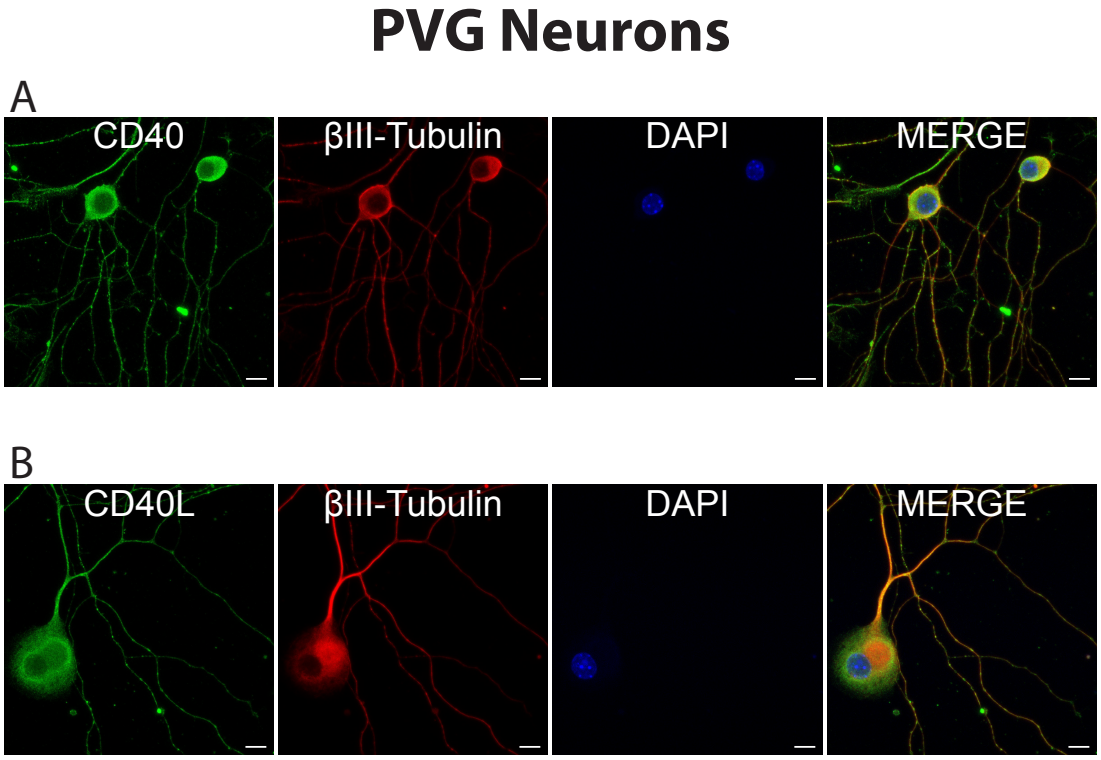

Figure 4.3. CD40 and CD40L Expression in Po PVG Neurons. (A) Representative images of PVG neurons from Po wild-type mice. Sympathetic neurons were labelled with anti-CD40 (green), anti-β-III tubulin (red), and DAPI was used to stain nuclei. **(B)** Representative images of PVG neurons from Po wild-type mice. Sympathetic neurons were labelled with anti-CD40L (green), anti-β-III tubulin (red), and DAPI was used to stain nuclei. Scale bars represent 10 μm. Each image is representative of at least 30 images. n=3 for each condition. PVG: prevertebral ganglia (coeliac and superior mesenteric ganglia).

Representative images demonstrated that CD40 (Fig. 4.4A) and CD40L (Fig. 4.4B) proteins were also expressed and localised in the cell soma and neurite processes of dissociated Po SCG neurons (Fig. 4.4). Quantification of triple labelled SCG neurons showed that 89 ± 2.9% of βIII tubulin-labelled neurons were also labelled by anti-CD40 antibody and 85 ± 2.4% by anti-CD40L antibody.

These results suggest that the majority of PVG neurons (at least 80%, as the percentages of CD40 and CD40L expression are both individually higher than 90%) co-express CD40 and CD40L proteins in their cell soma and neurite processes at the developmental stage when these sympathetic neurons are innervating their target organs. A similar co-expression pattern of CD40 and CD40L was also seen in SCG neurons, verifying previous reports of CD40-CD40L co-localisation in this sympathetic neuron population (McWilliams et al. 2015).

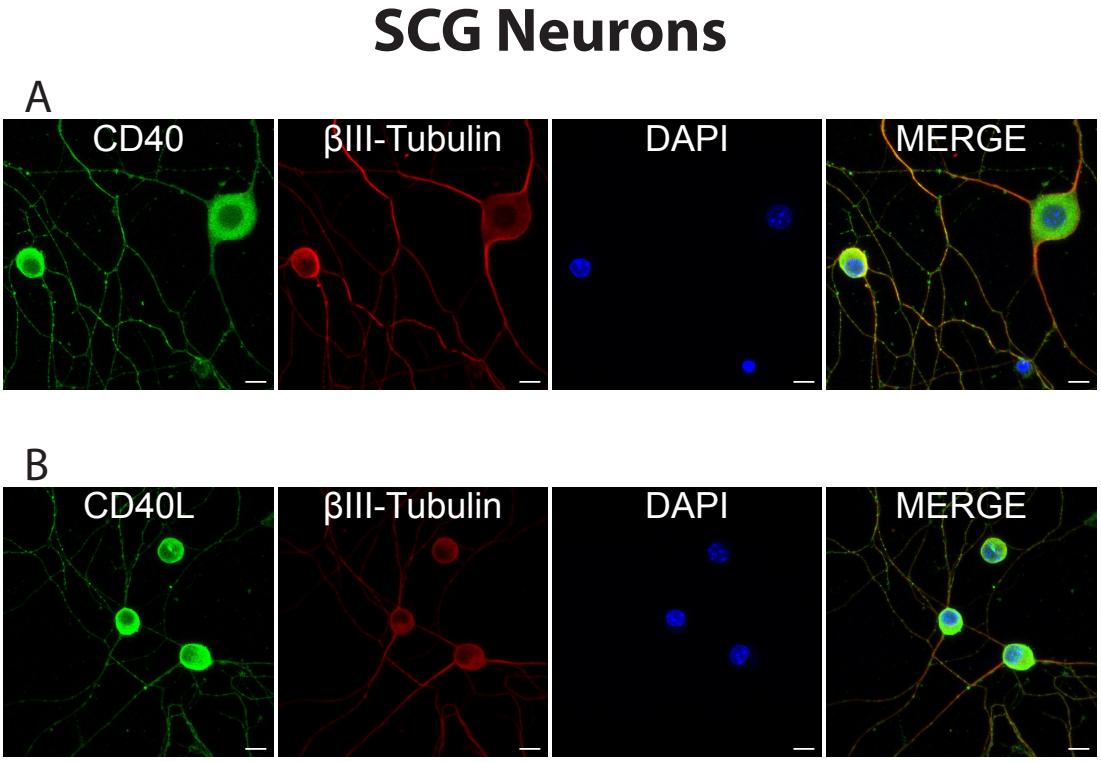

Figure 4.4. CD40 and CD40L Expression in Po SCG Neurons. (A) Representative images of SCG neurons from Po wild-type mice. Sympathetic neurons were labelled with anti-CD40 (green), anti-β-III tubulin (red), and DAPI was used to stain nuclei. **(B)** Representative images of SCG neurons from Po wild-type mice. Sympathetic neurons were labelled with anti-CD40L (green), anti-β-III tubulin (red), and DAPI was used to stain nuclei. Scale bars represent 10 μm. Each image is representative of at least 30 images. n=3 for each condition. SCG: superior cervical ganglia.

4.2.2 CD40-CD40L Autocrine Signalling Suppresses NGF-Promoted Neurite Outgrowth from PVG Neurons

A number of previous studies have demonstrated that the co-expression of TNFSF and TNFRSF members within the same neurons is indicative of an autocrine signalling loop that regulates neuronal process growth (O'Keeffe et al. 2008; Gavalda et al. 2009; McWilliams et al. 2015; Carriba and Davies 2017; Howard et al. 2018). From these studies, the findings of McWilliams *et al.* are of particular interest to the current study as they demonstrated that CD40-CD40L autocrine signalling enhances NGF-promoted axon growth and branching from SCG neurons *in vitro* and *in vivo* (McWilliams et al. 2015). The co-expression of CD40 and CD40L in both the cell bodies and processes of PVG neurons raises the question as to whether process outgrowth from PVG neurons may be modulated through CD40-CD40L autocrine signalling in a similar manner to SCG neurons. Blocking the interaction between CD40 and CD40L would eliminate any potential CD40-CD40L autocrine loop, and help identify its contribution to regulating neurite outgrowth from PVG neurons.

To test the contribution of CD40-CD40L autocrine signalling in regulating process outgrowth from PVG neurons, neuronal cultures were established from PVG and SCG (as a positive control) dissected from Po $Cd40^{+/+}$ and $Cd40^{-/-}$ mice. For each experimental repeat, paravertebral and prevertebral ganglia were pooled (separately) from at least three different mice per genotype. Dissociated PVG and SCG neurons were seeded into extremely low-density, non-contiguous, cultures in the presence of 1 ng/ml NGF to sustain neuron survival and to promote neurite growth.

A visual comparison of cultured PVG neurons from $Cd40^{+/+}$ and $Cd40^{-/-}$ mice after 24 h incubation clearly indicates that knockout of CD40 enhanced NGF-promoted neurite growth and branching from PVG neurons (Fig. 4.5A). Quantification of the neurite morphology of PVG neurons revealed that $Cd40^{-/-}$ neurons had significantly longer mean neurite lengths (Fig. 4.5B, $p<0.001$) and a higher mean number of branch points (Fig. 4.5C, $p<0.05$) than $Cd40^{+/+}$ neurons. The Sholl profiles of PVG neurons, plotted by counting the number of

intersections that neurites make with virtual concentric rings at different distances from the soma, demonstrated that *Cd40*$^{-/-}$ neurons had more complex neurites than neurons from *Cd40*$^{+/+}$ mice (Fig. 4.5D).

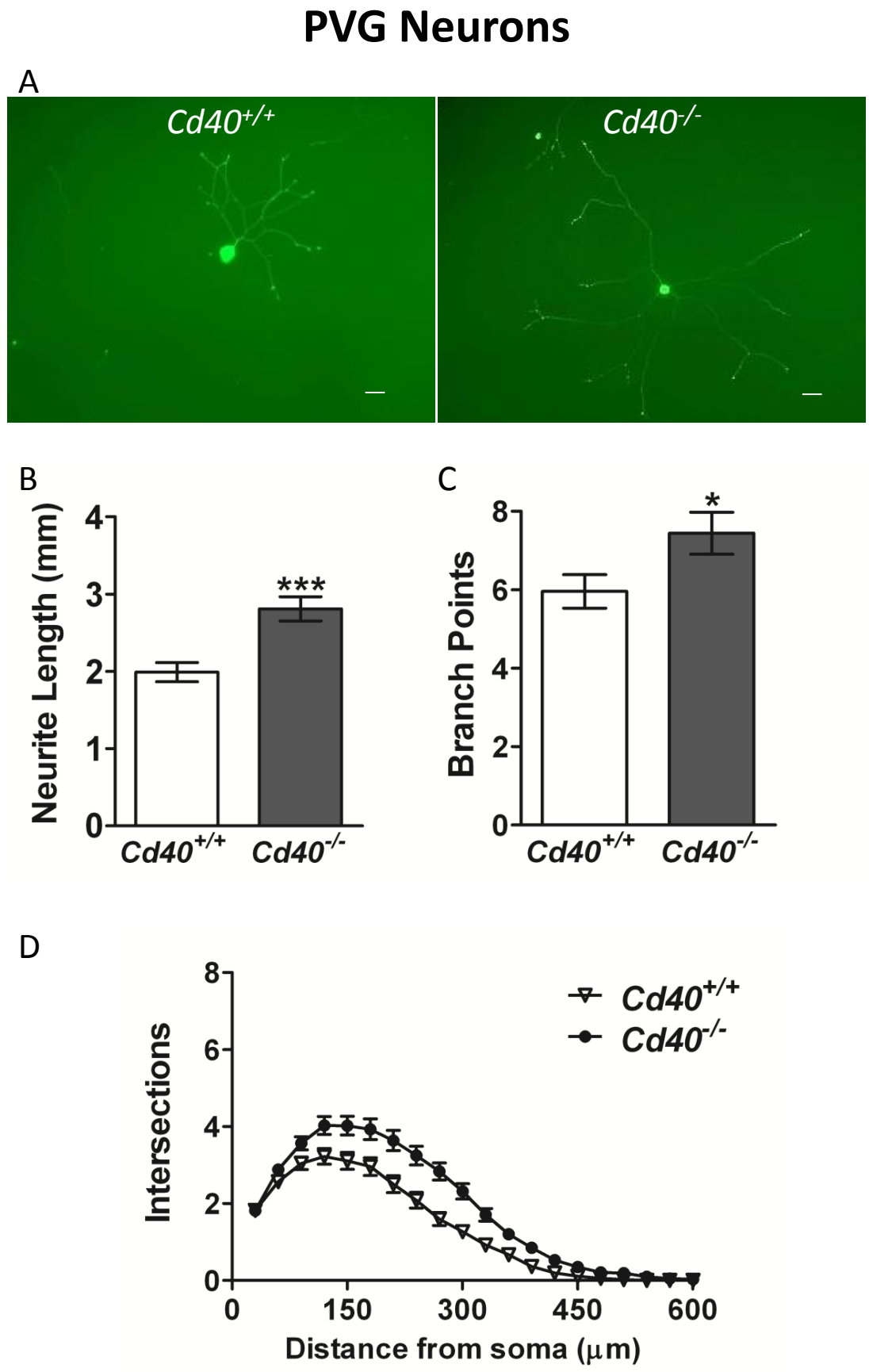

Fig. 4.5. Legend on following page.

Figure 4.5. CD40-CD40L Autocrine Signalling Suppresses NGF-Promoted Outgrowth of Po PVG Neurites. (A) Representative images of calcein-AM stained PVG neurons from Po *Cd40*$^{+/+}$ and *Cd40*$^{-/-}$ mice treated with 1 ng/ml NGF. Scale bars represent 50 μm. Each image is representative of 180 images from at least three independent experiments. **(B&C)** Quantification of neurite lengths **(B)** and branch points **(C)** of Po *Cd40*$^{+/+}$ and *Cd40*$^{-/-}$ PVG neurons treated as described in (A). Data are presented as the mean ± standard error. Results were collected from the analysis of at least 180 neurons per condition, with at least three separate experiments performed for each condition (60 to 80 neurons analysed per experiment). *: $p<0.05$, ***: $p<0.001$ (Mann-Whitney test). **(D)** Sholl analysis of Po *Cd40*$^{+/+}$ and *Cd40*$^{-/-}$ PVG neurons treated as described in (A). Data are presented as the mean ± standard error. At least three separate experiments were performed for each condition (60 to 80 neurons analysed per experiment). NGF: nerve growth factor; PVG: prevertebral ganglia (coeliac and superior mesenteric ganglia).

In contrast, knockout of CD40 protein in SCG neurons resulted in suppressed neurite outgrowth and branch development as shown in Fig. 4.6A. Analysis of cultured SCG neurons from *Cd40*$^{+/+}$ and *Cd40*$^{-/-}$ mice demonstrated that neurons from *Cd40*$^{-/-}$ mice had significantly shorter (Fig. 4.6B, $p<0.001$), and less branched processes (Fig. 4.6C, $p<0.001$) than neurons from wild-type littermates. Sholl profiles illustrate that cultured SCG neurons from *Cd40*$^{-/-}$ animals had clearly less complex morphologies than SCG neurons from *Cd40*$^{+/+}$ mice (Fig. 4.6D).

These findings indicate that deletion of CD40 impacts NGF-promoted neurite outgrowth and complexity in PVG neurons as in SCG neurons. Surprisingly, however, deletion of CD40 has opposite effects on the extent of neurite outgrowth from PVG and SCG neurons. This suggests that whilst CD40-CD40L autocrine signalling functions to promote neurite outgrowth in wild-type SCG neurons, in wild-type PVG neurons it functions instead to suppress neurite outgrowth.

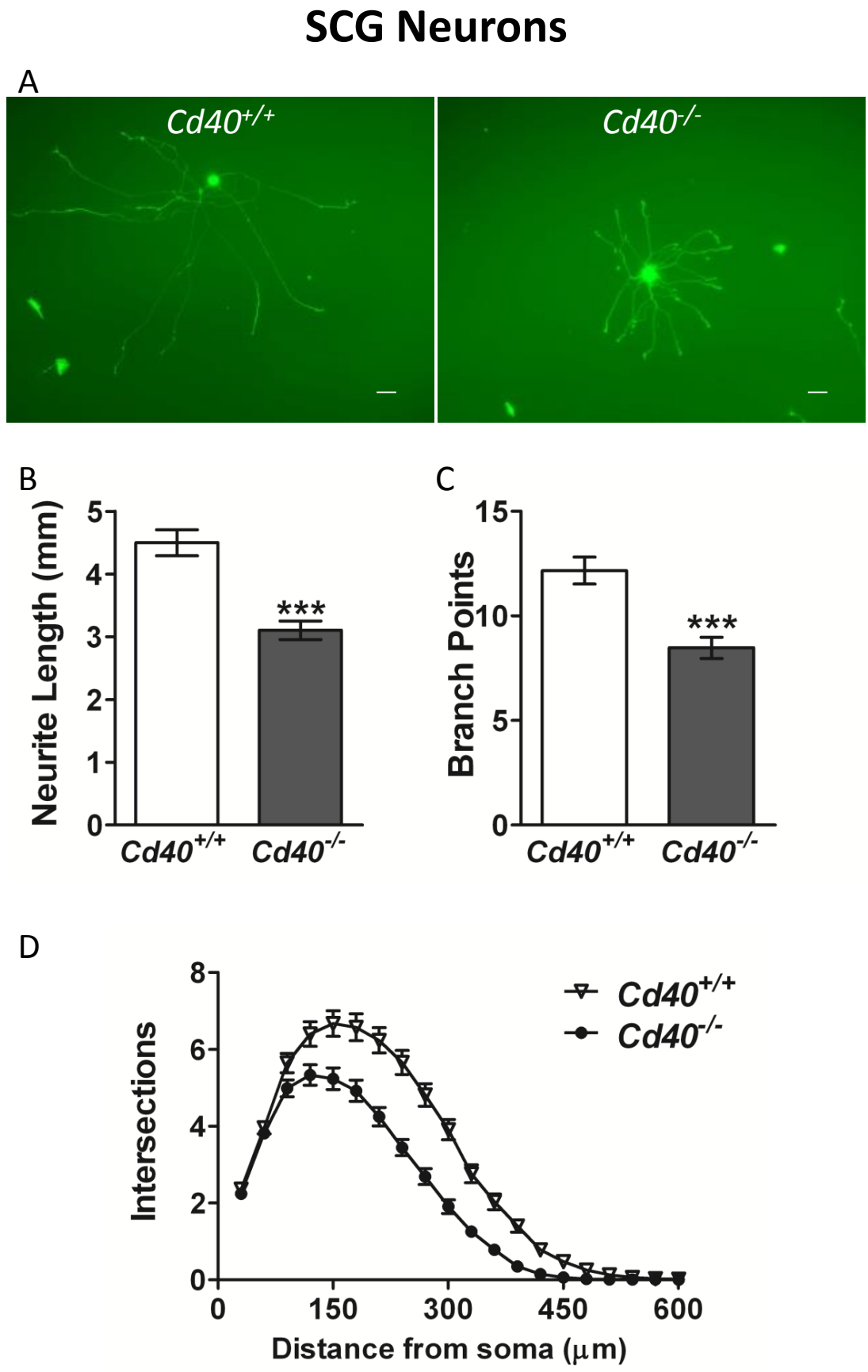

Fig. 4.6. Legend on following page.

Figure 4.6. CD40-CD40L Autocrine Signalling Enhances NGF-Promoted Outgrowth of Po SCG Neurites. **(A)** Representative images of calcein-AM stained SCG neurons from Po *Cd40*$^{+/+}$ and *Cd40*$^{-/-}$ mice treated with 1 ng/ml NGF. Scale bars represent 50 μm. Each image is representative of 180 images from at least three experiments. **(B&C)** Quantification of neurite lengths **(B)** and branch points **(C)** of Po *Cd40*$^{+/+}$ and *Cd40*$^{-/-}$ SCG neurons treated as described in (A). Data are presented as the mean ± standard error. Results were collected from the analysis of at least 180 neurons per condition, with at least three separate experiments performed for each condition (60 to 80 neurons analysed per experiment). ***: $p<0.001$ (Mann-Whitney test). **(D)** Sholl analysis of Po *Cd40*$^{+/+}$ and *Cd40*$^{-/-}$ SCG neurons treated as described in (A). Data are presented as the mean ± standard error. At least three separate experiments were performed for each condition (60 to 80 neurons analysed per experiment). NGF: nerve growth factor; SCG: superior cervical ganglia.

4.2.3 CD40L Reverse Signalling Modulates NGF-promoted Neurite Growth in Both PVG and SCG Neurons

One of the significant findings by McWilliams *et al.* was that CD40-CD40L autocrine signalling enhances NGF-promoted neurite growth and complexity in cultured SCG neurons by a reverse signalling mechanism (McWilliams et al. 2015). Similarly, data in the previous chapter suggested that TNF-α-reverse signalling regulates process growth from SCG neurons, but not PVG neurons (see **Section 3.2.2** in **Chapter 3**). To better understand the influence of TNFSF and TNFRSF members in the development of the SNS, it was important to determine whether autocrine CD40-CD40L reverse signalling was also limited to paravertebral neurons or whether it operates in both paravertebral and prevertebral sympathetic neurons. To investigate whether autocrine CD40-CD40L signalling suppressed the growth of PVG neuron processes by forward or reverse signalling, NGF-supplemented PVG and SCG (as a positive control) neuron cultures were established from Po *Cd40*$^{+/+}$ and *Cd40*$^{-/-}$ littermates. It was reasoned that if reverse signalling was operating, treating *Cd40*$^{-/-}$ sympathetic neurons with CD40-Fc chimera (in which the extracellular domain of CD40 is linked to the Fc part of human IgG1) would rescue *Cd40*$^{-/-}$ PVG neurons from the significant increase in their neurite length compared to *Cd40*$^{+/+}$ neurons, by restoring CD40-activated CD40L-mediated reverse signalling.

In PVG neuron cultures supplemented with NGF, disruption of CD40-CD40L signalling caused a significant increase in mean neurite length of *Cd40*$^{-/-}$ neurons compared with *Cd40*$^{+/+}$ neurons (Fig. 4.7A, $p<0.05$). However, the addition of CD40-Fc to CD40 knockout PVG neuron cultures significantly reduced mean neurite lengths to levels similar to those seen in *Cd40*$^{+/+}$ neuron cultures (Fig. 4.7A, $p<0.05$). On the other hand, while mean neurite lengths of SCG neurons in NGF-supplemented cultures established from *Cd40*$^{-/-}$ mice were significantly less than in cultures established from *Cd40*$^{+/+}$ mice (Fig. 4.7B, $p<0.05$), CD40-Fc treatment significantly increased the length of *Cd40*$^{-/-}$ SCG neuron neurites to wild-type levels (Fig. 4.7B, $p<0.05$). The addition of Fc

fragment (as a control of CD40-Fc), and CD40L (as a control for CD40 signalling) to *Cd40*$^{-/-}$ PVG (Fig. 4.7A) and SCG (Fig. 4.7B) cultures did not affect neurite length.

These data demonstrate that CD40-Fc reverses the changes in the extent of neurite outgrowth from CD40-deficient PVG and SCG neurons compared to wild-type neurons in cultures supplemented with NGF and returns the level of neurite outgrowth to that seen in cultures of wild-type neurons. This therefore indicates that autocrine CD40-CD40L reverse signalling modulates NGF-promoted process outgrowth in both SCG and PVG neurons.

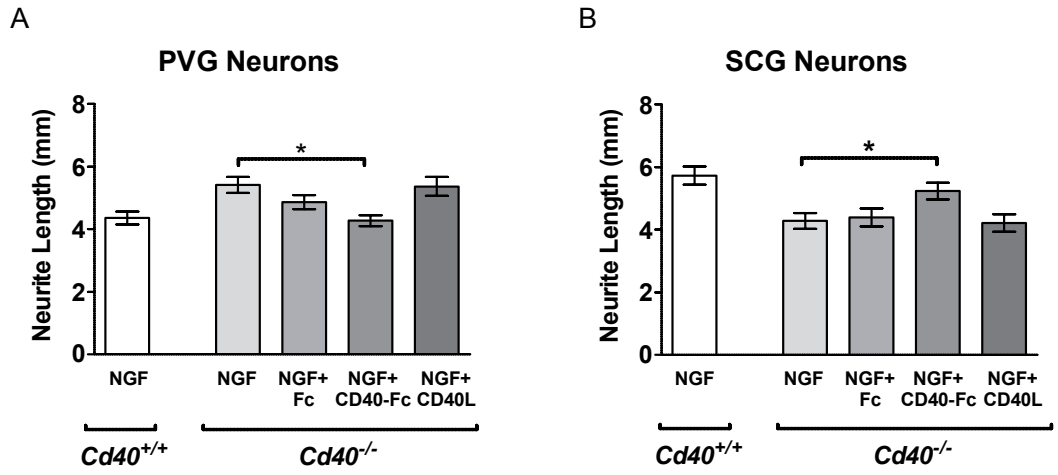

Figure 4.7. Reverse Signalling Underlies the Effect of CD40-CD40L Autocrine Signalling on NGF-Promoted Outgrowth of Po PVG and SCG Neurites. (A&B) Quantification of neurite lengths of Po *Cd40*$^{+/+}$ and *Cd40*$^{-/-}$ PVG **(A)** and SCG **(B)** neurons. Neurons were treated with 1 ng/ml NGF alone, or in addition to 1 µg/ml Fc control, 1 µg/ml CD40-Fc, or 1 µg/ml CD40L. Data are presented as the mean ± standard error. n=3 for each condition, *: $p<0.05$ (Kruskal-Wallis, with Dunn's *post-hoc* analysis). NGF: nerve growth factor; PVG: prevertebral ganglia (coeliac and superior mesenteric ganglia); SCG: superior cervical ganglia.

4.2.4 CD40-CD40L Signalling Acts on PVG and SCG Neurons in a Similar Developmental Period

To help understand the potential physiological context of the opposing effects of autocrine CD40-CD40L reverse signalling on process outgrowth from PVG and SCG neurons, the time period over which this signalling loop was able to modulate process outgrowth from PVG neurons was investigated and compared to SCG neurons. McWilliams *et al.* previously demonstrated that CD40-CD40L autocrine reverse signalling enhances NGF-promoted neurite outgrowth from SCG neurons in a time window between E17 and P5, which encompasses the period of development in which SCG neurons are reaching and innervating their peripheral target organs, and are still heavily dependent on NGF for their survival (McWilliams et al. 2015). To investigate whether a similar developmental window exists for the effects of CD40-CD40L signalling on PVG neurons, NGF (1 ng/ml) supplemented, low-density dissociated PVG and SCG neuron cultures were established from *Cd40*$^{+/+}$ and *Cd40*$^{-/-}$ mice at a range of developmental ages (E18, P0, P3 and P5). Sympathetic neurons were incubated for 24 h, then labelled by the fluorescent vital dye, calcein-AM, to enable imaging of processes.

At E18, quantification of the lengths of PVG and SCG neuron processes in cultures established from CD40-deficient and wild-type mice revealed that disruption of autocrine CD40-CD40L reverse signalling resulted in significantly increased mean neurite lengths in PVG neuron cultures (Fig. 4.8A, $p<0.05$), and a significant reduction in mean neurite lengths in SCG neuron cultures (Fig. 4.8B, $p<0.05$). This pattern was also seen at P0 (Fig. 4.8, $p<0.001$ for both PVG and SCG neurons). Statistical differences between the length of CD40-deficient and wild-type PVG and SCG neuron processes persisted at P3 (Fig. 4.8, $p<0.05$ for both PVG and SCG neurons). However, by P5, knockout of CD40 and disruption of the autocrine CD40-CD40L reverse signalling loop no longer affected the extent of neurite outgrowth in both PVG and SCG neuron cultures. The age at which CD40 knockout had the most statistically significant effect on mean neurite length was P0.

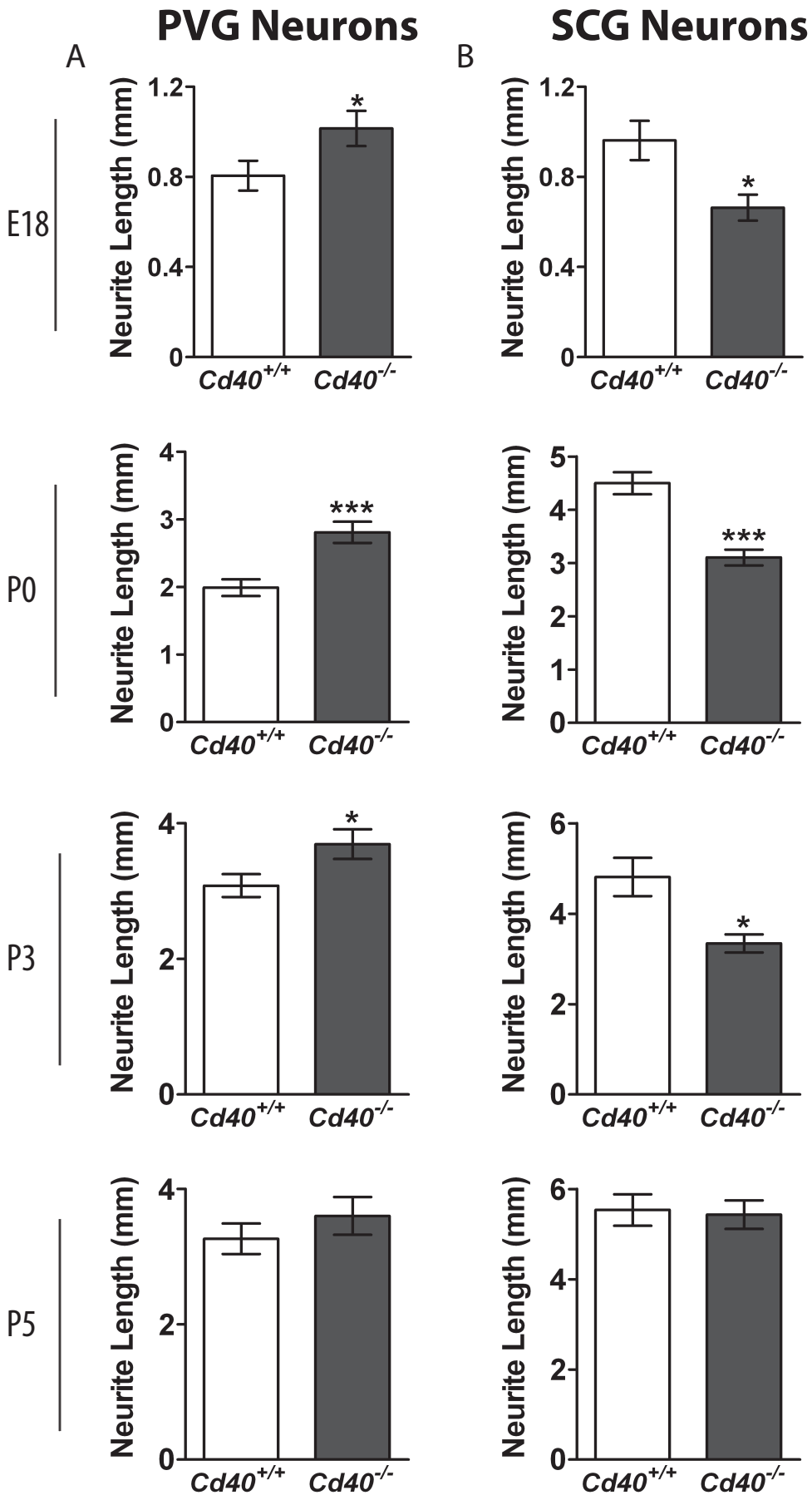

Fig. 4.8. Legend on following page.

Figure 4.8. Autocrine CD40-CD40L Reverse Signalling Affects PVG and SCG Neuron Neurite Lengths Across Late Embryonic and Early Postnatal Periods. (A&B) Quantification of neurite lengths of *Cd40*$^{+/+}$ and *Cd40*$^{-/-}$ PVG **(A)** and SCG **(B)** neurons at E18, P0, P3, and P5. Neurons were treated with 1 ng/ml NGF. Data are presented as the mean ± standard error. n=3 for each condition, **: $p<0.01$ (Mann-Whitney test). NGF: nerve growth factor; PVG: prevertebral ganglia (coeliac and superior mesenteric ganglia); SCG: superior cervical ganglia.

A similar developmental pattern over the E18 to P5 experimental window was also seen in the number of branch points exhibited by the processes of cultured *Cd40*$^{-/-}$ and *Cd40*$^{+/+}$ PVG and SCG neurons (Fig. 4.9). At E18 and P0, CD40 knockout significantly increased the number of neurite bifurcations in PVG neuron cultures (Fig. 4.9A, $p<0.05$ at both ages) and had the opposite effect in SCG neuron cultures (Fig. 4.9B, $p<0.001$ at both ages). By P3, differences between the number of branch points on the neurites of PVG neurons from *Cd40*$^{-/-}$ mice and wild-type mice had disappeared (Fig. 4.9A). However, in the case of SCG neurons, CD40 knockout neurons still exhibited reduced neurite branching compared to wild-type neurons, although the extent of the reduction and its statistical significance was less than at P0 (Fig. 4.9B, $p<0.05$). At P5, there were no differences in the number of neurite branch points between PVG neuron cultures established from *Cd40*$^{-/-}$ mice and wild-type mice. Surprisingly, cultured P5 CD40-deficient SCG neurons showed a significantly *increased* number of branch points compared with wild-type neurons ($p<0.01$). As with neurite length, the developmental age at which CD40 knockout had the most prominent effect on neurite branch point number was P0 for both PVG and SCG neurons.

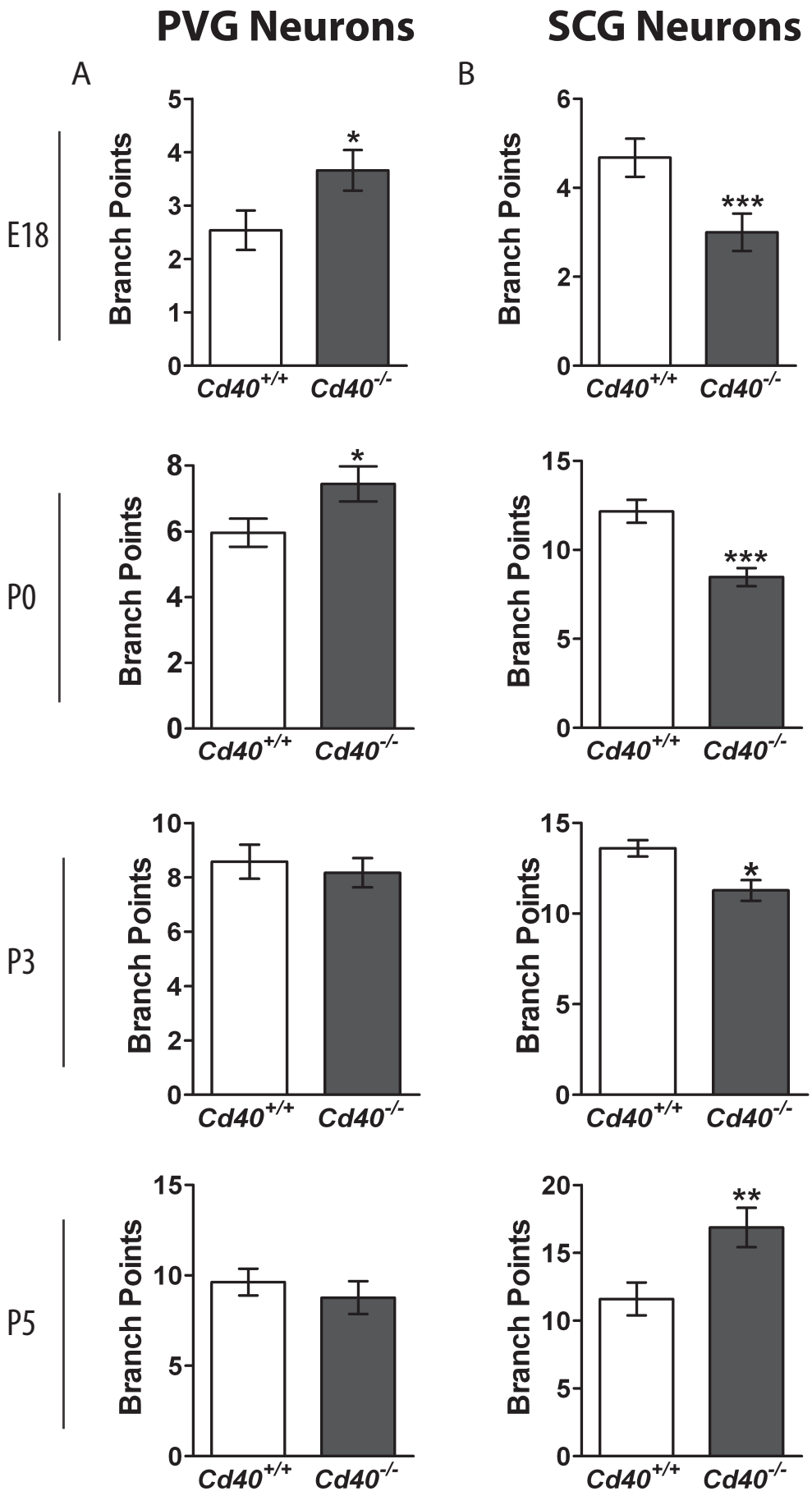

Fig. 4.9. Legend on following page.

Figure 4.9. Autocrine CD40-CD40L Reverse Signalling Affects PVG and SCG Neuron Branch Point Numbers Across Late Embryonic and Early Postnatal Periods. (A&B) Quantification of branch point numbers of *Cd40*$^{+/+}$ and *Cd40*$^{-/-}$ PVG **(A)** and SCG **(B)** neurons at E18, P0, P3, and P5. Neurons were treated with 1 ng/ml NGF. Data are presented as the mean ± standard error. n=3 for each condition, **: $p<0.01$ (Mann-Whitney test). NGF: nerve growth factor; PVG: prevertebral ganglia (coeliac and superior mesenteric ganglia); SCG: superior cervical ganglia.

Differences in neurite complexity between CD40-deficient and wild-type neurons from PVG and SCG are demonstrated by Sholl analysis (Fig. 4.10). At E18, the Sholl profiles of cultured *Cd40*$^{-/-}$ and wild-type PVG neurons are almost overlapping, indicating only a marginal increase in neurite complexity in the absence of autocrine CD40-CD40L reverse signalling. In contrast, CD40-deficient SCG neurons showed a clear reduction in the number of neurite intersections at distances from the cell soma of between 90 and 300 μm when compared with neurons from wild-type littermates. At P0, both PVG and SCG CD40-deficient neurons showed clear differences in their neurite morphology when compared with wild-type neurons. In the case of PVG neurons, CD40-deficient neurons displayed a higher neurite complexity than wild-type neurons, whereas in the case of SCG neurons CD40 knockout reduced neurite complexity compared to wild-type neurons. The obvious morphological differences between *Cd40*$^{-/-}$ and wild-type PVG neurons, as displayed by Sholl analysis, had largely disappeared by P3, although the number of intersections at distances from the cell soma of between 210 and 300 μm were still higher in *Cd40*$^{-/-}$ neurons compared to *Cd40*$^{+/+}$ neurons. Less complex neurite outgrowth from CD40-deficient neurons compared to wild-type neurons was still obvious in the Sholl profiles of P3 SCG neurons. The differences between the effects of CD40 knockout on the Sholl profiles, and hence neurite complexity, of PVG and SCG neurons persisted at P5. At this timepoint, no difference in neurite complexity was seen between wild-type and CD40-deficient PVG neurons. Sholl profiles of P5 SCG neurons indicate that whereas CD40-deficient SCG neurons displayed greater neurite complexity than wild-type neurons at shorter distances from the soma (between 120 and 210 μm), neurites from wild-type neurons made more intersections than *Cd40*$^{-/-}$ neurons at distances from the soma of between 300 and 420 μm.

In summary, disruption of autocrine CD40-CD40L reverse signalling by CD40 knockout caused a significant increase in mean neurite length and number of neurite branch points in cultured PVG neurons at E18 and P0, and an increase in mean neurite length at P3. The most statistically significant

increases were observed at P0, and differences were not discernible by P5. On the whole, the efficacy of autocrine CD40-CD40L reverse signalling in modulating NGF-promoted process outgrowth follows the same time course as that seen in SCG neurons. This coincides with the developmental period over which sympathetic neurons are innervating their target organs and remain dependent on NGF for their survival. Finally, the SCG data in this section corroborated the previous report from McWilliams *et al*. that demonstrated that autocrine CD40-CD40L reverse signalling modulates the extent of process outgrowth from SCG neurons during a defined developmental time window (McWilliams et al. 2015).

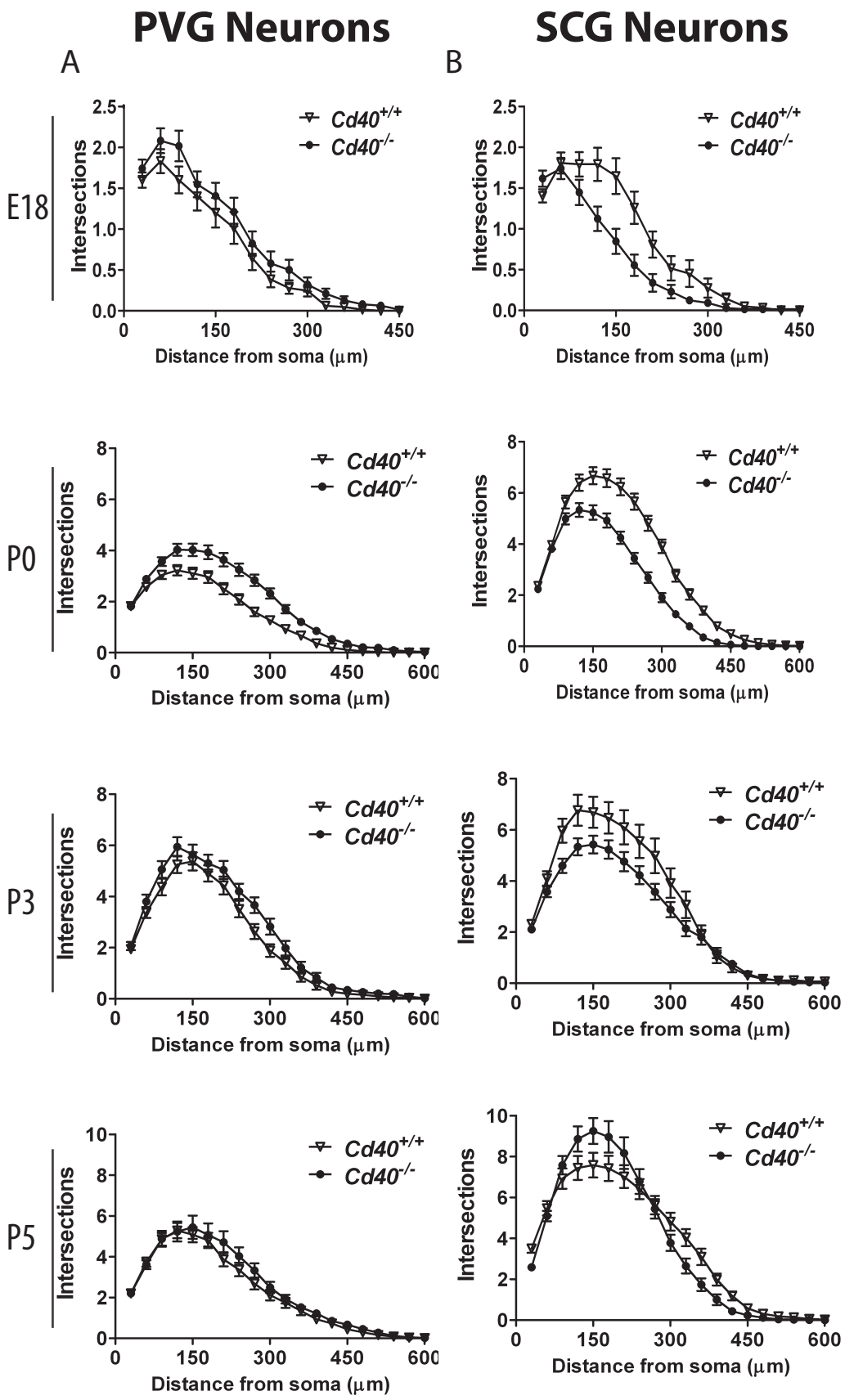

Fig. 4.10. Legend on following page.

Figure 4.10. Autocrine CD40-CD40L Reverse Signalling Affects PVG and SCG Neuronal Morphologies Across Late Embryonic and Early Postnatal Periods. (A&B) Sholl analysis of *Cd40*$^{+/+}$ and *Cd40*$^{-/-}$ PVG **(A)** and SCG **(B)** neurons at E18, P0, P3, and P5. Neurons were treated with 1 ng/ml NGF. Data are presented as the mean ± standard error. n=3 for each condition. NGF: nerve growth factor; PVG: prevertebral ganglia (coeliac and superior mesenteric ganglia); SCG: superior cervical ganglia.

4.2.5 NGF Sensitivity of CD40-CD40L Signalling in Sympathetic Neurons

As CD40 influences the development of PVG neurons over a time period in which they are still heavily dependent on NGF for survival and target field innervation, the next step was to investigate whether the efficacy of CD40-CD40L reverse signalling in suppressing process outgrowth from PVG neurons is dependent on the concentration of NGF that the neurons are exposed to, or indeed whether CD40-CD40L reverse signalling requires any NGF to operate. Previously, it was demonstrated that CD40-CD40L signalling only enhances process outgrowth from SCG neurons *in vitro* at NGF concentrations between 0.01 and 1 ng/ml (McWilliams et al. 2015). To characterise the possible interactions between NGF and CD40-CD40L signalling in developing PVG neurons, sympathetic neuron cultures were established from Po *Cd40*$^{+/+}$ and *Cd40*$^{-/-}$ PVG and SCG (as a control). All cultures were supplemented with the broad-spectrum caspase inhibitor, Boc-D-FMK to prevent apoptosis in conditions with little or no NGF (Kisiswa et al. 2013; McWilliams et al. 2015). Sympathetic neurons were incubated for 24 h, then labelled by calcein-AM to allow imaging of processes.

The NGF dependence of CD40-CD40L regulation of neurite growth (Fig. 4.11), branch point number (Fig. 4.12), and overall neurite complexity (Fig. 4.13) was tested in cultures of PVG and SCG neurons containing either no NGF or with NGF concentrations ranging from 0.01 to 10 ng/ml NGF. In the absence of NGF in the culture media, analysis of Po PVG and SCG neurons found no difference in neurite lengths between *Cd40*$^{+/+}$ and *Cd40*$^{-/-}$ neurons (Fig. 4.11). At 0.01 ng/ml NGF, while CD40 knockout had still no effect on PVG neurite lengths, the neurite lengths of CD40-deficient SCG neurons were significantly reduced compared with wild-type neurons (Fig. 4.11, $p<0.05$), indicating that in wild-type SCG neurons CD40-CD40L reverse signalling was operating to enhance NGF-promoted neurite outgrowth. When the NGF concentration was increased to 0.1 and 1 ng/ml, CD40-deficient neurites were significantly longer in PVG cultures (Fig. 4.11, $p<0.01$) and significantly shorter in SCG cultures (Fig.

4.11, $p<0.001$) compared with the wild-type counterparts of those neurons. Finally, at 10 ng/ml NGF, CD40-deficient PVG neurons had neurite lengths that were still significantly longer than wild-type PVG neurons (Fig. 4.11, $p<0.01$); however, at this NGF concentration *Cd40*$^{+/+}$ and *Cd40*$^{-/-}$ SCG neurons did not show any differences in neurite length.

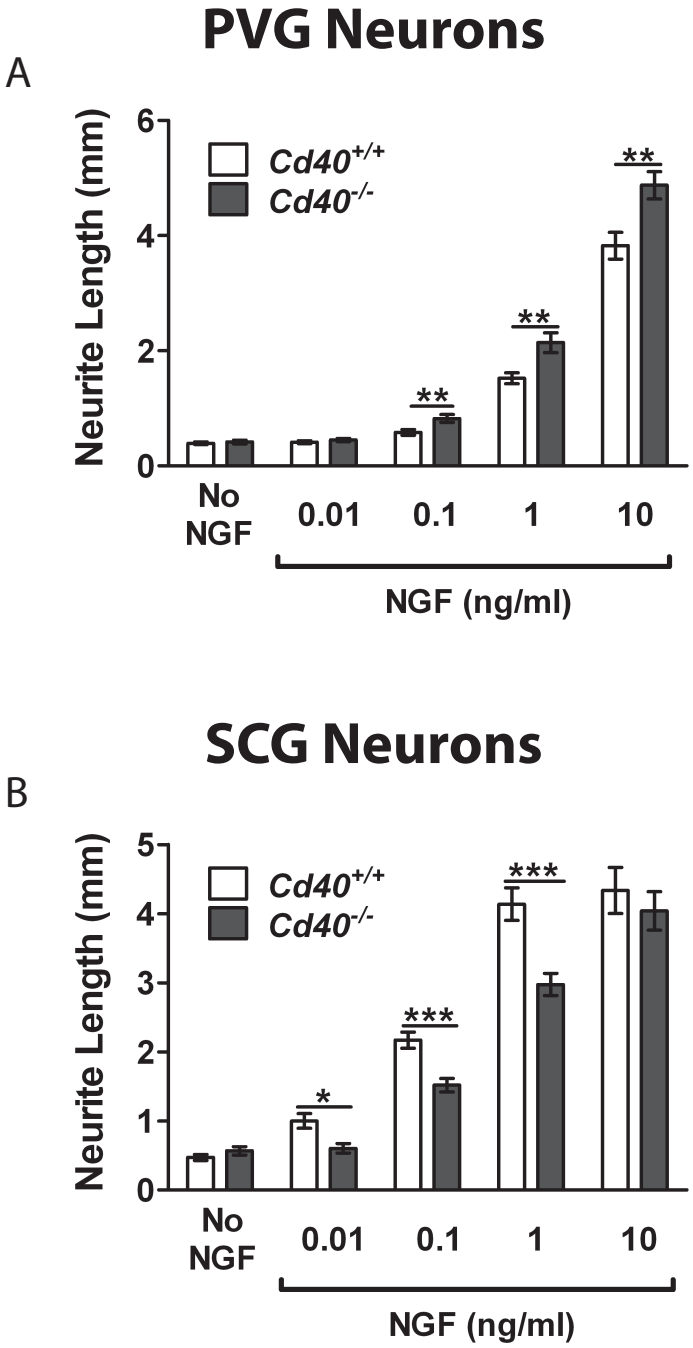

Figure 4.11. NGF Sensitivity of CD40-CD40L Signalling in Po PVG and SCG Neurons – Effect on Neurite Lengths. (A&B) Quantification of neurite lengths of Po *Cd40*$^{+/+}$ and *Cd40*$^{-/-}$ PVG **(A)** and SCG **(B)** neurons. Neurons were either cultured without NGF, or treated with NGF at concentrations between 0.01 and 10 ng/ml. Data are presented as the mean ± standard error. n=3 for each condition. *: $p<0.05$, **: $p<0.01$, ***: $p<0.001$ (Kruskal-Wallis, with Dunn's *post-hoc* analysis). NGF: nerve growth factor; PVG: prevertebral ganglia (coeliac and superior mesenteric ganglia); SCG: superior cervical ganglia.

Fig. 4.12 shows the effect of different NGF concentrations on the regulation of neurite branch point number in sympathetic neurons through autocrine CD40-CD40L reverse signalling. Similar to the effect of CD40 knockout on the length of sympathetic neuron neurites, *Cd40*$^{+/+}$ and *Cd40*$^{-/-}$ PVG and SCG neurons did not show any significant differences in the number of branch points in the absence of NGF. In cultures supplemented with 0.01 ng/ml NGF, *Cd40*$^{+/+}$ and *Cd40*$^{-/-}$ PVG neurons still displayed the same number of branch points; however, *Cd40*$^{-/-}$ SCG neurons had significantly less branch points than *Cd40*$^{+/+}$ SCG neurons at this NGF concentration (p<0.05). In the presence of 0.1 and 1 ng/ml NGF, while *Cd40*$^{-/-}$ PVG neurons had significantly increased number of branch points compared to *Cd40*$^{+/+}$ PVG neurons (p<0.01 at 0.1 ng/ml NGF and p<0.05 at 1 ng/ml NGF), *Cd40*$^{-/-}$ SCG neurons had significantly fewer branch points than *Cd40*$^{+/+}$ SCG neurons (p<0.01 at 0.1 and 1 ng/ml NGF). At 10 ng/ml NGF, *Cd40*$^{-/-}$ PVG neurons still had significantly more branch points than *Cd40*$^{+/+}$ PVG neurons (p<0.05); however, at this high NGF concentration there was no significant effect of CD40-CD40L reverse signalling on the branching of SCG neurons.

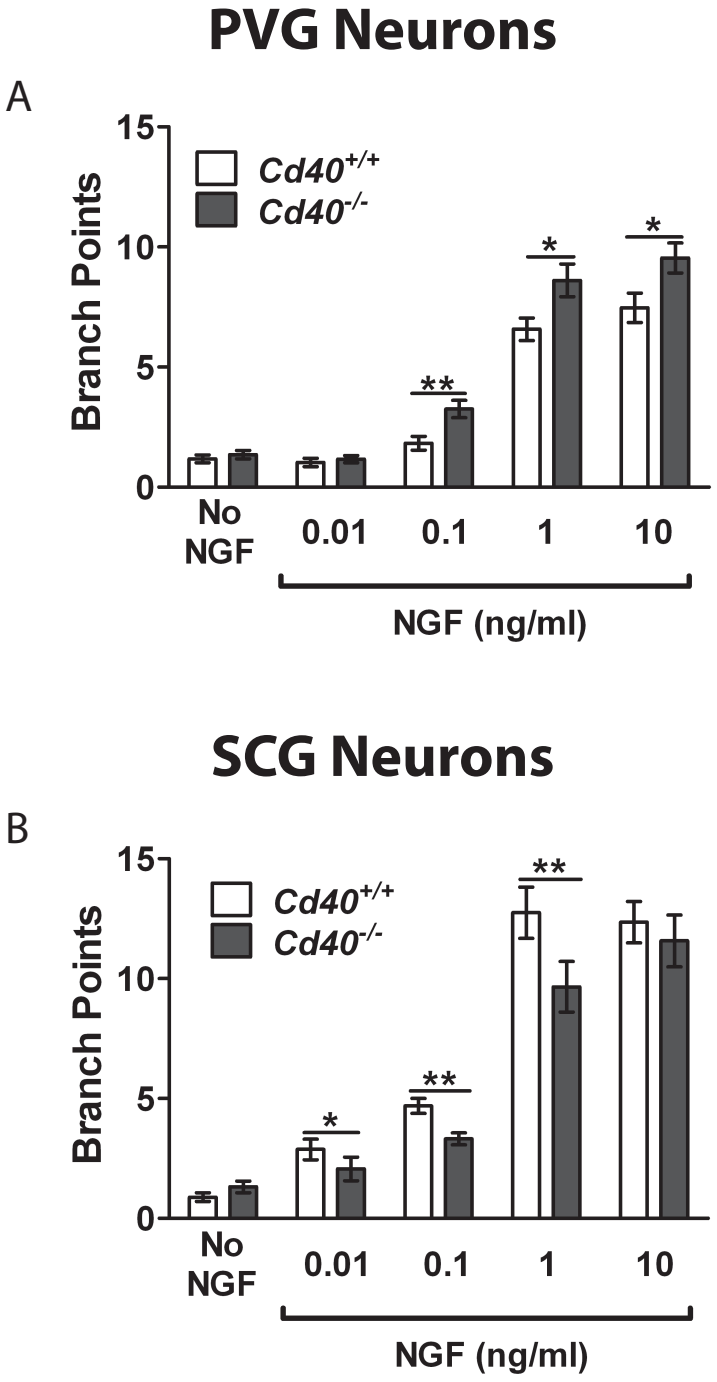

Figure 4.12. NGF Sensitivity of CD40-CD40L Signalling in Po PVG and SCG Neurons – Effect on Branch Points. (A&B) Quantification of branch points of Po *Cd40*$^{+/+}$ and *Cd40*$^{-/-}$ PVG **(A)** and SCG **(B)** neurons. Neurons were either cultured without NGF, or treated with NGF at concentrations between 0.01 and 10 ng/ml. Data are presented as the mean ± standard error. n=3 for each condition. *: $p<0.05$, **: $p<0.01$ (Kruskal-Wallis, with Dunn's *post-hoc* analysis). NGF: nerve growth factor; PVG: prevertebral ganglia (coeliac and superior mesenteric ganglia); SCG: superior cervical ganglia.

The importance of NGF concentration on the efficacy of CD40-CD40L reverse signalling in modulating overall neurite complexity is illustrated by the Sholl profiles of *Cd40*$^{+/+}$ and *Cd40*$^{-/-}$ PVG and SCG neurons cultured with different concentrations of NGF (Fig. 4.13). There were no obvious differences in the Sholl profiles of *Cd40*$^{+/+}$ and *Cd40*$^{-/-}$ PVG and SCG neurons cultured in the absence of NGF. Whereas knockout of CD40 in the presence of 0.01 ng/ml NGF did not impact the complexity of PVG neurons, a clear reduction in the complexity of *Cd40*$^{-/-}$ SCG neuron neurites compared to wild-type SCG neurons was observed at this low NGF concentration. As NGF concentrations increased to 0.1 and 1 ng/ml, loss of CD40 expression clearly altered the Sholl profiles of PVG and SCG neurons compared to wild-type neurons, reflecting the ability of autocrine CD40-CD40L reverse signalling to modulate the extent of process outgrowth from PVG and SCG neurons at these higher concentrations of NGF. Once again, the deletion of CD40 did not alter the extent of process outgrowth compared to wild-type neurons in SCG neuron cultures supplemented with 10 ng/ml NGF, as demonstrated by the overlapping Sholl profiles displayed by both SCG neuron genotypes. However, at this high NGF concentration, *Cd40*$^{-/-}$ PVG neurons made many more intersections than wild-type neurons at distances between 120 and 300 μm from the neuron soma, indicating an increased complexity of PVG neuron processes in the absence of autocrine CD40-CD40L reverse signalling.

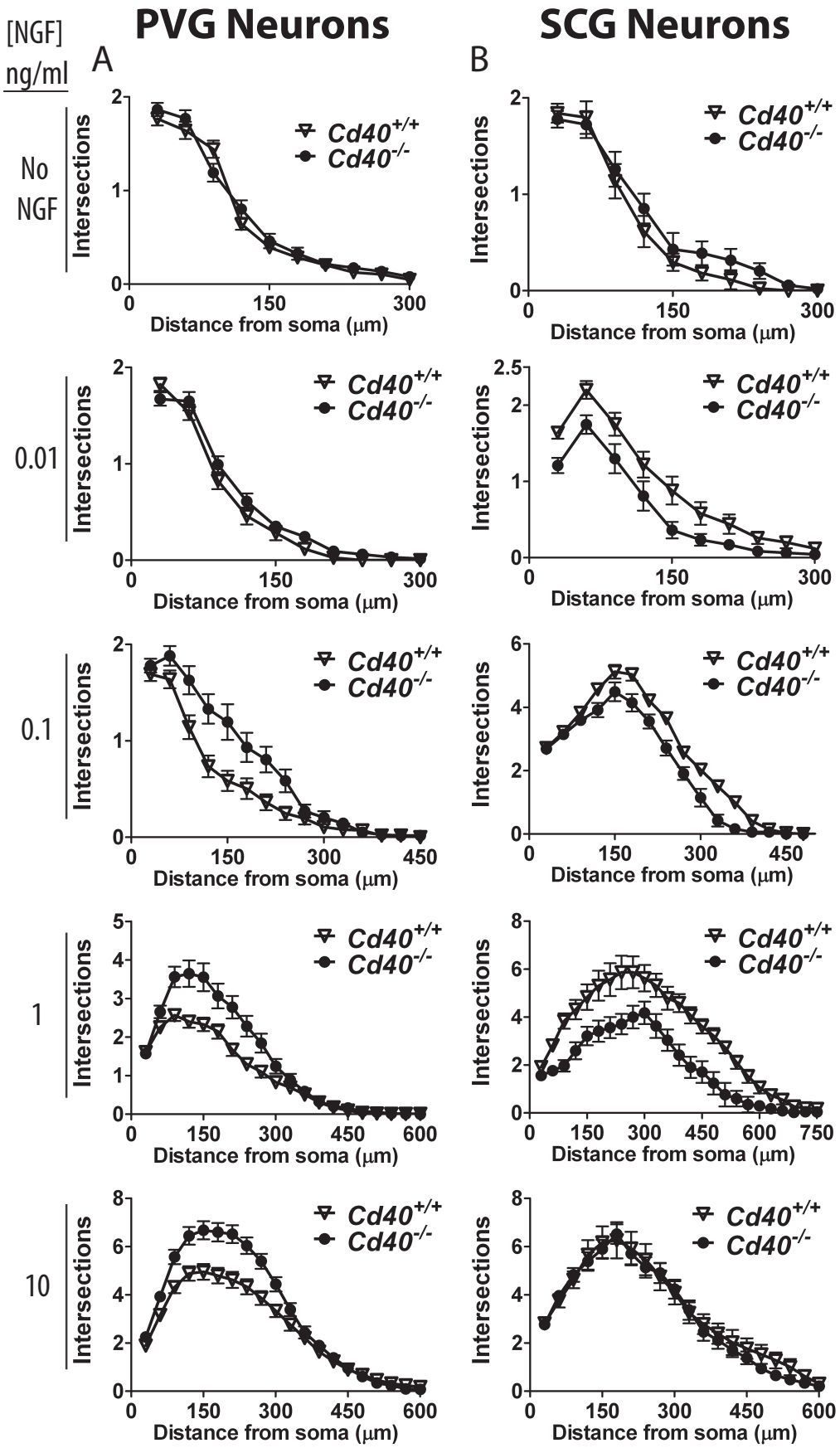

Fig. 4.13. Legend on following page.

Figure 4.13. NGF Sensitivity of CD40-CD40L Signalling in Po PVG and SCG Neurons – Effect on Neuronal Morphology. (A&B) Sholl plots of Po *Cd40*$^{+/+}$ and *Cd40*$^{-/-}$ PVG **(A)** and SCG **(B)** neurons. Neurons were either cultured without NGF or treated with NGF at concentrations between 0.01 and 10 ng/ml. Data are presented as the mean ± standard error. n=3 for each condition. NGF: nerve growth factor; PVG: prevertebral ganglia (coeliac and superior mesenteric ganglia); SCG: superior cervical ganglia.

4.2.6 NGF Regulates the Expression of CD40 mRNA in PVG and SCG Neurons

It has previously been shown that the expression of *Cd40* mRNA and CD40 protein are negatively regulated by NGF in cultured SCG neurons, with the result that the autocrine CD40-CD40L reverse signalling loop only enhances NGF-promoted process outgrowth from SCG neurons at low concentrations of NGF (McWilliams et al. 2015). The persistence of the modulatory effects of CD40-CD40L reverse signalling on process outgrowth from cultured PVG neurons, but not SCG neurons, at 10 ng/ml NGF raised the possibility that NGF may not be a negative regulator of CD40 expression in PVG neurons. To address this possibility, the regulation of *Cd40* mRNA expression by NGF was investigated in both PVG and SCG neuron cultures. Dissociated, wild-type Po PVG and SCG neurons were cultured either in the absence of NGF or with 10 ng/ml NGF in media supplemented with Boc-D-FMK caspase inhibitors to prevent apoptosis in the absence of NGF. After 24 h incubation, total RNA was extracted from cultured neurons and *Cd40* mRNA levels, relative to the expression of the reference mRNAs, *Gapdh*, *Sdha* and *Hprt1*, were determined by RT-qPCR.

Fig. 4.14 shows the influence of 10 ng/ml NGF on *Cd40* mRNA expression in PVG and SCG neurons. Quantification of relative *Cd40* transcript levels (after normalisation to endogenous reference genes) in PVG and SCG neurons demonstrated that 10 ng/ml NGF caused a 2-fold decrease in *Cd40* mRNA levels in PVG neurons compared to neurons cultured in the absence of NGF (control), whereas SCG neurons incubated with 10 ng/ml NGF had 25-fold lower *Cd40* transcript levels compared to control neurons.

These data indicate that whilst *Cd40* mRNA expression is negatively regulated by NGF in both PVG and SCG neurons, SCG neurons show much greater sensitivity to NGF regulation than PVG neurons.

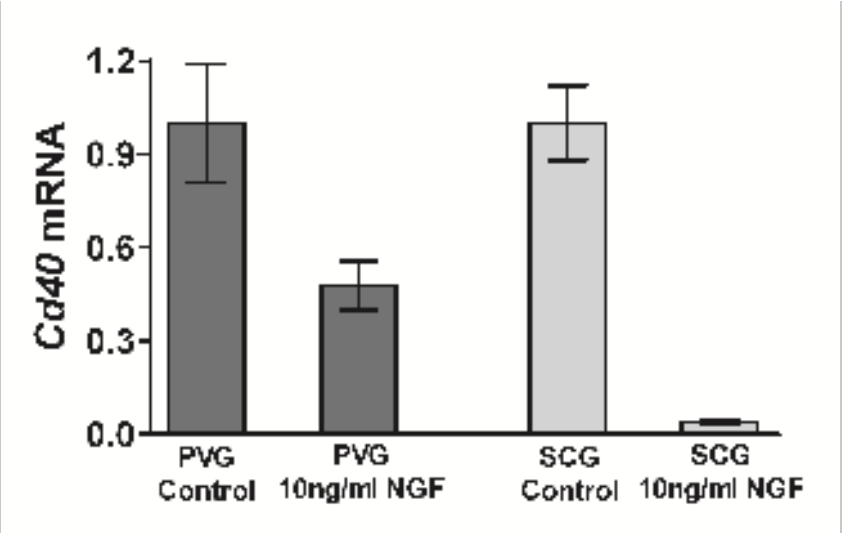

Figure 4.14. Effect of NGF on CD40 mRNA Expression Levels in Po PVG and SCG Neurons. *Cd40* mRNA expression levels in PVG and SCG neurons from Po wild-type mice cultured without NGF or with 10 ng/ml NGF. mRNA levels were normalised to those of the housekeeping genes *Gapdh*, *Hprt1* and *Sdha*. Data are presented as the mean ± standard error. Each sample (with neurons pooled from at least 5 animals from the same litter) was analysed in triplicate wells for each gene (with the mean value of the triplicates used as one repeat), and n=3 independent experiments. NGF: nerve growth factor; PVG: prevertebral ganglia (coeliac and superior mesenteric ganglia); SCG: superior cervical ganglia.

4.2.7 Expression of NGF Transcripts in PVG and SCG Target Organs

Data in **Section 4.2.6** suggest that autocrine CD40-CD40L reverse signalling in PVG neurons is less sensitive to negative regulation by NGF compared to SCG neurons. Previous *in vivo* experiments identified that NGF expression levels in SCG-target tissues dramatically impacts the effect of CD40 knockout on target tissue innervation (McWilliams et al. 2015). SCG target tissues expressing low levels of NGF (thymus and periorbital tissue) have significantly reduced sympathetic innervation in CD40-deficient mice compared to wild-type mice, as CD40-CD40L reverse signalling operates in wild-type mice to enhance NGF-promoted innervation of these target tissues. In contrast, innervation density is unaffected in CD40-deficient mice compared to wild-type mice in SCG target tissues expressing high levels of NGF (SMG and nasal tissue), as CD40-CD40L reverse signalling is prevented by the high levels of NGF in these tissue in wild-type mice and therefore does not contribute to their innervation (McWilliams et al. 2015).

To understand the potential physiological relevance of the decreased sensitivity of PVG neurons to the regulation of CD40 expression by NGF, and to relate NGF levels in PVG neuron target tissues to those seen in SCG target tissues, the expression levels of NGF were determined in target tissues innervated by PVG neurons *in vivo*. Spleen, stomach, and kidney tissues were analysed, since these tissues receive their sympathetic innervation predominantly from prevertebral neurons. Retrograde tracing experiments show that CG-SMG (prevertebral ganglia) neuron fibres establish a diffuse perivascular plexus alongside the branches of the coeliac artery and supply an extensive network of sympathetic fibres for the innervation of the stomach, together with some minimal innervation from paravertebral ganglia (Phillips and Powley 2007; Petersohn 2011; Browning and Travagli 2014). Analyses with fluorescent retrograde tracers and surgical experiments demonstrate that the spleen receives sympathetic innervation mostly from CG and SMG neurons (Bellinger et al. 1989; Nance and Burns 1989). Similarly, the kidneys are another tissue richly innervated by sympathetic fibres from CG and splanchnic nerves

(Sata et al. 2018). To determine the relative levels of *Ngf* mRNA expressed in PVG target tissues, *Ngf* mRNA was assayed by RT-qPCR in total RNA extracted from these tissues. *Ngf* mRNA levels were also determined in total RNA extracted from thymus and submandibular gland to compare NGF expression levels in PVG neuron targets with previously characterised SCG neuron targets known to express both high (submandibular gland) and low (thymus) levels of NGF.

Fig. 4.15 shows the expression levels of *Ngf* mRNA, relative to the expression levels of the reference mRNAs *Gapdh*, *Sdha* and *Hprt1*, in SCG neuron targets (thymus and submandibular gland) and PVG neuron targets (spleen, stomach, and kidney). The highest level of *Ngf* mRNA expression was found in submandibular gland tissue and the lowest in the thymus, with an approximately 130-fold difference in expression levels between the two organs. In PVG neuron target tissues, *Ngf* mRNA levels were found to lie between these two extremes. Relative to the levels in the submandibular gland, the spleen was found to express 7.5-fold less *Ngf* mRNA, the stomach 14-fold less, and finally the kidney was found to express 9-fold less *Ngf* mRNA than the submandibular gland.

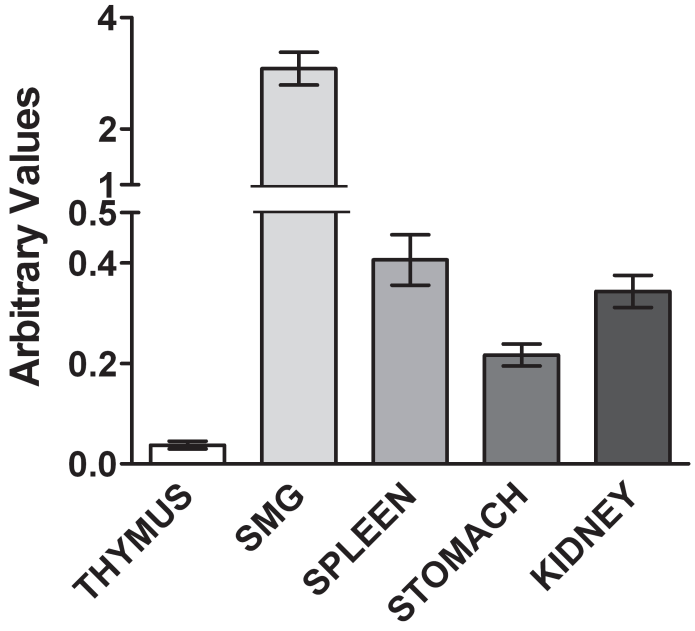

Figure 4.15. mRNA Expression Levels of CD40 Signalling Components in Paravertebral and Prevertebral Target Organs. *Cd40* mRNA expression levels in thymus and submandibular gland (as paravertebral target organs), and spleen, stomach, and kidney (as prevertebral target organs) of Po wild-type mice. mRNA levels were normalised to those of the housekeeping genes *Gapdh*, *Hprt1* and *Sdha*. Each sample was analysed in triplicate wells for each gene (with the mean value of the triplicates used as one repeat), and n=3 independent experiments. Data are presented as the mean ± standard error. SMG: Submandibular gland.

4.2.8 Sympathetic Innervation of PVG Target Tissues is Regulated by CD40-CD40L Reverse Signalling

In vitro studies have consistently shown that developing CD40-deficient PVG neurons display a significant increase in neurite size and complexity compared with wild-type neurons, suggesting that autocrine CD40-CD40L reverse signalling acts to suppress NGF-promoted process outgrowth from wild-type neurons. However the physiological relevance of this reverse signalling loop in regulating target field innervation by PVG neurons has not been verified *in vivo*. To determine the role of CD40-CD40L reverse signalling in establishing the innervation of PVG target tissues *in vivo*, sympathetic innervation of stomach, spleen and kidney were analysed in P10 *Cd40*$^{+/+}$, *Cd40*$^{+/-}$ and *Cd40*$^{-/-}$ mice by using immunolabeling-enabled three-dimensional imaging of solvent-cleared organs (iDISCO) (Renier et al. 2014) employing an antibody against tyrosine hydroxylase (TH) to label sympathetic axons. These tissues were selected as they receive their sympathetic innervation predominantly from prevertebral neurons (Gattone et al. 1986; Chevendra and Weaver 1991; Trudrung et al. 1994; Quinson et al. 2001; Emanuilov et al. 2018). P10 was chosen for analysis, as by this age sympathetic fibres have completed innervation of target tissues (Kisiswa et al. 2013).

TH-expressing sympathetic fibres are seen on the visceral surface of representative images of spleen tissue from *Cd40*$^{+/+}$, *Cd40*$^{+/-}$, and *Cd40*$^{-/-}$ mice (Fig. 4.16). Quantification of sympathetic fibres in *Cd40*$^{-/-}$ spleen tissues revealed a significant increase in innervating fibre density (127 ± 14%, $p<0.05$, $n=7$) compared with tissues from wild-type littermates. There was also an increase in sympathetic density between heterozygous (114 ± 28%, $n=9$) and wild-type spleen tissues (100 ± 17%, $n=6$); however, this was not statistically significant. The difference between innervation density of spleen tissues from *Cd40*$^{+/-}$ and *Cd40*$^{-/-}$ mice was not statistically significant either.

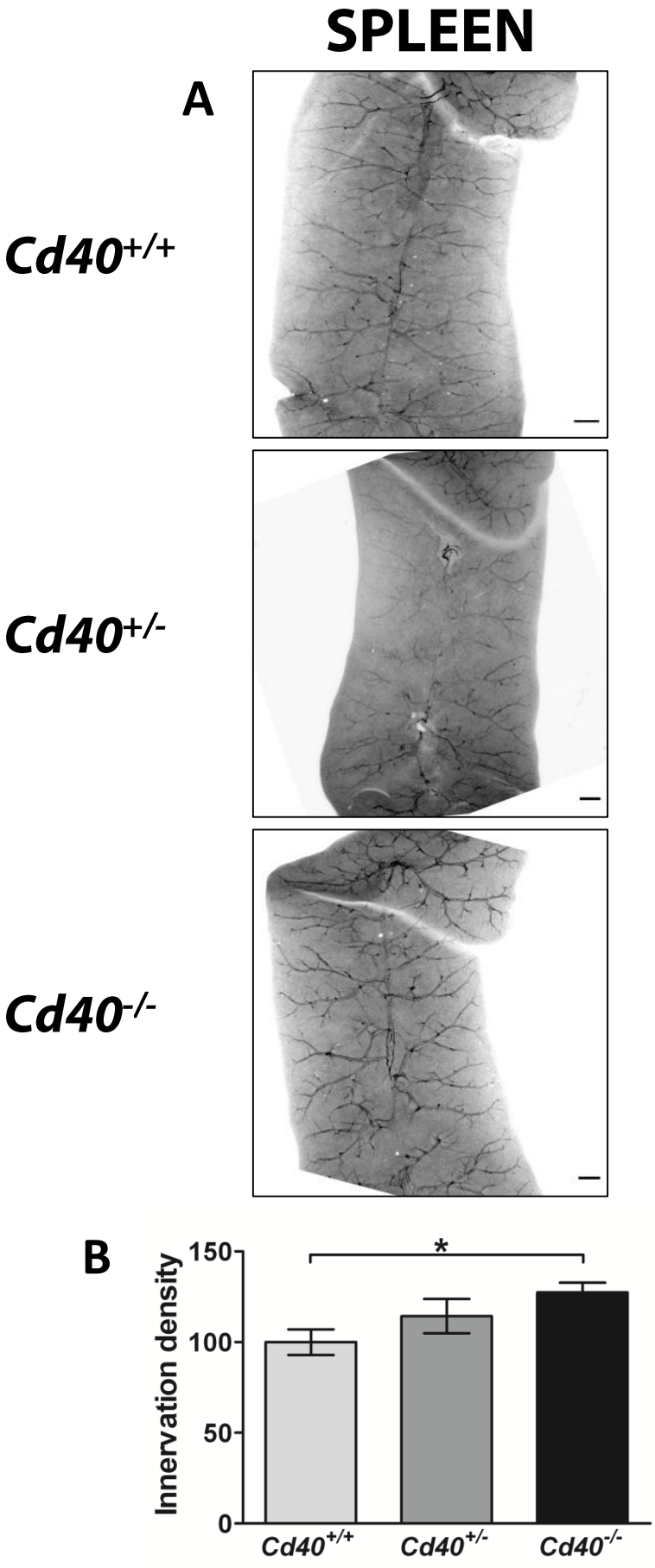

Fig. 4.16. Legend on following page.

Figure 4.16. Sympathetic Innervation of the PVG-Innervated Spleen in Wild-Type and *Cd40* Knockout Mice. **(A)** Representative images of iDISCO-stained whole mount spleens from P10 *Cd40* wild-type and knockout mice. Sympathetic nerves were labelled with an anti-tyrosine hydroxylase antibody. Scale bars represent 100 µm. Each image is representative of 6 $Cd40^{+/+}$, 9 $Cd40^{+/-}$, and 7 $Cd40^{-/-}$ animals. **(B)** Quantification of innervation density of sympathetic fibres in spleens from P10 *Cd40* wild-type and knockout mice. Values were normalised to those obtained from wild-type animals, and data are presented as the mean ± standard error. n is as stated in (A). *: $p<0.05$ (one-way ANOVA, with Dunnett's *post-hoc* analysis). PVG: prevertebral ganglia (coeliac and superior mesenteric ganglia).

Fig. 4.17 shows representative images of sympathetic innervation of stomach tissue from wild-type, heterozygous and homozygous *Cd40* knockout mice. Images clearly illustrate that sympathetic neuron axons enter the stomach from the cardia area beneath the oesophagus and ramify into other areas of the stomach. Visual inspection indicated that $Cd40^{-/-}$ stomach tissues were more densely innervated by sympathetic fibres compared with those from $Cd40^{+/+}$ animals. Quantification of the TH-stained sympathetic processes revealed that innervation density of $Cd40^{-/-}$ stomach tissues was significantly higher than those from wild-type littermates ($p<0.01$; $Cd40^{-/-}$: 167 ± 13%, $n=8$; $Cd40^{+/+}$: 100 ± 13%, $n=6$). However, there were no statistically significant changes detected in innervation density between $Cd40^{+/+}$ and $Cd40^{+/-}$ stomach tissues, or $Cd40^{+/-}$ and $Cd40^{-/-}$ stomach tissues.

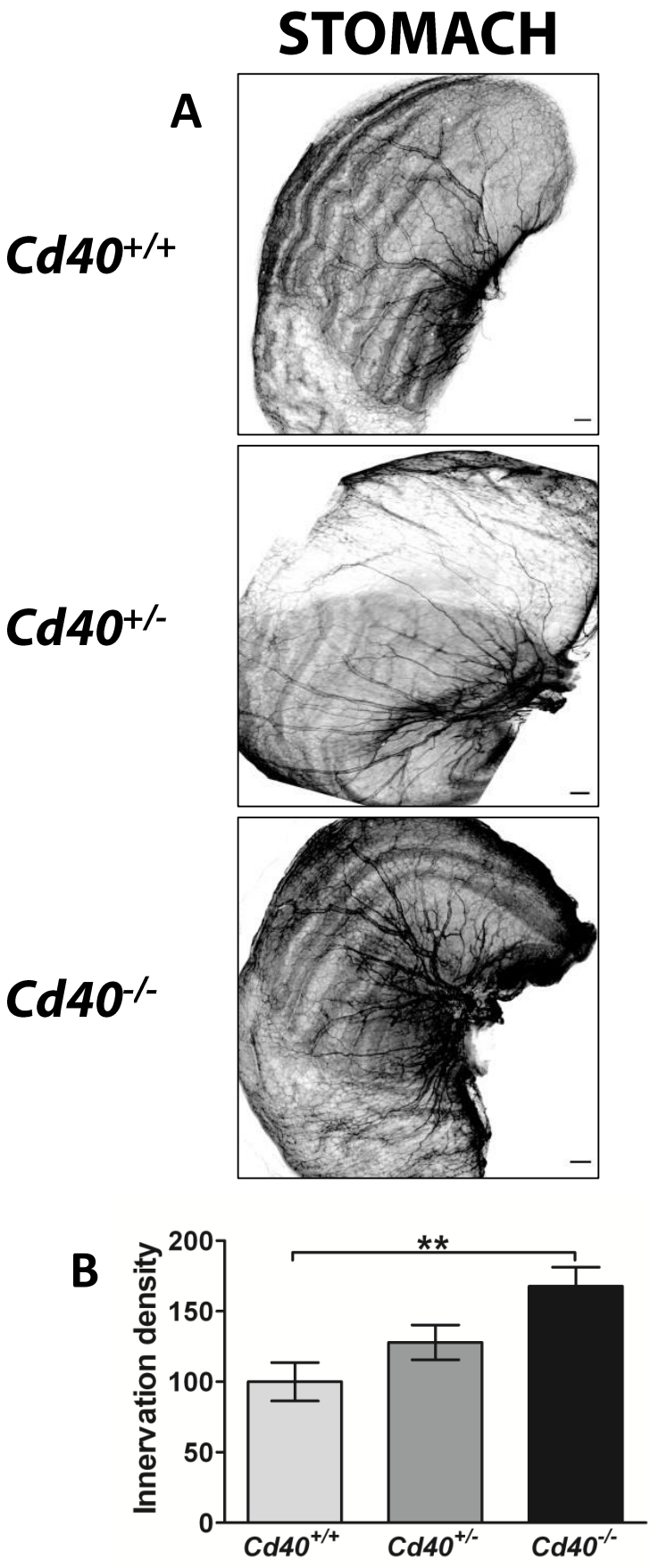

Fig. 4.17. Legend on following page.

Figure 4.17. Sympathetic Innervation of the PVG-Innervated Stomach in Wild-Type and *Cd40* Knockout Mice. **(A)** Representative images of iDISCO-stained whole mount stomachs from P10 *Cd40* wild-type and knockout mice. Sympathetic nerves were labelled with an anti-tyrosine hydroxylase antibody. Scale bars represent 100 μm. Each image is representative of at least 6 $Cd40^{+/+}$, 9 $Cd40^{+/-}$, and 8 $Cd40^{-/-}$ animals. **(B)** Quantification of innervation density of sympathetic fibres in stomach from P10 *Cd40* wild-type and knockout mice. Values were normalised to those obtained from wild-type animals, and data are presented as the mean ± standard error. n is as stated in (A). **: $p<0.01$ (one-way ANOVA, with Dunnett's *post-hoc* analysis). PVG: prevertebral ganglia (coeliac and superior mesenteric ganglia).

The kidney was the last tissue in which innervation density was analysed by iDISCO preparations. Fig. 4.18 shows representative images of full kidney innervation in wild-type, heterozygous and homozygous *Cd40* knockout mice. TH-stained sympathetic fibres begin innervating the kidney from the helius area, before ramifying throughout the kidney parenchyma and other major areas. Representative images indicate that there was an increase in sympathetic fibre innervation when CD40 protein expression was reduced or deleted. Analysis of sympathetic fibres demonstrated that $Cd40^{-/-}$ kidney tissues had significantly more sympathetic neuron projections per surface area than $Cd40^{+/+}$ kidney tissues ($p<0.001$; $Cd40^{-/-}$: 172 ± 26%, $n=9$; $Cd40^{+/+}$: 100 ± 37%, $n=12$). $Cd40^{+/-}$ kidney tissues also showed a significant increase in innervation density ($p<0.05$; $Cd40^{+/-}$: 140 ± 26%, $n=9$) compared with $Cd40^{+/+}$ kidney tissues; however, there was no statistically significant difference between $Cd40^{+/-}$ and $Cd40^{-/-}$ kidney innervation.

These *in vivo* observations clearly demonstrate that autocrine CD40-CD40L reverse signalling plays a significant physiological role in the innervation of the PVG neuron target tissues examined. iDISCO analysis demonstrated that while deletion of CD40 resulted in a statistically significant increase in sympathetic innervation of all target tissues examined compared with those from wild-type littermates, the loss of only one *Cd40* allele only caused a significant increase in sympathetic innervation density in the kidney. These data suggest that autocrine CD40-CD40L reverse signalling acts to limit the sympathetic innervation of PVG target tissues in developing wild-type mice.

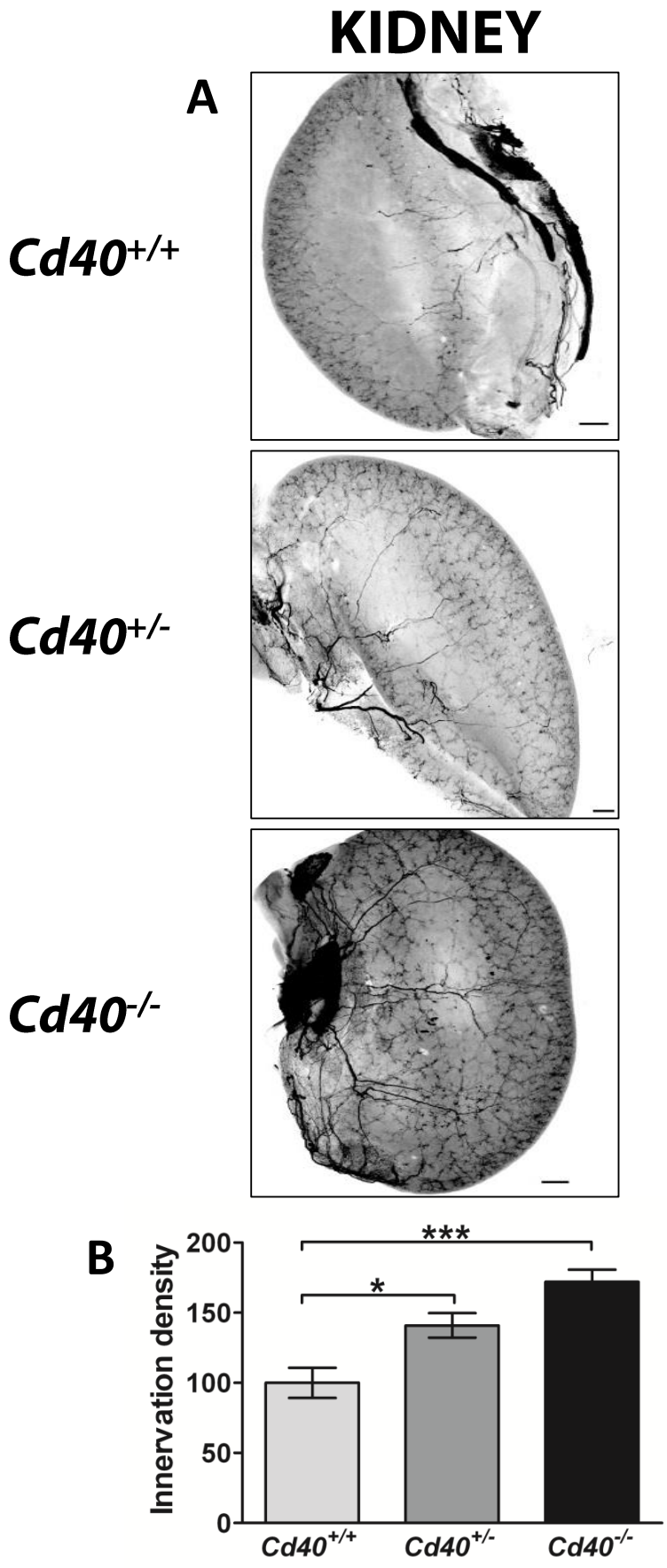

Fig. 4.18. Legend on following page.

Figure 4.18. Sympathetic Innervation of the PVG-Innervated Kidney in Wild-Type *Cd40* Knockout Mice. **(A)** Representative images of iDISCO-stained whole mount kidneys from P10 *Cd40* wild-type and knockout mice. Sympathetic nerves were labelled with an anti-tyrosine hydroxylase antibody. Scale bars represent 100 µm. Each image is representative of at least 12 $Cd40^{+/+}$, 9 $Cd40^{+/-}$, and 9 $Cd40^{-/-}$ animals. **(B)** Quantification of innervation density of sympathetic fibres in kidney from P10 *Cd40* wild-type and knockout mice. Values were normalised to those obtained from wild-type animals, and data are presented as the mean ± standard error. n is as stated in (A). *: $p<0.05$, ***: $p<0.001$ (one-way ANOVA, with Dunnett's *post-hoc* analysis). PVG: prevertebral ganglia (coeliac and superior mesenteric ganglia).

4.3 DISCUSSION

The aim of this chapter was to determine the efficacy of CD40-CD40L signalling in regulating process outgrowth from prevertebral sympathetic neurons during the developmental period when they are innervating their target fields, and to identify similarities and differences with the established role of CD40-CD40L signalling in regulating target field innervation by paravertebral sympathetic neurons of the SCG (McWilliams et al. 2015).

Several key findings are reported in this chapter. CD40 and CD40L proteins were both found to be expressed by prevertebral sympathetic neurons and an autocrine CD40-CD40L signalling loop was shown to modulate process outgrowth from these neurons. Strikingly, CD40-CD40L signalling had an opposite effect on the outgrowth of PVG neuron processes to that seen in previously studied SCG neurons, suppressing neurite outgrowth from PVG neurons. Furthermore, reverse signalling by TNFSF members was detected in prevertebral sympathetic neurons for the first time, whereas previously this signalling modality had only been found in paravertebral sympathetic neurons. Lastly, CD40 expression, and by implication CD40-CD40L reverse signalling, was found to be negatively regulated by NGF in PVG neurons, as previously reported in SCG neurons, although CD40 expression in PVG neurons was found to be less sensitive to regulation by NGF than in SCG neurons. The physiological relevance of these *in vitro* findings was confirmed by *in vivo* experiments which found that knockout of CD40 resulted in hyperinnervation of prevertebral sympathetic neuron target tissues, in contrast to the hypoinnervation previously reported in paravertebral sympathetic neuron target tissues of *Cd40*$^{-/-}$ animals (McWilliams et al. 2015).

CD40 autocrine signalling is a well-established mechanism in non-neuronal cell populations (Pamukcu et al. 2011; Li et al. 2013; Kim et al. 2015; Hillis et al. 2016). One common indicator of autocrine signalling is the expression of both ligand and receptor within the same compartments of individual cells. The expression of both receptor and ligand in the soma and neurite compartments of individual neurons has previously been observed in

SCG neurons for several TNFSF members, including LIGHT-HVEM (Gavalda et al. 2009), GITR-GITRL (O'Keeffe et al. 2008), and BCMA-TWE-PRIL (Howard et al. 2018), and recent studies have identified TNFSF members that use this cell-autonomous signalling mechanism in developing SCG neurons (O'Keeffe et al. 2008; McWilliams et al. 2015; Howard et al. 2018; Howard et al. 2019). In this chapter, the co-expression of CD40L and CD40 in both the cell soma and neurites was confirmed in SCG neurons and identified for the first time in PVG neurons, suggesting that both compartments of the SNS can utilise a CD40-CD40L autocrine signalling loop. McWilliams *et al.* previously showed that CD40-CD40L autocrine signalling has a neurite growth-enhancing role in paravertebral SCG neurons, contributing to the innervation of paravertebral target tissues by those neurons. To confirm autocrine signalling in this chapter, neurite development was examined in SCG and PVG neuron cultures established from *Cd40*$^{-/-}$ mice. In low density cultures, where neurons are not in close proximity to each other, knockout of CD40 prevented the normal outgrowth of both PVG and SCG neuron processes, strongly suggesting that a CD40-CD40L autocrine signalling loop modulates neurite length and complexity in PVG neurons as previously seen with SCG neurons. Currently, the exact mechanism by which CD40-CD40L autocrine signalling occurs in neurons and non-neuronal cells remains unclear. Wnt5a is a member of the Wnt protein family, which also mediates paravertebral sympathetic innervation via Wnt5a-Ror autocrine signalling (Ryu et al. 2013). Wnts are highly hydrophobic proteins due to posttranslational modifications, particularly N-terminal palmitoylation. These lipid modifications are particularly important because lipid-modified Wnt proteins tend to stick tightly to the cell membrane due to their hydrophobicity (Port and Basler 2010). Thus, it is suggested that these modifications, together with positively charged residues on Wnt proteins, facilitate Wnt5a-Ror interactions and autocrine signalling (Ryu et al. 2013). However, very little is known about the detailed biochemistry of CD40-CD40L autocrine signalling, despite the fact that it is a widespread signalling mechanism for various cell types. CD40 is known to undergo several different posttranslational modifications (van Kooten et al. 2000), although there is no

evidence currently showing that palmitoylation occurs as one of CD40 or CD40L post-translational modifications. However, it is possible that hydrophobic residues (Armitage et al. 1992; Laman et al. 2017) in CD40 and CD40L limit secreted protein diffusion, and facilitate instead interaction between CD40 and CD40L on the cell surface to promote forward or reverse autocrine signalling. Further work is required to establish the precise biochemical forces that promote CD40-CD40L autocrine signalling in sympathetic neurons.

The TNFSF contains several members that use bi-directional signalling (Sun and Fink 2007). In the previous chapter, one of the key differences identified in TNF-α signalling between developing PVG and SCG neurons was the differential impact of TNF-α-reverse signalling, with an effect seen in SCG neurons but not PVG neurons. Whether this was due to a functional difference between the subpopulations of sympathetic neurons, wherein only SCG neurons had the capacity to use reverse signalling (e.g. the specific localisation of TNFR1), was unclear. In CD40-deficient PVG and SCG neurons, in which CD40-CD40L autocrine signalling is abolished, the addition of soluble CD40-Fc chimera restored the efficacy of the CD40-CD40L signalling pathway. This is highly suggestive that soluble CD40 receptor, acting as a ligand and binding to membrane-bound CD40L, can affect neuronal process outgrowth by reverse signalling. Whilst CD40-Fc-mediated rescue of enhanced process outgrowth from knockout SCG neurons confirmed that reverse signalling mediates the CD40-CD40L signalling pathway in SCG neurons (as reported by (McWilliams et al. 2015)), of more relevance to the current study is that it demonstrated a similarity between PVG and SCG neurons in that they both use autocrine CD40-CD40L reverse signalling to modulate neuronal process outgrowth during the period of target field innervation. These findings are the first demonstration of a reverse signalling mechanism playing a role in the development of prevertebral sympathetic neurons, and increases the need to consider both forward and reverse signalling when studying the role of TNFSF members in the context of SNS development.

Identifying the developmental time period over which a particular extracellular signal functions is crucial to understanding the potential roles of that signal on developmental processes. Results presented here highlight a further similarity between SCG and PVG neurons, in that CD40-CD40L-reverse signalling acts on neurite growth during the same developmental window in both neuron types. CD40-CD40L reverse signalling shows a regulatory role on the development of PVG and SCG sympathetic neurons between E18 and P3. This developmental period encompasses several developmental processes in the SNS, such as: target field innervation by sympathetic axons and the subsequent ramification of axons within target fields, growth and maturation of postganglionic sympathetic neuron dendrites, synaptogenesis between preganglionic and postganglionic sympathetic neurons, and the NGF-dependent survival of sympathetic neurons (Glebova and Ginty 2005). Whilst it is possible that CD40-CD40L-reverse signalling may play a role in all of these developmental events, it has previously been shown that CD40-CD40L reverse signalling does not regulate the survival of developing SCG neurons (McWilliams et al. 2015). Whether CD40-CD40L signalling plays a role in dendrite growth and maturation or synaptogenesis within sympathetic ganglia has not yet been tested. The effects of CD40-CD40L-reverse signalling on regulating the growth and branching of PVG and SCG processes was observed to disappear by age P5. The relatively limited time window over which CD40-CD40L reverse signalling acts to regulate process outgrowth and target field innervation suggests that this signalling mechanism serves a complementary, "fine tuning" role in directing functional target field innervation by sympathetic axons, rather than being a major driver of this process. Target field innervation by mouse sympathetic axons begins at E16.5 and continues until P0.5, and the period of axon arborisation within target fields extends from E18 to approximately P10 (Rubin 1985; Fagan et al. 1996; Glebova 2004; Glebova and Ginty 2005; Armstrong et al. 2011). Although NGF has been shown to play an essential role in this process, the requirement for NGF for correct functional target field innervation is somewhat heterogeneous. Some sympathetic target fields, like the submandibular gland, are totally devoid of sympathetic

innervation in NGF-deficient mice; others, like the heart, kidney and stomach, have greatly reduced (heart) or modestly reduced (kidney and stomach) sympathetic innervation in the absence of NGF, and some target fields, like the trachea, do not appear to require NGF for sympathetic innervation (Glebova 2004). The heterogeneous requirement for NGF in establishing the correct innervation of sympathetic target fields implies that other factors must co-operate with NGF to ensure functional target field innervation. Indeed, TNF-α (Kisiswa et al. 2013; Kisiswa et al. 2017; Erice et al. 2019), Wnt5a (Bodmer et al. 2009; Ryu et al. 2013), Frizzled3 (Armstrong et al. 2011), RANK-RANKL|, GITR-GITRL, BCMA-TWE-PRIL, and CD40-CD40L (McWilliams et al. 2015) have all previously been shown to have a regulatory role in establishing correct sympathetic target field innervation. Therefore, data presented in this study showing that CD40-CD40L reverse signalling can modulate NGF-promoted process outgrowth from prevertebral sympathetic neurons between E18 and P3 suggest that CD40-CD40L-reverse signalling co-operates with NGF to ensure the correct innervation of PVG neuron targets during the latter stages of target field innervation and during the period of axonal arborisation within target fields.

Despite revealing several similarities between SCG and PVG neurons, the most striking findings to emerge in this chapter involve the differences in CD40-CD40L signalling between the two neuron types. Autocrine CD40-CD40L reverse signalling was found to modulate neuronal process outgrowth from both PVG and SCG neurons *in vitro* and alter innervation density of their target fields *in vivo*. *In vitro* experiments using neurons from *Cd40*$^{-/-}$ mice treated with soluble CD40-Fc confirmed the previous report that CD40-CD40L-reverse signalling enhances NGF-promoted neurite growth and branching from paravertebral SCG neurons. Surprisingly, however, CD40-CD40L-reverse signalling had the opposite effect on prevertebral sympathetic neurons, suppressing neurite length and reducing the number of neurite branch points. An opposite regulatory role of CD40L-reverse signalling on the elaboration of neuronal processes has also been shown in the developing CNS. CD40-CD40L

reverse signalling plays a crucial role in promoting axon and dendrite growth and enhancing dendrite branching in glutamatergic pyramidal neurons from the CA1 region of the developing mouse hippocampus. In contrast, CD40-CD40L reverse signalling prevents growth and elaboration of GABA-ergic medium spiny neuron dendrites in the developing striatum (Carriba and Davies 2017). The molecular mechanisms by which CD40L mediates downstream intracellular signalling cascades in reverse signalling remains unclear, as mCD40L has a short cytoplasmic domain with no known enzymatic activity (Sun and Fink 2007). Therefore, the processes underling the opposing functions of CD40-CD40L reverse signalling in different neuron types are unknown. CD40-CD40L reverse signalling is known to trigger activation of JNK (Brenner et al. 1997a) and induce tyrosine phosphorylation of PLC-γ in T-lymphocytes, phosphorylation of which correlates with activation of PKC (Brenner et al. 1997b). In the CNS, CD40-CD40L reverse signalling is dependent on two PKC isoforms, PKC-β and PKC-γ, which are reported to mediate the effects of CD40-CD40L reverse signalling in the development of hippocampal and striatal neurons (Carriba and Davies 2017; Carriba et al. 2020). More recently, it has been shown that CD40-CD40L-reverse signalling phosphorylates proteins in the PKC, ERK and JNK pathways to regulate neuronal process outgrowth and branching in developing hippocampal neurons (Carriba and Davies 2020). Thus, the possibility exists that CD40-CD40L-reverse signalling may interact with proteins in these pathways to regulate the growth of developing prevertebral and paravertebral sympathetic neuron processes. Further research should explore the signalling cascades that arise from CD40-activated CD40L to determine whether CD40-CD40L-reverse signalling either enhances or suppresses process outgrowth in developing sympathetic neurons.

A key focus of this chapter has been the role of NGF in modulating the effects of CD40-CD40L reverse signalling. Previous work by McWilliams *et al.* (2015) found that CD40-CD40L reverse signalling cannot promote neurite growth and branching from developing SCG neurons in the absence of NGF, rather it enhances NGF-promoted process outgrowth over a defined range of

NGF concentrations. In this chapter, examining the effects of increasing concentrations of NGF on CD40-CD40L-mediated signalling in sympathetic neurons, confirmed the NGF-dependence of CD40-CD40L signalling in SCG neurons, and identified the same phenomena in PVG neurons. Initial results found that neurons from *Cd40*$^{-/-}$ mice have either decreased (SCG) or increased (PVG) neurite outgrowth compared to their wild-type counterparts in cultures containing 1 ng/ml NGF, indicating that CD40-CD40L signalling is affecting neurite outgrowth. When the same experiments were performed in the absence of NGF in the culture media there were no differences in the extent of neurite outgrowth between wild-type and CD40-deficient SCG or PVG neurons, confirming the findings of McWilliams *et al.* (2015) in the case of SCG neurons, and demonstrating that CD40-CD40L reverse signalling suppresses NGF-promoted process outgrowth from PVG neurons rather than reducing process outgrowth per se. In accordance with the present study, previous studies have reported the same NGF-dependence for the modulatory roles of other TNFSF and TNFRSF members on neurite outgrowth from developing sympathetic neurons (O'Keeffe et al. 2008; Howard et al. 2018).

A key observation to emerge from experiments examining the effects of increasing concentrations of NGF on CD40-CD40L-mediated signalling in sympathetic neurons was the different sensitivities of CD40-CD40L reverse signalling to NGF in PVG and SCG neurons. PVG neurons required higher concentrations of NGF (0.1 ng/ml) than SCG neurons (0.01 ng/ml) to begin affecting neurite outgrowth via CD40-CD40L reverse signalling. Furthermore, in SCG neurons the efficacy of CD40-CD40L-reverse signalling in enhancing NGF-promoted neurite outgrowth disappeared at higher NGF concentrations (10 ng/ml). This is consistent with data from McWilliams *et al.* who also reported that the autocrine CD40-CD40L-reverse signalling loop failed to enhance NGF-promoted neurite outgrowth from cultured neonatal SCG neuron when the NGF concentration was increased to 10 ng/ml (McWilliams et al. 2015). Unlike SCG neurons, the effects of CD40-CD40L reverse signalling on the growth and complexity of PVG neuron neurites were still observable at 10 ng/ml

NGF. A possible rationale for these findings may lie in the regulation of CD40 expression by NGF. In SCG neurons, the negative regulation of both CD40L (at the protein level) and CD40 (at the protein and mRNA level) expression by NGF had been previously reported (McWilliams et al. 2015). In the present study, RT-qPCR analysis revealed that the expression of *Cd40* mRNA was also negatively regulated by NGF in PVG neurons. However, the down-regulation of *Cd40* mRNA expression by 10 ng/ml NGF was much more dramatic in SCG neurons (25-fold) than in PVG neurons (only 2-fold), possibly explaining why the effects of CD40-CD40L-reverse signalling on the extent of neurite outgrowth from PVG neurons is still observable at 10 ng/ml NGF, whereas the same NGF concentration ablates the effects of CD40-CD40L reverse signalling on neurite outgrowth from SCG neurons. The signalling mechanism underlying the differential regulation of CD40 expression by NGF in prevertebral and paravertebral sympathetic neurons remains to be determined. Future work should focus on ERK signalling as a potential intermediate, as it has been reported that CD40-CD40L forward signalling contributes to NGF-promoted ERK activation in the regulation of DRG sensory neuron process outgrowth (Howard et al. 2019).

In vivo investigations were used to examine the physiological relevance of the *in vitro* data demonstrating that autocrine CD40-CD40L reverse signalling suppresses NGF-promoted process outgrowth and branching from PVG neurons. *In vivo* experiments were designed to address two key questions: 1) Does CD40-CD40L-reverse signalling play a physiological role in the innervation of prevertebral target organs? 2) Does NGF-induced down-regulation of CD40 expression in prevertebral neurons affect CD40L-reverse signalling *in vivo*, as previously described for SCG neurons? McWilliams *et al.* (2015) demonstrated that CD40-deficient mice showed deficits in the sympathetic innervation of SCG neuron target tissues expressing low levels of NGF (thymus and periorbital tissue), but not target tissues expressing high levels of NGF (submandibular gland and nasal tissue). Given that NGF is a strong negative regulator of CD40 expression in SCG neurons, this implies that

CD40-CD40L reverse signalling does not operate to enhance target field innervation by SCG neurons in target tissues expressing high levels of NGF, because the high levels of NGF lead to significant down-regulation of CD40 expression by SCG neurons, thus extinguishing the autocrine CD40-CD40L reverse signalling loop.

In vivo data in this chapter demonstrated that prevertebral sympathetic neuron target tissues (spleen, kidney and stomach) express detectable levels of *Ngf* mRNA that are in between the levels expressed in the submandibular gland, an SCG target tissue that expresses very high levels of NGF, and the thymus, an SCG neuron target tissue that expresses very low levels of NGF but still demonstrates functional CD40-CD40L reverse signalling *in vivo*. Thus it can be hypothesised that the levels of NGF expressed in prevertebral neuron target fields are high enough to permit the CD40-CD40L reverse signalling loop to operate in innervating PVG neurons, but not so high as to lead to the down-regulation of CD40 expression by PVG neurons and the consequential shutdown of autocrine CD40-CD40L reverse signalling. This latter point seems likely given that *Cd40* mRNA expression is less sensitive to down-regulation by NGF in PVG neurons compared to SCG neurons. If this hypothesis is correct, spleen, stomach and kidney from CD40-deficient mice should display hyperinnervation compared to tissues from wild-type mice if autocrine CD40-CD40L reverse signalling operates *in vivo* to suppress NGF-promoted target field innervation by PVG neurons, as suggested by *in vitro* experiments. iDISCO analysis of the sympathetic innervation density of PVG neuron innervated target tissues in *Cd40*$^{-/-}$ and wild-type mice did indeed demonstrate that a lack of CD40 caused hyperinnervation in all three prevertebral target organs. This confirmed both 1) the physiological relevance of the *in vitro* data indicating that autocrine CD40-CD40L reverse signalling suppresses NGF-promoted process outgrowth from PVG neurons, and 2) that NGF levels in the PVG neuron target tissues examined are high enough to permit operation of the autocrine CD40-CD40L reverse signalling loop *in vivo*, but not so high as to suppress the functioning of this signalling loop.

In the iDISCO experiments within this chapter tyrosine hydroxylase was used as a marker to detect sympathetic fibres innervating prevertebral target organs, as a great majority of the sympathetic neurons are catecholaminergic and use tyrosine hydroxylase to synthesise catecholamine (Emanuilov et al. 2018; Kaestner et al. 2019). However, it is known that some sub-populations of rat, avian and mouse sensory neurons e.g., nodose neurons and DRG neurons, may also have catecholaminergic characteristics, and thus can display TH-immunoreactivity (Katz et al. 1983; Xue et al. 1985; Brumovsky et al. 2012). A few studies indicated that some of those TH-positive sub-populations of nodose sensory neurons may innervate visceral organs, including the stomach (Zhuo 1997) of the squirrel monkey (Gwyn et al. 1985) and rat (Sharkey et al. 1984), as well as prevertebral sympathetic neurons. Unfortunately, these studies do not state the percentage or ratio of these sensory neurons to total neurons innervating the stomach; neither do they map out the exact location in the stomach that these sub-populations of sensory neurons are innervating. However, in their retrograde neuronal tracing experiments Kummer et al. reported that only 5% of the total innervation in the pylorus area of the stomach tissue is provided by TH-positive nodose neurons in the rat (Kummer et al. 1993). Although TH-positive sub-populations of nodose ganglia might have interfered with the *in vivo* results demonstrating the physiological role of CD40-CD40L reverse signalling in PVG neuron target innervation, this is highly unlikely for two reasons. First, during the collection of the organs, stomach tissues were dissected from the intersection between the sulcus intermedius and lesser curvature, so the pyloric regions of the stomach, such as the pyloric orifice, pyloric sphincter, and some parts of the pylorus very close to the duodenum, were excluded to prevent any innervation interference from the duodenum. Moreover, the stomach still contains milk at this stage of development, which causes uneven surfaces on the stomach tissue for standardised quantification. Therefore, the innervation density of the stomach tissues was measured based on the most intensely innervated regions of all stomach tissues analysed, which were the lesser curvature area, cardia, fundus and the upper half of the body area. The pylorus area was not included in the

analysis of the stomach tissues. Second, sensory nodose ganglion neurons are BDNF-dependent for their survival. Unpublished data from experiments investigating the role of CD40-CD40L signalling in these neurons revealed that E18 nodose ganglion neurons cultured from *Cd40*$^{+/+}$ and *Cd40*$^{-/-}$ mice show no significant differences in total neurite length or complexity over a range of BDNF concentrations (0.01 to 10 ng/ml; personal communication with Prof. Alun Davies FRS, Cardiff University). Therefore, it seems unlikely that a lack of CD40 expression in a small population of nodose ganglion neurons innervating the stomach tissue would have had a significant impact on the overall interpretation of *in vivo* results presented in this chapter. In future analysis of stomach tissue innervation by prevertebral sympathetic neurons, neuropeptide Y should also be used as a second sympathetic marker together with TH since 80% of coeliac ganglion sympathetic neurons also express neuropeptide Y, whereas TH-positive nodose ganglion sensory neurons do not express neuropeptide Y (Kummer et al. 1993; Emanuilov et al. 2018; Kaestner et al. 2019).

In conclusion, the *in vivo* results from this chapter, combined with the *in vitro* characterisation of CD40-CD40L signalling in SCG and PVG neurons, further expand our understanding of the role of neurotrophic factors in the development of the sympathetic nervous system, and identify further similarities and differences between the paravertebral and prevertebral divisions of the SNS. In future work it will be important to identify the precise signalling mechanisms downstream of CD40 binding to CD40L, to understand why CD40-CD40L-reverse signalling has opposing effects in prevertebral neurons to those seen in paravertebral neurons. It will also be critical to investigate *in vivo*, the effect of CD40 knockout on PVG target organs expressing either very high or low levels of NGF, compared to the tissues analysed here. This would help confirm and understand the role of NGF on CD40-CD40L signalling.

Chapter 5

The Regulatory Roles of NGF and NT-3 in the Outgrowth and Survival of Paravertebral and Prevertebral Sympathetic Neurons

5.1 Introduction

The development of the peripheral nervous system (PNS) relies on coordination between target organ maturation and the processes driving their innervation by peripheral neurons. According to the neurotrophic hypothesis, it is the requirement for innervation by target organs that regulates the amount of neurotrophic factor synthesised and secreted. Controlled synthesis and secretion of these factors limits the survival of peripheral neurons and ensures precise innervation of target organs (Davies 2003).

The first neurotrophic factor identified, nerve growth factor (NGF), plays a highly important role in the development of the PNS, and is essential for the survival of several different classes of peripheral neurons, including sympathetic neurons, a concept well-established by both *in vitro* and *in vivo* experiments (Levi-Montalcini and Booker 1960; Levi-Montalcini and Angeletti 1968; Angeletti and Levi-Montalcini 1971; Davies et al. 1987; Levi-Montalcini 1987; Martin et al. 1988; Crowley et al. 1994; Deshmukh and Johnson 1997; Lockhart et al. 1997; Cowan 2001). *In vitro* application of NGF anti-serum results in an almost total loss of sympathetic neurons in mammals (Greene 1977; Martin et al. 1988; Deshmukh and Johnson 1997). Similarly, mice lacking NGF display profound neuron loss in sympathetic ganglia *in vivo*, and many studies have confirmed that other neurotrophins are not able to compensate for the loss of NGF in the peripheral nervous system (Levi-Montalcini and Booker 1960; Angeletti and Levi-Montalcini 1971; Davies et al. 1987; Crowley et al. 1994; Middleton and Davies 2001).

NGF also has an important role in promoting process outgrowth from sympathetic neurons. Neonatal SCG neurons deprived of NGF display significant reductions in neurite elaboration *in vitro* (Campenot 1994; Deckwerth et al. 1996), whereas injection of NGF antiserum results in a reduction in the size of sympathetic ganglia *in vivo* (Levi-Montalcini and Booker 1960). In addition, overexpression of mouse NGF from epidermal tissue (an organ innervated by sympathetic neurons) causes hypertrophy of sympathetic nerves and ganglia enlargement (Albers et al. 1994). *In vivo* studies have shown

that NGF is not required for proximal outgrowth of sympathetic neurons, however both embryonically and postnatally it is essential for distal outgrowth of SCG neurons to their target organs, including the eye, trachea, and submandibular glands (Kuruvilla et al. 2004). In an *Ngf* knockout mouse model (in which *Bax* was also knocked down to prevent SCG death due to NGF deficiency), prevertebral neurons were also shown to require NGF for their development. In this model, prevertebral target organs including the stomach, spleen, and kidneys, showed a reduction in innervation which largely presented as a reduction in the terminal branching of the sympathetic neurons, and not as a full absence of innervation (Glebova 2004).

As suggested by its name, neurotrophin-3 (NT-3) was the third identified and characterised neurotrophin, following NGF and brain-derived neurotrophic factor (BDNF) (Ernfors et al. 1990; Hohn et al. 1990; Jones and Reichardt 1990; Kaisho et al. 1990; Maisonpierre et al. 1990; Rosenthal et al. 1990). Identification of NT-3 was facilitated by its striking sequence similarities to NGF and BDNF. Initial characterisation of NT-3 was completed on early embryonic chicken sensory ganglia, in which NT-3 supports the survival and differentiation of sensory neurons; later research expanded on these findings and demonstrated that NT-3 also supports the survival and outgrowth of cultured sympathetic neurons. NT-3 mRNA is expressed in target tissues of peripheral neurons during the developmental window when other neurotrophins are also functioning in peripheral neuron development. This indicated that these neurotrophins may work synergistically during the development of the PNS (Ernfors et al. 1992; Pirvola et al. 1992; Arumäe et al. 1993; Buchman and Davies 1993; DiCicco-Bloom et al. 1993; Davies 1994; Hallbook et al. 1995; Davies 2000).

NT-3 plays an essential role in the survival of SCG neurons in the same developmental window in which NGF regulates survival. Serial sections of SCG from mice carrying an *Ntf3* deletion showed 50% cell loss towards the end of sympathetic neuron development (P12-P16), indicative of its key role in neuronal cell survival (Ernfors et al. 1994; Fariñas et al. 1994). This neuronal loss derives from relatively late in development. Wyatt *et al.* found no neuronal loss

in E16 SCGs from *Ntf3* knockout mice; however, significant SCG neuronal cell death had occurred by E18 (Wyatt et al. 1997). They hypothesised therefore that NT-3 deficiency does not affect the early stages of development, such as the proliferation of sympathetic neuron precursors in the SCG, but instead is limited to later stages (Wyatt et al. 1997). Further *in vivo* analysis supported this hypothesis. No neuronal loss was identified in SCGs from *Ntf3*-null mice at E13.5 and E15.5, instead the first decrease in neuron number was detected at E17.5, and further continued at P0 (Francis et al. 1999). Although NGF and NT-3 function in the same developmental window, and substantial neuronal loss has been observed in both knockout mouse models, *Ngf* knockout mice showed more severe SCG neuron loss than *Ntf3* knockout mice. In addition, neuronal loss was not further increased in double knockout mouse models in which both NGF and NT-3 were ablated when compared to *Ngf* single knockout mouse models, suggesting that NT-3- dependent SCG neurons are a subset of NGF-dependent SCG neurons (Francis et al. 1999).

NT-3 can also stimulate SCG outgrowth both *in vitro* and *in vivo* (Elshamy et al. 1996; Belliveau et al. 1997; Francis et al. 1999; Kuruvilla et al. 2004). NT-3 increases neurite network density and total neurite length of cultured SCG neurons, and promotes expression of growth-associated genes in cultured neonatal SCG neurons (Belliveau et al. 1997). *In vivo*, NT-3 is expressed at high levels in intermediate organs found *en route* to target organs, such as the vasculature, as well as in the target organs themselves (Francis et al. 1999; Kuruvilla et al. 2004). This intermediate organ-derived NT-3 promotes both proximal and distal outgrowth of SCG neurons (Francis et al. 1999; Kuruvilla et al. 2004). Several studies using immunohistochemical approaches to analyse sympathetic target organs from *Ntf3* knockout mice revealed a developmental failure in target organ innervation, highlighting the importance of NT-3 in sympathetic axon growth *in vivo* (Elshamy et al. 1996; Francis et al. 1999; Kuruvilla et al. 2004).

The cell survival and neurite outgrowth promoting activities of NGF and NT-3 are mediated by their relationship with the tropomyosin receptor kinase A

(TrkA) (Davies et al. 1995; Fagan et al. 1996; Belliveau et al. 1997; Tessarollo et al. 1997; Kuruvilla et al. 2004). Target tissue-derived NGF binds its cognate receptor TrkA, and this receptor-ligand complex in turn is retrogradely transported to the soma where it triggers downstream cellular responses (Deinhardt and Chao 2014). Similarly, although TrkC is the cognate receptor for NT-3, evidence to date indicates that NT-3 also signals through TrkA, rather than TrkC, during the regulation of sympathetic neuronal survival and process outgrowth in the later embryonic stages (Davies et al. 1995; Fagan et al. 1996; Belliveau et al. 1997; Tessarollo et al. 1997; Kuruvilla et al. 2004). Characterisation of the role of the TrkC receptor in the development of sympathetic neurons revealed it had no significant effects on either the survival or process outgrowth of SCG neurons. Deletion of *Ntrk3* (TrkC gene) in a mouse model did not affect neurogenesis, neuronal survival, the expression of neuronal markers, or the initial outgrowth of SCG neurons (Davies et al. 1995; Fagan et al. 1996; Tessarollo et al. 1997). Furthermore, while TrkC expression decreases dramatically after E15.5, TrkA expression increases and is relatively high from E15.5 onwards (Qiu and Green 1992; Fagan et al. 1996; Kuruvilla et al. 2004). These expression profiles also strongly suggest that TrkA is a key component in both NGF and NT-3 signalling during the developmental of sympathetic neurons. Despite this shared receptor, there is a key difference between the downstream pathways activated by NGF and NT-3. Unlike NGF/TrkA, NT-3/TrkA complexes are not retrogradely transported to the cell soma of SCG neurons; therefore, NT-3 likely does not function as a target-derived survival factor. Instead, NT-3/TrkA signalling is required for proximal axon growth and target field innervation in a subset of SCG sympathetic neurons. Neuron loss of SCG neurons in a *Ntf3* knockout mouse model results from a failure of some SCG neurons to reach their target fields and thus gain access to NGF (Kuruvilla et al. 2004).

In addition to the Trk receptors, neurotrophins can also modulate sympathetic nervous system development through the receptor $p75^{NTR}$ (Bibel and Barde 2000). *In vitro* experiments strongly indicate that the balanced

expression of TrkA and $p75^{NTR}$ receptors influences neurotrophin-induced developmental events (Horton et al. 1997). Overexpression of the TrkA receptor accelerates NGF-induced neurite elaboration in PC12 cells via its tyrosine kinase activity (Hempstead et al. 1992). Conversely, reduced expression of $p75^{NTR}$ increases the responsiveness of the same cells to NT-3, manifesting as a significant increase in neurite outgrowth when this ligand is added (Benedetti et al. 1993; Clary and Reichardt 1994). Interestingly, it is the activity of NT-3 which is most susceptible to changes in the TrkA:$p75^{NTR}$ ratio. A high $p75^{NTR}$ expression suppresses the ability of NT-3 to bind TrkA; in contrast NT-3/TrkA signalling is stronger in postnatal SCG neurons from *Ngfr* ($p75^{NTR}$ gene) knockout mice (Lee et al. 1994b; Davies et al. 1995). *In vivo*, $p75^{NTR}$ can also influence the outgrowth of sympathetic neurons. In $p75^{NTR}$ knockout mice, disrupted innervation of the pineal gland and sweat glands of the foot was observed (Lee et al. 1994a). (This is likely due to reduced efficacy of NGF in promoting innervation of these target tissues, independent of NT-3 signalling). These findings suggest that $p75^{NTR}$ may be able to alter the specificity of NT-3 binding to TrkA, and regulate survival and outgrowth responses of sympathetic neurons.

NGF and NT-3 clearly play a critical role in the development of SCG neurons, both *in vitro* and *in vivo*. Previous chapters in this thesis have highlighted significant differences in the response of SCG (paravertebral) and PVG (prevertebral) sympathetic neurons to receptors and ligands from the TNF and TNFR superfamilies. These differences are only partially explained by variations in the regional localisation of the receptors and their ligands. This raised the question as to whether the differences seen between SCG and PVG neurons, in part originate at more fundamental levels of cell signalling. Altered responses to the neurotrophins NGF and NT-3, the central drivers of neuronal survival and outgrowth, could generate an underlying signalling environment dissimilar enough to explain the sometimes contrasting responses of SCG and PVG neurons to TNF superfamily members. This chapter will investigate the responses of SCG and PVG neurons to neurotrophins, particularly in the context

of neuronal survival and process outgrowth, to understand whether this may partially explain findings from the previous chapters.

Past studies have clearly illustrated that the characteristics of SCG neurons change throughout development, over both embryonic and postnatal periods (Davies 1994; Horton et al. 1997; Wyatt et al. 1997; Davies 2000). Therefore, this chapter will investigate the responses of SCG and PVG neurons to NGF and NT-3 across both embryonic and postnatal periods.

5.2 RESULTS

5.2.1 NGF and NT-3 Regulate Paravertebral and Prevertebral Neuron Outgrowth

Previous studies have clearly demonstrated that NGF and NT-3 play an essential role in promoting the outgrowth of processes from mouse SCG neurons after these neurons become NGF-dependent at E14 (Wyatt and Davies 1993; Davies 1994; Davies et al. 1995; Wyatt and Davies 1995; Horton et al. 1997; Wyatt et al. 1997; Kuruvilla et al. 2004). After this point, both NGF and NT-3 promote neuronal process outgrowth from SCG neurons over the embryonic and postnatal periods (Glebova and Ginty 2005). Despite robust investigations into the primary roles of neurotrophins and their receptors in the survival of various neuronal populations in the PNS (Glebova and Ginty 2005), the characterisation of their role in outgrowth of neural processes has not been fully explored. Better understanding of these other functions, in conjunction with their role in neuronal survival, will provide a more thorough map of their significance during the establishment of the sympathetic nervous system. To achieve this objective, this section aims to undertake the first comprehensive examination of the role of NGF and NT-3 in the outgrowth of sympathetic neuronal processes, in the developmental window in which these neurons are innervating their target fields. To examine whether NT-3 and NGF promote process outgrowth from PVG neurons, as in SCG neurons, during embryonic and postnatal development, SCG and PVG neurons were dissected from CD1 mice at ages ranging from E16 to P5. In this experimental set-up, isolated SCG and PVG neurons were cultured at extremely low-density (≤ 100 neurons per 35 mm^2 dish), and treated with increasing concentrations of neurotrophins, ranging from 0.01 to 100 ng/ml NGF and 0.1 to 1000 ng/ml NT-3. To compare the response of PVG and SCG neurons, mean neurite lengths and numbers of branch points were quantified. In addition, Sholl profiles of SCG and PVG neurons were constructed to more clearly illustrate the morphological changes

occurring in response to increasing concentrations of NGF and NT-3 at each developmental age.

5.2.1.1 Sympathetic Neuron Process Outgrowth at E16

The first embryonic age investigated was E16. This age represents the earliest timepoint from which isolated SCG neurons are clearly and consistently responsive to NGF, thus characterisation of PVG neurons began at this age.

5.2.1.1.1 Effect of NGF

Fig. 5.1 shows the effect of increasing concentrations of NGF (0 to 100 ng/ml) on the mean neurite length (Fig. 5.1A), mean number of branch points (Fig. 5.1B), and overall complexity (Fig. 5.1C) of E16 paravertebral and prevertebral sympathetic neurons. The addition of sufficient levels of NGF to sympathetic neuron cultures significantly increased mean neurite length and mean number of branch points compared to those cultured without NGF. NGF increasingly promoted neurite outgrowth and complexity in both PVG and SCG neurite arbours with increasing concentrations. Surprisingly, at almost all concentrations tested, NGF exhibited a less potent effect on E16 PVG neurons compared with their SCG counterparts, promoting neurite outgrowth and branch complexity in PVG neurons to lower magnitudes than those seen in paravertebral SCG neurons.

In outgrowth assays, 0.1 ng/ml NGF was sufficient to induce significant increases in the mean length of SCG neuron processes compared to neurons cultured without NGF ($p<0.001$); however, 1 ng/ml NGF was needed to induce a significant increase in PVG neurite lengths compared to neurons cultured without NGF ($p<0.001$). In the case of SCG neurons, each 10-fold increase in NGF concentration, between 0.01 and 10 ng/ml, resulted in significant increases in neurite length (Fig. 5.1A, 0.01 vs. 0.1 ng/ml, $p<0.01$; 0.1 vs. 1 ng/ml, $p<0.001$; 1 vs. 10 ng/ml, $p<0.01$). In the case of PVG neurons, significant increases in neurite length were also seen over 10-fold changes in NGF concentrations, up to 10 ng/ml; however, this began at 1 ng/ml NGF (Fig. 5.1A, 0.1 vs. 1 ng/ml, $p<0.001$; 1 vs. 10 ng/ml, $p<0.05$). There was no significant difference in neurite length for

either PVG or SCG neurons between 10 and 100 ng/ml NGF, suggesting that by this concentration NGF had reached saturation.

Fig. 5.1B displays the increase in the mean number of branch points exhibited by processes of PVG and SCG neurons in response to increasing NGF concentrations. Whilst 0.1 ng/ml NGF was sufficient to induce a significant increase in the number of branch points displayed by the processes of SCG neurons compared to neurons cultured without NGF (p<0.001), PVG neurons required a minimum of 1 ng/ml NGF before a significant increase in branch point number compared to no NGF was seen (p<0.001). 10-fold increases in NGF concentrations significantly increased the number of neurite bifurcations in both PVG (0.1 vs. 1 ng/ml, p<0.001) and SCG (0.01 vs. 0.1 ng/ml, 0.1 vs. 1 ng/ml, p<0.001) neuron cultures, although this occurred over a wider concentration range in SCG neurons. There was no further increase in the branching of PVG or SCG neurons at concentrations above 1 ng/ml NGF, suggesting saturation between 0.1 and 1 ng/ml NGF.

Strikingly, although NGF promoted elongation and branching of the processes of both PVG and SCG neurons, increases in these parameters were smaller in PVG than SCG neurons at each NGF concentration tested (PVG vs SCG, neurite length: Fig. 5.1A, 0.01 ng/ml, p<0.01; 0.1, 1, 10, and 100 ng/ml, p<0.001; branch point numbers: Fig. 5.1B, 0.1, 1, 10, and 100 ng/ml NGF, p<0.001). The only exception was at 0.01 ng/ml NGF, where no significant differences in branch point numbers was seen between PVG or SCG neurites (Fig. 5.1B).

Differences in neurite complexity between PVG and SCG neurons in response to increasing NGF concentrations are demonstrated by Sholl analysis (Fig. 5.1C). Sholl plots highlighted no discernible differences between PVG and SCG neuron cultures incubated without NGF. In contrast, at 0.01 ng/ml NGF, PVG neurons showed a decrease in the number of intersections at distances between 150 and 300 μm from the cell soma, when compared with SCG neurons. At higher concentrations (0.1, 1, 10, and 100 ng/ml), the difference in the number of intersections in PVG neurons compared to SCG neurons was even more dramatic, and occurred over a wider range of distances from the cell soma.

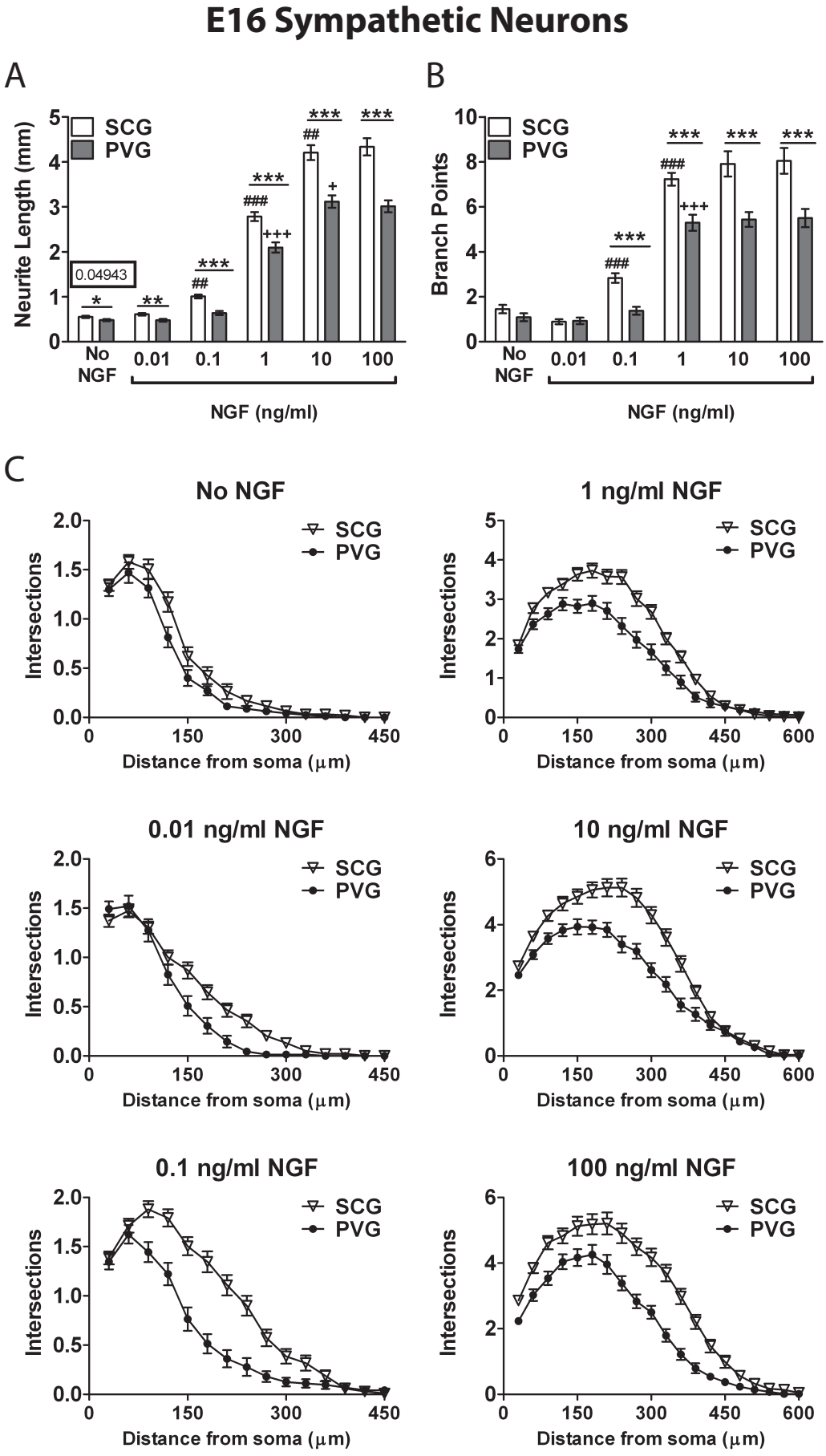

Fig. 5.1. Legend on following page.

Figure 5.1. NGF Concentration-Dependent Outgrowth of E16 SCG and PVG Neurons. (A&B) Quantification of neurite lengths **(A)** and branch points **(B)** of E16 wild-type SCG and PVG neurons cultured without NGF, or treated with NGF at concentrations between 0.01 and 10 ng/ml. Data are presented as the mean ± standard error. n=3 for each condition. * denotes significant differences between SCG and PVG neurons at each concentration point, *: $p<0.05$, **: $p<0.01$, ***: $p<0.001$; # denotes significant differences across 10-fold concentration increases in SCG neurons, ##: $p<0.01$, ###: $p<0.001$; + denotes significant differences across 10-fold concentration increases in PVG neurons, +: $p<0.05$, +++: $p<0.001$ (Kruskal-Wallis, with Dunn's *post-hoc* analysis). **(C)** Sholl analysis of E16 wild-type SCG and PVG neurons as described in (A). Data are presented as the mean ± standard error. n=3 for each condition. NGF: nerve growth factor; PVG: prevertebral ganglia (coeliac and superior mesenteric ganglia); SCG: superior cervical ganglia.

5.2.1.1.2 Effect of NT-3

Fig. 5.2 illustrates the effect of increasing concentrations of NT-3 (0 to 1000 ng/ml) on the mean neurite length (Fig. 5.2A), mean number of branch points (Fig. 5.2B), and overall neurite complexity (Fig. 5.2C) of E16 PVG and SCG neurons. NT-3 significantly increased neurite elongation and branching of PVG and SCG neurons compared with those incubated without NT-3. 10-fold increases in NT-3 concentration significantly further increased neurite growth in both PVG and SCG neurons, until saturation by 100 (length) or 10 (branching) ng/ml NT-3. However, similar to NGF, the effect of NT-3 was less potent in PVG than SCG neurons, at each concentration tested.

SCG neurons incubated with as little as 0.1 ng/ml NT-3 had significantly longer neurites than those incubated without NT-3 (Fig. 5.2A, $p<0.001$). In PVG neurons however, the lowest NT-3 concentration at which a significant increase was observed in neurite outgrowth was 10-fold higher, at 1 ng/ml (Fig. 5.2A, $p<0.001$). In SCG neurons, 10-fold increases in concentration significantly increased the length of neurite processes between 0.1 and 1 ng/ml ($p<0.05$), and again between 10 and 100 ng/ml ($p<0.01$). In PVG neurons, similar significant increases in neurite length were detected at each 10-fold increase in concentration between 0.1 and 100 ng/ml (0.1 vs. 1 ng/ml, $p<0.001$; 1 vs. 10 ng/ml, 10 vs. 100 ng/ml, $p<0.01$).

Significant increases in branch point numbers were identified in SCG neurons cultured with 0.1 ng/ml NT-3, when compared to neurons cultured without NT-3 (Fig. 5.2B, $p<0.05$). However, as with neurite length, an effect on branch point numbers was not seen in PVG neurons until much higher NT-3 concentrations, in this case 10 ng/ml ($p<0.001$).

Similar to NGF, NT-3 had less potent effects on PVG compared to SCG neurons. At each concentration tested, PVG neurons showed shorter neurite lengths (Fig. 5.2A, 0.1, 1, 10, 100, and 1000 ng/ml, $p<0.001$), and a fewer number of branch points (Fig. 5.2B, 0.1, 1, 10, and 1000 ng/ml, $p<0.001$; 100 ng/ml, $p<0.01$) compared to SCG neurons. An unexpected result in E16 sympathetic neurons was a significant decrease in the length (Fig. 5.2A, $p=0.0429$) and branching (Fig.

5.2B, $p<0.05$) of PVG neurites compared with SCG neurites when these neurons were incubated without NT-3.

Fig. 5.2C shows Sholl analysis comparing the effect of increasing NT-3 concentrations on the overall neurite complexity of PVG and SCG neurons. Sholl analysis showed no clear difference in the number of intersections close to the cell body – within a Sholl radius of 120 μm – between PVG and SCG neurons cultured without NT-3. However, at distances from the neuron soma of 150 μm and greater there were clear differences between the number of intersection made by SCG and PVG neurons in the absence of NT-3. When NT-3 was added to cultures, PVG neurons had less complex neurite morphologies than SCG neurons at all distances within the whole Sholl radius.

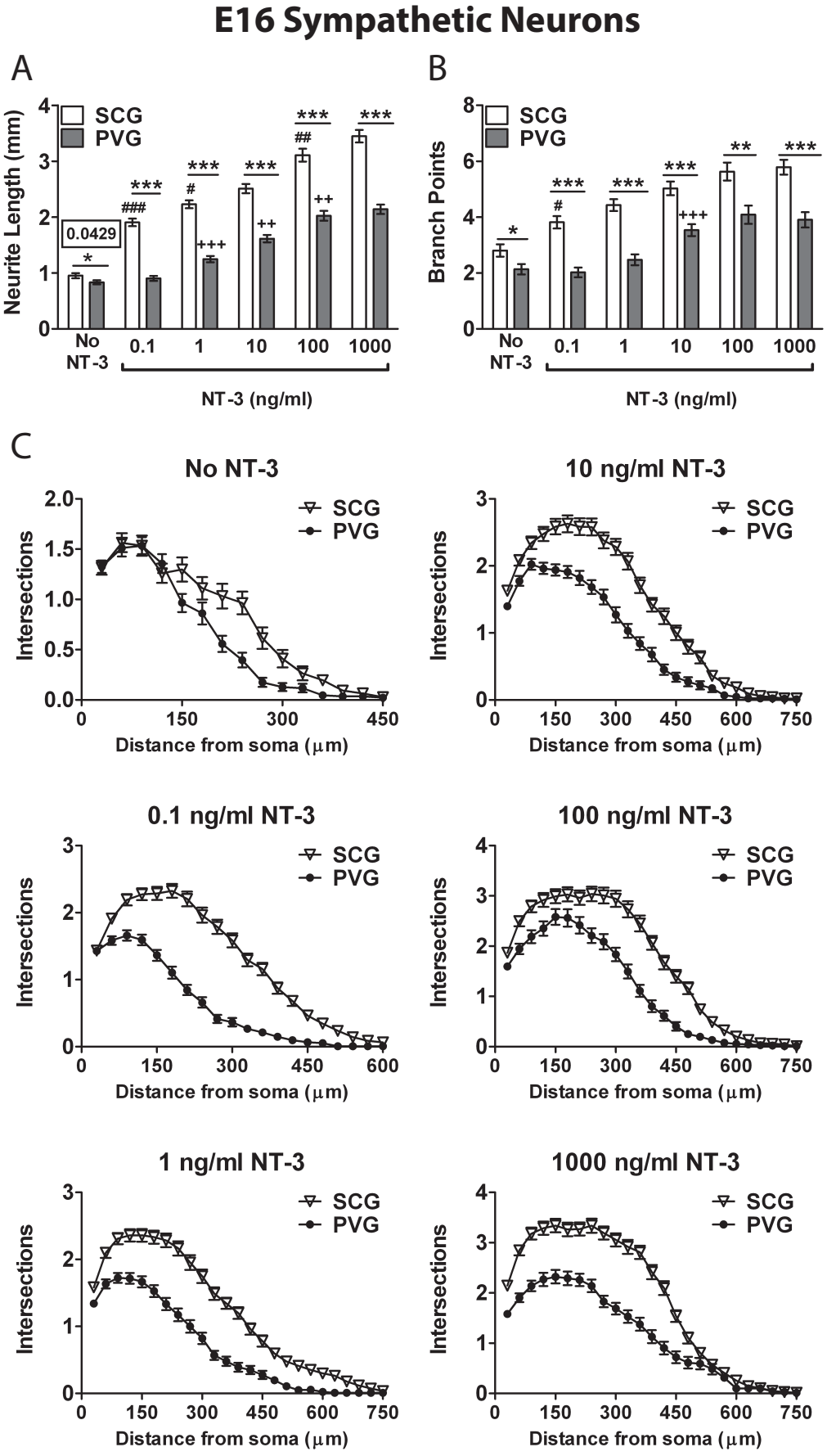

Fig. 5.2. Legend on following page.

Figure 5.2. NT-3 Concentration-Dependent Outgrowth of E16 SCG and PVG Neurons. (A&B) Quantification of neurite lengths **(A)** and branch points **(B)** of E16 wild-type SCG and PVG neurons cultured without NT-3 or treated with NT-3 at concentrations between 0.1 and 1000 ng/ml. Data are presented as the mean ± standard error. n=3 for each condition. * denotes significant differences between SCG and PVG neurons at each concentration point, *: $p<0.05$, **: $p<0.01$, ***: $p<0.001$; # denotes significant differences across 10-fold concentration increases in SCG neurons, #: $p<0.05$, ##: $p<0.01$, ###: $p<0.001$; + denotes significant differences across 10-fold concentration increases in PVG neurons, ++: $p<0.01$, +++: $p<0.001$ (Kruskal-Wallis, with Dunn's *post-hoc* analysis). **(C)** Sholl analysis of E16 wild-type SCG and PVG neurons treated as described in (A). Data are presented as the mean ± standard error. n=3 for each condition. NT-3: neurotrophin-3; PVG: prevertebral ganglia (coeliac and superior mesenteric ganglia); SCG: superior cervical ganglia.

5.2.1.2 Sympathetic Neuron Process Outgrowth at E18

Next, the effects of NT-3 and NGF were investigated in E18 PVG and SCG neurons. By this age the vast majority of SCG neurons are NGF-dependent; therefore, outgrowth and branching responses to neurotrophins are greater at E18 compared to E16 (Wyatt and Davies 1995).

5.2.1.2.1 Effect of NGF

Fig. 5.3 presents E18 sympathetic neurons cultured in increasing concentrations of NGF (0 to 100 ng/ml). At this age, the addition of NGF induced significant increases in neurite length (Fig. 5.3A) and branch point numbers (Fig. 5.3B) in both PVG and SCG neurons. Moreover, over 10-fold increases in NGF concentration, further increases in the neurite length of PVG and SCG neurons were seen, before a plateau was reached by 10 ng/ml NGF. Similar to results at E16, NGF had weaker effects on the outgrowth of E18 PVG neurons compared with SCG neurons; accordingly, PVG neurons had significantly shorter neurites and less complex branches than SCG neurites at each NGF concentration tested.

Although at E16, SCG neurons were responsive to a lower NGF concentration than PVG neurons, neurite length data at E18 showed that both SCG and PVG neurons required at least 1 ng/ml to induce a significant increase in neurite outgrowth compared to neurons grown without NGF (Fig. 5.3A; $p<0.001$). Significant changes in the neurite lengths of both PVG and SCG neurons were seen over 10-fold increases in NGF concentration between each step from 0.1 to 10 ng/ml (0.1 vs. 1 ng/ml; 1 vs. 10 ng/ml, $p<0.001$ for both PVG and SCG neurons). No significant change was observed in the neurite lengths of PVG and SCG neurons when the concentration was increased from 10 to 100 ng/ml NGF.

Fig. 5.3B shows the increase in branching of E18 PVG and SCG neurons as a result of increasing NGF concentrations. SCG neurons cultured with 0.01 ng/ml NGF had significantly more branch points than neurons cultured without NGF (Fig. 5.3B, $p<0.05$). PVG neurons required a higher concentration of NGF – 1 ng/ml – to induce a significant change in branch point number ($p<0.001$). A

10-fold increase in the NGF concentration, from 0.01 to 0.1 ng/ml, did not cause any significant changes in the neurite branch numbers of either PVG or SCG neurons. However, the 10-fold increase from 0.1 to 1 ng/ml significantly increased branching of both PVG and SCG neurons ($p<0.001$). Analysis found no further significant increases in the number of neurite branches displayed by PVG or SCG neurons in either of the 10-fold increases between 1 and 100 ng/ml NGF.

The effect of NGF on E18 sympathetic neurons was, similar to that on E16 sympathetic neurons, less potent in promoting the outgrowth of prevertebral PVG neurons than paravertebral SCG neurons. Analysis of E18 sympathetic neurons clearly showed that PVG neurons had significantly shorter (Fig. 5.3A, 0.01 ng/ml, $p<0.05$; 0.1 ng/ml $p<0.01$; 1, 10, and 100 ng/ml, $p<0.001$) and less branched (Fig. 5.3B, 0.01 ng/ml, $p<0.05$; 0.1 ng/ml $p<0.01$; 1, 10, and 100 ng/ml, $p<0.001$) neurites than SCG neurons at all NGF concentrations tested. PVG and SCG neurons incubated without NGF did not show any significant difference in their neurite outgrowth, indicating that PVG neurons did not have intrinsically less complicated neurites than SCG neurons, but instead the addition of NGF led to less substantial increases in the growth of PVG neurons than SCG neurons.

The changes in overall neurite structures of PVG and SCG neurons in response to increasing NGF concentrations is illustrated by Sholl plots (Fig. 5.3C). PVG and SCG neurons did not show any difference in their morphology when they were cultured without NGF and only very small differences emerged between the two neuron types with the addition of 0.01 ng/ml NGF. However, with the addition of greater concentrations of NGF to the culture media, PVG neurons displayed less complex neurite morphology than SCG neurons at each NGF concentration tested.

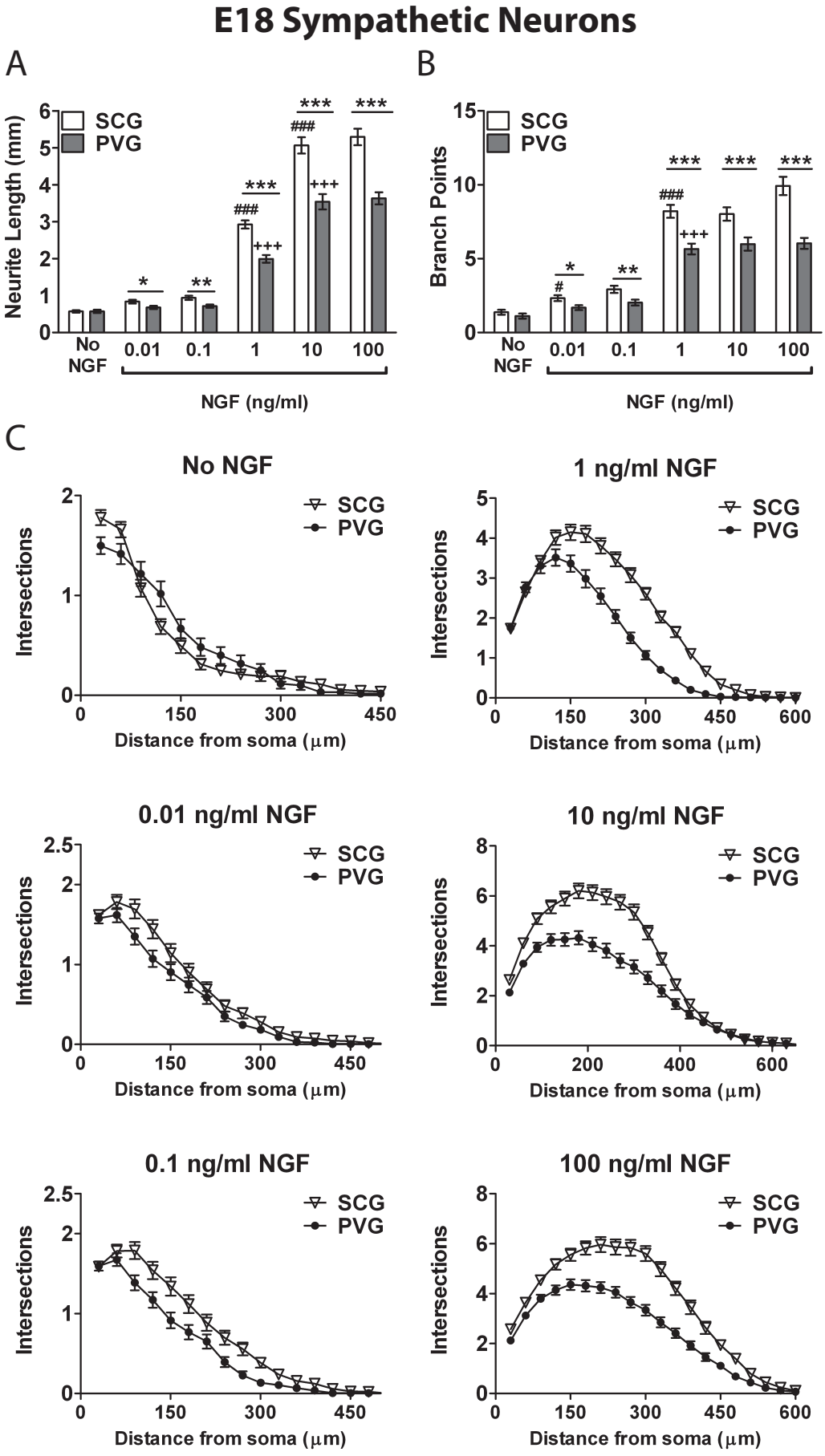

Fig. 5.3. Legend on following page.

Figure 5.3. NGF Concentration-Dependent Outgrowth of E18 SCG and PVG Neurons. (A&B) Quantification of neurite lengths **(A)** and branch points **(B)** of E18 wild-type SCG and PVG neurons cultured without NGF or treated with NGF at concentrations between 0.01 and 100 ng/ml. Data are presented as the mean ± standard error. n=3 for each condition. * denotes significant differences between SCG and PVG neurons at each concentration point, *: $p<0.05$, **: $p<0.01$, ***: $p<0.001$; # denotes significant differences across 10-fold concentration increases in SCG neurons, #: $p<0.05$, ###: $p<0.001$; + denotes significant differences across 10-fold concentration increases in PVG neurons, +++: $p<0.001$ (Kruskal-Wallis, with Dunn's *post-hoc* analysis). **(C)** Sholl analysis of E18 wild-type SCG and PVG neurons treated as described in (A). Data are presented as the mean ± standard error. n=3 for each condition. NGF: nerve growth factor; PVG: prevertebral ganglia (coeliac and superior mesenteric ganglia); SCG: superior cervical ganglia.

5.2.1.2.2 Effect of NT-3

Fig. 5.4 shows the effect of NT-3 on neurite length (Fig. 5.4A) and bifurcation (Fig. 5.4B) in E18 paravertebral and prevertebral sympathetic neuron cultures, with Sholl plots illustrating changes in neurite morphology in response to increasing NT-3 concentrations (Fig. 5.4C). 0.1 ng/ml NT-3 was able to increase neurite elongation and branching from both PVG and SCG neurons, and larger responses were seen with increasing NT-3 concentrations. The effects of NT-3 were less potent on PVG neurons than on SCG neurons, although this difference was largely seen at mid-high concentrations of NT-3.

In terms of neurite length, both PVG and SCG neurons were responsive to the minimum NT-3 concentration tested, 0.1 ng/ml (Fig. 5.4A, $p<0.001$). Over the 10-fold increase from 0.1 to 1 ng/ml NT-3, there was no significant change in the length of sympathetic neuron neurites. Each subsequent 10-fold increase in NT-3 concentration, from 1 to 1000 ng/ml, resulted in significantly longer PVG and SCG neuron neurites (PVGs: 1 vs. 10 ng/ml, $p<0.01$; 10 vs. 100 ng/ml, $p<0.001$; 100 vs. 1000 ng/ml, $p<0.05$; SCGs: 1 vs. 10 ng/ml; 10 vs. 100 ng/ml; 100 vs. 1000 ng/ml, $p<0.001$).

Figure 5.4B shows the changes in the mean branch point numbers with changing NT-3 concentrations. Branching in both PVG and SCG neurons showed a significant increase at 0.1 ng/ml NT-3 compared to control cultures (both neuron types: $p<0.001$). Quantification of branch points on sympathetic neuron processes revealed that a 10-fold increase in NT-3 concentration from 0.1 to 1 ng/ml did not significantly affect arborisation of sympathetic neuron neurites. However, each 10-fold increase in NT-3 concentration from 1 to 100 ng/ml significantly increased the extent of branching in both PVG (1 vs. 10 ng/ml, $p<0.01$; 10 vs. 100 ng/ml, $p<0.001$) and SCG neuron processes (1 vs. 10 ng/ml; 10 vs. 100 ng/ml, $p<0.001$). Increasing the NT-3 concentration to 1000 ng/ml did not significantly increase neurite branch point number compared to 100 ng/ml NT-3 in either PVG or SCG neuron cultures.

The weaker effect of NT-3 in promoting the growth of PVG neurites compared to SCG neurites was also seen in E18 sympathetic neuron cultures.

While there was no statistically significant difference between the neurite lengths of PVG and SCG neurons when they were incubated with 0.1 and 1 ng/ml NT-3, PVG neurons had significantly shorter neurite lengths than SCG neurons at higher NT-3 concentrations (Fig. 5.4A, 10, 100, and 1000 ng/ml, $p<0.001$). Similarly, the extent of branching displayed by PVG neuron neurites was significantly less compared to SCG neurons at both low and high NT-3 concentrations tested, with an exception of 1 ng/ml at which no significant difference was detected (Fig. 5.4B, 0.1 ng/ml, $p<0.05$; 10 ng/ml, $p<0.001$; 100 and 1000 ng/ml, $p<0.01$).

Sholl plots of PVG and SCG neurons illustrate the effect of increasing NT-3 concentrations on the overall complexity of E18 neuron sympathetic neuron neurites (Fig. 5.4C). No discernible difference was seen between the Sholl plots of PVG and SCG neurons cultured without NT-3, or with low concentrations of NT-3 (0.1 and 1 ng/ml). However, at 10, 100, and 1000 ng/ml NT-3, PVG neurons displayed a decreased number of intersections between 150 and 450 μm from the cell soma. In addition, Sholl plots revealed that SCG neurites were able to make intersections at further distances from the soma compared to PVG neurons at NT-3 concentrations of 10 ng/ml and higher. These results suggest that although PVG and SCG neurons show similar patterns in their neurite elaboration in response to increasing NT-3 concentrations, NT-3 promotes the outgrowth of PVG neurons to a lesser extent than SCG neurons.

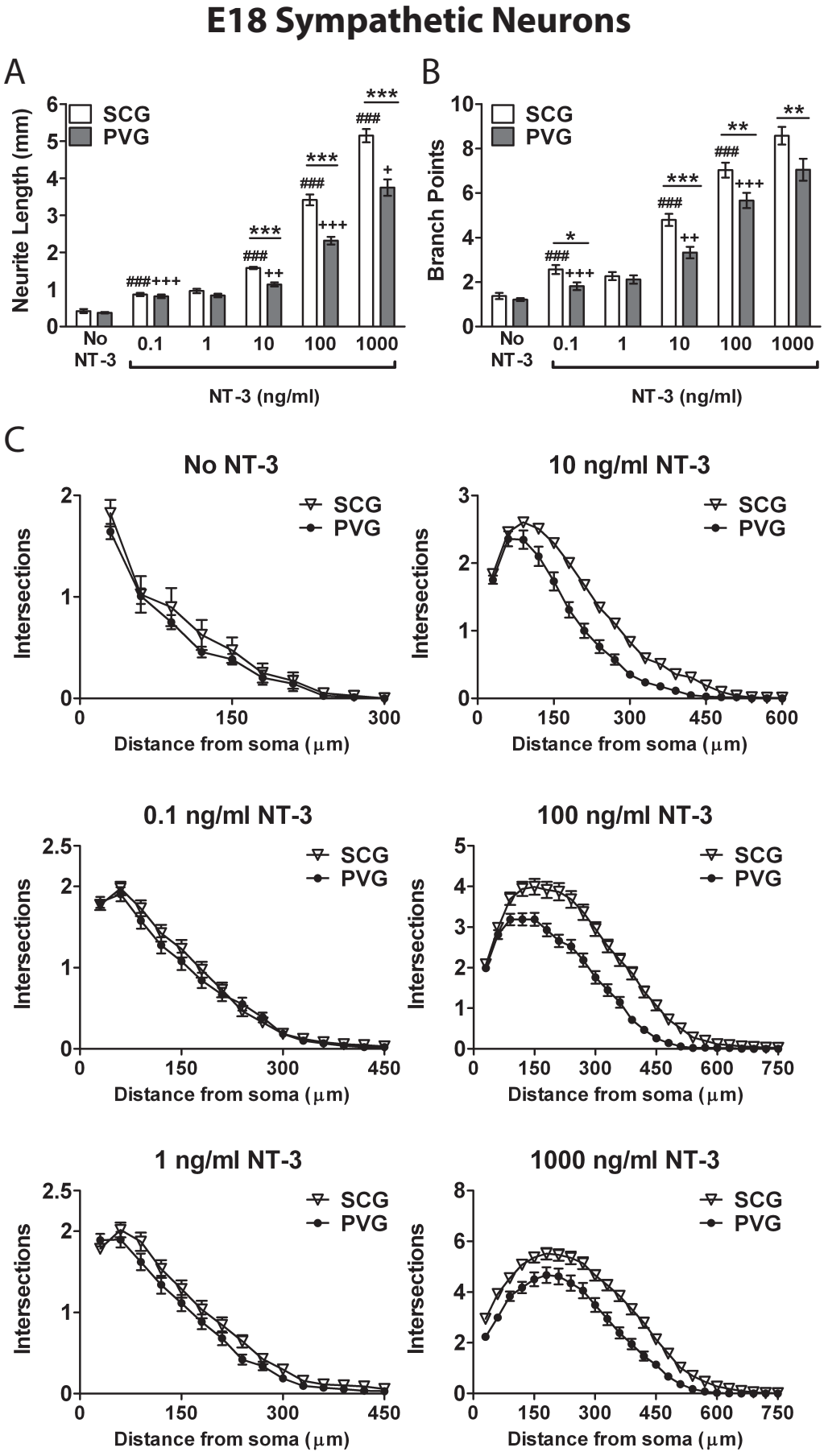

Fig. 5.4. Legend on following page.

Figure 5.4. NT-3 Concentration-Dependent Outgrowth of E18 SCG and PVG Neurons. (A&B) Quantification of neurite lengths **(A)** and branch points **(B)** of E18 wild-type SCG and PVG neurons cultured without NT-3 or treated with NT-3 at concentrations between 0.1 and 1000 ng/ml. Data are presented as the mean ± standard error. n=3 for each condition. * denotes significant differences between SCG and PVG neurons at each concentration point, *: $p<0.05$, **: $p<0.01$, ***: $p<0.001$; # denotes significant differences across 10-fold concentration increases in SCG neurons, ###: $p<0.001$; + denotes significant differences across 10-fold concentration increases in PVG neurons, +: $p<0.05$, ++: $p<0.01$, +++: $p<0.001$ (Kruskal-Wallis, with Dunn's *post-hoc* analysis). **(C)** Sholl analysis of E18 wild-type SCG and PVG neurons treated as described in (A). Data are presented as the mean ± standard error. n=3 for each condition. NT-3: neurotrophin-3; PVG: prevertebral ganglia (coeliac and superior mesenteric ganglia); SCG: superior cervical ganglia.

5.2.1.3 Sympathetic Neuron Process Outgrowth at Po

Neurotrophic factor regulation of Po sympathetic neuron process growth was examined to understand the differences between PVG and SCG neurons in the developmental period immediately post-birth.

5.2.1.3.1 Effect of NGF

Fig. 5.5 shows the effect of increasing NGF concentrations on the mean neurite length (Fig. 5.5A), the mean number of branch points (Fig. 5.5B), and Sholl profiles (Fig. 5.5C) of Po PVG and SCG neurons. NGF significantly increased the length and complexity of PVG and SCG neuron neurites compared with those incubated without NGF (Fig. 5.A, B & C). Similar to previous ages studied, NGF affected neurite length and branching of Po PVG neurons less potently than their SCG counterparts, at both lower and higher NGF concentrations tested.

Analysis of the neurite length of sympathetic neurons revealed that the length of SCG neuron processes in cultures supplemented with 0.1 ng/ml NGF was significantly greater than those cultured without NGF (Fig. 5.5A, $p<0.001$). On the other hand, PVG neurons did not show any significant increase in neurite length compared to controls until 1 ng/ml NGF was added to cultures (Fig. 5.5A, $p<0.001$). At 1 ng/ml NGF, both PVG and SCG neurons had significantly increased neurite lengths compared with those treated with 0.1 ng/ml (Fig 5.5A, $p<0.001$). At 10 and 100 ng/ml NGF, the lengths of PVG and SCG neuron neurites were not significantly longer compared to neurons in cultures supplemented with 1 ng/ml NGF (Fig. 5.5A).

Analysis of branch point number found that both PVG and SCG neurons incubated with 0.01 ng/ml NGF had significantly more neurite branch points compared to those cultured without NGF (Fig. 5.5B, $p<0.01$ and $p<0.001$ for PVG and SCG neurons, respectively). Whereas SCG neurons cultured with 0.1 ng/ml NGF had significantly more branch points than those cultured with 0.01 ng/ml NGF ($p<0.05$), PVG neurons did not show any changes in their branching over this 10-fold increase in NGF concentration. When the NGF concentration was increased from 0.1 ng/ml to 1 ng/ml, neurite bifurcations in both PVG and SCG

neurons were significantly increased (p<0.001). At higher concentrations – 10 and 100 ng/ml – the extent of branching in PVG and SCG neuron neurites did not significantly increase compared to neurons cultured with 1 ng/ml NGF.

At this age, NGF continued to have a weaker efficacy on the outgrowth of PVG neurites than SCG neurites. Quantification of PVG and SCG neurons demonstrated that PVG neurons were significantly shorter (Fig. 5.5A, 0.1 ng/ml, p<0.001; 1 ng/ml, p<0.05; 10 and 100 ng/ml, p<0.01) and had fewer branch points (Fig. 5.5B, 0.1 ng/ml, p<0.001; 1 and 10 ng/ml, p<0.05) than SCG neurons, when cultured with 0.1, 1 and 10 ng/ml NGF.

Sholl plots of sympathetic neurons illustrate the changing neurite morphologies of Po PVG and SCG neurons in response to increasing NGF concentrations (Fig. 5.5C). In the absence of NGF and with 0.01 ng/ml NGF, Sholl plots of SCG and PVG neurites were almost overlapping. However, at all concentrations between 0.1 and 100 ng/ml NGF, Sholl graphs illustrate that PVG neurites had less complex morphologies than SCG neurites, reflected by a reduced number of intersections, at almost every distance measured from the cell soma, in agreement with results from the neurite length and branching analyses (Fig. 5.5A & B).

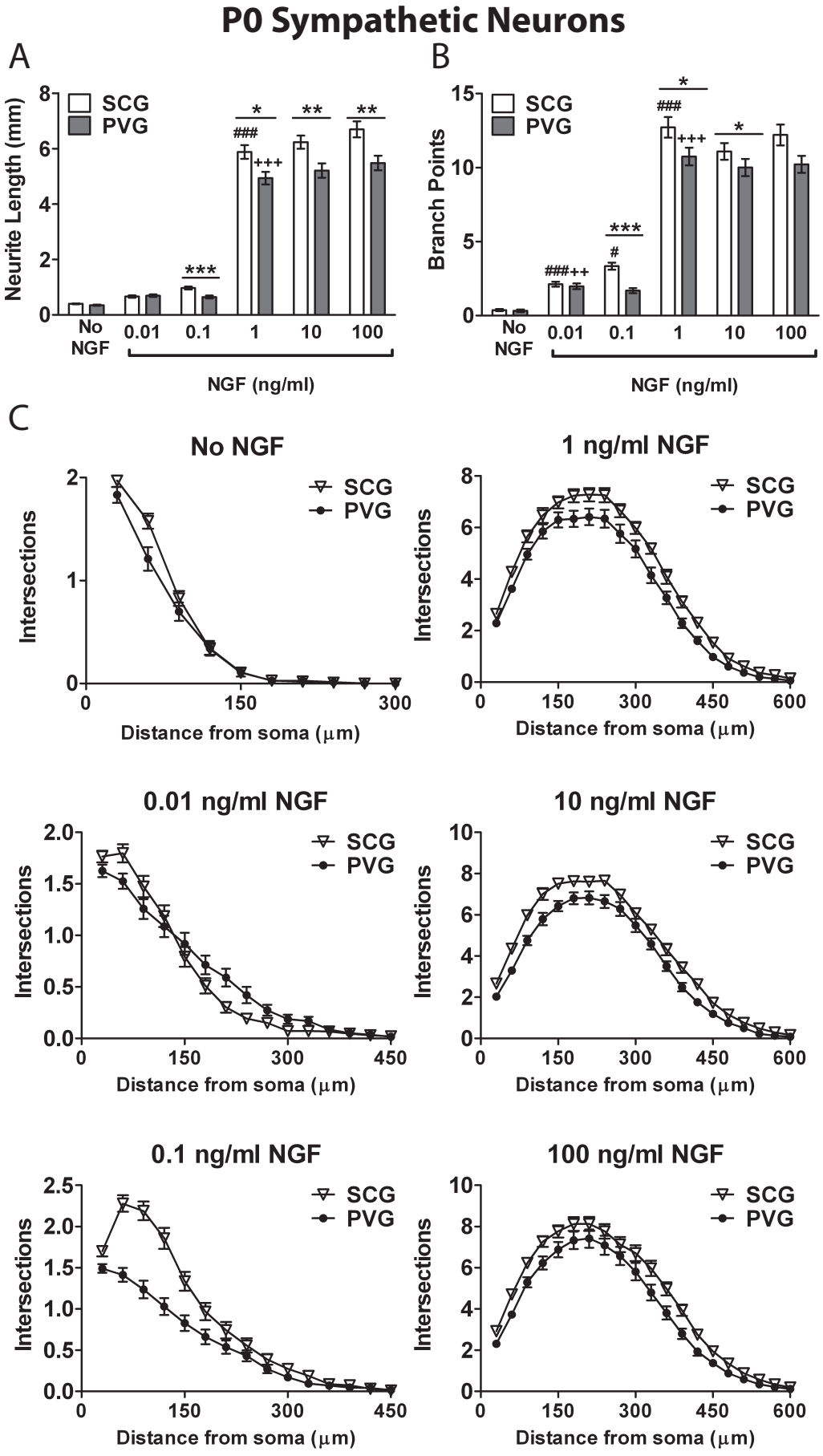

Fig. 5.5. Legend on following page.

Figure 5.5. NGF Concentration-Dependent Outgrowth of Po SCG and PVG Neurons. (A&B) Quantification of neurite lengths **(A)** and branch points **(B)** of Po wild-type SCG and PVG neurons cultured without NGF or treated with NGF at concentrations between 0.01 and 100 ng/ml. Data are presented as the mean ± standard error. n=3 for each condition. * denotes significant differences between SCG and PVG neurons at each concentration point, *: $p<0.05$, **: $p<0.01$, ***: $p<0.001$; # denotes significant differences across 10-fold concentration increases in SCG neurons, #: $p<0.05$, ###: $p<0.001$; + denotes significant differences across 10-fold concentration increases in PVG neurons, +: $p<0.05$, ++: $p<0.01$, +++: $p<0.001$ (Kruskal-Wallis, with Dunn's *post-hoc* analysis). **(C)** Sholl analysis of Po wild-type SCG and PVG neurons treated as described in (A). Data are presented as the mean ± standard error. n=3 for each condition. NGF: nerve growth factor; PVG: prevertebral ganglia (coeliac and superior mesenteric ganglia); SCG: superior cervical ganglia.

5.2.1.3.2 Effect of NT-3

Fig. 5.6 shows that NT-3 has a significant role in promoting the growth (Fig. 5.6A) and bifurcation (Fig. 5.6B) of P0 paravertebral and prevertebral sympathetic neuron processes. The changes in the complexity of sympathetic neurites occurring in response to increasing concentrations of NT-3 are illustrated by Sholl plots (Fig. 5.6C). Whilst NT-3 was able to induce significant changes in neurite length and branching at P0, relatively higher concentrations of the neurotrophin were needed to produce significant changes in neurite length when compared with previous ages. At this age, the reduced potency of NT-3 in promoting neurite elongation and branching from PVG neurons compared to SCG neurons seen at earlier ages had largely disappeared, particularly in the context of neurite branching.

At P0, the lowest concentration of NT-3 able to induce a significant increase in neurite length compared to control cultures was relatively high, 10 ng/ml in SCG neurons (Fig. 5.6A, $p<0.05$), and 100 ng/ml in PVG neurons ($p<0.001$). Further increases in the length of SCG neurons were seen at each subsequent 10-fold increase in NT-3 concentration (10 vs. 100 ng/ml; 100 vs. 1000 ng/ml, $p<0.001$). The 10-fold increase from 100 to 1000 ng/ml NT-3 also induced a further increase in the neurite lengths of PVG neurons ($p<0.05$).

Branching analysis revealed that at this age, both PVG and SCG neurons were still able to respond to the lowest concentration of NT-3 tested, 0.1 ng/ml (Fig. 5.6B, $p<0.05$). With the exception of the 10-fold increase to 1 ng/ml NT-3, each of the subsequent 10-fold concentration increases, up to 100 ng/ml NT-3, resulted in a significant increase in the branching of PVG (1 vs. 10 ng/ml, $p<0.05$; 10 vs. 100 ng/ml, $p<0.001$) and SCG neurons (1 vs. 10 ng/ml, $p<0.05$; 10 vs. 100 ng/ml, $p<0.001$). The further increase in NT-3 concentration to 1000 ng/ml only produced a further significant increase in the number of branch points in SCG neurons ($p<0.05$).

The differential efficacy of NT-3 on PVG and SCG neuron process outgrowth seemed to be largely absent at P0, particularly in the case of branch point number. A reduced effect of NT-3 on the branching of PVG neurons was

only seen at the highest concentration tested, 1000 ng/ml (Fig. 5.6B, $p<0.001$). On the other hand, PVG neurite elongation still appeared less responsive to NT-3 signalling compared to SCG neurons (Fig. 5.6A). Significant differences in the outgrowth of the two neuron types were seen at 1, 10 ($p<0.05$), and 1000 ng/ml NT-3 ($p<0.001$).

Fig. 5.6C shows the overall morphologies of sympathetic P0 PVG and SCG neurons cultured with increasing concentrations of NT-3. Sholl plots of PVG and SCG neurons overlapped when they were grown either without NT-3 or with 0.1 ng/ml NT-3. In contrast, at 1 and 10 ng/ml NT-3, PVG neurons had less intersections than SCG neurons at distances from the soma between 90 and 240 μm; such differences were consistent with reductions in the neurite length of PVG neurons compared with SCG neurons at the same NT-3 concentrations (Fig. 5.6A). Sholl plots of both SCG and PVG neurons displayed more prominent peaks beginning at 100 ng/ml NT-3, at which concentration SCG neurons exhibited a higher number of intersections closer to the cell soma. At 1000 ng/ml, the influence of NT-3 on PVG neurites was less prominent compared with SCG neurites, with PVG neurons displaying less complex neurite structures at distances between 120 and 390 μm from the cell soma.

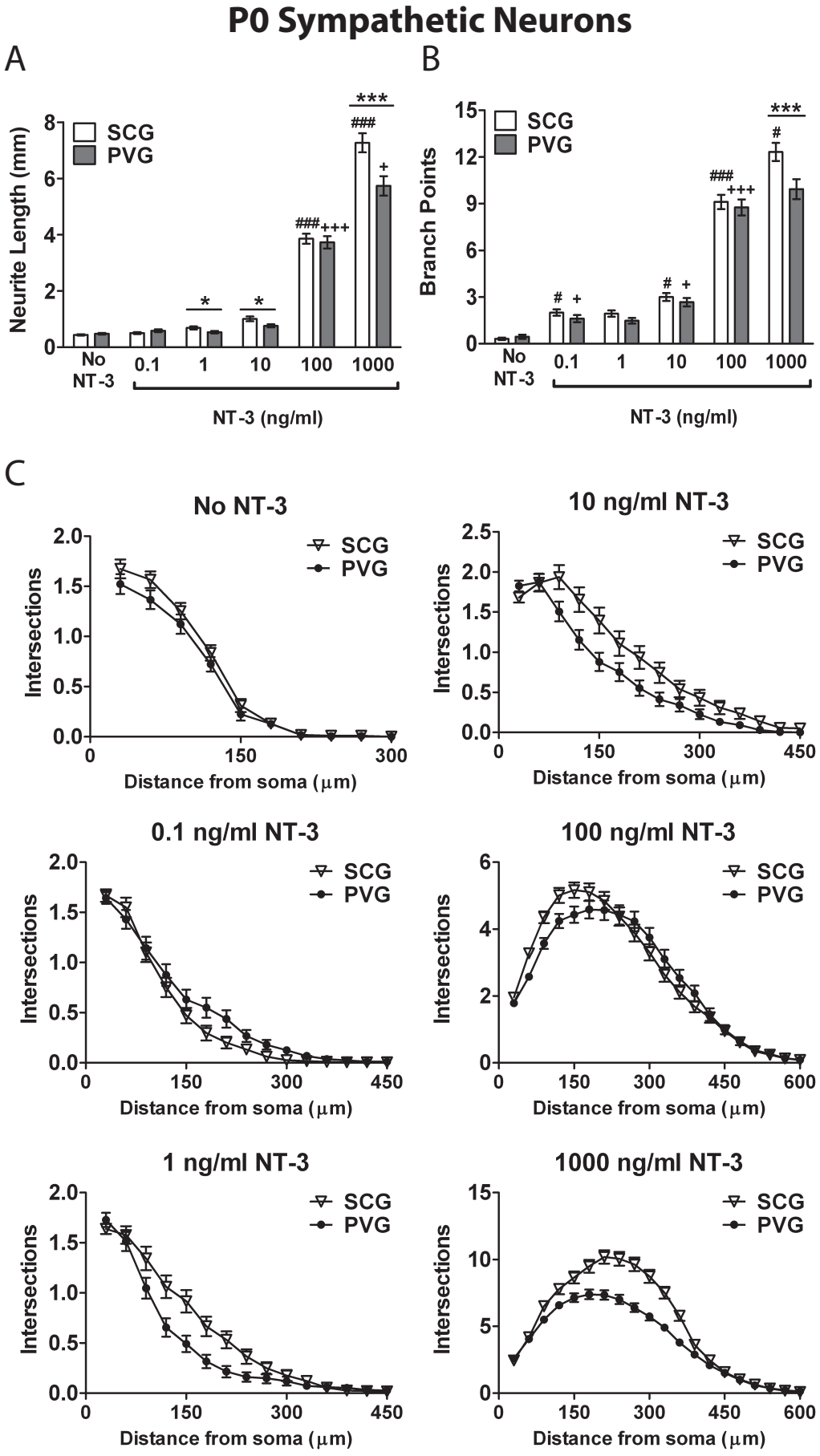

Fig. 5.6. Legend on following page.

Figure 5.6. NT-3 Concentration-Dependent Outgrowth of Po SCG and PVG Neurons. (A&B) Quantification of neurite lengths **(A)** and branch points **(B)** of Po wild-type SCG and PVG neurons cultured without NT-3 or treated with NT-3 at concentrations between 0.1 and 1000 ng/ml. Data are presented as the mean ± standard error. n=3 for each condition. * denotes significant differences between SCG and PVG neurons at each concentration point, *: $p<0.05$, ***: $p<0.001$; # denotes significant differences across 10-fold concentration increases in SCG neurons, #: $p<0.05$, ###: $p<0.001$; + denotes significant differences across 10-fold concentration increases in PVG neurons, +: $p<0.05$, +++: $p<0.001$ (Kruskal-Wallis, with Dunn's *post-hoc* analysis). **(C)** Sholl analysis of Po wild-type SCG and PVG neurons treated as described in (A). Data are presented as the mean ± standard error. n=3 for each condition. NT-3: neurotrophin-3; PVG: prevertebral ganglia (coeliac and superior mesenteric ganglia); SCG: superior cervical ganglia.

5.2.1.4 Sympathetic Neuron Process Outgrowth at P5

To characterise neurotrophic factor regulation of sympathetic neuron process outgrowth towards the end of target organ innervation, the efficacy of NGF and NT-3 in promoting neurite elongation and branching from SCG and PVG neurons was investigated at P5.

5.2.1.4.1 Effect of NGF

Fig. 5.7 illustrates how increasing NGF concentrations affect neurite length (Fig. 5.7A) and branching (Fig. 5.7B) of P5 paravertebral and prevertebral sympathetic neurons. The changes in the complexity of sympathetic neurites in response to increases in NGF concentrations are illustrated by Sholl plots (Fig. 5.7C). As at earlier ages, NGF promoted neurite elongation and branching of P5 PVG neurons less effectively than SCG neurons, particularly in the case of neurite branching.

The neurites of PVG and SCG neurons only showed significant increases in length compared to control cultures at NGF concentrations of 1 ng/ml and above (Fig. 5.7A). However, each 10-fold increase in NGF concentration between 0.1 to 10 ng/ml resulted in a significant increase in the lengths of PVG and SCG neuron neurites (0.1 vs. 1 ng/ml; 1 vs. 10 ng/ml, $p<0.001$). The effect of NGF on the length of sympathetic neuron processes reached saturation between 1 and 10 ng/ml NGF, as no significant increase was detected between the neurite lengths of sympathetic neurons incubated with 10 ng/ml NGF and those incubated with 100 ng/ml NGF.

NGF also promoted the branching of P5 SCG and PVG neuron neurites (Fig. 5.7B). Significant increases in branching compared to control cultures were seen following the addition of 1 and 0.1 ng/ml NGF to PVG and SCG neuron cultures, respectively (PVG: $p<0.001$; SCG: $p<0.05$). Significant increases in neurite branching were seen between 0.1 and 1 ng/ml NGF, and 1 and 10 ng/ml NGF ($p<0.001$) in both PVG and SCG neurons. However, increasing the concentration of NGF to 100 ng/ml did not further increase the extent of neurite branching in PVG and SCG neuron cultures compared to 10 ng/ml NGF.

Investigations into process outgrowth from P5 sympathetic neurons demonstrated that while NGF promoted neurite elongation from PVG and SCG neurons to a similar extent at lower NGF concentrations (0.01, 0.1, and 1 ng/ml), at 10 and 100 ng/ml NGF PVG neurons had significantly shorter neurite extensions than SCG neurons (Fig. 5.7A, 10 and 100 ng/ml, $p<0.001$). Conversely, in the case of neurite branch points, NGF had a reduced capacity to increase branch point number in PVG neuron neurites across a much wider NGF concentration range, with PVG neurons showing less elaborate branching than SCG neurons at each NGF concentration tested (Fig. 5.7B, 0.01 and 0.1 ng/ml, $p<0.05$; 1 ng/ml, $p<0.01$; 10 and 100 ng/ml, $p<0.001$).

Sholl profiles of sympathetic neurons incubated without NGF showed that PVG and SCG neurites had similar neurite complexities after 24 h in culture (Fig. 5.7C). However, at 0.01 and 0.1 ng/ml NGF, PVG neurons displayed differences in the number of intersections compared to SCG neurons at distances between 30 μm and 90 μm from the cell soma. Similarly, at 1 ng/ml, the complexity of PVG neuron neurites was less at distances from the soma of between 120 μm and 240 μm. At 10 and 100 ng/ml, PVG neuron neurites had clearly lower numbers of intersections compared to SCG neuron neurites at most distances from the soma.

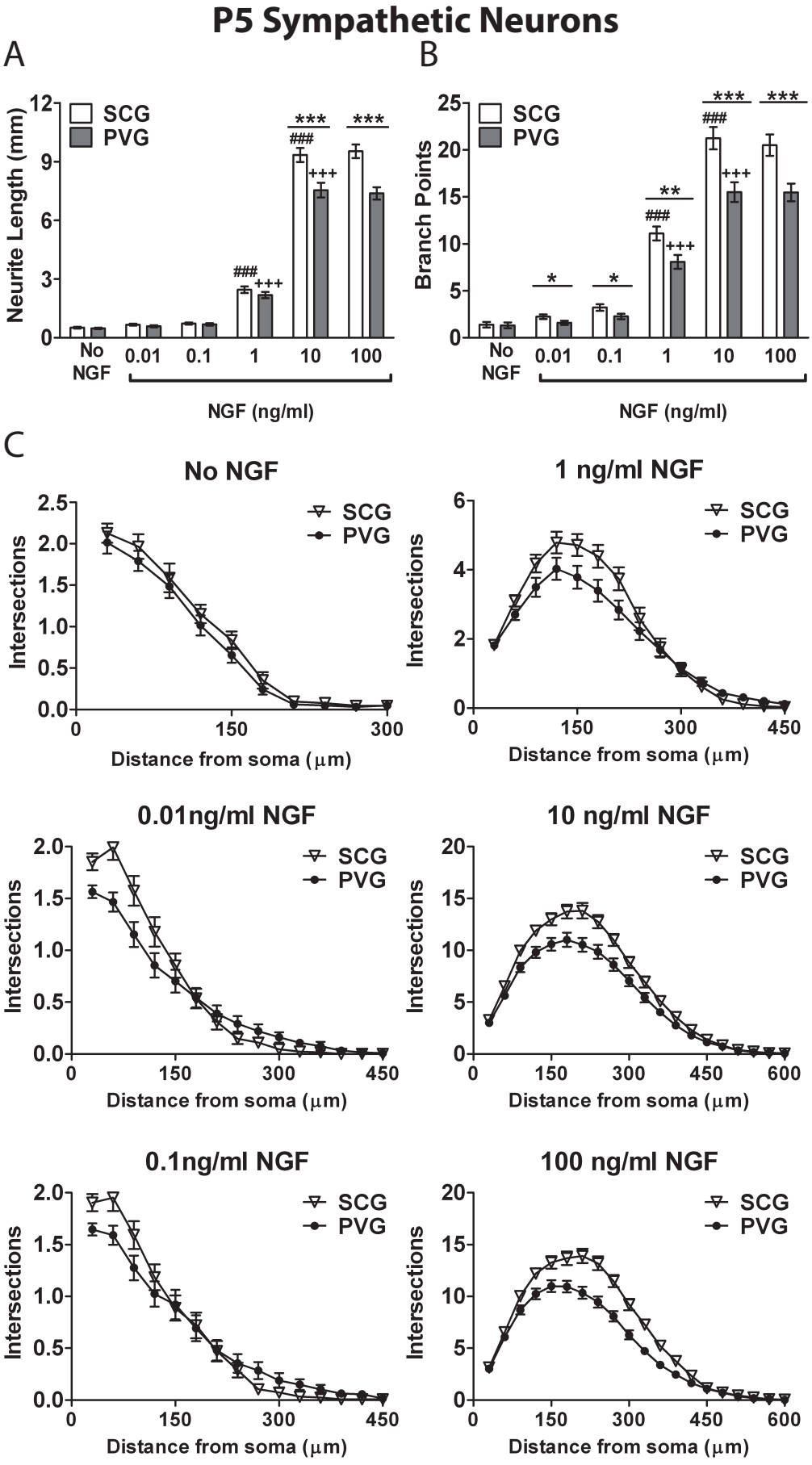

Fig. 5.7. Legend on following page.

Figure 5.7. NGF Concentration-Dependent Outgrowth of P5 SCG and PVG Neurons. (A&B) Quantification of neurite lengths **(A)** and branch points **(B)** of P5 wild-type SCG and PVG neurons cultured without NGF or treated with NGF at concentrations between 0.01 and 100 ng/ml. Data are presented as the mean ± standard error. n=3 for each condition. * denotes significant differences between SCG and PVG neurons at each concentration point, *: $p<0.05$, **: $p<0.01$, ***: $p<0.001$; # denotes significant differences across 10-fold concentration increases in SCG neurons, ###: $p<0.001$; + denotes significant differences across 10-fold concentration increases in PVG neurons, +++: $p<0.001$ (Kruskal-Wallis, with Dunn's *post-hoc* analysis). **(C)** Sholl analysis of P5 wild-type SCG and PVG neurons treated as described in (A). Data are presented as the mean ± standard error. n=3 for each condition. NGF: nerve growth factor; PVG: prevertebral ganglia (coeliac and superior mesenteric ganglia); SCG: superior cervical ganglia.

5.2.1.4.2 Effect of NT-3

Fig. 5.8 shows the effect of NT-3 on the length (Fig.5.8A) and number of branch points (Fig. 5.8B) of P5 prevertebral and paravertebral sympathetic neuron processes. Neurite complexity changes in response to different NT-3 concentrations are illustrated by Sholl plots (Fig. 5.8C). At P5, NT-3 was able to significantly increase neurite lengths, number of branch points, and total complexity of both PVG and SCG neurons. Furthermore, NT-3 had a significantly weaker effect on PVG neurons compared to SCG neurons across the whole concentration range.

The lowest concentration of NT-3 able to induce significant increases in neurite length was 10 and 0.1 ng/ml for PVG (Figure 5.8A, $p<0.01$) and SCG neurons ($p<0.05$) respectively. The only significant increases detected in neurite length over 10-fold increases in NT-3 concentration were between 10 and 100 ng/ml NT-3 ($p<0.001$ in both PVG and SCG neurons).

Fig. 5.8B shows that NT-3 promoted the branching of P5 sympathetic neuron processes. As with length analysis, PVG neurons required a higher concentration of NT-3 to induce a significant increase in branching compared to control cultures (1 ng/ml NT-3 ($p<0.05$)), compared to SCG neurons, which underwent a significant increase in branching with 0.1 ng/ml NT-3 ($p<0.001$). The only further significant increase in neurite branch point numbers seen over 10-fold increases in NT-3 concentration was between 10 and 100 ng/ml in both PVG and SCG neurons ($p<0.001$ for PVG and SCG neurons).

Strikingly, the efficacy of NT-3 in promoting increased PVG neuron process outgrowth and branching was significantly less than that for SCG neurons at every NT-3 concentration tested (Fig. 5.8A and B) (neurite length: 0.1, 10 and 1000 ng/ml NT-3, $p<0.05$; 1 and 100 ng/ml NT-3, $p<0.01$; branch points: 0.1 and 1 ng/ml NT-3, $p<0.001$; 10 and 100 ng/ml NT-3, $p<0.01$; 1000 ng/ml NT-3, $p<0.05$).

The differences seen in the extent of neurite outgrowth and branching between P5 PVG and SCG neurons in response to increasing NT-3 concentrations, is reflected in the associated Sholl plots (Fig. 5.8C). PVG and

SCG neurons showed no difference in their neurite morphology when these neurons were cultured without NT-3. However, after supplementing cultures with NT-3, PVG neurons showed less complex neurite morphologies at all NT-3 concentrations tested.

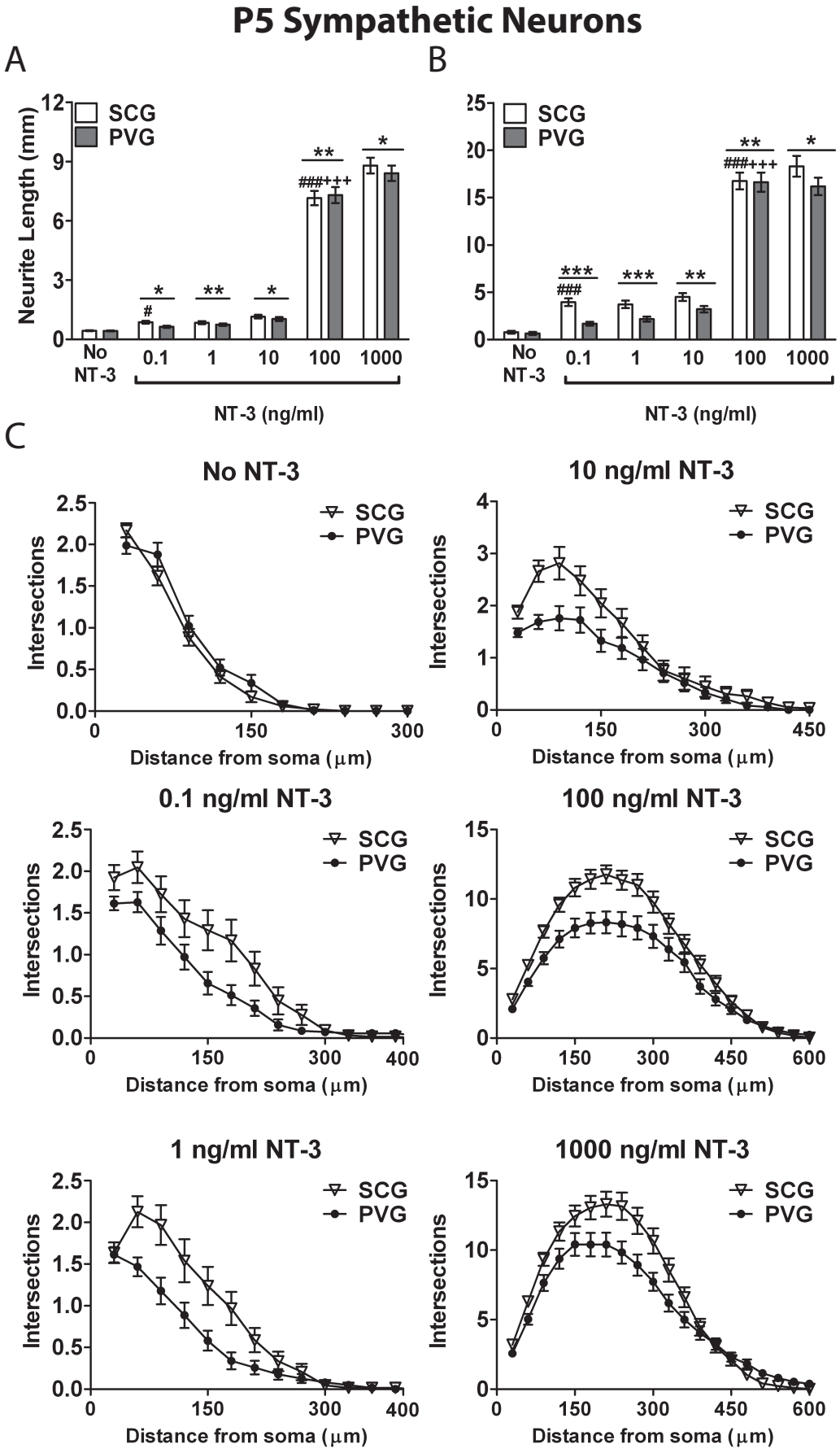

Fig. 5.8. Legend on following page.

Figure 5.8. NT-3 Concentration-Dependent Outgrowth of P5 SCG and PVG Neurons. (A&B) Quantification of neurite lengths **(A)** and branch points **(B)** of P5 wild-type SCG and PVG neurons cultured without NT-3 or treated with NT-3 at concentrations between 0.1 and 1000 ng/ml. Data are presented as the mean ± standard error. n=3 for each condition. * denotes significant differences between SCG and PVG neurons at each concentration point, *: $p<0.05$, ***: $p<0.001$; # denotes significant differences across 10-fold concentration increases in SCG neurons, #: $p<0.05$, ###: $p<0.001$; + denotes significant differences across 10-fold concentration increases in PVG neurons, +++: $p<0.001$ (Kruskal-Wallis, with Dunn's *post-hoc* analysis). **(C)** Sholl analysis of P5 wild-type SCG and PVG neurons treated as described in (A). Data are presented as the mean ± standard error. n=3 for each condition. NT-3: neurotrophin-3; PVG: prevertebral ganglia (coeliac and superior mesenteric ganglia); SCG: superior cervical ganglia.

5.2.2 Neurotrophin Regulation of Paravertebral and Prevertebral Sympathetic Neuron Survival

Aside from their role in the promotion of sympathetic neuronal outgrowth, NGF and NT-3 are primarily responsible for supporting the survival of sympathetic neurons throughout development (Glebova and Ginty 2005; Skaper 2018). Both *in vitro* and *in vivo* studies have shown that NGF and NT-3 play an irreplaceable role in the survival of SCG neurons during both embryonic stages (immediately after they become dependent on NGF at E14), and in the postnatal period (Davies 2003; Davies 2009). SCG neurons show concentration-dependent survival profiles, with their survival increasing with increasing concentrations of either NGF or NT-3 (Wyatt and Davies 1993; Belliveau et al. 1997; Horton et al. 1997; Wyatt et al. 1997; Kuruvilla et al. 2004). As the data above clearly identify significant differences between the efficacies of NGF and NT-3 in promoting process outgrowth and branching from SCG and PVG neurons, this raised the question as to whether these two sympathetic neuron populations would also differ in their response to NGF and NT-3 in the context of survival. SCG and PVG neurons were isolated from wild-type CD1 mice between ages E16 and P5. Isolated neurons were cultured in poly-ornithine/laminin-coated dishes at a density of 600-800 neurons per dish. 4 to 6 h after plating, the number of attached neurons were counted, and the mean of these counts taken as the initial number of neurons for the experiment. After 24 h and 48 h incubation, neuronal survival in the absence or presence of different concentrations of NGF or NT-3 was calculated by counting the number of surviving neurons. Results are presented as a percentage of the initial number of attached neurons. In each experiment, triplicate cultures were set-up for all conditions and each experiment was repeated three times. To determine if paravertebral and prevertebral neurons differ in their survival response to NGF and NT-3, the percentage survival of SCG and PVG neurons were ascertained at NGF concentrations between 0.01 and 100 ng/ml, and NT-3 concentrations between 0.1 and 1000 ng/ml.

Surprisingly, there were no significant differences in the percentage survival of PVG neurons compared to SCG neurons for both NGF and NT-3; this was true at all developmental ages and concentrations of NGF and NT-3 tested. The only difference emerging from these experiments was that both SCG and PVG neuron survival reached saturation at 10 ng/ml NGF at E16 (Fig. 5.9A), E18 (Fig. 5.10A), P0 (Fig. 5.11A), and P5 (Fig. 5.12A). On the other hand, at E16 (Fig. 5.9B) and P5 (Fig. 5.12B), SCG and PVG neuron survival reached saturation at the highest NT-3 concentration tested (1000 ng/ml NT-3), whereas no saturation was reached for NT-3-promoted survival at E18 (Fig. 5.10B) and P0 (Fig. 5.11B), even at 1000 ng/ml NT-3. Thus, although considerable differences were seen in neurotrophin-induced process outgrowth between paravertebral and prevertebral sympathetic neurons, no such difference was found in NGF- and NT-3-induced survival responses.

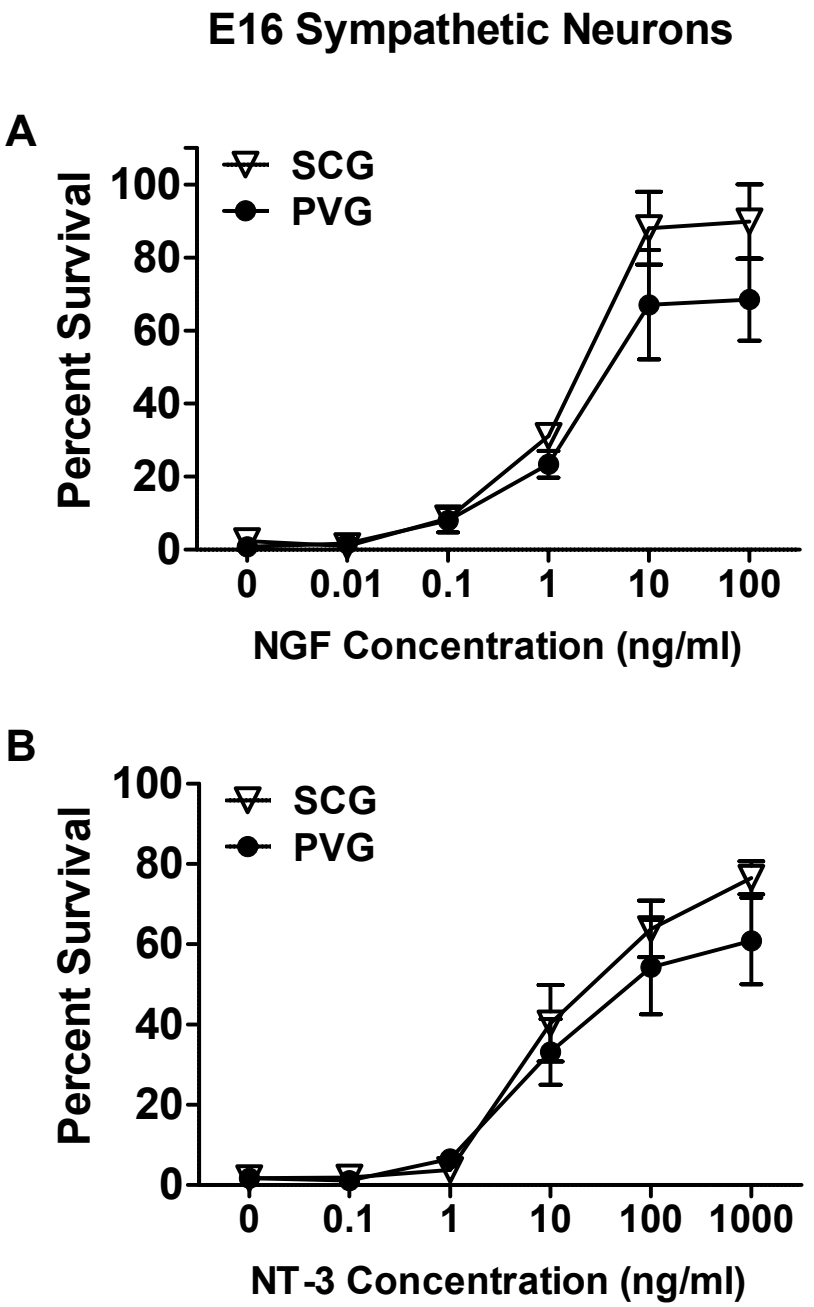

Figure 5.9. NGF- and NT-3 Concentration-Dependent Survival of E16 SCG and PVG Neurons. (A&B) Quantification of percentage neuronal survival of E16 wild-type SCG and PVG neurons cultured without NGF or with NGF at concentrations between 0.01 and 100 ng/ml **(A)**, or cultured without NT-3 or with NT-3 at concentrations between 0.1 and 1000 ng/ml **(B).** Percentage neuronal survival was calculated as the number of cells surviving at 48 h as a percentage of cells attaching to the dish on day 0 (after 4 h incubation). Data are presented as the mean ± standard error. n=3 for each condition. NGF: nerve growth factor; NT-3: neurotrophin-3; PVG: prevertebral ganglia (coeliac and superior mesenteric ganglia); SCG: superior cervical ganglia.

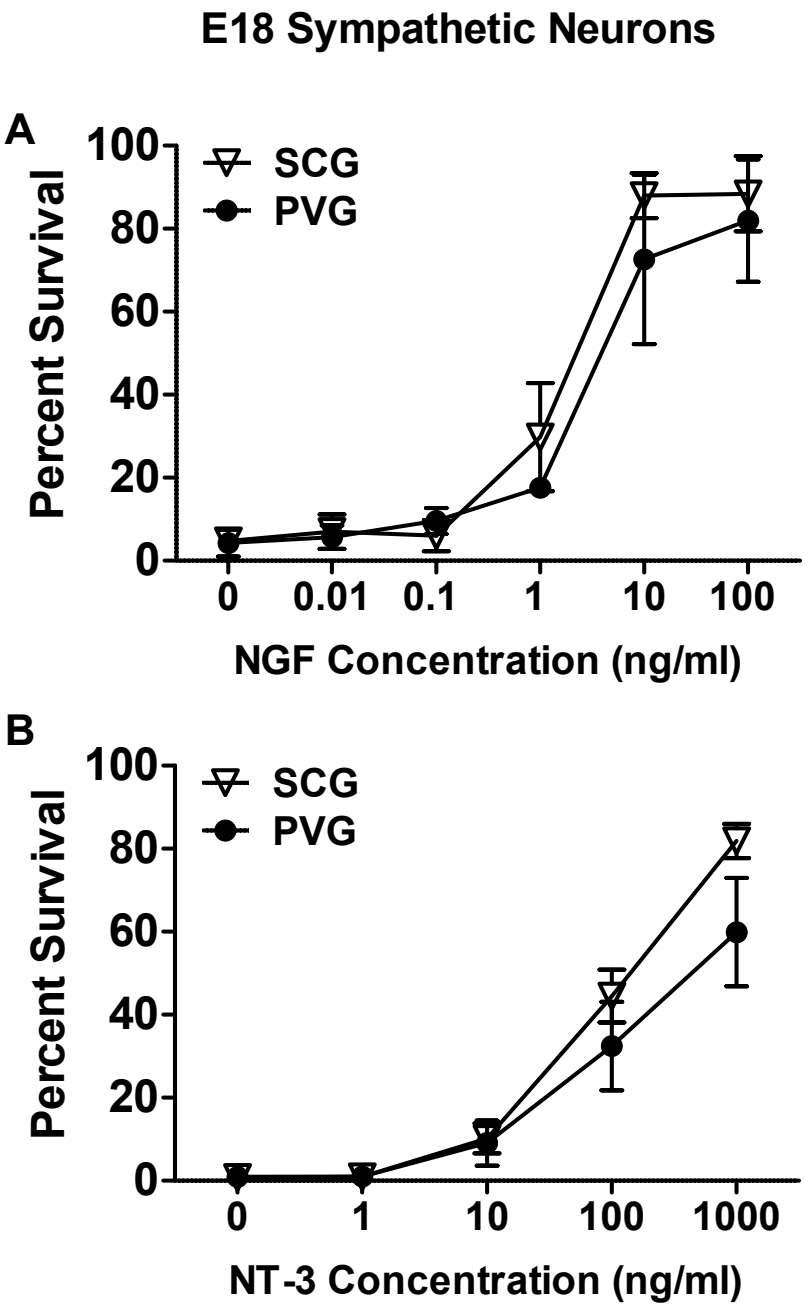

Figure 5.10. NGF- and NT-3 Concentration-Dependent Survival of E18 SCG and PVG Neurons. (A&B) Quantification of percentage neuronal survival of E18 wild-type SCG and PVG neurons cultured without NGF or with NGF at concentrations between 0.01 and 100 ng/ml **(A)**, or cultured without NT-3 or with NT-3 at concentrations between 0.1 and 1000 ng/ml **(B).** Percentage neuronal survival was calculated as the number of cells surviving at 48 h as a percentage of cells attaching to the dish on day 0 (after 4 h incubation). Data are presented as the mean ± standard error. n=3 for each condition. NGF: nerve growth factor; NT-3: neurotrophin-3; PVG: prevertebral ganglia (coeliac and superior mesenteric ganglia); SCG: superior cervical ganglia.

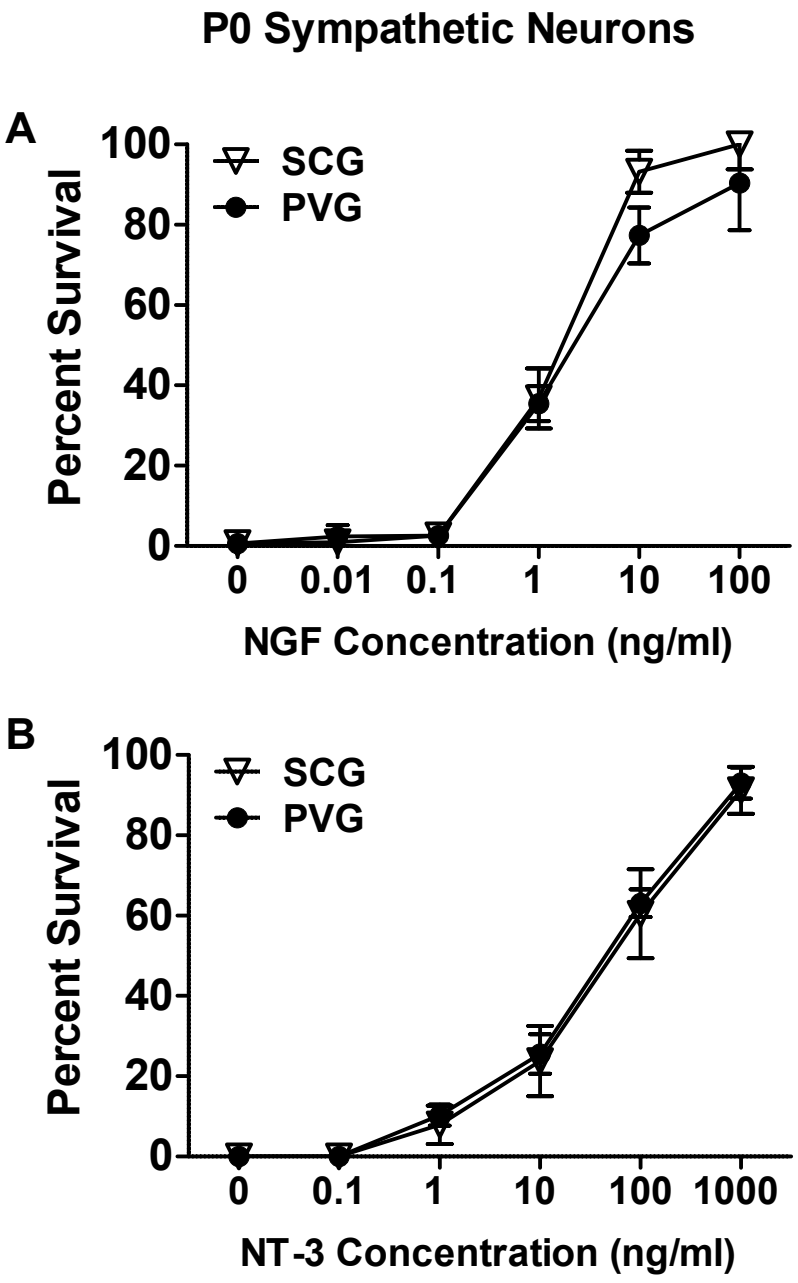

Figure 5.11. NGF- and NT-3 Concentration-Dependent Survival of Po SCG and PVG Neurons. (A&B) Quantification of percentage neuronal survival of Po wild-type SCG and PVG neurons cultured without NGF or with NGF at concentrations between 0.01 and 100 ng/ml **(A)**, or cultured without NT-3 or with NT-3 at concentrations between 0.1 and 1000 ng/ml **(B).** Percentage neuronal survival was calculated as the number of cells surviving at 48 h as a percentage of cells attaching to the dish on day 0 (after 4 h incubation). Data are presented as the mean ± standard error. n=3 for each condition. NGF: nerve growth factor; NT-3: neurotrophin-3; PVG: prevertebral ganglia (coeliac and superior mesenteric ganglia); SCG: superior cervical ganglia.

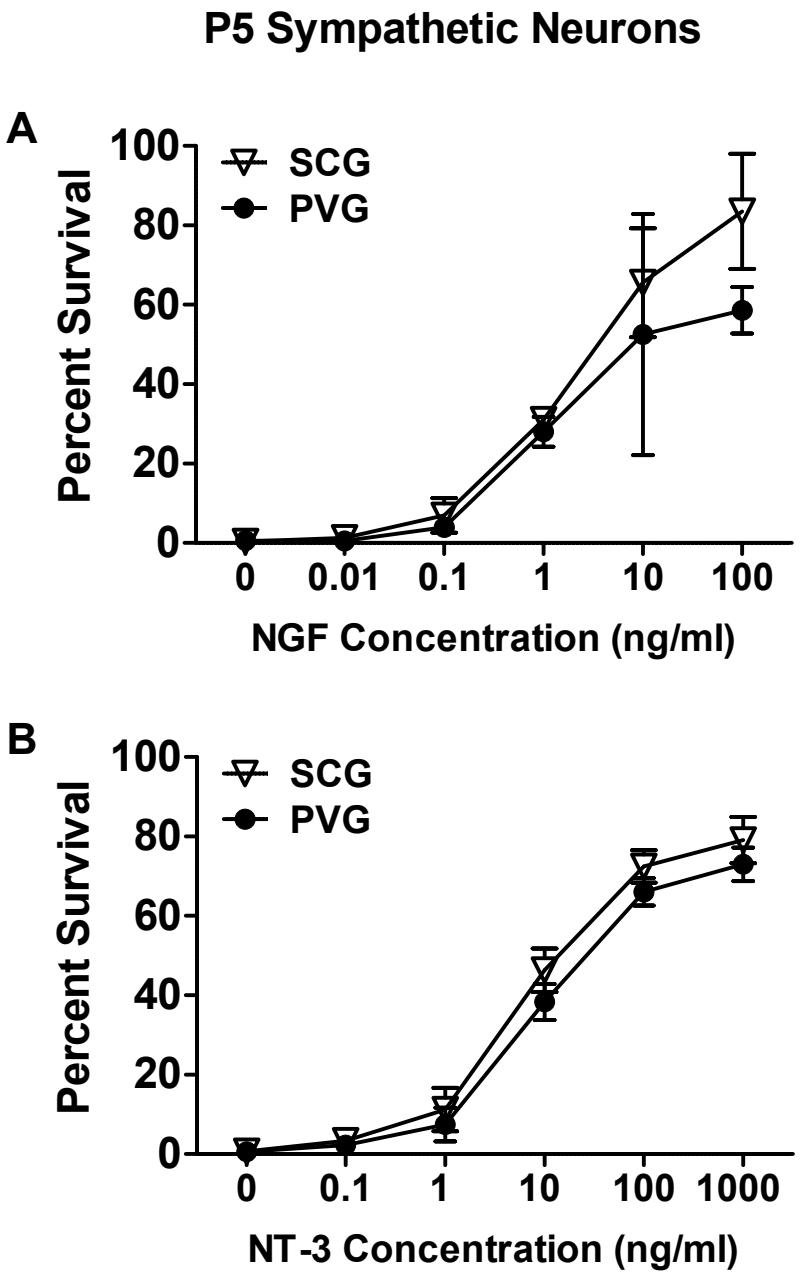

Figure 5.12. NGF- and NT-3 Concentration-Dependent Survival of P5 SCG and PVG Neurons. (A&B) Quantification of percentage neuronal survival of P5 wild-type SCG and PVG neurons cultured without NGF or with NGF at concentrations between 0.01 and 100 ng/ml **(A)**, or cultured without NT-3 or with NT-3 at concentrations between 0.1 and 1000 ng/ml **(B).** Percentage neuronal survival was calculated as the number of cells surviving at 48 h as a percentage of cells attaching to the dish on day 0 (after 4 h incubation). Data are presented as the mean ± standard error. n=3 for each condition. NGF: nerve growth factor; NT-3: neurotrophin-3; PVG: prevertebral ganglia (coeliac and superior mesenteric ganglia); SCG: superior cervical ganglia.

5.3 Discussion

Work presented in **Chapter 3** and **Chapter 4** showed that TNF and TNFR superfamily members may use different signalling mechanisms to modulate the neuronal process outgrowth of SCG and PVG neurons during development. In this chapter, the aim was to understand whether SCG and PVG neurons differ at a more fundamental level in their survival and process outgrowth responses to NGF and NT-3. The data presented in this chapter are the first detailed characterisation of the response of SCG and PVG neurons to increasing concentrations of NGF and NT-3 over a wide developmental window. The data support a number of conclusions. First, NGF and NT-3 mediate increased elongation and branching of cultured PVG neuron neurites in the developmental period between E16 and P5, as previously seen in SCG neurons. Second, PVG neurites are less sensitive to lower concentrations of exogenous NGF (0.01 and 0.1 ng/ml) and NT-3 (0.1 and 1 ng/ml) compared to SCG neurons. Third, SCG neurons have longer and more complex neurites than PVG neurons at almost every NGF and NT-3 concentration tested and at every developmental age tested. Lastly, NGF and NT-3 play similar roles in the survival of SCG and PVG neurons between the developmental ages of E16 and P5, ages when these neurons are reaching out and innervating target organs *in vivo*.

NGF and NT-3 promoted concentration-dependent increases in neurite outgrowth in sympathetic prevertebral and paravertebral neurons, between E16 and P5. The concentration-dependent regulatory role of NGF in promoting process outgrowth from cultured neonatal rat paravertebral sympathetic neurons was previously demonstrated using mid-to-high range NGF concentrations (between 10 to 200 ng/ml) at P1 (Belliveau et al. 1997). In this chapter, NGF dose response experiments on mouse SCG neurons confirm this previous report, whilst also expanding these findings to characterise the process outgrowth response at much lower NGF concentrations (0.01, 0.1 and 1 ng/ml NGF) and over a greater developmental window (E16 to P5). The current data demonstrate that NGF elicits concentration-dependent neurite outgrowth from mouse SCG neurons over large concentration and time ranges. More

importantly, the analysis of the effects of different concentrations of NGF on PVG neurons suggests that neurites from the prevertebral division respond to NGF in a similar fashion to that observed in neurites from the paravertebral division. Over the same developmental window, PVG neurite length and complexity increases with increasing NGF concentrations. Data in this chapter demonstrate that NT-3 also promotes the elongation and increased complexity of sympathetic neuron neurites in a concentration-dependent manner. Although previous research has clearly demonstrated that NT-3 induces neurite extension and elaboration in rat and mouse SCG neurons throughout development, most of these studies examined only one concentration of NT-3 (Belliveau et al. 1997; Kuruvilla et al. 2004). In this chapter, the concentration-dependent nature of both paravertebral and prevertebral neuron responses to NT-3 was clearly demonstrated. Data in this chapter allow further understanding of the regulation of neuronal process outgrowth from developing sympathetic neurons, confirming that NGF and NT-3 are key neurotrophic factors for promoting process outgrowth from paravertebral neurons throughout their development. In addition, it shows for the first time that developing prevertebral sympathetic neurons respond to NGF and NT-3 with similar concentration-dependent dynamics as previously seen in the paravertebral division.

One of the most striking observations from this chapter was that SCG neurons consistently have significantly longer and more exuberant neurites than PVG neurons at nearly every concentration of NGF tested and throughout the period between E16 and P5. One of the possible explanations is differential expression of signalling components involved in the NGF signalling pathway. NGF promotes neurite growth and arborisation of SCG neurons by activation of its cognate receptor, TrkA, and the $p75^{NTR}$ receptor (Kuruvilla et al. 2004). An increased expression of either TrkA or $p75^{NTR}$ would allow SCG neurons to respond more vigorously to NGF than their PVG neuron counterparts. Alternatively, an altered ratio of TrkA/$p75^{NTR}$ expression may underlie these changes. Use of a mutated version of NGF, only able to bind TrkA but not

$p75^{NTR}$, identified that blocking the NGF/$p75^{NTR}$ interaction negatively impacted SCG neuronal sensitivity to NGF at P4 (Horton et al. 1997). This effect was not seen at E17. The authors hypothesised that this was due to different ratios of $p75^{NTR}$ to TrkA, as $p75^{NTR}$:TrkA is 0.56 at E17, and approximately 1 at P4 (Horton et al. 1997). Similarly, postnatal sensory neurons from $p75^{NTR}$ knockout mice were 4- to 5-fold less sensitive to the effects of NGF than wild-type neurons (Davies et al. 1993). It would therefore, not be surprising if altered $p75^{NTR}$:TrkA ratios explained the reduced sensitivity of PVG neurons to NGF signalling, compared to SCG neurons, across development.

It follows that it may be possible that NGF regulates the expression of TrkA and $p75^{NTR}$ receptors and other neurite growth-related proteins with different molecular mechanisms and dynamics in SCG and PVG neurons. For example, regulation of $p75^{NTR}$ and other neurite growth-related genes show dissimilarities at transcriptional and post-transcriptional levels when compared between SCG and PC12 cells (Belliveau et al. 1997). The expression of NGF receptors is well-characterised in SCG neurons. TrkA mRNA is first detectable at E14, and its expression increases up until the postnatal period. NGF is also known to regulate $p75^{NTR}$ receptor mRNA expression in SCG neurons at E14. The proportion of neurons responding to NGF increases with increasing age; *in vivo* and *in vitro*, almost 90% of neurons respond by E18 (Wyatt and Davies 1995). To date there has been no analysis of NGF receptor mRNA or protein levels in PVG neurons, but altered expression levels, and/or regulation of expression, could explain the differential neurite outgrowth responses to NGF between the two neuron types. Alternatively, the signalling pathways downstream of activated $p75^{NTR}$ and TrkA may be different, or differentially activated, between SCG and PVG neurons. Further characterisation is still needed to determine the molecular and cellular mechanisms underlying the significantly weakened sensitivity of PVG neurons to NGF signalling, and whether this explains the altered NGF-induced outgrowth of neuronal processes seen.

Similar to NGF, PVG neurons treated with NT-3 had significantly smaller and less complex neurite structures than age-matched SCG neurons for NT-3 concentrations between 0.1-1000 ng/ml, at ages E16 through to P5. Studies using the *Ntf3* knockout mouse model identified the role of NT-3 in sympathetic neurite outgrowth *in vivo* (Belliveau et al. 1997; Kuruvilla et al. 2004). These studies found impaired SCG neurite outgrowth, and deficiencies in the density of sympathetic organ innervations when NT-3 expression was ablated. NT-3 has been shown to induce expression of growth-associated genes, and promote neurite extension, in SCG neurons by binding to TrkA, rather than its cognate receptor, TrkC (Belliveau et al. 1997). The ratio of the TrkA receptor to $p75^{NTR}$ appears to also play a key role in NT-3/TrkA signalling (Horton et al. 1997; Kuruvilla et al. 2004). For example, phosphorylation of TrkA induced by NT-3 increases when wild-type $p75^{NTR}$ expression is reduced in *in vitro* experiments with PC12 cells (Benedetti et al. 1993), or TrkA is overexpressed in PC12 cells (Hempstead et al. 1992). By contrast, in cultured SCG neurons with a higher $p75^{NTR}$/TrkA ratio the activation of TrkA by NT-3 significantly decreased (Belliveau et al. 1997). Other studies have identified that target-derived NGF supports $p75^{NTR}$ expression in SCG neurons, altering the $p75^{NTR}$:TrkA ratio in favour of $p75^{NTR}$, and consequently diminishing the ability of NT-3 to activate TrkA. This in turn, reduces the neurite outgrowth-promoting effect of NT-3 *in vivo* (Kuruvilla et al. 2004). Findings so far indicate that NGF, NT-3, TrkA and $p75^{NTR}$ are closely linked in the coordination of SCG neurite outgrowth. Therefore, the significant difference observed between the neurite outgrowth of SCG and PVG neurons in response to NT-3 may be related to the differential expression or regulation of TrkA and $p75^{NTR}$ in these neurons and/or NGF and NT-3 in the targets of these neurons.

Future experiments are required to characterise the mechanisms driving the attenuated sensitivity of PVG neurons to both NGF and NT-3. Examining the levels of TrkA/$p75^{NTR}$ mRNA and protein expression in SCG and PVG neurons (across the developmental window) will help understand if there is a significant difference in both the total expression of these receptors between

the two neurons types, and in the ratio of TrkA to $p75^{NTR}$. In addition, analysis of the expression levels of NGF/NT-3 in the target fields of SCG and PVG neurons, and the timing of this expression, would help identify the physiological relevance of the altered sensitivity of paravertebral and prevertebral neurons to target organ-secreted neurotrophins. Moreover, characterising the efficacy of TrkA and $p75^{NTR}$ coupling to downstream signalling targets (i.e. TrkA phosphorylation and $p75^{NTR}$ recruitment of TRAF proteins) may provide a further avenue to understand the differential responses to NGF and NT-3. *In vivo* findings suggest that the cognate TrkC receptor has no detectable role in the development of SCG neurons after E15.5 (Fariñas et al. 1994; Fagan et al. 1996). However, the possible role of TrkC in the development of prevertebral neurons has yet to be investigated, and could provide an alternative explanation for the findings in this chapter. These experiments will clarify the exact molecular mechanisms driving the difference in the efficacy of neurotrophin-promoted neuronal process outgrowth from SCG and PVG neurons, and may even shed further light into the interactions between NGF, NT-3, TrkA and $p75^{NTR}$ that promote correct sympathetic neuron target field innervation *in vivo*.

Another striking finding in this chapter was that NGF and NT-3 could promote the survival of PVG neurons to the same extent as age-matched SCG neurons over the developmental window tested. Previously, the concentration-dependent NGF- and NT-3- promoted survival of SCG neurons was illustrated over 0.001 to 10 ng/ml NGF, and 0.08 to 250 ng/ml NT-3, in mice between E15 to E19 (Davies et al. 1993). Results from this chapter are in agreement with previous findings, and show that even at higher concentrations (100 ng/ml NGF and 1000 ng/ml NT-3) paravertebral neurons still show concentration-dependent responses towards these neurotrophins.

Data from this chapter clearly show that NGF and NT-3 can both support the survival of developing PVG neurons in culture. Surprisingly, PVG neurons showed very similar concentration-dependent survival in response to both neurotrophins compared to that seen in SCG neurons, showing no significant difference in survival percentages at tested concentrations points within all ages

tested. This is interesting given that NGF and NT-3 have been shown to promote SCG neuron survival via the same receptors, TrkA and $p75^{NTR}$, that mediate neurotrophin-promoted neurite outgrowth from sympathetic neurons (Wyatt and Davies 1993; Ernfors et al. 1994; Fariñas et al. 1994; Davies et al. 1995; Wyatt and Davies 1995; Fagan et al. 1996; Belliveau et al. 1997; Francis et al. 1999; Davies 2000; Kuruvilla et al. 2004). Whereas these neurotrophin/receptor interactions lead to a significant difference between the extent of neurite outgrowth from SCG and PVG neurons, the same ligand/receptor coupling on the same neurons does not result in any significant differences in survival between the two neuron types. Kuruvilla *et al*. suggested that NGF/NT-3-mediated neuronal survival and neurite outgrowth may be functioning at distinct neuronal sites. Using compartmentalised cultures, they postulated that NT-3 is not able to support the survival of SCG neurons *in vivo*, as, unlike NGF, the NT-3 survival signal cannot be retrogradely transported from axon terminals in distal targets to SCG neuron soma (Kuruvilla et al. 2004). In contrast, local NT-3 signalling can promote growth and branching at axon terminals. Use of microfluidics chambers will help identify if the involvement of spatially distinct sites of neurotrophin/receptor interaction can explain the altered sensitivity of PVG neurons to NGF and NT-3 in terms of process outgrowth and survival. Results to date suggest that neurite outgrowth and survival of paravertebral sympathetic neurons may be regulated by different downstream effector proteins and signalling mechanisms (Glebova and Ginty 2005). Thus, it may be informative to carry out more detailed studies to discover the signalling mechanisms underlying neurite outgrowth and neuronal survival in prevertebral sympathetic neurons.

In summary, this chapter has focused on comparing the roles of NGF and NT-3 in promoting neuronal process outgrowth from, and survival of, prevertebral and paravertebral sympathetic neurons. Data have demonstrated that NGF and NT-3 promote neurite outgrowth from, and survival of, prevertebral sympathetic neurons, in a similar manner to SCG neurons between the ages of E16 and P5. However, PVG neurons are less sensitive to NGF and NT-

3 in terms of neurite outgrowth compared with SCG neurons. PVG neurons had significantly shorter and less complex neurite structures at almost every concentration point tested compared with SCG neurons. Further investigations examining the expression levels of NGF and NT-3 in target fields, and their relevant receptors, TrkA and $p75^{NTR}$ in neurons, are needed to understand the molecular mechanisms underlying the observed differences between SCG and PVG neurons. Survival analyses of sympathetic neurons identified that PVG neuron survival is supported by NGF and NT-3 within the same developmental period as these neurotrophins support the survival of SCG neurons. Surprisingly however, the survival rates of PVG neurons showed no significant differences compared to SCG neurons in response to NGF and NT-3. This is intriguing, as in the regulation of both neurite outgrowth and survival NGF and NT-3 act through TrkA and $p75^{NTR}$ receptors, yet the sensitivity differences seen in neurite outgrowth are not seen in neuronal survival. Further research is required to identify the specific signalling mechanisms underlying this difference.

Chapter 6

GENERAL DISCUSSION

This thesis aimed to identify whether findings established so far in the paravertebral division of the sympathetic nervous system (SNS) can also be seen in the prevertebral nervous system, the other half of the SNS. Identification of the similarities and differences between these two divisions is important for two main reasons. Firstly, as the majority of research into the development of the SNS has been conducted using SCG neurons of the paravertebral division (which have been well-characterised and are relatively easy to access (Kisiswa et al. 2013)), it is critical to understand if the mechanisms established in the paravertebral system are universal to the SNS. If this is the case, future research looking to understand the development of the SNS can continue to focus primarily on the paravertebral division, using SCG neurons as the model cell type of sympathetic neurons. Secondly, if the signalling mechanisms in prevertebral neurons diverge from the paravertebral division, there is great research potential in identifying and understanding the reasons for such differences, as this could significantly advance our understanding of SNS development. Notably, in this thesis several similarities and significant differences were identified in the development of paravertebral and prevertebral neurons. These differences were found not only in the neurite growth regulatory effects of the TNF superfamily, but also in the more fundamental responses to members of the neurotrophin family, NGF and NT-3.

The role of the TNF superfamily in the development of the nervous system has been well-established (O'Keeffe et al. 2008; Gutierrez et al. 2013; Kisiswa et al. 2013; McWilliams et al. 2015; Kisiswa et al. 2017; Howard et al. 2018; Howard et al. 2019; Carriba et al. 2020; Carriba and Davies 2020; Horton and Davies 2020). Several members of the family, and their receptors, have been recently shown to modulate neuronal process outgrowth in the developing central and peripheral nervous system (McWilliams et al. 2015; Carriba and Davies 2017; Howard et al. 2019; Carriba et al. 2020; Carriba and Davies 2020). In the SNS, multiple TNF superfamily members have been shown to regulate neurite outgrowth from paravertebral SCG neurons, and the innervation of their target organs. This regulation can either be positive – promoting outgrowth and

complexity of neurites (e.g. CD40 (McWilliams et al. 2015), GITRL (O'Keeffe et al. 2008), and TNF-α reverse signalling (Kisiswa et al. 2013)) – or negative – inhibiting outgrowth and reducing the ramification of neuron processes into target fields (e.g. TNF-α (Nolan et al. 2014) and RANKL (Gutierrez et al. 2013)). Importantly, the ability of TNF family members to modulate neuronal process outgrowth from paravertebral sympathetic neurons is restricted to the developmental period when sympathetic neurons are reaching out to, and ramifying within, their target organs.

Working in the same developmental window (between E16 and P5), this thesis has demonstrated for the first time that these signalling molecules can play a different role in the coeliac and superior mesenteric ganglia (CG and SMG) of the prevertebral division of the SNS, as to that established previously in SCG neurons. Several key findings emerged from the data within **Chapters 3**, **4** and **5** of this thesis. TNF-α reverse signalling, previously shown to enhance the innervation of target organs by paravertebral sympathetic neurons (Kisiswa et al. 2013), was instead ineffective in regulating the innervation of prevertebral sympathetic neuron target organs *in vivo* (with a single exception in the spleen, where ablation of *Tnfrsf1a* increased innervation) (**Chapter 3**). *In vitro* findings demonstrated similar disparities, with TNF-α reverse signalling increasing process outgrowth from SCG but not PVG neurons. **Chapter 4** describes similar findings in the context of CD40 and its ligand CD40L, although the differences in the response of the two divisions were more dramatic, as CD40L-mediated reverse signalling stimulated process outgrowth from SCG neurons, but had the opposite effect, inhibiting process outgrowth, from PVG neurons. These *in vitro* findings were consistent with *in vivo* findings, in which CD40 signalling was shown to enhance innervation of paravertebral sympathetic neuron target organs, and attenuate innervation in organs targeted by prevertebral sympathetic neurons. In addition, **Chapter 5** demonstrated that PVG neurons were less responsive to NGF and NT-3 than their SCG counterparts in terms of neurite outgrowth and neuronal complexity. Surprisingly, these neurotrophic

factors did not show any significant differential effect in neurotrophin-mediated neuronal survival between SCG and PVG neurons.

Significant differences identified in the response of SCG and PVG neurons to extracellular TNF superfamily proteins and neurotrophins occurred despite their highly shared lineage. This raises the possibility that these differences instead derived from the nature of the target fields that these neurons innervate, which provide neurotrophic support to developing sympathetic neurons. These findings add further clarity to previous research into SNS development. Although there are only limited previous *in vitro* studies using prevertebral neurons, several differences between the two SNS divisions have been reported. This includes differences in their intrinsic electrophysiological properties (demonstrated in guinea-pigs (Cassell et al. 1986) and cats (Szurszewski 1981)), extent of innervation (Szurszewski 1981), and neuropeptide content (Elfvin et al. 1993). There have also been previous indications that the separate divisions of the SNS differentially respond to factors regulating neuronal outgrowth and survival. A study from the 1960s revealed that whereas injection of anti-NGF serum into newborn rats causes the loss of 90-95% of neurons from the paravertebral ganglia, a substantial subset of prevertebral neurons are resistant to the adverse effects of anti-NGF (Zaimis et al. 1965). Later findings also supported initial discoveries, showing that in neonatal rats treated with daily anti-NGF serum, CG, SMG and splanchnic ganglia target organs were less affected by NGF removal than paravertebral targets when organ innervation was investigated at 4 and 8 weeks of age (Hill et al. 1985). Studies using knockout mice also confirmed previous results. In a study by Glebova *et al.* knockout embryonic and neonatal mice lacking both *Ngf* and *Bax* expression displayed diminished sympathetic innervation of both paravertebral and prevertebral target fields compared to mice lacking *Bax* expression alone, but this occurred to a much greater extent in paravertebral neuron target fields (Glebova 2004). For example, whereas the sympathetic innervation of SCG targets, such as the eye and the salivary gland, were completely lacking in both embryonic and perinatal mice, in prevertebral

neuron targets (such as the stomach, spleen, and kidneys) there were deficiencies in sympathetic innervation, but not a complete absence. Furthermore, whilst the reduction in innervation encompassed the entire length of paravertebral neurons, only the terminal branches of prevertebral neurons were affected in these animals (Glebova 2004).

Given these findings, several suggestions were put forward to explain the reduced NGF-dependency of PVG neurons. The most considered notion was put forward based on a previous hypothesis by Dixon and McKinnon *et al.* (Dixon and McKinnon 1994), who postulated that prevertebral ganglia targets produce a neurotrophic factor(s), in addition to NGF, and the neurons themselves would express proteins to allow them to respond to such cues. In this paper, they were able to demonstrate that while CG and SMG ganglia express both full length (kinase domain-containing) and truncated (kinase domain-deficient) TrkB receptors, SCGs only express soluble truncated TrkB (Dixon and McKinnon 1994). As only the full length version of the receptor is able to mediate the complete downstream effects of BDNF and NT-4, this suggests that PVG neurons have a distinct advantage over SCG neurons in terms of being able to respond to these neurotrophins. Supporting the idea that PVG neurons have access to further neurotrophins, NT-4 and NT-3 mRNA expression has been identified in the rat stomach (Hohn et al. 1990; Berkemeier et al. 1991), a target organ for PVG neurons. *In vitro* analysis in **Chapter 5** also supported this, demonstrating that PVG neurons were responsive to NT-3, at least in the restricted developmental window tested.

However, it is now known that both SCG and PVG neurons have access to neurotrophins in addition to NGF, such as NT-3, during their development (Glebova and Ginty 2005). As such, this 'second neurotrophin' notion is unlikely to be the only explanation for the difference between SCGs and PVGs. Studies so far demonstrated that both NGF and NT-3 act through TrkA to promote neuron survival and neurite outgrowth (Kuruvilla et al. 2004). However, NT-3 may act through TrkB, instead of or in addition to TrkA, in PVG neurons. It would be highly interesting to clarify whether this expression of full length TrkB

on PVG neurons can explain the reduced responsiveness of PVG neurons to NGF and NT-3 signalling in the context of neurite outgrowth. It is possible that the expression of full length TrkB on PVG, but not SCG, neurons, downregulates the efficacy of both NT-3 and NGF signalling through TrkA. In addition, it is important to consider the role of $p75^{NTR}$ (for detailed discussion see **Chapter 5**) in NGF and NT-3 mediated neurite outgrowth and target field innervation. Any new model attempting to explain the diminished responsiveness of PVG neurons to NGF and NT-3 compared to SCG neurons should thus consider NGF, NT-3, TrkA, TrkB and $p75^{NTR}$. In addition, the activation of downstream signalling elements could also potentially explain the differences between the response of SCG and PVG neurons to neurotrophins. ERK1/2, PI3-kinase, JNK and Akt are some of the known downstream signalling pathways of Trk receptors (see Fig. 1.7), and their activation upon neurotrophin binding was previously demonstrated in SCG neurons (Crowder and Freeman 1998; Anderson and Tolkovsky 1999; Vizard et al. 2015). Therefore, investigation of these potential signalling pathways in PVG neurons will help understand the diminished responsiveness of PVG neurons.

Differences between PVG and SCG neurons have been described in both their response to TNF superfamily signalling (**Chapters 3 & 4**), and neurotrophin-mediated signalling (**Chapter 5**). These could be due to different expression levels and distributions of receptor and/or ligand in each signalling pathway as discussed in **Chapter 3** in detail. It could also be due to the signalling components downstream of TNF and CD40L and whether they are expressed in SCG or PVG neurons (see **Section 4.3** in **Chapter 4** for a more detailed discussion of the downstream signalling cascades activated by CD40L). Alternatively, if the TNF superfamily and neurotrophin signalling pathways were intertwined, changes in just one of these receptor/ligand pairs could contribute to all of the differences between the two divisions of the SNS described in this thesis. This latter hypothesis becomes more attractive given a very recent study from the Deppmann lab (Kuhn et al. 2020). This laboratory identified a novel interaction between TNF superfamily members and

neurotrophin signalling in the development of SCG neurons. $p75^{NTR}$ is able to mediate forward signalling upon binding of neurotrophins (Kuhn et al. 2020). Similar to TNF-α promoted TNFR1-mediated forward signalling, $p75^{NTR}$-mediated forward signalling is also able to suppress axon growth and branch arborisation, however in this case it is dependent on the presence of membrane TNFR1. The two receptors were found to both co-localise and physically interact (forming heterotrimers), and in the absence of TNFR1, $p75^{NTR}$ activation (in this case by BDNF) was not able to suppress axonal outgrowth (Kuhn et al. 2020).

The localisation of TNFR1 expression is different between SCG and PVG neurons; both neuron types expressed the receptor in the cell soma, but only in PVG neurons was it also found on neurites (**Chapter 3**). One of the most important points identified in Kuhn *et al*. found that $p75^{NTR}$ forward signalling and TNFR1-promoted TNF-α-reverse signalling are functionally antagonistic (Kuhn et al. 2020). Therefore, a lack of TNFR1 expression in the terminal branches of SCG neurons would prevent not only the inhibitory role of TNFR1-mediated forward signalling in neurite outgrowth, but would prevent the newly defined antagonistic activity of $p75^{NTR}$ signalling on the neurite-promoting effect of TNF-α-reverse signalling. In addition to its recently defined role in neurite growth through the interaction with TNFR1 in SCG neurons, it should be also be considered that $p75^{NTR}$ has the capacity to bind to pro-neurotrophins, as well as mature neurotrophins (Meeker and Williams 2015). Howard *et al*. demonstrated that pro-NGF promotes the growth of SCG neurons through a $p75^{NTR}$-dependent mechanism (Howard et al. 2013); therefore, it would not be surprising if pro-neurotrophins have, at least a partial, role in the marked differences observed between SCG and PVG neurons through either $p75^{NTR}$ or TNFR1 receptors, or via the newly identified interaction between these two receptors.

In addition to the Kuhn *et al.* findings, future research should also consider whether other interactions exist between receptors of the TNF superfamily. Both $p75^{NTR}$ and TNFR1 are members of the TNF receptor superfamily; it would be intriguing therefore to investigate whether similar

relationships exist between other receptor pairs, either in the forward or reverse signalling context. In this thesis, both TNFR1 and CD40 were implicated in the regulation of neurite process outgrowth of sympathetic neurons. Use of knockout mouse models in which both TNFR1 and CD40 were ablated would identify whether these proteins have any dependencies on each other in regulating neurite outgrowth from sympathetic neurons, and would identify any possible interactions between these receptors during their signalling.

These physiological differences in the development of prevertebral and paravertebral neurons are mirrored in selective vulnerabilities to pathological conditions. One such condition is sympathetic neuronal axonal dystrophy occurring during diabetes. Prevertebral neurons show a markedly increased vulnerability to diabetes-related neuropathies, with increased susceptibility to degenerative changes compared to SCG neurons (Schmidt and Plurad 1986). Furthermore, whilst NGF can function as a protective factor in SCG neurons undergoing *in vitro* hypoglycaemia conditions, this protective activity is absent in PVG neurons (Semra et al. 2009). A better understanding of the signalling mechanism regulating neuronal growth and complexity in paravertebral and prevertebral neurons may help explain the selective vulnerability of sympathetic neuron subpopulations, and open new research avenues for their treatment and prevention.

In conclusion, data in this thesis clearly demonstrated that paravertebral and prevertebral sympathetic neurons show evident differences in response to factors affecting outgrowth and complexity of sympathetic neuron processes. Therefore, it is important to bring prevertebral neurons into focus in future research related to the development of the SNS. This would help discern the complex interactions between the many players that regulate SNS development. In addition, as seen in this thesis, these players may have unique roles in the two divisions of the SNS. Inclusion of both PVG and SCG neurons in future research will clarify the different downstream signalling mechanisms inducible by factors involved in SNS development, and help identify the different molecular pathways leading to these outcomes.

References

Adrain, C. et al. 2012. Tumor Necrosis Factor Signaling Requires iRhom2 to Promote Trafficking and Activation of TACE. *Science* 335(6065), pp. 225–228. doi: 10.1126/science.1214400.

Aggarwal, B.B. et al. 1985. Human tumor necrosis factor. Production, purification, and characterization. *The Journal of Biological Chemistry* 260(4), pp. 2345–54.

Aggarwal, B.B. 2003. Signalling pathways of the TNF superfamily: A double-edged sword. *Nature Reviews Immunology* 3(9), pp. 745–756. doi: 10.1038/nri1184.

Aggarwal, B.B. et al. 2012. Historical perspectives on tumor necrosis factor and its superfamily: 25 years later, a golden journey. *Blood* 119(3), pp. 651–665. doi: 10.1182/blood-2011-04-325225.

Aird, W.C. 2007. Phenotypic Heterogeneity of the Endothelium. *Circulation Research* 100(2), pp. 158–173. doi: 10.1161/01.RES.0000255691.76142.4a.

Albers, T.M. et al. 1994. Overexpression of nerve growth factor in epidermis of transgenic mice causes hypertrophy of the peripheral nervous system. *Journal of Neuroscience* 14(3 II), pp. 1422–1432. doi: 10.1523/jneurosci.14-03-01422.1994.

Anderson, C.N.G. and Tolkovsky, A.M. 1999. A Role for MAPK/ERK in Sympathetic Neuron Survival: Protection against a p53-Dependent, JNK-Independent Induction of Apoptosis by Cytosine Arabinoside. *The Journal of Neuroscience* 19(2), pp. 664–673. doi: 10.1523/JNEUROSCI.19-02-00664.1999.

Ang, S.-L. and Behringer, R.R. 2002. Anterior-Posterior Patterning of the Mouse Body Axis at Gastrulation. In: *Mouse Development*. Elsevier, pp. 37–53. doi: 10.1016/B978-012597951-1/50005-6.

Angeletti, P.U. and Levi-Montalcini, R. 1971. Growth regulation of the sympathetic nervous system: immunosympathectomy and chemical sympathectomy. *European Journal of Clinical and Biological Research* 16(9), pp.

866–74.

Antoniades, C. et al. 2009. The CD40/CD40 Ligand System. *Journal of the American College of Cardiology* 54(8), pp. 669–677. doi: 10.1016/j.jacc.2009.03.076.

Armitage, R.J. et al. 1992. Molecular and biological characterization of a murine ligand for CD40. *Nature* 357(6373), pp. 80–82. doi: 10.1038/357080a0.

Armstrong, A. et al. 2011. Frizzled3 Is Required for Neurogenesis and Target Innervation during Sympathetic Nervous System Development. *Journal of Neuroscience* 31(7), pp. 2371–2381. doi: 10.1523/JNEUROSCI.4243-10.2011.

Arumäe, U. et al. 1993. Neurotrophins and their receptors in rat peripheral trigeminal system during maxillary nerve growth. *Journal of Cell Biology* 122(5), pp. 1053–1065. doi: 10.1083/jcb.122.5.1053.

Ashkenazi, A. 1998. Death Receptors: Signaling and Modulation. *Science* 281(5381), pp. 1305–1308. doi: 10.1126/science.281.5381.1305.

Ba, H. et al. 2017. Transmembrane tumor necrosis factor-α promotes the recruitment of MDSCs to tumor tissue by upregulating CXCR4 expression via TNFR2. *International Immunopharmacology* 44, pp. 143–152. doi: 10.1016/j.intimp.2016.12.028.

Banchereau, J. et al. 1994. The CD40 Antigen and its Ligand. *Annual Review of Immunology* 12(1), pp. 881–926. doi: 10.1146/annurev.iy.12.040194.004313.

Banchereau, J. et al. 1995. Functional CD40 antigen on B cells, dendritic cells and fibroblasts. *Advances in Experimental Medicine and Biology* 378, pp. 79–83. doi: 10.1007/978-1-4615-1971-3_16.

Barde, Y.A. et al. 1978. New factor released by cultured glioma cells supporting survival and growth of sensory neurones. *Nature* 274(5673), pp. 818–818. doi: 10.1038/274818a0.

Barde, Y.A. et al. 1982. Purification of a new neurotrophic factor from mammalian brain. *The EMBO Journal* 1(5), pp. 549–53.

Barker, V. et al. 2001. TNFα contributes to the death of NGF-dependent neurons during development. *Nature Neuroscience* 4(12), pp. 1194–1198. doi: 10.1038/nn755.

Barral, J.-P. and Croibier, A. 2009. Autonomic nervous system. In: *Manual Therapy for the Cranial Nerves*. Elsevier, pp. 255–264. doi: 10.1016/B978-0-7020-3100-7.50034-3.

Bashaw, G.J. and Klein, R. 2010. Signaling from Axon Guidance Receptors. *Cold Spring Harbor Perspectives in Biology* 2(5), pp. a001941–a001941. doi: 10.1101/cshperspect.a001941.

Bellinger, D.L. et al. 1989. Origin of noradrenergic innervation of the spleen in rats. *Brain, Behavior, and Immunity* 3(4), pp. 291–311. doi: 10.1016/0889-1591(89)90029-9.

Belliveau, D.J. et al. 1997. NGF and Neurotrophin-3 Both Activate TrkA on Sympathetic Neurons but Differentially Regulate Survival and Neuritogenesis. *Journal of Cell Biology* 136(2), pp. 375–388. doi: 10.1083/jcb.136.2.375.

Benedetti, M. et al. 1993. Differential expression of nerve growth factor receptors leads to altered binding affinity and neurotrophin responsiveness. *Proceedings of the National Academy of Sciences* 90(16), pp. 7859–7863. doi: 10.1073/pnas.90.16.7859.

Bennett, M.. et al. 2002. Neuronal cell death, nerve growth factor and neurotrophic models: 50 years on. *Autonomic Neuroscience* 95(1–2), pp. 1–23. doi: 10.1016/S1566-0702(01)00358-7.

Berkemeier, L.R. et al. 1991. Neurotrophin-5: A novel neurotrophic factor that activates trk and trkB. *Neuron* 7(5), pp. 857–866. doi: 10.1016/0896-6273(91)90287-A.

Bibel, M. and Barde, Y.A. 2000. Neurotrophins: Key regulators of cell fate and cell shape in the vertebrate nervous system. *Genes and Development* 14(23), pp. 2919–2937. doi: 10.1101/gad.841400.

Bishop, G.A. et al. 2007. TRAF proteins in CD40 signaling. *Advances in Experimental Medicine and Biology* 597, pp. 131–151. doi: 10.1007/978-0-387-70630-6_11.

Black, R.A. 2002. Tumor necrosis factor-α converting enzyme. *The International Journal of Biochemistry & Cell Biology* 34(1), pp. 1–5. doi: 10.1016/S1357-2725(01)00097-8.

Bodmer, D. et al. 2009. Wnt5a Mediates Nerve Growth Factor-Dependent Axonal Branching and Growth in Developing Sympathetic Neurons. *Journal of Neuroscience* 29(23), pp. 7569–7581. doi: 10.1523/JNEUROSCI.1445-09.2009.

Boyd, H.D. et al. 1996. Three electrophysiological classes of guinea pig sympathetic postganglionic neurone have distinct morphologies. *The Journal of Comparative Neurology* 369(3), pp. 372–387. doi: 10.1002/(SICI)1096-9861(19960603)369:3<372::AID-CNE4>3.0.CO;2-2.

Bradley, J. 2008. TNF-mediated inflammatory disease. *The Journal of Pathology* 214(2), pp. 149–160. doi: 10.1002/path.2287.

Brennan, F.M. et al. 2002. Evidence that rheumatoid arthritis synovial T cells are similar to cytokine-activated T cells: Involvement of phosphatidylinositol 3-kinase and nuclear factor κB pathways in tumor necrosis factor α production in rheumatoid arthritis. *Arthritis and Rheumatism* 46(1), pp. 31–41. doi: 10.1002/1529-0131(200201)46:1<31::AID-ART10029>3.0.CO;2-5.

Brenner, B. et al. 1997a. Evidence for a novel function of the CD40 ligand as a signalling molecule in T-lymphocytes. *FEBS Letters* 417(3), pp. 301–306. doi: 10.1016/S0014-5793(97)01306-9.

Brenner, B. et al. 1997b. The CD40 Ligand Directly Activates T-Lymphocytes via Tyrosine Phosphorylation Dependent PKC Activation. *Biochemical and Biophysical Research Communications* 239(1), pp. 11–17. doi: 10.1006/bbrc.1997.7415.

Brenner, S. 2000. GENOMICS:The End of the Beginning. *Science*

287(5461), pp. 2173–2174. doi: 10.1126/science.287.5461.2173.

Browning, K.N. and Travagli, R.A. 2014. Central Nervous System Control of Gastrointestinal Motility and Secretion and Modulation of Gastrointestinal Functions. In: *Comprehensive Physiology*. Hoboken, NJ, USA: John Wiley & Sons, Inc., pp. 1339–1368. doi: 10.1002/cphy.c130055.

Brumovsky, P.R. et al. 2012. Dorsal root ganglion neurons innervating pelvic organs in the mouse express tyrosine hydroxylase. *Neuroscience* 223, pp. 77–91. doi: 10.1016/j.neuroscience.2012.07.043.

Buchman, V.L. and Davies, A.M. 1993. Different neurotrophins are expressed and act in a developmental sequence to promote the survival of embryonic sensory neurons. *Development* 118(3), pp. 989–1001.

Butte, M.J. et al. 1998. Crystal Structure of Neurotrophin-3 Homodimer Shows Distinct Regions Are Used To Bind Its Receptors. *Biochemistry* 37(48), pp. 16846–16852. doi: 10.1021/bi9812540.

Butte, M.J. 2001. Neurotrophic factor structures reveal clues to evolution, binding, specificity, and receptor activation. *Cellular and Molecular Life Sciences* 58(8), pp. 1003–1013. doi: 10.1007/PL00000915.

Calhan, O.Y. et al. 2019. CD40L reverse signaling suppresses prevertebral sympathetic axon growth and tissue innervation. *Developmental Neurobiology* 79(11–12), pp. 949–962. doi: 10.1002/dneu.22735.

Campenot, R.B. 1994. NGF and the local control of nerve terminal growth. *Journal of Neurobiology* 25(6), pp. 599–611. doi: 10.1002/neu.480250603.

Carbone, E. et al. 1997. A New Mechanism of NK Cell Cytotoxicity Activation: The CD40–CD40 Ligand Interaction. *The Journal of Experimental Medicine* 185(12), pp. 2053–2060. doi: 10.1084/jem.185.12.2053.

Carriba, P. et al. 2020. CD40L Reverse Signaling Influences Dendrite Spine Morphology and Expression of PSD-95 and Rho Small GTPases. *Frontiers in Cell and Developmental Biology* 8. doi: 10.3389/fcell.2020.00254.

Carriba, P. and Davies, A.M. 2017. CD40 is a major regulator of dendrite

growth from developing excitatory and inhibitory neurons. *eLife* 6. doi: 10.7554/eLife.30442.

Carriba, P. and Davies, A.M. 2020. How CD40L reverse signaling regulates axon and dendrite growth. *Cellular and Molecular Life Sciences : CMLS* . doi: 10.1007/s00018-020-03563-2.

Cassell, J.F. et al. 1986. Characteristics of phasic and tonic sympathetic ganglion cells of the guinea-pig. *The Journal of Physiology* 372(1), pp. 457–483. doi: 10.1113/jphysiol.1986.sp016020.

Causing, C.G. et al. 1997. Synaptic Innervation Density Is Regulated by Neuron-Derived BDNF. *Neuron* 18(2), pp. 257–267. doi: 10.1016/S0896-6273(00)80266-4.

Chan, F.K. et al. 2000. A Domain in TNF Receptors That Mediates Ligand-Independent Receptor Assembly and Signaling. *Science* 288(5475), pp. 2351–2354. doi: 10.1126/science.288.5475.2351.

Cheng, G. et al. 1995. Involvement of CRAF1, a relative of TRAF, in CD40 signaling. *Science* 267(5203), pp. 1494–1498. doi: 10.1126/science.7533327.

Chevendra, V. and Weaver, L.C. 1991. Distribution of splenic, mesenteric and renal neurons in sympathetic ganglia in rats. *Journal of the Autonomic Nervous System* 33(1), pp. 47–53. doi: 10.1016/0165-1838(91)90017-W.

Chuntharapai, A. et al. 2001. Isotype-Dependent Inhibition of Tumor Growth In Vivo by Monoclonal Antibodies to Death Receptor 4. *The Journal of Immunology* 166(8), pp. 4891–4898. doi: 10.4049/jimmunol.166.8.4891.

Clary, D.O. and Reichardt, L.F. 1994. An alternatively spliced form of the nerve growth factor receptor TrkA confers an enhanced response to neurotrophin 3. *Proceedings of the National Academy of Sciences* 91(23), pp. 11133–11137. doi: 10.1073/pnas.91.23.11133.

Colgan, L.A. et al. 2018. PKCα integrates spatiotemporally distinct Ca2+ and autocrine BDNF signaling to facilitate synaptic plasticity. *Nature Neuroscience* 21(8), pp. 1027–1037. doi: 10.1038/s41593-018-0184-3.

Contin, C. et al. 2003. Membrane-anchored CD40 Is Processed by the Tumor Necrosis Factor-α-converting Enzyme. *Journal of Biological Chemistry* 278(35), pp. 32801–32809. doi: 10.1074/jbc.M209993200.

Cory, S. and Adams, J.M. 2002. The BCL2 family: Regulators of the cellular life-or-death switch. *Nature Reviews Cancer* 2(9), pp. 647–656. doi: 10.1038/nrc883.

Cottin, V. et al. 1999. Phosphorylation of Tumor Necrosis Factor Receptor CD120a (p55) by p42 mapk/erk2 Induces Changes in Its Subcellular Localization. *Journal of Biological Chemistry* 274(46), pp. 32975–32987. doi: 10.1074/jbc.274.46.32975.

Cowan, W.M. 2001. Viktor Hamburger and Rita Levi-Montalcini: The path to the discovery of nerve growth factor. *Annual Review of Neuroscience* 24(1), pp. 551–600. doi: 10.1146/annurev.neuro.24.1.551.

Crane, J.F. and Trainor, P.A. 2006. Neural Crest Stem and Progenitor Cells. *Annual Review of Cell and Developmental Biology* 22(1), pp. 267–286. doi: 10.1146/annurev.cellbio.22.010305.103814.

Crowder, R.J. and Freeman, R.S. 1998. Phosphatidylinositol 3-kinase and Akt protein kinase are necessary and sufficient for the survival of nerve growth factor-dependent sympathetic neurons. *Journal of Neuroscience* 18(8), pp. 2933–2943. doi: 10.1523/jneurosci.18-08-02933.1998.

Crowley, C. et al. 1994. Mice lacking nerve growth factor display perinatal loss of sensory and sympathetic neurons yet develop basal forebrain cholinergic neurons. *Cell* 76(6), pp. 1001–1011. doi: 10.1016/0092-8674(94)90378-6.

Davies, A.M. et al. 1986. Different factors from the central nervous system and periphery regulate the survival of sensory neurones. *Nature* 319, p. 497.

Davies, A.M. 1986. The survival and growth of embryonic proprioceptive neurons is promoted by a factor present in skeletal muscle. *Developmental Biology* 115(1), pp. 56–67. doi: https://doi.org/10.1016/0012-1606(86)90227-7.

Davies, A.M. et al. 1987. Timing and site of nerve growth factor synthesis in developing skin in relation to innervation and expression of the receptor. *Nature* 326(6111), pp. 353–358. doi: 10.1038/326353a0.

Davies, A.M. et al. 1993. p75-Deficient trigeminal sensory neurons have an altered response to NGF but not to other neurotrophins. *Neuron* 11(4), pp. 565–574. doi: 10.1016/0896-6273(93)90069-4.

Davies, A.M. 1994. Neurotrophic Factors: Switching neurotrophin dependence. *Current Biology* 4(3), pp. 273–276. doi: 10.1016/S0960-9822(00)00064-6.

Davies, A.M. 1995. Cranial sensory neurons. In: James, C. and Wilkin, G. P. eds. *Neural cell culture: A Practical Approach*. New York: Oxford University Press, pp. 153–176.

Davies, A.M. et al. 1995. Developmental changes in NT3 signalling via TrkA and TrkB in embryonic neurons. *EMBO Journal* 14(18), pp. 4482–4489. doi: 10.1002/j.1460-2075.1995.tb00127.x.

Davies, A.M. 1996. The neurotrophic hypothesis: where does it stand? *Philosophical Transactions: Biological Sciences* 351(1338), pp. 389 LP – 394.

Davies, A.M. 2000. Neurotrophins: Neurotrophic modulation of neurite growth. *Current Biology* 10(5), pp. 198–200. doi: 10.1016/S0960-9822(00)00351-1.

Davies, A.M. 2003. New EMBO Member's Review: Regulation of neuronal survival and death by extracellular signals during development. *The EMBO Journal* 22(11), pp. 2537–2545. doi: 10.1093/emboj/cdg254.

Davies, A.M. 2008. Neurotrophins giveth and they taketh away. *Nature Neuroscience* 11(6), pp. 627–628. doi: 10.1038/nn0608-627.

Davies, A.M. 2009. Extracellular signals regulating sympathetic neuron survival and target innervation during development. *Autonomic Neuroscience* 151(1), pp. 39–45. doi: 10.1016/j.autneu.2009.07.011.

Dechant, G. and Neumann, H. 2013. The Trk family of neurotrophins transmembrane receptors. In: *Madame Curie Bioscience Database [Internet]*.

Austin (TX): Landes Bioscience

Deckwerth, T.L. et al. 1996. BAX is required for neuronal death after trophic factor deprivation and during development. *Neuron* 17(3), pp. 401–411. doi: 10.1016/S0896-6273(00)80173-7.

Deinhardt, K. and Chao, M. V. 2010. Neurotrophin Signaling in Development. In: *Handbook of Cell Signaling*. Elsevier, pp. 1913–1917. doi: 10.1016/B978-0-12-374145-5.00234-5.

Deinhardt, K. and Chao, M. V. 2014. Trk receptors. *Handbook of Experimental Pharmacology* 220, pp. 103–119. doi: 10.1007/978-3-642-45106-5_5.

Deshmukh, M. and Johnson, E.M. 1997. Programmed cell death in neurons: Focus on the pathway of nerve growth factor deprivation-induced death of sympathetic neurons. *Molecular Pharmacology* 51(6), pp. 897–906. doi: 10.1124/mol.51.6.897.

Deuchars, S.A. and Lall, V.K. 2015. Sympathetic preganglionic neurons: Properties and inputs. *Comprehensive Physiology* 5(2), pp. 829–869. doi: 10.1002/cphy.c140020.

DiCicco-Bloom, E. et al. 1993. NT-3 stimulates sympathetic neuroblast proliferation by promoting precursor survival. *Neuron* 11(6), pp. 1101–1111. doi: 10.1016/0896-6273(93)90223-E.

Dickson, B.J. 2002. Molecular Mechanisms of Axon Guidance. *Science* 298(5600), pp. 1959 LP – 1964.

Dixon, J.E. and McKinnon, D. 1994. Expression of the trk gene family of neurotrophin receptors in prevertebral sympathetic ganglia. *Developmental Brain Research* 77(2), pp. 177–182. doi: 10.1016/0165-3806(94)90194-5.

Domonkos, A. et al. 2001. Receptor-like properties of the 26 kDa transmembrane form of TNF. *European cytokine network* 12(3), pp. 411–9.

Dostert, C. et al. 2019. The TNF Family of Ligands and Receptors: Communication Modules in the Immune System and Beyond. *Physiological Reviews* 99(1), pp. 115–160. doi: 10.1152/physrev.00045.2017.

Downs, K.M. 2009. The enigmatic primitive streak: prevailing notions and challenges concerning the body axis of mammals. *BioEssays : News and Reviews in Molecular, Cellular and Developmental Biology* 31(8), pp. 892–902. doi: 10.1002/bies.200900038.

Eissner, G. et al. 2000. Reverse Signaling Through Transmembrane TNF Confers Resistance to Lipopolysaccharide in Human Monocytes and Macrophages. *The Journal of Immunology* 164(12), pp. 6193–6198. doi: 10.4049/jimmunol.164.12.6193.

Eissner, G. et al. 2004. Ligands working as receptors: Reverse signaling by members of the TNF superfamily enhance the plasticity of the immune system. *Cytokine and Growth Factor Reviews* 15(5), pp. 353–366. doi: 10.1016/j.cytogfr.2004.03.011.

Elfvin, L.-G.G. et al. 1993. The chemical neuroanatomy of sympathetic ganglia. *Annual Review of Neuroscience* 16(1), pp. 471–507. doi: 10.1146/annurev.ne.16.030193.002351.

Elgueta, R. et al. 2009. Molecular mechanism and function of CD40/CD40L engagement in the immune system. *Immunological Reviews* 229(1), pp. 152–172. doi: 10.1111/j.1600-065X.2009.00782.x.

Elmore, S. 2007. Apoptosis: A Review of Programmed Cell Death. *Toxicologic Pathology* 35(4), pp. 495–516. doi: 10.1080/01926230701320337.

Elshamy, W.M. et al. 1996. Prenatal and postnatal requirements of NT-3 for sympathetic neuroblast survival and innervation of specific targets. *Development* 122(2), pp. 491–500.

Emanuilov, A.I. et al. 2018. Sympathetic Innervation of Stomach in Postnatal Development. *Doklady Biological Sciences* 483(1), pp. 219–221. doi: 10.1134/S0012496618060017.

Enari, M. et al. 1998. A caspase-activated DNase that degrades DNA during apoptosis, and its inhibitor ICAD. *Nature* 391, p. 43. doi: 10.0.4.14/34112.

Enomoto, H. et al. 2001. RET signaling is essential for migration, axonal

growth and axon guidance of developing sympathetic neurons. *Development* 128(20), pp. 3963–3974.

Erice, C. et al. 2019. Regional Differences in the Contributions of TNF Reverse and Forward Signaling to the Establishment of Sympathetic Innervation. *Developmental Neurobiology* 79(4), pp. 317–334. doi: 10.1002/dneu.22680.

Ernfors, P. et al. 1990. Molecular cloning and neurotrophic activities of a protein with structural similarities to nerve growth factor: Developmental and topographical expression in the brain. *Proceedings of the National Academy of Sciences of the United States of America* 87(14), pp. 5454–5458. doi: 10.1073/pnas.87.14.5454.

Ernfors, P. et al. 1992. Cells Expressing mRNA for Neurotrophins and their Receptors During Embryonic Rat Development. *European Journal of Neuroscience* 4(11), pp. 1140–1158. doi: 10.1111/j.1460-9568.1992.tb00141.x.

Ernfors, P. et al. 1994. Lack of neurotrophin-3 leads to deficiencies in the peripheral nervous system and loss of limb proprioceptive afferents. *Cell* 77(4), pp. 503–512. doi: 10.1016/0092-8674(94)90213-5.

Fagan, A.M. et al. 1996. TrkA, But Not TrkC, Receptors Are Essential for Survival of Sympathetic Neurons In Vivo. *The Journal of Neuroscience* 16(19), pp. 6208–6218. doi: 10.1523/JNEUROSCI.16-19-06208.1996.

Falvo, J. V et al. 2010. Transcriptional control of the TNF Gene. *Current Directions in Autoimmunity* 11(table 1), pp. 27–60. doi: 10.1159/000289196.

Fariñas, I. et al. 1994. Severe sensory and sympathetic deficits in mice lacking neurotrophin-3. *Nature* 369(6482), pp. 658–661. doi: 10.1038/369658a0.

Faustman, D. and Davis, M. 2010. TNF receptor 2 pathway: Drug target for autoimmune diseases. *Nature Reviews Drug Discovery* 9(6), pp. 482–493. doi: 10.1038/nrd3030.

Feinberg, B. et al. 1988. A phase I trial of intravenously-administered recombinant tumor necrosis factor-alpha in cancer patients. *Journal of Clinical*

Oncology 6(8), pp. 1328–1334. doi: 10.1200/JCO.1988.6.8.1328.

Feldman, B. 2015. Taking the Middle Road: Vertebrate Mesoderm Formation and the Blastula-Gastrula Transition. In: *Principles of Developmental Genetics: Second Edition*., pp. 203–236. doi: 10.1016/B978-0-12-405945-0.00012-0.

Fenner, B.M. 2012. Truncated TrkB: Beyond a dominant negative receptor. *Cytokine & Growth Factor Reviews* 23(1–2), pp. 15–24. doi: 10.1016/j.cytogfr.2012.01.002.

Ferran, C. et al. 1994. Anti-tumor necrosis factor modulates anti-CD3-triggered T cell cytokine gene expression in vivo. *Journal of Clinical Investigation* 93(5), pp. 2189–2196. doi: 10.1172/JCI117215.

Fischer, R. et al. 2011. Ligand-induced internalization of TNF receptor 2 mediated by a di-leucin motif is dispensable for activation of the NFκB pathway. *Cellular Signalling* 23(1), pp. 161–170. doi: 10.1016/j.cellsig.2010.08.016.

Francis, N. et al. 1999. NT-3, like NGF, is required for survival of sympathetic neurons, but not their precursors. *Developmental Biology* 210(2), pp. 411–427. doi: 10.1006/dbio.1999.9269.

Fries, K.M. et al. 1995. CD40 Expression by human fibroblasts. *Clinical Immunology and Immunopathology* 77(1), pp. 42–51. doi: 10.1016/0090-1229(95)90135-3.

Furness, J.B. 2015. Peripheral Autonomic Nervous System. In: *The Rat Nervous System*. Elsevier, pp. 61–76. doi: 10.1016/B978-0-12-374245-2.00004-8.

Gallo, G. and Letourneau, P.C. 1998. Localized sources of neurotrophins initiate axon collateral sprouting. *The Journal of Neuroscience* 18(14), pp. 5403–5414.

Gammill, L.S. and Bronner-Fraser, M. 2003. Neural crest specification: Migrating into genomics. *Nature Reviews Neuroscience* 4(10), pp. 795–805. doi: 10.1038/nrn1219.

Gattone, V.H. et al. 1986. Extrinsic innervation of the rat kidney: a retrograde tracing study. *American Journal of Physiology-Renal Physiology*

250(2), pp. F189–F196. doi: 10.1152/ajprenal.1986.250.2.F189.

Gavalda, N. et al. 2009. Developmental Regulation of Sensory Neurite Growth by the Tumor Necrosis Factor Superfamily Member LIGHT. *Journal of Neuroscience* 29(6), pp. 1599–1607. doi: 10.1523/JNEUROSCI.3566-08.2009.

Gendron, R.L. et al. 1991. Expression of Tumor Necrosis Factor Alpha in the Developing Nervous System. *International Journal of Neuroscience* 60(1), pp. 129–136. doi: 10.3109/00207459109082043.

Gilbert, S. 2000. The Neural Crest. In: *Developmental Biology*. 6th ed. Sunderland: Sinauer Associates

Gilbey, M.P. and Michael Spyer, K. 1993. Essential organization of the sympathetic nervous system. *Baillière's Clinical Endocrinology and Metabolism* 7(2), pp. 259–278. doi: 10.1016/S0950-351X(05)80177-6.

Gillespie, L.N. 2003. Regulation of axonal growth and guidance by the neurotrophin family of neurotrophic factors. *Clinical and Experimental Pharmacology and Physiology* 30(10), pp. 724–733. doi: 10.1046/j.1440-1681.2003.03909.x.

Glebova, N.O. 2004. Heterogeneous Requirement of NGF for Sympathetic Target Innervation In Vivo. *Journal of Neuroscience* 24(3), pp. 743–751. doi: 10.1523/JNEUROSCI.4523-03.2004.

Glebova, N.O. and Ginty, D.D. 2005. Growth and Survival Signals Controlling Sympathetic Nervous System Development. *Annual Review of Neuroscience* 28(1), pp. 191–222. doi: 10.1146/annurev.neuro.28.061604.135659.

Graf, D. et al. 1995. A soluble form of TRAP (CD40 ligand) is rapidly released after T cell activation. *European Journal of Immunology* 25(6), pp. 1749–1754. doi: 10.1002/eji.1830250639.

Graham, J.P. et al. 2009. Roles of the TRAF2/3 binding site in differential B cell signaling by CD40 and its viral oncogenic mimic, LMP1. *Journal of immunology* 183(5), pp. 2966–73. doi: 10.4049/jimmunol.0900442.

Green, D.R. and Reed, J.C. 1998. Mitochondria and apoptosis. (Cover

story). *Science* 281(5381), p. 1309.

Greene, L.A. 1977. Quantitative in vitro studies on the nerve growth factor (NGF) requirement of neurons. *Developmental Biology* 58(1), pp. 96–105. doi: 10.1016/0012-1606(77)90076-8.

Grell, M. et al. 1994. TNF receptors TR60 and TR80 can mediate apoptosis via induction of distinct signal pathways. *The Journal of Immunology* 153(5), pp. 1963 LP – 1972.

Grell, M. et al. 1995. The transmembrane form of tumor necrosis factor is the prime activating ligand of the 80 kDa tumor necrosis factor receptor. *Cell* 83(5), pp. 793–802. doi: 10.1016/0092-8674(95)90192-2.

Grell, M. et al. 1998. The type 1 receptor (CD120a) is the high-affinity receptor for soluble tumor necrosis factor. *Proceedings of the National Academy of Sciences* 95(2), pp. 570–575. doi: 10.1073/pnas.95.2.570.

Grivennikov, S.I. et al. 2006. Intracellular Signals and Events Activated by Cytokines of the Tumor Necrosis Factor Superfamily: From Simple Paradigms to Complex Mechanisms. *International Review of Cytology* 252(06), pp. 129–161. doi: 10.1016/S0074-7696(06)52002-9.

Gross, A. et al. 1999. BCL-2 family members and the mitochondria in apoptosis BCL-2 family members and the mitochondria in apoptosis. *Genes & Development* 13, pp. 1899-1911Gross, A., Mcdonnell, J. M., Korsmeyer,. doi: 10.1101/gad.13.15.1899.

Gruss, H.J. and Dower, S.K. 1995. Tumor necrosis factor ligand superfamily: involvement in the pathology of malignant lymphomas. *Blood* 85(12), pp. 3378 LP – 3404.

Gundersen, R.W. and Barrett, J.N. 1980. Characterization of the turning response of dorsal root neurites toward nerve growth factor. *Journal of Cell Biology* 87(3), pp. 546–554. doi: 10.1083/jcb.87.3.546.

Gutierrez, H. et al. 2008. Nuclear Factor B Signaling Either Stimulates or Inhibits Neurite Growth Depending on the Phosphorylation Status of p65/RelA.

Journal of Neuroscience 28(33), pp. 8246–8256. doi: 10.1523/JNEUROSCI.1941-08.2008.

Gutierrez, H. et al. 2013. Regulation of neurite growth by tumour necrosis superfamily member RANKL. *Open Biology* 3(1), pp. 120150–120150. doi: 10.1098/rsob.120150.

Gutierrez, H. and Davies, A.M. 2007. A fast and accurate procedure for deriving the Sholl profile in quantitative studies of neuronal morphology. 163, pp. 24–30. doi: 10.1016/j.jneumeth.2007.02.002.

Gwyn, D.G. et al. 1985. Observations on the afferent and efferent organization of the vagus nerve and the innervation of the stomach in the squirrel monkey. *The Journal of Comparative Neurology* 239(2), pp. 163–175. doi: 10.1002/cne.902390204.

Hallbook, F. et al. 1995. Neurotrophins and their receptors in chicken neuronal development. *The International journal of developmental biology* 39(5), pp. 855–68.

Hallböök, F. et al. 1991. Evolutionary studies of the nerve growth factor family reveal a novel member abundantly expressed in xenopus ovary. *Neuron* 6(5), pp. 845–858. doi: https://doi.org/10.1016/0896-6273(91)90180-8.

Hedger, J.H. and Webber, R.H. 1976. Anatomical study of the cervical sympathetic trunk and ganglia in the albino rat (Mus norvegicus albinus). *Cells Tissues Organs* 96(2), pp. 206–217. doi: 10.1159/000144674.

Hempstead, B.L. et al. 1992. Overexpression of the trk tyrosine kinase rapidly accelerates nerve growth factor-induced differentiation. *Neuron* 9(5), pp. 883–896. doi: 10.1016/0896-6273(92)90241-5.

Henn, V. et al. 1998. CD40 ligand on activated platelets triggers an inflammatory reaction of endothelial cells. *Nature* 391(6667), pp. 591–594. doi: 10.1038/35393.

Higuchi, M. and Aggarwal, B.B. 1994. TNF induces internalization of the p60 receptor and shedding of the p80 receptor. *Journal of Immunology* 152(7),

pp. 3550–8.

Hill, C.E. et al. 1985. Subpopulations of sympathetic neurones differ in their sensitivity to nerve growth factor antiserum. *Developmental Brain Research* 23(1), pp. 121–130. doi: 10.1016/0165-3806(85)90011-2.

Hillis, J. et al. 2016. Neurotrophins and B-cell malignancies. *Cellular and molecular life sciences : CMLS* 73(1), pp. 41–56. doi: 10.1007/s00018-015-2046-4.

Hohn, A. et al. 1990. Identification and characterization of a novel member of the nerve growth factor/brain-derived neurotrophic factor family. *Nature* 344(6264), p. 339. doi: 10.1038/344339a0.

Honma, Y. et al. 2002. Artemin Is a Vascular-Derived Neurotropic Factor for Developing Sympathetic Neurons. *Neuron* 35(2), pp. 267–282. doi: 10.1016/S0896-6273(02)00774-2.

Horiuchi, T. et al. 2010. Transmembrane TNF-α: Structure, function and interaction with anti-TNF agents. *Rheumatology* 49(7), pp. 1215–1228. doi: 10.1093/rheumatology/keq031.

Horton, A. et al. 1997. NGF Binding to p75 Enhances the Sensitivity of Sensory and Sympathetic Neurons to NGF at Different Stages of Development. *Molecular and Cellular Neuroscience* 10(3–4), pp. 162–172. doi: 10.1006/mcne.1997.0650.

Horton, A.R. and Davies, A.M. 2020. Initial axon growth rate from embryonic sensory neurons is correlated with birth date. *Developmental Neurobiology* 80(3–4), pp. 126–131. doi: 10.1002/dneu.22743.

Hou, H. et al. 2008. Modulation of neuronal differentiation by CD40 isoforms. *Biochemical and Biophysical Research Communications* 369(2), pp. 641–647. doi: 10.1016/j.bbrc.2008.02.094.

Howard, L. et al. 2013. ProNGF promotes neurite growth from a subset of NGF-dependent neurons by a p75NTR-dependent mechanism. *Development* 140(10), pp. 2108–2117. doi: 10.1242/dev.085266.

Howard, L. et al. 2018. TWE-PRIL reverse signalling suppresses

sympathetic axon growth and tissue innervation. *Development (Cambridge)* 145(22). doi: 10.1242/dev.165936.

Howard, L. et al. 2019. CD40 forward signalling is a physiological regulator of early sensory axon growth. *Development* 146(18), p. dev176495. doi: 10.1242/dev.176495.

Hsu, H. et al. 1995. The TNF receptor 1-associated protein TRADD signals cell death and NF-κB activation. *Cell* 81(4), pp. 495–504. doi: 10.1016/0092-8674(95)90070-5.

Hu, H.M. et al. 1994. A novel RING finger protein interacts with the cytoplasmic domain of CD40. *The Journal of biological chemistry* 269(48), pp. 30069–72.

Huang, E.J. and Reichardt, L.F. 2003. Trk Receptors: Roles in Neuronal Signal Transduction. *Annual Review of Biochemistry* 72(1), pp. 609–642. doi: 10.1146/annurev.biochem.72.121801.161629.

Huang, X. and Saint-Jeannet, J.P. 2004. Induction of the neural crest and the opportunities of life on the edge. *Developmental Biology* 275(1), pp. 1–11. doi: 10.1016/j.ydbio.2004.07.033.

Huber, A.B. et al. 2003. Signaling at the Growth Cone: Ligand-Receptor Complexes and the Control of Axon Growth and Guidance. *Annual Review of Neuroscience* 26(1), pp. 509–563. doi: 10.1146/annurev.neuro.26.010302.081139.

Ichikawa, K. et al. 2001. Tumoricidal activity of a novel anti-human DR5 monoclonal antibody without hepatocyte cytotoxicity. *Nature Medicine* 7(8), pp. 954–960. doi: 10.1038/91000.

Ip, N.Y. et al. 1992. Mammalian neurotrophin-4: structure, chromosomal localization, tissue distribution, and receptor specificity. *Proceedings of the National Academy of Sciences of the United States of America* 89(7), pp. 3060–4. doi: 10.1073/pnas.89.7.3060.

Itoh, K. and Sokol, S.Y. 2015. Early Development of Epidermis and Neural Tissue. In: *Principles of Developmental Genetics: Second Edition*. Elsevier Inc.,

pp. 189–201. doi: 10.1016/B978-0-12-405945-0.00011-9.

Itoh, N. and Nagata, S. 1993. A novel protein domain required for apoptosis. Mutational analysis of human Fas antigen. *The Journal of Biological Chemistry* 268(15), pp. 10932–7.

Jänig, W. and McLachlan, E.M. 1992. Specialized functional pathways are the building blocks of the autonomic nervous system. *Journal of the Autonomic Nervous System* 41(1–2), pp. 3–13. doi: 10.1016/0165-1838(92)90121-V.

Jones, K.R. and Reichardt, L.F. 1990. Molecular cloning of a human gene that is a member of the nerve growth factor family. *Proceedings of the National Academy of Sciences of the United States of America* 87(20), pp. 8060–8064. doi: 10.1073/pnas.87.20.8060.

Joza, N. et al. 2001. Essential role of the mitochondrial apoptosis-inducing factor in programmed cell death. *Nature* 410(6828), pp. 549–554. doi: 10.1038/35069004.

Juhász, K. et al. 2013. Importance of reverse signaling of the TNF superfamily in immune regulation. *Expert Review of Clinical Immunology* 9(4), pp. 335–348. doi: 10.1586/eci.13.14.

Kaestner, C.L. et al. 2019. Immunohistochemical analysis of the mouse celiac ganglion: An integrative relay station of the peripheral nervous system. *Journal of Comparative Neurology* 527(16), pp. 2742–2760. doi: 10.1002/cne.24705.

Kaisho, Y. et al. 1990. Cloning and expression of a cDNA encoding a novel human neurotrophic factor. *FEBS Letters* 266(1–2), pp. 187–191. doi: 10.1016/0014-5793(90)81536-W.

Kameda, Y. 2014. Signaling molecules and transcription factors involved in the development of the sympathetic nervous system, with special emphasis on the superior cervical ganglion. *Cell and Tissue Research* 357(3), pp. 527–548. doi: 10.1007/s00441-014-1847-3.

Kandel, E.R. et al. 2013. Principles of Neural Science. In: *Principles of*

Neural Science. Fifth. NewYork: McGraw-Hill, pp. 21–24.

Kandel, E.R. et al. 2014. *Principles of Neural Science, Fifth Edition*. doi: 10.1036/0838577016.

Karpusas, M. et al. 1995. 2 A crystal structure of an extracellular fragment of human CD40 ligand. *Structure* 3(10), pp. 1031–9. doi: 10.1016/S0969-2126(01)00239-8.

Katz, D.M. et al. 1983. Expression of catecholaminergic characteristics by primary sensory neurons in the normal adult rat in vivo. *Proceedings of the National Academy of Sciences* 80(11), pp. 3526–3530. doi: 10.1073/pnas.80.11.3526.

Kawabe, T. et al. 1994. The immune responses in CD40-deficient mice: Impaired immunoglobulin class switching and germinal center formation. *Immunity* 1(3), pp. 167–178. doi: 10.1016/1074-7613(94)90095-7.

Kelley, S.K. et al. 2001. Preclinical studies to predict the disposition of Apo2L/tumor necrosis factor-related apoptosis-inducing ligand in humans: characterization of in vivo efficacy, pharmacokinetics, and safety. *The Journal of pharmacology and experimental therapeutics* 299(1), pp. 31–8.

Kim, H. et al. 2006. Hierarchical regulation of mitochondrion-dependent apoptosis by BCL-2 subfamilies. *Nature Cell Biology* 8(12), pp. 1348–1358. doi: 10.1038/ncb1499.

Kim, H.S. et al. 2015. Autocrine stimulation of IL-10 is critical to the enrichment of IL-10-producing CD40 hi CD5 + regulatory B cells in vitro and in vivo. *BMB Reports* 48(1), pp. 54–59. doi: 10.5483/BMBRep.2015.48.1.213.

Kinder, S.J. et al. 2001. The organizer of the mouse gastrula is composed of a dynamic population of progenitor cells for the axial mesoderm. *Development* 128(18), pp. 3623 LP – 3634.

Kisiswa, L. et al. 2013. TNFα reverse signaling promotes sympathetic axon growth and target innervation. *Nature Neuroscience* 16(7), pp. 865–873. doi: 10.1038/nn.3430.

Kisiswa, L. et al. 2017. T-type Ca2+ channels are required for enhanced

sympathetic axon growth by TNFα reverse signalling. *Open Biology* 7(1), p. 160288. doi: 10.1098/rsob.160288.

Kolodkin, A.L. and Tessier-Lavigne, M. 2011. Mechanisms and Molecules of Neuronal Wiring: A Primer. *Cold Spring Harbor Perspectives in Biology* 3(6), pp. a001727–a001727. doi: 10.1101/cshperspect.a001727.

van Kooten, C. et al. 2000. CD40-CD40 ligand. *Journal of Leukocyte Biology* 67(1), pp. 2–17. Available at: http://doi.wiley.com/10.1002/jlb.67.1.2.

van Kooten, C. and Banchereau, J. 1997. Functions of CD40 on B cells, dendritic cells and other cells. *Current Opinion in Immunology* 9(3), pp. 330–7.

Körner, H. et al. 1997. Distinct roles for lymphotoxin-α and tumor necrosis factor in organogenesis and spatial organization of lymphoid tissue. *European Journal of Immunology* 27(10), pp. 2600–2609. doi: 10.1002/eji.1830271020.

Kotzbauer, P.T. et al. 1994. Postnatal development of survival responsiveness in rat sympathetic neurons to leukemia inhibitory factor and ciliary neurotrophic factor. *Neuron* 12(4), pp. 763–773. doi: 10.1016/0896-6273(94)90329-8.

Krammer, P.H. 2000. CD95's deadly mission in the immune system. *Nature* 407(6805), pp. 789–795. doi: 10.1038/35037728.

Kriegstein, A. and Alvarez-Buylla, A. 2009. The Glial Nature of Embryonic and Adult Neural Stem Cells. *Annual Review of Neuroscience* 32(1), pp. 149–184. doi: 10.1146/annurev.neuro.051508.135600.

Krippner-Heidenreich, A. et al. 2002. Control of Receptor-induced Signaling Complex Formation by the Kinetics of Ligand/Receptor Interaction. *Journal of Biological Chemistry* 277(46), pp. 44155–44163. doi: 10.1074/jbc.M207399200.

Kuhn, K.D. et al. 2020. Molecular dissection of TNFR-TNFα bidirectional signaling reveals both cooperative and antagonistic interactions with p75 neurotrophic factor receptor in axon patterning. *Molecular and Cellular*

Neuroscience 103(October 2019), p. 103467. doi: 10.1016/j.mcn.2020.103467.

Kummer, W. et al. 1993. Tyrosine-hydroxylase-containing vagal afferent neurons in the rat nodose ganglion are independent from neuropeptide-Y-containing populations and project to esophagus and stomach. *Cell & Tissue Research* 271(1), pp. 135–144. doi: 10.1007/BF00297551.

Kuruvilla, R. et al. 2004. A neurotrophin signaling cascade coordinates sympathetic neuron development through differential control of TrkA trafficking and retrograde signaling. *Cell* 118(2), pp. 243–255. doi: 10.1016/j.cell.2004.06.021.

Ladd, F.V.L. et al. 2014. Stereological and Allometric Studies on Neurons and Axo-Dendritic Synapses in Superior Cervical Ganglia. In: *International Review of Cell and Molecular Biology*. 1st ed. Elsevier Inc., pp. 123–155. doi: 10.1016/B978-0-12-800179-0.00002-7.

Laman, J.D. et al. 2017. Functions of CD40 and Its Ligand, gp39 (CD40L). *Critical Reviews in Immunology* 37(2–6), pp. 371–420. doi: 10.1615/CritRevImmunol.v37.i2-6.100.

Lawson, A. 2003. Epiblast and primitive-streak origins of the endoderm in the gastrulating chick embryo. *Development* 130(15), pp. 3491–3501. doi: 10.1242/dev.00579.

Lee, K.F. et al. 1994a. Dependence on p75 for innervation of some sympathetic targets. *Science* 263(5152), pp. 1447–1449. doi: 10.1126/science.8128229.

Lee, K.F. et al. 1994b. p75-deficient embryonic dorsal root sensory and neonatal sympathetic neurons display a decreased sensitivity to NGF. *Development* 120(4), pp. 1027–1033.

Lee, R. 2001. Regulation of Cell Survival by Secreted Proneurotrophins. *Science* 294(5548), pp. 1945–1948. doi: 10.1126/science.1065057.

Lee, W.-H. et al. 2019. Reverse Signaling of Tumor Necrosis Factor Superfamily Proteins in Macrophages and Microglia: Superfamily Portrait in the

Neuroimmune Interface. *Frontiers in Immunology* 10. doi: 10.3389/fimmu.2019.00262.

Leibrock, J. et al. 1989. Molecular cloning and expression of brain-derived neurotrophic factor. *Nature* 341(6238), pp. 149–152. doi: 10.1038/341149a0.

Levi-Montalcini, R. 1987. The nerve growth factor 35 years later. *Science* 237(4819), pp. 1154–1162. doi: 10.1126/science.3306916.

Levi-Montalcini, R. and Angeletti, P.U. 1968. *Nerve Growth Factor*. doi: 10.1152/physrev.1968.48.3.534.

Levi-Montalcini, R. and Booker, B. 1960. Destruction of the sympathetic ganglia in mammals by an antiserum to a nerve-growth protein. *Proceedings of the National Academy of Sciences* 46(3), pp. 384–391. doi: 10.1073/pnas.46.3.384.

Li, D. et al. 2013. Autocrine TNF-α-mediated NF-κB activation is a determinant for evasion of CD40-induced cytotoxicity in cancer cells. *Biochemical and Biophysical Research Communicationsochemical* 436(3), pp. 467–72. doi: 10.1016/j.bbrc.2013.05.128.

Li, L.Y. et al. 2001. Endonuclease G is an apoptotic DNase when released from mitochondria. *Nature* 412, p. 95.

Linden, R. 1994. The survival of developing neurons: A review of afferent control. *Neuroscience* 58(4), pp. 671–682. doi: 10.1016/0306-4522(94)90447-2.

Lockhart, S.T. et al. 1997. Nerve growth factor modulates synaptic transmission between sympathetic neurons and cardiac myocytes. *Journal of Neuroscience* 17(24), pp. 9573–9582. doi: 10.1523/jneurosci.17-24-09573.1997.

Lowery, L.A. and Van Vactor, D. 2009. The trip of the trip: understanding the growth cone machinery. *Nature Reviews Molecular Cell Biology* 10(5), pp. 332–343. doi: 10.1038/nrm2679.The.

Ludwig, M. and Leng, G. 2006. Dendritic peptide release and peptide-dependent behaviours. *Nature Reviews Neuroscience* 7(2), pp. 126–136. doi: 10.1038/nrn1845.

Ludwig, M. and Pittman, Q.J. 2003. Talking back: dendritic

neurotransmitter release. *Trends in Neurosciences* 26(5), pp. 255–261. doi: 10.1016/S0166-2236(03)00072-9.

Lumsden, A.G.S. and Davies, A.M. 1983. Earliest sensory nerve fibres are guided to peripheral targets by attractants other than nerve growth factor. *Nature* 306(5945), pp. 786–788. doi: 10.1038/306786a0.

MacEwan, D.J. 2002. TNF ligands and receptors - A matter of life and death. *British Journal of Pharmacology* 135(4), pp. 855–875. doi: 10.1038/sj.bjp.0704549.

Maina, F. et al. 1998. Multiple Roles for Hepatocyte Growth Factor in Sympathetic Neuron Development. *Neuron* 20(5), pp. 835–846. doi: 10.1016/S0896-6273(00)80466-3.

Maina, F. and Klein, R. 1999. Hepatocyte growth factor, a versatile signal for developing neurons. *Nature Neuroscience* 2(3), pp. 213–217. doi: 10.1038/6310.

Maisonpierre, P.C. et al. 1990. Neurotrophin-3: a neurotrophic factor related to NGF and BDNF. *Science* 247(4949), pp. 1446–1451. doi: 10.1126/science.2321006.

Makita, T. et al. 2008. Endothelins are vascular-derived axonal guidance cues for developing sympathetic neurons. *Nature* 452(7188), pp. 759–763. doi: 10.1038/nature06859.

Martin, D.P. et al. 1988. Inhibitors of protein synthesis and RNA synthesis prevent neuronal death caused by nerve growth factor deprivation. *Journal of Cell Biology* 106(3), pp. 829–844. doi: 10.1083/jcb.106.3.829.

Mazzei, G.J. et al. 1995. Recombinant Soluble Trimeric CD40 Ligand Is Biologically Active. *Journal of Biological Chemistry* 270(13), pp. 7025–7028. doi: 10.1074/jbc.270.13.7025.

McCorry, L.K. et al. 2007. Physiology of the autonomic nervous system. *American journal of pharmaceutical education* 71(4), p. 78. doi: 10.5688/aj710478.

McDermott, M.F. et al. 1999. Germline Mutations in the Extracellular Domains of the 55 kDa TNF Receptor, TNFR1, Define a Family of Dominantly

Inherited Autoinflammatory Syndromes. *Cell* 97(1), pp. 133–144. doi: 10.1016/S0092-8674(00)80721-7.

McWilliams, T.G. et al. 2015. Regulation of autocrine signaling in subsets of sympathetic neurons has regional effects on tissue innervation. *Cell Reports* 10(9), pp. 1443–1449. doi: 10.1016/j.celrep.2015.02.016.

Meeker, R.B. and Williams, K.S. 2015. The p75 neurotrophin receptor: At the crossroad of neural repair and death. *Neural Regeneration Research* 10(5), pp. 721–725. doi: 10.4103/1673-5374.156967.

Michels, M. et al. 2015. CD40-CD40 Ligand Pathway Is a Major Component of Acute Neuroinflammation and Contributes to Long-term Cognitive Dysfunction after Sepsis. *Molecular Medicine* 21(1), pp. 219–226. doi: 10.2119/molmed.2015.00070.

Middleton, G. and Davies, A.M. 2001. Populations of NGF-dependent neurones differ in their requirement for BAX to undergo apoptosis in the absence of NGF/TrkA signalling in vivo. *Development (Cambridge, England)* 128(23), pp. 4715–4728.

Miolan, J.P. and Niel, J.P. 1996. The mammalian sympathetic prevertebral ganglia: integrative properties and role in the nervous control of digestive tract motility. *Journal of the Autonomic Nervous System* 58(3), pp. 125–138. doi: 10.1016/0165-1838(95)00128-X.

Mitsuoka, K. et al. 2017. Morphological relationship between the superior cervical ganglion and cervical nerves in Japanese cadaver donors. *Brain and Behavior* 7(2), p. e00619. doi: 10.1002/brb3.619.

Naismith, J.H. and Sprang, S.R. 1998. Modularity in the TNF-receptor family. *Trends in Biochemical Sciences* 23(2), pp. 74–79. doi: 10.1016/S0968-0004(97)01164-X.

Nance, D.M. and Burns, J. 1989. Innervation of the spleen in the rat: Evidence for absence of afferent innervation. *Brain, Behavior, and Immunity* 3(4), pp. 281–290. doi: 10.1016/0889-1591(89)90028-7.

Nechushtan, A. et al. 2001. Bax and Bak Coalesce into Novel Mitochondria-Associated Clusters during Apoptosis. *The Journal of Cell Biology* 153(6), pp. 1265 LP – 1276.

Nishino, J. et al. 1999. GFRa3, a component of the artemin receptor, is required for migration and survival of the superior cervical ganglion. *Neuron* 23(4), pp. 725–736. doi: 10.1016/S0896-6273(01)80031-3.

Nolan, A.M. et al. 2014. The neurite growth inhibitory effects of soluble TNFα on developing sympathetic neurons are dependent on developmental age. *Differentiation* 88(4–5), pp. 124–130. doi: 10.1016/j.diff.2014.12.006.

O'Keeffe, G.W. et al. 2008. NGF-promoted axon growth and target innervation requires GITRL-GITR signaling. *Nature Neuroscience* 11(2), pp. 135–142. doi: 10.1038/nn2034.

Oppenheim, R.W. 1985. Naturally occurring cell death during neural development. *Trends in Neurosciences* 8(November), pp. 487–493. doi: 10.1016/0166-2236(85)90175-4.

Oppenheim, R.W. 1989. The neurotrophic theory and naturally occurring motoneuron death. *Trends in Neurosciences* 12(7), pp. 252–255. doi: 10.1016/0166-2236(89)90021-0.

Pallai, A. et al. 2016. Transmembrane TNF-α Reverse Signaling Inhibits Lipopolysaccharide-Induced Proinflammatory Cytokine Formation in Macrophages by Inducing TGF-β: Therapeutic Implications. *The Journal of Immunology* 196(3), pp. 1146–1157. doi: 10.4049/jimmunol.1501573.

Pamukcu, B. et al. 2011. The CD40-CD40L system in cardiovascular disease. *Annals of Medicine* 43(5), pp. 331–340. doi: 10.3109/07853890.2010.546362.

Parameswaran, N. and Patial, S. 2010. Tumor necrosis factor-a signaling in macrophages. *Critical Reviews in Eukaryotic Gene Expression* 20(2), pp. 87–103. doi: 10.1615/CritRevEukarGeneExpr.v20.i2.10.

Paves, H. and Saarma, M. 1997. Neurotrophins as in vitro growth cone

guidance molecules for embryonic sensory neurons. *Cell and tissue research* 290(2), pp. 285–97.

Peschon, J.J. et al. 1998. TNF receptor-deficient mice reveal divergent roles for p55 and p75 in several models of inflammation. *Journal of Immunology* 160(2), pp. 943–52.

Petersohn, J.D. 2011. Sympathetic Neural Blockade. In: *Pain Procedures in Clinical Practice*. Elsevier, pp. 507–519. doi: 10.1016/B978-1-4160-3779-8.10042-9.

Pfeffer, K. et al. 1993. Mice deficient for the 55 kd tumor necrosis factor receptor are resistant to endotoxic shock, yet succumb to L. monocytogenes infection. *Cell* 73(3), pp. 457–467. doi: 10.1016/0092-8674(93)90134-C.

Pfisterer, U. and Khodosevich, K. 2017. Neuronal survival in the brain: Neuron type-specific mechanisms. *Cell Death and Disease* 8(3), pp. e2643-14. doi: 10.1038/cddis.2017.64.

Phillips, R.J. and Powley, T.L. 2007. Innervation of the gastrointestinal tract: Patterns of aging. *Autonomic Neuroscience* 136(1–2), pp. 1–19. doi: 10.1016/j.autneu.2007.04.005.

Pirvola, U. et al. 1992. Brain-derived neurotrophic factor and neurotrophin 3 mRNAs in the peripheral target fields of developing inner ear ganglia. *Proceedings of the National Academy of Sciences* 89(20), pp. 9915–9919. doi: 10.1073/pnas.89.20.9915.

Port, F. and Basler, K. 2010. Wnt Trafficking: New Insights into Wnt Maturation, Secretion and Spreading. *Traffic* 11(10), pp. 1265–1271. doi: 10.1111/j.1600-0854.2010.01076.x.

Powell, W.C. et al. 1999. The metalloproteinase matrilysin proteolytically generates active soluble Fas ligand and potentiates epithelial cell apoptosis. *Current Biology* 9(24), pp. 1441–1447. doi: 10.1016/S0960-9822(00)80113-X.

Probert, L. 2015. TNF and its receptors in the CNS: The essential, the desirable and the deleterious effects. *Neuroscience* 302, pp. 2–22. doi:

10.1016/j.neuroscience.2015.06.038.

Pullen, S.S. et al. 1999. High-Affinity Interactions of Tumor Necrosis Factor Receptor-Associated Factors (TRAFs) and CD40 Require TRAF Trimerization and CD40 Multimerization. *Biochemistry* 38(31), pp. 10168–10177. doi: 10.1021/bi9909905.

Purves, D. et al. 2001. The Sympathetic Division of the Visceral Motor System. In: *Neuroscience*. 2nd Editio. Sunderland: Sinauer Associates

Qiu, M.-S. and Green, S.H. 1992. PC12 cell neuronal differentiation is associated with prolonged p21ras activity and consequent prolonged ERK activity. *Neuron* 9(4), pp. 705–717. doi: 10.1016/0896-6273(92)90033-A.

Qu, Y. et al. 2017. Forward and Reverse Signaling Mediated by Transmembrane Tumor Necrosis Factor-Alpha and TNF Receptor 2: Potential Roles in an Immunosuppressive Tumor Microenvironment. *Frontiers in Immunology* 8. doi: 10.3389/fimmu.2017.01675.

Quinson, N. et al. 2001. Locations and Innervation of Cell Bodies of Sympathetic Neurons Projecting to the Gastrointestinal Tract in the Rat. *Archives of Histology and Cytology* 64(3), pp. 281–294. doi: 10.1679/aohc.64.281.

Ramirez, S.H. et al. 2010. Dyad of CD40/CD40 Ligand Fosters Neuroinflammation at the Blood-Brain Barrier and Is Regulated via JNK Signaling: Implications for HIV-1 Encephalitis. *Journal of Neuroscience* 30(28), pp. 9454–9464. doi: 10.1523/JNEUROSCI.5796-09.2010.

Renier, N. et al. 2014. Resource iDISCO : A Simple , Rapid Method to Immunolabel Large Tissue Samples for Volume Imaging. *Cell* 159(4), pp. 896–910. doi: 10.1016/j.cell.2014.10.010.

Roelen, B.A.J. 2018. Epiblast development. In: *Encyclopedia of Reproduction*. Elsevier, pp. 341–346. doi: 10.1016/B978-0-12-801238-3.64480-X.

Rohrer, H. 1990. The Role of Growth Factors in the Control of Neurogenesis. *European Journal of Neuroscience* 2(12), pp. 1005–1015. doi: 10.1111/j.1460-9568.1990.tb00013.x.

Ronn, L.C.B. et al. 2000. A simple procedure for quantification of neurite outgrowth based on stereological principles. *Journal of Neuroscience Methods* 100(1–2), pp. 25–32. doi: 10.1016/S0165-0270(00)00228-4.

Roosen, A. et al. 2001. Lack of Neurotrophin-4 Causes Selective Structural and Chemical Deficits in Sympathetic Ganglia and Their Preganglionic Innervation. *The Journal of Neuroscience* 21(9), pp. 3073–3084. doi: 10.1523/JNEUROSCI.21-09-03073.2001.

Rosas-Ballina, M. et al. 2008. Splenic nerve is required for cholinergic antiinflammatory pathway control of TNF in endotoxemia. *Proceedings of the National Academy of Sciences* 105(31), pp. 11008–11013. doi: 10.1073/pnas.0803237105.

Rosenthal, A. et al. 1990. Primary structure and biological activity of a novel human neurotrophic factor. *Neuron* 4(5), pp. 767–773. doi: 10.1016/0896-6273(90)90203-R.

Rossol, M. et al. 2007. Interaction between Transmembrane TNF and TNFR1/2 Mediates the Activation of Monocytes by Contact with T Cells. *The Journal of Immunology* 179(6), pp. 4239–4248. doi: 10.4049/jimmunol.179.6.4239.

Rothstein, M. et al. 2018. The molecular basis of neural crest axial identity. *Developmental Biology* 444, pp. S170–S180. doi: 10.1016/j.ydbio.2018.07.026.

Rubin, E. 1985. Development of the rat superior cervical ganglion: ganglion cell maturation. *The Journal of Neuroscience* 5(3), pp. 673–684. doi: 10.1523/JNEUROSCI.05-03-00673.1985.

Ruhrberg, C. and Schwarz, Q. 2010. In the beginning. *Cell Adhesion & Migration* 4(4), pp. 622–630. doi: 10.4161/cam.4.4.13502.

Ryu, Y.K. et al. 2013. An autocrine Wnt5a-Ror signaling loop mediates sympathetic target innervation. *Developmental Biology* 377(1), pp. 79–89. doi: 10.1016/j.ydbio.2013.02.013.

Sadler, T.W. 2005. Embryology of neural tube development. *American Journal of Medical Genetics Part C: Seminars in Medical Genetics* 135C(1), pp. 2–8. doi: 10.1002/ajmg.c.30049.

Saraste, A. 2000. Morphologic and biochemical hallmarks of apoptosis. *Cardiovascular Research* 45(3), pp. 528–537. doi: 10.1016/S0008-6363(99)00384-3.

Sata, Y. et al. 2018. Role of the Sympathetic Nervous System and Its Modulation in Renal Hypertension. *Frontiers in Medicine* 5. doi: 10.3389/fmed.2018.00082.

Sato, Y. et al. 1998. Three-dimensional multi-scale line filter for segmentation and visualization of curvilinear structures in medical images. *Medical Image Analysis* 2(2), pp. 143–168. doi: 10.1016/S1361-8415(98)80009-1.

Schindelin, J. et al. 2012. Fiji: an open-source platform for biological-image analysis. *Nature Methods* 9(7), pp. 676–682. doi: 10.1038/nmeth.2019.

Schmidt, R.E. and Plurad, S.B. 1986. Ultrastructural and Biochemical Characterization of Autonomic Neuropathy in Rats with Chronic Streptozotocin Diabetes. *Journal of Neuropathology and Experimental Neurology* 45(5), pp. 525–544. doi: 10.1097/00005072-198609000-00004.

Schneider, P. et al. 1999. BAFF, a novel ligand of the tumor necrosis factor family, stimulates B cell growth. *The Journal of Experimental Medicine* 189(11), pp. 1747–56. doi: 10.1084/jem.189.11.1747.

Schober, A. and Unsicker, K. 2001. Growth and neurotrophic factors regulating development and maintenance of sympathetic preganglionic neurons. In: *International Review of Cytology*., pp. 37–76. doi: 10.1016/S0074-7696(01)05002-1.

Schönbeck, U. and Libby, P. 2001. CD40 Signaling and Plaque Instability. *Circulation Research* 89(12), pp. 1092–1103. doi: 10.1161/hh2401.101272.

Sedger, L.M. and McDermott, M.F. 2014. TNF and TNF-receptors: From mediators of cell death and inflammation to therapeutic giants – past, present

and future. *Cytokine & Growth Factor Reviews* 25(4), pp. 453–472. doi: 10.1016/j.cytogfr.2014.07.016.

Selleck, M.A. and Bronner-Fraser, M. 1995. Origins of the avian neural crest: the role of neural plate-epidermal interactions. *Development* 121(2), pp. 525 LP – 538.

Semra, Y.K. et al. 2009. NGF protects paravertebral but not prevertebral sympathetic neurons against exposure to high glucose in vitro. *Brain Research* 1285, pp. 164–173. doi: 10.1016/j.brainres.2009.05.089.

Sharkey, K.A. et al. 1984. Sensory substance P innervation of the stomach and pancreas. Demonstration of capsaicin-sensitive sensory neurons in the rat by combined immunohistochemistry and retrograde tracing. *Gastroenterology* 87(4), pp. 914–21.

Sharma, N. et al. 2010. Long-Distance Control of Synapse Assembly by Target-Derived NGF. *Neuron* 67(3), pp. 422–434. doi: 10.1016/j.neuron.2010.07.018.

Skaper, S.D. 2018. Neurotrophic Factors: An Overview., pp. 1–17. doi: 10.1007/978-1-4939-7571-6_1.

Smeyne, R.J. et al. 1994. Severe sensory and sympathetic neuropathies in mice carrying a disrupted Trk/NGF receptor gene. *Nature* 368(6468), pp. 246–249. doi: 10.1038/368246a0.

Smith, C.A. et al. 1994. The TNF receptor superfamily of cellular and viral proteins: Activation, costimulation, and death. *Cell* 76(6), pp. 959–962. doi: 10.1016/0092-8674(94)90372-7.

Solomon, K.A. et al. 1999. Cutting edge: a dominant negative form of TNF-alpha converting enzyme inhibits proTNF and TNFRII secretion. *Journal of Immunology* 163(8), pp. 4105–8.

Srinivasula, S.M. et al. 1998. Autoactivation of procaspase-9 by Apaf-1-mediated oligomerization. *Molecular Cell* 1(7), pp. 949–957. doi: 10.1016/S1097-2765(00)80095-7.

Stoeckli, E.T. 2018. Understanding axon guidance: are we nearly there yet? *Development* 145(10), p. dev151415. doi: 10.1242/dev.151415.

Sun, M. and Fink, P.J. 2007. A New Class of Reverse Signaling Costimulators Belongs to the TNF Family. *The Journal of Immunology* 179(7), pp. 4307–4312. doi: 10.4049/jimmunol.179.7.4307.

Szurszewski, J.H. 1981. Physiology of Mammalian Prevertebral Ganglia. *Annual Review of Physiology* 43(1), pp. 53–68. doi: 10.1146/annurev.ph.43.030181.000413.

Szurszewski, J.H. and Linden, D.R. 2012. Physiology of Prevertebral Sympathetic Ganglia. In: *Physiology of the Gastrointestinal Tract*. Elsevier, pp. 583–627. doi: 10.1016/B978-0-12-382026-6.00020-8.

Tam, P.P.L. and Behringer, R.R. 1997. Mouse gastrulation: the formation of a mammalian body plan. *Mechanisms of Development* 68(1–2), pp. 3–25. doi: 10.1016/S0925-4773(97)00123-8.

Tan, J. 2002. CD40 is expressed and functional on neuronal cells. *The EMBO Journal* 21(4), pp. 643–652. doi: 10.1093/emboj/21.4.643.

Tartaglia, L.A. et al. 1993. A novel domain within the 55 kd TNF receptor signals cell death. *Cell* 74(5), pp. 845–853. doi: 10.1016/0092-8674(93)90464-2.

Tassew, N.G. et al. 2017. Exosomes Mediate Mobilization of Autocrine Wnt10b to Promote Axonal Regeneration in the Injured CNS. *Cell Reports* 20(1), pp. 99–111. doi: 10.1016/j.celrep.2017.06.009.

Taylor, A.M. et al. 2005. A microfluidic culture platform for CNS axonal injury, regeneration and transport. *Nature Methods* 2(8), pp. 599–605. doi: 10.1038/nmeth777.

Tecklenborg, J. et al. 2018. The role of the immune system in kidney disease. *Clinical & Experimental Immunology* 192(2), pp. 142–150. doi: 10.1111/cei.13119.

Teng, H.K. et al. 2005. ProBDNF induces neuronal apoptosis via activation of a receptor complex of p75NTR and sortilin. *Journal of Neuroscience*

25(22), pp. 5455–5463. doi: 10.1523/JNEUROSCI.5123-04.2005.

Terauchi, A. et al. 2016. Retrograde fibroblast growth factor 22 (FGF22) signaling regulates insulin-like growth factor 2 (IGF2) expression for activity-dependent synapse stabilization in the mammalian brain. *eLife* 5. doi: 10.7554/eLife.12151.

Tessarollo, L. et al. 1997. Targeted deletion of all isoforms of the trkC gene suggests the use of alternate receptors by its ligand neurotrophin-3 in neuronal development and implicates trkC in normal cardiogenesis. *Proceedings of the National Academy of Sciences of the United States of America* 94(26), pp. 14776–14781. doi: 10.1073/pnas.94.26.14776.

Thoenen, H. and Barde, Y.A. 1980. Physiology of nerve growth factor. *Physiological Reviews* 60(4), pp. 1284–1335. doi: 10.1152/physrev.1980.60.4.1284.

Tone, M. et al. 2001. Regulation of CD40 function by its isoforms generated through alternative splicing. *Proceedings of the National Academy of Sciences* 98(4), pp. 1751–1756. doi: 10.1073/pnas.98.4.1751.

Trudrung, P. et al. 1994. Locations and Chemistries of Sympathetic Nerve Cells that Project to the Gastrointestinal Tract and Spleen. *Archives of Histology and Cytology* 57(2), pp. 139–150. doi: 10.1679/aohc.57.139.

Utsumi, T. et al. 2001. Transmembrane TNF (pro-TNF) is palmitoylated. *FEBS Letters* 500(1–2), pp. 1–6. doi: 10.1016/S0014-5793(01)02576-5.

Verdi, J.M. et al. 1996. A reciprocal cell-cell interaction mediated by NT-3 and neuregulins controls the early survival and development of sympathetic neuroblasts. *Neuron* 16(3), pp. 515–27. doi: 10.1016/s0896-6273(00)80071-9.

Vicente, C. 2015. An interview with Lewis Wolpert. *Development* 142(15), pp. 2547–2548. doi: 10.1242/dev.127373.

Vilar, M. 2017. Structural Characterization of the p75 Neurotrophin Receptor. In: *Vitamins and Hormones*. 1st ed. Elsevier Inc., pp. 57–87. doi: 10.1016/bs.vh.2016.10.007.

Vizard, T.N. et al. 2015. ERK signaling mediates CaSR-promoted axon

growth. *Neuroscience Letters* 603, pp. 77–83. doi: 10.1016/j.neulet.2015.07.019.

Wajant, H. 2002. The Fas signaling pathway: More than a paradigm. *Science* 296(5573), pp. 1635–1636. doi: 10.1126/science.1071553.

Wajant, H. and Siegmund, D. 2019. TNFR1 and TNFR2 in the Control of the Life and Death Balance of Macrophages. *Frontiers in Cell and Developmental Biology* 7(May), pp. 1–14. doi: 10.3389/fcell.2019.00091.

Wang, H.S. and McKinnon, D. 1995. Potassium currents in rat prevertebral and paravertebral sympathetic neurones: control of firing properties. *The Journal of Physiology* 485(2), pp. 319–335. doi: 10.1113/jphysiol.1995.sp020732.

Wehrwein, E.A. et al. 2016. Overview of the Anatomy, Physiology, and Pharmacology of the Autonomic Nervous System. In: *Comprehensive Physiology*. Hoboken, NJ, USA: John Wiley & Sons, Inc., pp. 1239–1278. doi: 10.1002/cphy.c150037.

White, F. a et al. 1998. Widespread elimination of naturally occurring neuronal death in Bax-deficient mice. *The Journal of Neuroscience* 18(4), pp. 1428–1439. doi: 10.1523/jneurosci.1446-05.2005.

Wielockx, B. et al. 2001. Inhibition of matrix metalloproteinases blocks lethal hepatitis and apoptosis induced by tumor necrosis factor and allows safe antitumor therapy. *Nature Medicine* 7(11), pp. 1202–1208. doi: 10.1038/nm1101-1202.

Wlizla, M. and Zorn, A.M. 2015. Vertebrate Endoderm Formation. In: *Principles of Developmental Genetics: Second Edition.*, pp. 237–253. doi: 10.1016/B978-0-12-405945-0.00013-2.

Wolpert, L. (Lewis) et al. 2002. Principles of Development. In: *Principles of Developmental*. Second. NewYork: Oxford University Press, pp. 375–414.

Wright, E.M. et al. 1992. Neurotrophic factors promote the maturation of developing sensory neurons before they become dependent on these factors for survival. *Neuron* 9(1), pp. 139–150. doi: 10.1016/0896-6273(92)90229-7.

Wyatt, S. et al. 1997. Sympathetic neuron survival and TrkA expression in NT3-deficient mouse embryos. *The EMBO Journal* 16(11), pp. 3115–3123. doi: 10.1093/emboj/16.11.3115.

Wyatt, S. and Davies, A.M. 1993. Regulation of expression of mRNAs encoding the nerve growth factor receptors p75 and trkA in developing sensory neurons. *Development* 119(3), pp. 635–648.

Wyatt, S. and Davies, A.M. 1995. Regulation of nerve growth factor receptor gene expression in sympathetic neurons during development. *Journal of Cell Biology* 130(6), pp. 1435–1446. doi: 10.1083/jcb.130.6.1435.

Xue, Z.G. et al. 1985. Differentiation of Catecholaminergic Cells in Cultures of Embryonic Avian Sensory Ganglia. *Proceedings of the National Academy of Sciences of the United States of America* 82(24), pp. 8800–8804.

Yang, S. et al. 2018. Role of TNF-TNF receptor 2 signal in regulatory T cells and its therapeutic implications. *Frontiers in Immunology* 9(APR). doi: 10.3389/fimmu.2018.00784.

Ye, L.L. et al. 2018. The significance of tumor necrosis factor receptor type II in CD8+ regulatory T cells and CD8+ effector T cells. *Frontiers in Immunology* 8(MAR), p. 22. doi: 10.3389/fimmu.2018.00583.

Zaimis, E. et al. 1965. Morphological, Biochemical and Functional Changes in the Sympathetic Nervous System of Rats Treated with Nerve Growth Factor-Antiserum. *Nature* 206(4990), pp. 1220–1222. doi: 10.1038/2061220a0.

Zhou, J.X. and Li, X. 2015. Apoptosis in Polycystic Kidney Disease: From Pathogenesis to Treatment. In: *Polycystic Kidney Disease*. Brisbane: Codon Publications, pp. 197–230. doi: 10.15586/codon.pkd.2015.ch9.

Zhuo, H. 1997. Neurochemistry of the Nodose Ganglion. *Progress in Neurobiology* 52(2), pp. 79–107. doi: 10.1016/S0301-0082(97)00003-8.

Appendix

Tnf PCR Protocol

Primers

***Tnf* common forward**: 5'-CTC TTC TGT CTA CTG AAC-3'
***Tnf* WT reverse**: 5'-TTT ATC TCT TGC TTA TCC-3'
***Tnf* KO reverse**: 5'-TTC TAT CGC CTT CTT GAC-3'

Estimated band size

WT: 320 bp
KO: 398 bp

1x Reaction Mix

Buffer 10x: 2.5 µl
dNTPs: 0.2 µl
Tnfα common forward: 0.5 µl
Tnfα WT reverse: 1 µl
Tnfα KO reverse: 0.25 µl
Paq5000 enzyme: 0.4 µl
Nuclease free water: 18.15 µl

PCR mix: 23 µl
DNA: 2 µl

PCR Programme

Step 1: 95 °C 2 min

Step 2: 95 °C 30 sec
Step 3: 50 °C 30 sec
Step 4: 72 °C 30 sec
40 times

Step 5: 72 °C 3min

Step 6: 4 °C hold

Tnfrsf1a PCR Protocol

Primers

***Tnfrsf1a* common forward**: 5'-GGC TGC AGT CCA CGC ACT GG-3'
***Tnfrsf1a* WT reverse**: 5'-TGT GAA AAG GGC ACC TTT ACG GC-3'
***Tnfrsf1a* KO reverse**: 5'-ATT CGC CAA TGA CAA TGA CAA GAC GCT GG-3'

Estimated band size

WT: 470 bp
KO: 300 bp

1x Reaction Mix

Buffer 10x: 2.5 µl
dNTPs: 0.25 µl
Tnfrsf1a common forward: 0.6 µl
Tnfrsf1a WT reverse: 0.6 µl
Tnfrsf1a KO reverse: 0.6 µl
Paq5000 enzyme: 0.25 µl
Nuclease free water: 18.2 µl

PCR mix: 23 µl
DNA: 2 µl

PCR Programme

Step 1: 95 °C 2 min

Step 2: 95 °C 30 sec
Step 3: 58 °C 1 min
Step 4: 72 °C 1 min
} 40 times

Step 5: 72 °C 3min

Step 6: 4 °C hold

Cd40 PCR Protocol

Primers

CD40 common forward: 5'-GTG AGA TGC TAG CCC TCC TG-3'
CD40 WT reverse: 5'-CAC GTC ATC TGC TGG TTT TC-3'
CD40 KO reverse: 5'-CGT GCA ATC CAT CTT GTT CA-3'

Estimated band size

WT: 594 bp
KO: 685 bp

1x Reaction Mix

Buffer 10x: 2.5 µl
dNTPs: 0.25 µl
Cd40 common forward: 1 µl
Cd40 WT reverse: 1 µl
Cd40 KO reverse: 1 µl
Paq5000 enzyme: 0.25 µl
Nuclease free water: 17 µl

PCR mix: 23 µl
DNA: 2 µl

PCR Programme

Step 1: 95°C 2 min

Step 2: 95 °C 20 sec
Step 3: 59 °C 20 sec
Step 4: 72 °C 30 sec
} 40 times

Step 5: 72 °C 5min

Step 6: 4 °C hold